Table of Contents

List of figures

List of tables

Acknowledgements

Firstly, I would like to thank my supervisors, Prof. Bruno Frenguelli, Dr Kevin Moffat and Dr Calum Sutherland for their unending support, encouragement and patience during my PhD.

In addition, I would like to thank the following:

Prof Dario Alessi (Dundee University) for the original BRSK constructs.

Mrs Ellie Tucker for the cloning of human CaMKKα (Chapter 3).

Drs Mel Feany, Bingwei Lu and Koichi Iijima for the generous provision of fly stocks.

The MRC Neurodegenerative Diseases Brain Bank for access to post-mortem human brain tissue samples and Drs Diane Hanger and Wendy Noble (King's College London, UK) for advice on the design and analysis of the study contained in Chapter 6.

Past and present members of the Frenguelli, Moffat and Sutherland labs for support, encouragement, discussions and critique!

I would also like to acknowledge the generous financial support of Alzheimer's Research UK, which enabled me to carry out my PhD.

Declaration

The work contained in this thesis is the result of original research conducted by myself under the supervision of Prof. Bruno Frenguelli, Dr Kevin Moffat and Dr Calum Sutherland with the following exception:

- The sub-cloning of human CaMKKα into the *Drosophila* expression vector pUAST (Chapter 3) was performed by Mrs Ellie Tucker under my supervision.

None of the work contained in this thesis has been submitted for any previous degree and all sources of information have been acknowledged by means of references.

Ceri Lyn-Adams

March 2011

Summary

Brain-selective kinases (BRSK1 and BRSK2) are serine/threonine kinase members of the AMPK-related family of protein kinases, the majority of which are regulated by the upstream kinase LKB1 whilst AMPK itself is regulated by CaMKK. The BRSKs are highly expressed in brain and have been implicated in neuronal polarization and the regulation of neurotransmitter release. They have also been shown to be involved in the basal phosphorylation of tau at the Alzheimer's disease (AD) related residue, serine 262, and are highly expressed in areas of the brain affected by AD, namely the hippocampus and the cortex. I have utilised the model organism *Drosophila melanogaster* to investigate interactions between transgenically expressed human tau, human BRSKs and upstream regulators

Selective over-expression of 0N4R human tau in the *Drosophila* eye resulted in a disruption of eye morphology. In contrast, over-expression of human wild type BRSK2 (B-WT) had no obvious effect on the eye. However, co-expression of both tau and B-WT resulted in a neurodegenerative phenotype more severe than tau alone. This enhancement of phenotype was not observed when BRSK2 was expressed that either lacked the activating phosphorylation site (non-phosphorylatable, B-NP) or that is unable to bind ATP (kinase dead, B-KD). Co-expression of human tau and B-WT significantly elevated tau phosphorylation at S262, suggesting that S262 is a key residue for tau-induced toxic phenotypes and the BRSK/tau interaction I observe. In support of this, no phenotype was observed in flies expressing the S262A variant of human tau with or without B-WT.

To establish the upstream kinases responsible for activating human BRSK2 in *Drosophila* I removed endogenous *Drosophila* LKB1 by RNAi. This prevented the enhanced degeneration of the eye caused by tau/B-WT co-expression, demonstrating that LKB1 is a key upstream regulator of BRSK2. I also found that down regulation of the *Drosophila* CaMKK homologue, CG17698, by the same method, ameliorated B-WT induced eye degeneration implicating a calcium-dependent pathway in the regulation of BRSK. Over-expression of human CaMKKα in the CG17698 RNAi background prevented the rescue seen with CG17698 RNAi. Over-expression of cac1, a calcium channel subunit, in the presence of B-WT and human tau exacerbated the B-WT induced eye phenotype in a B-WT dependent manner, supporting the hypothesis that the human tau and B-WT interaction can be regulated in a calcium-dependent manner.

Expression of total BRSK2, LKB1 and CaMKK were not altered in human post-mortem AD brain tissue when compared to control. However, with the exception of LKB1, due to limited reagents and time constraints I was unable to investigate the proportion of phosphorylated (and thus active) to total kinase.

This study defines a novel Ca^{2+}-dependent regulatory pathway to tau, which may contribute to AD and other tauopathies.

Abbreviations and acronyms

AChEIs – Acetylcholinesterase inhibitors

AD – Alzheimer's disease

ADP – Adenosine diphosphate

AICD – APP intracellular domain

AMP – Adenosine monophospahte

AMPK – AMP-related protein kinase

ApoE – Apolipoprotein E

APP – Amyloid precursor protein

APS – Ammonium persulphate

ATM - Ataxia telangiectasia mutated

ATP – Adenosine triphosphate

ATR - ATM and Rad3-related

Aβ – Amyloid beta

BACE – β-site APP-cleaving enzyme

BAP – Bacterial alkaline phosphatase

B-CA – BRSK constitutively active

B-KD – BRSK kinase dead

BLASTp – Basic local alignment search tool for protein sequences

B-NP – BRSK non-phosphorylatable

bp – Base pair

BRSK – Brain Selective Kinase

BSA – Bovine serum albumin

B-WT – BRSK wild type

CA – Constitutively active

CAMKII – Calcium/calmodulin dependent protein kinase II

CaMKK – Calcium/calmodulin dependent kinase kinase

CBF – Cerebral blood flow

CBV – Cerebral blood volume

cdk5 - Cyclin-dependent kinase 5

Chk – Checkpoint kinase

CHO – Chinese hamster ovary

CSF – Cerebrospinal fluid

CT – Computed tomography

CTP – Cystidine triphosphate

DC – Distortion coefficient

DNA – Deoxyribonucleic acid

DPX – Mountant for microscopy consisting of dibutyl phthalate and xylene

ECL – Enhanced chemoluminescence

EDTA – Ethylenediamine tetraacetic acid

EGTA – Ethyleneglycol tetra-acetic acid

ER – Endoplasmic reticulum

ETC – Electron transport chain

FAD – Familial Alzheimer's disease

FAT – Fast axonal transport

FDG – 18^{F}-2-fluoro-2-deoxy-Dglucose

fMRI – Functional magnetic resonance imaging

GSK-3β - Glycogen synthase kinase-3β

GTP – Guanosine triphosphate

HEK – Human embryonic kidney

HRP – Horseradish peroxidase

IP_3 – Inositol triphosphate

KD – Kinase dead

kDa – Kilo dalton

LTP – Long-term potentiation

MARK – Microtubule affinity regulating kinases

MCI – Mild cognitive impairment

MCS – Multiple cloning site

MMSE – Mini mental state examination

MO25 – Mouse protein 25

MRI – Magnetic resonance imaging

mRIPA – Modified radioimmunoprecipitation assay buffer

mRNA – Messenger RNA

NFT – Neurofibrillary tangles

NICE – National Institute for Health and Clinical Excellence

NMDAR – *N*-methyl *D*-aspartate receptor

NP – Non-phosphorylatable

NSE – Neuron specific enolase

OGT – O-linked-β-N-acetylglucosamine transferase

PAR-1 – Partitioning defective-1

PBS – Phosphate Buffered saline

PBST – Phosphate butered saline containing 0.05% Tween-20

PCR – Polymerase chain reaction

PET – Positive emission topography

PFA – Paraformaldehyde

PHF – Paired helical filaments

PKA - Cyclic AMP-dependent protein kinase

PMD – Post-mortem delay

PMSF – Phenyl methyl sulfonyl fluoride

PP-2A - Phosphoseryl/phosphothreonyl protein phosphatase-2A

PP2B – Phosphoseryl/phosphothreonyl protein phosphatase-2B

PP-2C - Phosphoseryl/phosphothreonyl protein phosphatase-2C

PS1 – Presenilin 1

PS2 – Presenilin 2

QED – Quantitative edge detection

RNA – Ribonucleic acid

RNAi – RNA interference

ROS – Reactive oxygen species

SAD – Synapses of amphids defective

SARCO – Sarco/ER calcium-ATPase

SEM – Scanning electron microscopy/micrograph

SDS – Sodium dodecyl sulphate

SDS-PAGE – Sodium dodecyl sulfate polyacrylamide gel electrophoresis

SEM – Scanning electron microscopy

STRAD - STE20-related adaptor

TE – Transentorhinal cortex

TEMED – Tetra methyl ethylene diamine

Tris – 2-amino-2-hydroxymethyl-1,3-propanediol

TTP – Thymidine triphosphate

UAS – Upstream activation sequence

v/v – Volume by volume

VDRC – Vienna *Drosophila* RNAi collection

w/v – Weight by volume

WT – Wild type

^{18}F-FDDNP – ^{18}F-(2-(1-f6-[(2-[^{18}F]fluoroethyl)(methyl)amino]-2naphthylgethylidene)malononotrile)

1| Introduction

Dementia is the collective name for disorders affecting memory, thinking, emotion and behaviour. Most people will experience some form of dementia in their life time. With Alzheimer's disease (AD) accounting for nearly 60% of dementia cases and affecting more than 20 million people worldwide (Goedert and Spillantini, 2006), many people will have first-hand experience of this debilitating disease. A small percentage of AD cases are familial (inherited) and are linked to genetic mutations, but the majority of AD cases have no known cause and as such are sporadic (Robakis, 2010a). A major report commissioned by Alzheimer's Research UK into the social and economic impact of dementia in the UK, states that dementia treatment and care costs the UK £23 billion a year (Luengo-Fernandez et al., 2010). Another report commissioned by the Alzheimer's Society forecasts that 1.7 million people in the UK will have dementia by 2051 (Knapp et al., 2007). Thus, research into the cause(s) of dementia and the development of treatments has never been more vital.

1.1 A brief history of AD

AD was first described in 1901 by Dr Alois Alzheimer, a German psychiatrist. His patient was 51 year old Auguste D. who was presented to him by her distraught husband. Dr Alzheimer was intrigued by her condition and followed her progressive mental decline until her death in 1906, when he made his findings public. On November 3 1906 he made a presentation to the Meeting of the Psychiatrists of South West Germany describing his observation of 'tangles' and 'plaques' during his post mortem examination of Auguste's brain (Hardy, 2006) and in 1907 he published his findings. The disease was given its name by Dr Alzheimer's senior colleague, Kreapelin, in 1910 after he heard Dr Alzheimer's statement:

"We must not be satisfied to force it into the existing group of well known disease patterns."

Many of the original references are in German, as referenced in Hardy (2006) but there is an English translation of Alzheimer's original 1907 paper (Alzheimer et al., 1995).

After its initial discovery, AD faded into the background until the 1960s, when Blessed, Tomlinson and Roth, a trio of researchers from Newcastle, realised upon post mortem examination of brain tissue that the 'common' dementia they had been observing in elderly patients was in fact AD (Blessed et al., 1968; Tomlinson et al., 1968; Tomlinson et al., 1970). Their observations brought AD research back to the forefront of people's minds and it is largely down to this trio's rediscovery of the disease that advancements have been made in the understanding of AD in the last 50 years.

The next piece of the puzzle was put into place in the early 1980's, when it was discovered that the cerebral cortex of AD brain suffers a loss of the neurotransmitter acetylcholine, a vital chemical component of memory (Bartus et al., 1982). This discovery was the basis for the development of the first drugs for mild to moderate AD, acetylcholinesterase inhibitors (AChEIs), which block the degradation of acetylcholine by acetylcholinesterase.

A major leap in understanding of AD pathology was made in the mid to late 1980's upon the discovery, by several groups, of two proteins whose conformation in the brain was abnormal; amyloid beta (Aβ) and the microtubule-associated protein, tau (Glenner and Wong, 1984; Masters et al., 1985; Grundke-Iqbal et al., 1986; Kosik et al., 1986; Goedert et al., 1988). The discovery of these two proteins, and their recognition as the pathological species Alois Alzheimer had previously described, later split AD researchers into two 'camps' – the baptists and the tauists. The baptists believe in the amyloid cascade hypothesis, the principles of which state that genetic and environmental factors combine to cause the formation of aberrant fibrillar Aβ plaques (extracellular deposits composed predominantly of the $A\beta_{1-42}$ and $A\beta_{1-40}$ peptides, see Figure 1.1), followed by tau tangles (composed of accumulations of hyperphosphorylated filaments of tau in a helical conformation, see Figure 1.1), the combination of which causes AD (Hardy and Allsop, 1991; Selkoe, 1991; Hardy and Higgins, 1992). The tauists believe that hyperphosphorylated tau is the toxic species in AD because the presence of hyperphosphorylated tau tangles in the brain correlates well with the severity of dementia (Tomlinson et al., 1970; Arriagada et al., 1992). In addition, in the tauopathies (a spectrum of diseases that cause dementia), tau tangles but not Aβ plaques are present in the brain (Iqbal et al., 2005).

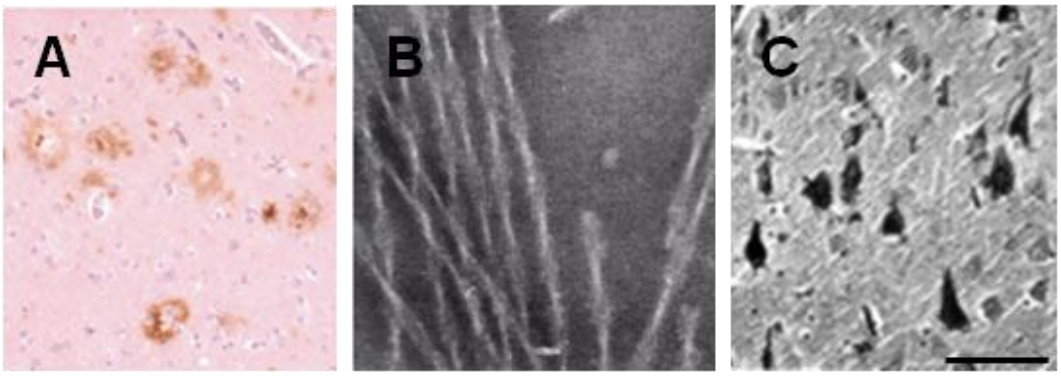

Figure 1.1: Examples of Alzheimer's disease pathology
A: Antibody stained β-amyloid plaques in the frontal isocortex. B: Electron micrograph of paired helical filaments isolated from Alzheimer brain. C: Bielschowsky stain of multiple neurons in the CA1 region of the hippocampus showing dense neurofibrillary tangle formation [1]. Scale bar 100µm applies to all panels.

[1] Images taken from:
(A) http://www.nature.com/modpathol/journal/v21/n2/fig_tab/3800994f4.html#figure-title
(B) http://www.mpasmb-hamburg.mpg.de/webpage_tau/figure9.gif
(C) http://brain.oxfordjournals.org/content/122/4/741.full

Since these initial discoveries, it has been established that AD brains undergo huge global cell loss. Brains from AD patients have approximately a 50% reduction in the size of the medial temporal lobe (Smith and Jobst, 1996) and also exhibit pan-cerebellar atrophy (Apostolova and Thompson, 2008). The medial temporal lobe is an area of the brain comprised of the hippocampus, subiculum, parahippocampal gyrus and amygdala – areas of the brain that are heavily affected by tau tangles (Arnold et al., 1991; Smith and Jobst, 1996). Indeed, medial temporal lobe atrophy correlates with both the density of tau tangles in the pyramidal cell layer of the hippocampus and with the degree of memory impairment (Nagy et al., 1996). In addition, cell loss from the hippocampus is usually very prominent (Smith and Jobst, 1996). Patients that undergo yearly temporal lobe-orientated x-ray computed tomography (CT), and more recently volumetric magnetic resonance imaging (MRI), scans during life have been demonstrated to have a rate of medial temporal lobe atrophy of up to 15% - more than 10 times higher than the approximately 1-1.5% yearly atrophy rate of age-matched control subjects (Jobst et al., 1992; Jobst et al., 1994; Apostolova and Thompson, 2008).

It has also been established that in the early stages of the disease, before any evidence of cell loss, Aβ accumulation or tau tangles, AD causes dramatic synaptic loss (Mucke et al., 2000; Selkoe, 2002; Brickman et al., 2009). Indeed, synaptic deterioration in AD brain correlates strongly with the severity of symptoms (Selkoe, 2002). Studies of post-mortem human AD brain tissue have established that the synaptic failure in AD is mainly due to changes in synaptic structural plasticity such as reductions in the number and/or density of structures such as presynaptic boutons and dendritic spines (Masliah et al., 1994; Mucke et al., 2000). Synaptic loss can be

detected in post mortem brain tissue simply by staining for synaptic markers such as synaptophysin and counting the number of synapses (Brickman et al., 2009). However, more recently, advances in brain imaging techniques have allowed the development of more sophisticated methods for determining synaptic loss in the brain. Functional MRI (fMRI), which relies on the fact that any synaptic changes will affect the rate of oxygen consumption in the brain, has been used to investigate synaptic loss (Brickman et al., 2009). Although fMRI can't directly measure oxygen consumption, it can measure correlates of oxygen consumption such as cerebral blood flow (CBF) and cerebral blood volume (CBV) (Small, 2003).

1.2 The clinical symptoms of AD

The clinical signs of AD are characterized by progressive cognitive deterioration beginning with mild memory loss, behavioural changes and a decrease in day to day activities. Often the first sign of AD is forgetting simple things such as where one lives or where the milk is kept. However, these symptoms can be put down to a number of different causes, such as stress and general old age. This progressive impairment may continue for many months affecting first declarative memory (memory which stores facts (semantic) and experiences (episodic)) and then non-declarative memory (Walsh and Selkoe, 2004). Over a period of many years, a more serious form of dementia develops which usually presents with a variety of symptoms affecting multiple cognitive and behavioural aspects such as language, learning, reasoning, attention, problem solving, emotion and memory. As there is no cure, death is inevitable and will usually be caused by a minor complication which

would not normally cause death in a healthy individual, such as pneumonia (Walsh and Selkoe, 2004).

1.2.1 The relationship between the clinical symptoms and the pathology of AD

There appears to be a close relationship between most of the identified pathological changes in AD brains and the severity of symptoms in life - with one notable exception: extracellular amyloid plaques. Extracellular accumulations of Aβ were one of the two original pathological hallmarks of AD identified by Alois Alzheimer (Alzheimer et al., 1995). However, it has now been established that the load and location of Aβ plaques in AD brain does not correlate with the severity of symptoms in life (Robakis, 2010a).

In contrast, the load and location of tau tangles, level of cell death and synaptic degeneration are known to correlate very well with the severity of dementia suffered in life (Grober et al., 1999). The correlation between tau tangle pathology and dementia gave rise to the original Braak scoring for post-mortem AD brain tissue (discussed further in section 1.3) (Braak and Braak, 1991; Braak and Braak, 1997).
The first area of the brain to be affected by tau pathology and cell death is the transentorhinal cortex (TE) which is a relay station between the cortex and hippocampus which filters sensory input (Braak and Braak, 1991; Braak and Braak, 1997; Taylor and Probst, 2008). As the disease progresses the pathology becomes more extensive and begins to affect the hippocampus and nearby amygdala (Braak and Braak, 1991; Braak and Braak, 1997). The hippocampi are located one on each side of the brain, in the temporal lobes and have been demonstrated to be critical in

the formation of new memories (Thompson, 1985). One of the most important studies showing the involvement of the hippocampi in memory formation was patient H.M. Patient H.M had both hippocampi and parts of the temporal lobes removed in order to treat severe epilepsy (Thompson, 1985; Bear et al., 2007). Although the surgery was successful in treating his epileptic seizures, patient H.M was left with a complete inability to create new memories – although his very immediate short term memory was unaffected. In addition, his memories from before the surgery were left intact, indicating that the hippocampi are not where memories are stored but are essential to the encoding of them (Thompson, 1985; Bear et al., 2007). The amygdala are also located deep within the temporal lobes and are thought to be important for the regulation of emotion, and in particular fear (Bear et al., 2007). Pathology in the amygdala is likely to give rise to some of the behavioural symptoms observed in AD such as distress, apathy, aggression and fear.

Whilst tangles, cell death and synaptic degeneration in the TE and hippocampus account for the memory deficits seen in AD patients, it is likely that pathology seen in the neocortex is responsible for symptoms affecting functions such as language, reasoning and attention (Nelson et al., 2009). The neocortex comprises the outer layer of the brain and is responsible for many higher-order processes such as vision, sensation, voluntary movement, imagination, consciousness and hearing (Bear et al., 2007). In short, the neocortex is what makes humans what they are. The progressive development of AD pathology and cell/synapse degeneration in the neocortex is undoubtedly responsible for such symptoms as dissorientation, lack of awareness and a general inability to perform daily tasks (Thompson, 1985). However, not all areas

of the neocortex are affected: hearing, vision and voluntary movement appear to be well preserved in AD patients.

1.3 Diagnosing AD

The diagnosis of Alzheimer's disease is notoriously difficult as subjects may present with varying symptoms easily mistaken for other disorders. There are several tests conducted in the clinic which are designed to assess the cognitive function of patients, the most well known being the mini mental state examination (MMSE). The MMSE consists of a brief 30 point questionnaire conducted over 10 minutes which is designed to test for cognitive impairment by asking the patient questions which probe his/her orientation to time/place, recall skills (short term memory), attention/registration, calculation and language amongst other aspects (Harvan and Cotter, 2006). A score below 24 is indicative of mild cognitive impairment (MCI), a score of 10-20 points is considered as moderate impairment and a score of <9 points is classed as severe impairment (see Table 1.1).

In addition to cognitive tests, patients with suspected AD may undergo brain scans to aid in the diagnosis. As previously discussed, fMRI can be utilised to assess the degree of synaptic deterioration due to the relationship between CBV/CBF with the oxygen demands of the brain (Small, 2003; Brickman et al., 2009). Additionally, positive emission topography (PET) scanning in combination with injection of the tracer 18^{F}-2-fluoro-2-deoxy-Dglucose (FDG) allows the measurement of regional cerebral glucose metabolism (Herholz et al., 2007). Glucose is the main energy supply in the brain and its metabolism is closely coupled to neuronal function both at

rest and during activation (Sokoloff, 1977). Characteristic reductions in regional cerebral glucose metabolism have been identified in several areas of AD brains such as the posterior cingulate and precuneus (Herholz et al., 2007). MRI and CT scans can be used to monitor the rate of atrophy in the brain. Brain atrophy has been demonstrated to be vastly increased in AD brain when compared to age-matched controls (Jobst et al., 1992; Jobst et al., 1994; Apostolova and Thompson, 2008). Positive emission topography (PET) scanning in combination with tracers such as ^{18}F-(2-(1-f6-[(2-[^{18}F]fluoroethyl)(methyl)amino]-2-naphthylgethylidene) malononitrile) (^{18}F-FDDNP), a molecule that binds to plaques and tangles, or Pittsburgh compound B, a compound that binds to Aβ aggregates, may also be used in order to visualise AD pathology in live brain (Small et al., 2006; Tolboom et al., 2009). Pittsburgh compound B has been shown to have high sensitivity when used to detect amyloid plaques *in vivo*, but there appears to be no increase in tracer signal during the progression of the disease, a disadvantage when trying to differentiate between subjects with MCI and AD (Engler et al., 2006; Herholz et al., 2007). However, despite having a weaker imaging signal than Pittsburgh compound B, use of ^{18}F-FDDNP confers the ability to differentiate between control, MCI and AD groups (Small et al., 2006).

Despite cognitive tests which can be carried out in life such as the MMSE, and the development of sophisticated brain scanning, a diagnosis of AD cannot be confirmed until the patient has died and a post-mortem is conducted. Upon post-mortem examination, the brains of patients with suspected AD undergo an examination for the two classical hallmarks of AD pathology (Aβ and tau tangles) and, historically, were scored according to Braak stages. Braak stage is a measure based on how many

tau tangles are present in the brain and their locations (Figure 1.2) (Braak and Braak, 1991; Braak and Braak, 1997). The location and load of tau tangles is known to correlate well with the MMSE score given in life (Table 1.1) (Grober et al., 1999). In order for a post-mortem diagnosis of AD to be made, there must be both tau tangles and Aβ plaques in the brain, and so some brain banks have begun to stage brains according to a new Brain Net Europe Consortium Scheme method which also takes into account the presence of amyloid plaque pathology (Alafuzoff et al., 2008).

More recently, a move has been made to attempt to identify biomarkers that could aid in the diagnosis of AD: since Aβ and tau are the two main pathological features of AD, much research has focussed upon these two proteins. A number of groups have shown a strong inverse relationship between cerebrospinal fluid (CSF) $A\beta_{1-42}$ concentrations and cortical Aβ deposition (Fagan et al., 2006; Grimmer et al., 2009). Additionally, a number of studies have demonstrated that CSF total tau and phosphorylated tau levels are elevated in AD, presumably as a result of cell death and subsequent lysis (Sunderland et al., 2003; Buerger et al., 2009; Mattsson et al., 2009). Although CSF total tau has been shown to increase following acute stroke and head trauma (Blennow and Nellgard, 2004; Ost et al., 2006; Yao et al., 2008), CSF phosphorylated tau appears to be a more specific marker for AD and has been shown to correlate with NFT load in post-mortem studies (Itoh et al., 2001; Buerger et al., 2006). However, both tau and Aβ species are found in the CSF of control populations and as such further characterisation of these proteins as potential biomarkers will be required in order to ensure sufficient sensitivity and specificity before they can be routinely utilised in the clinic (Fagan and Holtzman, 2010; Robakis, 2010b).

Diagnosis	Braak Stage	MMSE	Symptoms
Mild Cognitive Impairment (MCI)	2-3	26-30	Mild memory loss/impairment Normal cognitive abilities MCI is frequently a precursor to AD but does not lead to AD in all cases
Mild AD	3-4	20-26	Mild memory loss/impairment Slight decrease in cognitive function Mild behavioural changes
Moderate AD	4-5	11-19	Progressive memory loss Increasingly disorganised and confused thinking Increasing behavioural symptoms Need for assistance in everyday activities
Severe AD	5-6	0-10	Severe memory loss and dementia Agitation, aggression, paranoia and delusions Loss of motor skills Patients often require hospitalisation or long-term care

Table 1.1: Correlation of Braak stage and MMSE scores.
Braak stage and MMSE scores show an inverse correlation; a low MMSE score, based on decreasing cognitive ability, indicates severe dementia whereas a low Braak stage, based on the load and location of tau tangles, indicates mild cognitive impairment. Table taken from http://www.tau-rx.com/quiz/tangles.html

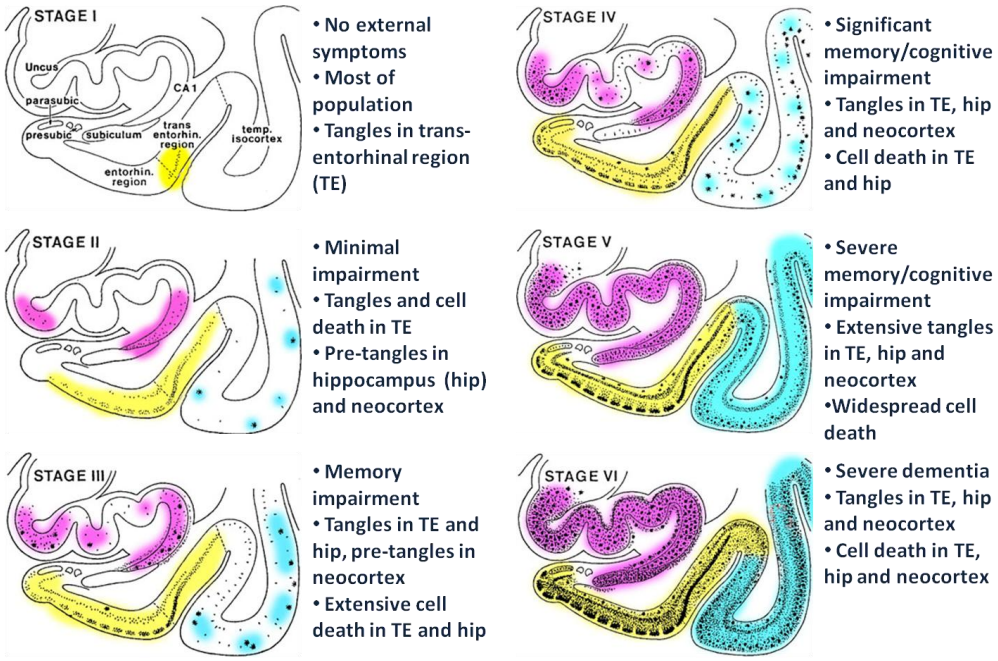

Figure 1.2: Braak staging of human brain

Braak staging is based upon the number and location of tau tangles in the brain. In Stage I there are minimal tangles present in the trans-entorhinal cortex (yellow). Most of the aged population will achieve this stage. As the Braak Stages increase the load of tau tangles in the trans-entorhinal cortex increases and tangles appear in the hippocampus (pink) and neocortex (blue). From Braak Stage III, extensive cell death is visible in the brain, first in the trans-entorhinal cortex, then in the hippocampus and neocortex. Tau tangles and cell death are accompanied with progressively significant memory problems culminating in severe dementia. Images taken from http://www.tau-rx.com/quiz/tangles.html

1.4 Treatment of AD

In the UK, there are currently four drugs licensed for the treatment of AD. Three of them, Aricept, Exelon and Reminyl are all acetylcholineesterase inhibitors (AChEIs) designed to prevent the degradation of acetylcholine by inhibiting the action of acetylcholinesterase. However, although the three drugs are effective in slowing cognitive decline, their efficacy is only seen in some patients, and ultimately their effects are limited to preserving simple daily activities and reducing the burden placed on caregivers (Rosler et al., 1999; Raskind et al., 2000; Rogers et al., 2000; Jacobsen, 2002). Current National Institute for Health and Clinical Excellence (NICE) guidelines on anti-Alzheimer's drugs recommend that people with moderate AD should be prescribed Aricept, Reminyl or Exelon. The fourth drug licensed in the UK for the treatment of AD is Ebixa (Memantine). Ebixa is an uncompetitive *N*-methyl *D*-aspartate receptor (NMDAR) antagonist which slows the rate of cognitive decline in patients with moderate to severe AD (Reisberg et al., 2003). In addition, when administered to patients with moderate to severe dementia already receiving Aricept, Ebixa was associated with significantly better outcomes than placebo (Tariot et al., 2004). However, treatment with Ebixa is not currently recommended as part of NHS care. Instead, the guidelines emphasize the importance of further clinical studies with Ebixa. Thus, there are currently no licensed drugs approved for the treatment of mild or severe AD.

Due to the limited efficacy of currently licensed pharmaceuticals, there is considerable interest in developing new compounds for the treatment of AD. However, it is proving difficult to develop new agents that successfully pass through all the phases of clinical trials. Compounds that have recently failed in phase III

clinical trials include Ginkgo Biloba (a widely used herbal treatment), Phenserine (a cholinesterase inhibitor reported to inhibit Aβ formation) and Tarenflurbil (a 'selective $A\beta_{42}$ lowering agent') (Sabbagh, 2009). Only limited success has been seen with the first trials of Aβ vaccines, but there are currently at least 9 'second generation' Aβ vaccines in various clinical trial phases (Hock et al., 2003; Orgogozo et al., 2003; Bayer et al., 2005; Gilman et al., 2005; Lee et al., 2005; Lemere and Masliah, 2010). Also in development are pharmaceutical compounds which target the formation of tau tangles (Bulic et al., 2009). The most promising candidates at present are Rember and LMT-X which are being developed and tested by a small company called TauRX[2]. Rember, based on methylthioninium chloride (better known as methylene blue), can block the formation of tau tangles and has been shown to be effective at dissolving tangles into tau monomers which can then be degraded by the cell. Phase III clinical trials for this compound are currently being prepared. LMT-X is a second generation derivative of Rember. It has shown a strong effect on tau pathology in transgenic models and in pre-clinical and early clinical trials. LMT-X is currently in phase III clinical trials.

1.5 Theories for the cause of Alzheimer's disease

There are many theories as to the causative agent in AD. Although much information has been gleaned from various animal models of AD, it is obvious from the literature that the scientific community is far from agreeing on a mechanism for the cause. There are many different types of transgenic models including worms,

[2] http://www.taurx.com/tau.htm#clinicalres

fruit flies and mice, expressing many different combinations of genes, both endogenous and exogenous. In the following section some of the most prevalent theories, such as the amyloid cascade hypothesis, will be summarised and because the experiments presented in this study were based upon the tau hyperphosphorylation theory, this hypothesis will be discussed in more detail.

1.5.1 The amyloid cascade hypothesis

As previously mentioned, the amyloid cascade hypothesis states that Aβ is the causative pathological agent in AD and that aberrant processing of the amyloid precursor protein (APP) leading to the production of Aβ, precedes formation of tau tangles. It is thought that altered APP processing is influenced by genetic and environmental factors and that the combination of Aβ and subsequently tau pathology leads to AD (Hardy and Allsop, 1991; Selkoe, 1991; Hardy and Higgins, 1992).

Various Aβ species (oligomers, diffusible ligands and fibrillar) have been shown to be toxic when applied to neurons (Deshpande et al., 2006). However, despite a strong amount of evidence supporting the amyloid cascade hypothesis, the quantity and formation of Aβ plaques do not correlate with the neurodegenerative decline observed in patients and it is still not clear whether Aβ plaques are the causative agent of the disease (Robakis, 2010a). Furthermore, it is possible to detect Aβ plaque loads similar to those seen in AD in control individuals. This strongly

suggests that fibrillar Aβ plaques do not cause neurodegeneration (Crystal et al., 1988; Davis et al., 1999).

1.5.1.1 APP processing

Full length APP (APP_{FL}) is a type I membrane protein consisting of a large ectodomain and a short cytoplasmic tail, the gene for which is on chromosome 21 (Evin et al., 2003; Thinakaran and Koo, 2008). The ectodomain can be shed from the membrane by way of two proteolytic pathways (Figure 1.3, adapted from Evin *et al.* (2003)). The default pathway, termed the non-amyloidogenic pathway, involves the cleavage of APP within the Aβ sequence by α-secretases to produce sAPPα and an 83 amino acid membrane associated C-terminal fragment (αCTF or C-83) (Wilson et al., 2003). C-83 can be further cleaved by either the γ-secretase/presenilin (PS) complex giving rise to a C-terminal fragment of the Aβ sequence, p3, and an APP intracellular domain (AICD), or by β-secretases giving rise to two N-terminally truncated variants of Aβ; $Aβ_{11-40}$ and $Aβ_{11-42}$ (Naslund et al., 1994). Roles for AICD in transcriptional activation, the modulation of inositol triphosphate (IP_3)-mediated calcium signalling and the suppression of neurogenesis have been proposed (Cao and Sudhof, 2001; Leissring et al., 2002; Ma et al., 2008).

During the course of the amyloidogenic pathway, β-secretases cleave APP_{FL} to release sAPPβ and a 99 amino acid membrane associated C-terminal fragment (βCTF or C-99) that contains the intact Aβ sequence (Evin et al., 2003). Further cleavage of C-99 by the γ-secretase/PS complex, at a number of residues, allows the release of $Aβ_{1-40}$ (the most common Aβ species), the less abundant but more

aggregating $A\beta_{1-42}$ (which is the primary species found in Aβ plaques in AD brain) and AICD (Selkoe, 1999; Evin et al., 2003).

Studies have identified α-secretases as zinc metalloproteinases and a number of proteins have been implicated as α-secretases, including members of the adamalysin family (Allinson et al., 2003). β-secretase has been identified as an aspartyl protease, BACE (β-site APP-cleaving enzyme) of which there are two isoforms, BACE1 and BACE2 (Thinakaran and Koo, 2008). The γ-secretase/PS complex has been identified to consist of four subunits: PS1 or PS2, nicastrin, PEN-2 and APH-1 (Iwatsubo, 2004).

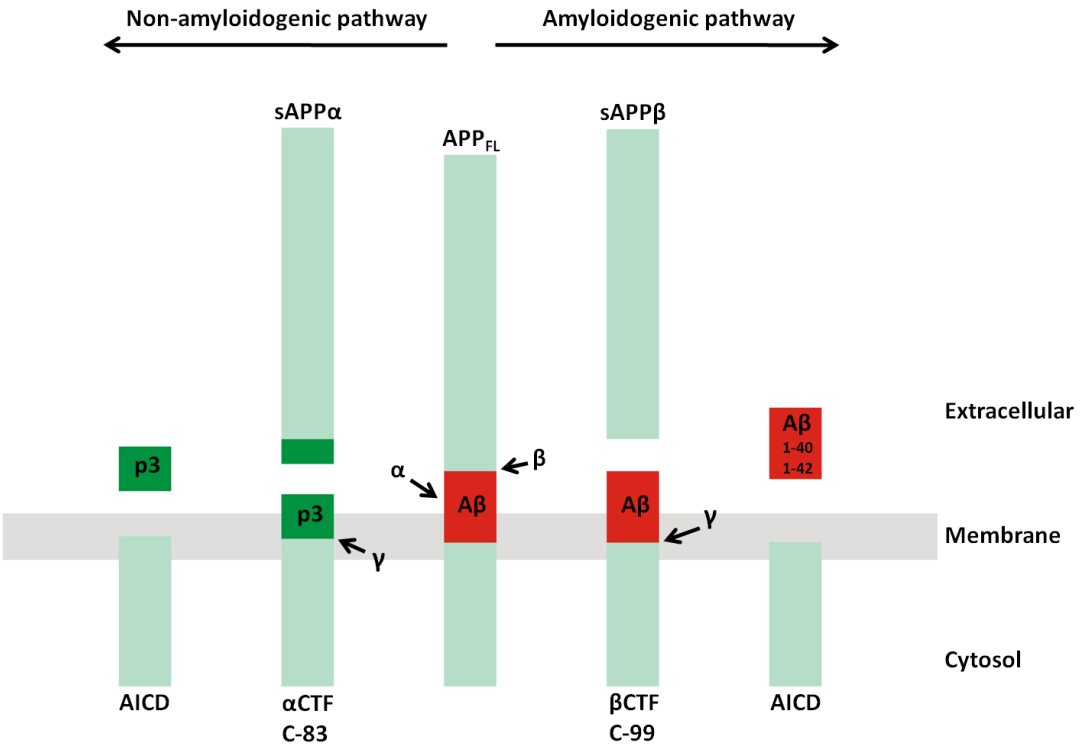

Figure 1.3: Schematic of the proteolytic processing of amyloid precursor protein (APP)

Full length APP (APP$_{FL}$) can be processed by two pathways; the non-amyloidogenic and the amyloidogenic pathways. The default is the non-amyloidogenic pathway whereby α-secretase cleaves within the Aβ domain to release sAPPα and an 83 amino acid membrane associated fragment (αCTF or C-83). Further cleavage of C-83 by γ-secretase releases the C-terminal fragment of Aβ, p3, and a fragment termed the APP intracellular domain (AICD). In the amyloidogenic pathway, β-secretase cleaves APP$_{FL}$ to release sAPPβ and a 99 amino acid membrane associated fragment (βCTF or C-99). γ-secretase can cleave C-99 at a number of sites, giving rise to Aβ$_{1-40}$ or Aβ$_{1-42}$ species and allowing the release of AICD. Figure adapted from Evin et al. (2003).

1.5.1.2 Mutations in APP and the presenilins

The amyloid cascade hypothesis was originally formulated on the basis that mutations in the APP gene (such as the London V717I mutation and the Swedish K670N and M671L mutations) or in the PS genes, affect the metabolism or production of $A\beta_{1-42}$ and are a rare cause of early-onset familial AD (FAD) (Hashimoto et al., 2000; Eckert et al., 2010). To date, only 10% of the known FAD-related mutations affect APP itself, with the majority (~140) affecting the presenilins, mainly PS1 (Randall et al., 2010). Despite the large variety of mutations found in APP and the presenilins, the vast majority result in an increased $A\beta_{1-42}$:$A\beta_{1-40}$ ratio which is suggestive of a toxic gain of function of $A\beta_{1-42}$ (Kumar-Singh et al., 2006). However, mutations in presenilins have also been associated with familial frontotemporal dementia, a disease where degeneration occurs in the absence of any Aβ pathology (Zekanowski et al., 2006). This would suggest that increased Aβ production and deposition are not the only consequences of presenilin mutations, and that the situation may be more complicated than it was first thought.

1.5.1.3 Soluble Aβ

More recently, it has been suggested that soluble Aβ species (as opposed to fibrillar Aβ which is found in extracellular Aβ plaques) may be important in the pathogenesis of AD. APP is a protein that localises to the plasma membrane, but it can also localise to the Golgi network, ER and lysosomal, endosomal and mitochondrial membranes (Mizuguchi et al., 1992; Xu et al., 1995; Kinoshita et al., 2003). Thus, should amyloidogenic APP cleavage occur at any of these locations, the liberated Aβ

would accumulate intracellularly. However, although soluble Aβ species have been shown to accumulate intracellularly, they are also detected in the CSF of most people and there is little evidence that the intracellular concentration of these species correlates with cognitive decline (Robakis, 2010b). Although this is a serious flaw in the theory that soluble Aβ species are the causative agents in AD, the effects of application of soluble Aβ to neuronal cells (see section 1.5.4), on mitochondria (see section 1.5.3) and at synapses (see section 1.5.1.4) make soluble Aβ species the subject of much interest and research.

1.5.1.4 APP, long-term potentiation and NMDA receptors

Long-term potentiation (LTP) has long been considered a neural correlate for memory. It results from the simultaneous activation of pre- and post-synaptic elements of the synapse leading to an increase in chemical transmission that can persist for long periods of time, typically hours *in vitro* and weeks or months *in vivo* (Cooke and Bliss, 2006). The increase in chemical transmission leads to the strengthening of synapses and it is this increase in strength that is thought to underlie memory formation. In the majority of glutamatergic synapses in the brain, LTP is mediated by the NMDAR.

A number of transgenic mouse models of AD have been constructed expressing wild type APP or APP with FAD-associated mutations either alone or in combination with other components of the APP processing pathway – most often mutated PS1 (Randall et al., 2010). APP transgenic models show an age-dependent increase in Aβ plaques and multiple behavioural and neurophysiological changes but do not replicate the tau

pathology, neurodegeneration or cell death exhibited in AD (Gotz and Ittner, 2008). In electrophysiological studies on brain slices from many of these models, a deficit in basal synaptic transmission and/or LTP has been observed (Randall et al., 2010). However, this observation is not made consistently in all APP transgenic models or even in the same model by different laboratories (Chapman et al., 1999; Fitzjohn et al., 2001; Jolas et al., 2002; Jacobsen et al., 2006; Townsend et al., 2010). These discrepancies are likely to depend on the combination of transgenes expressed in the various models. Also, different methods for the preparation of brain slices from transgenic animals, different brain slice incubation conditions and varying induction protocols for LTP would be expected to contribute to the variable results and as such it is difficult to compare results across laboratories and models (Randall et al., 2010). Nevertheless, it has been shown robustly that over expression of APP can cause a deficit in LTP in transgenic animal models. Whilst Aβ plaques are known to form extracellularly, and as such are unlikely to affect LTP *per-se*, intracellular soluble Aβ and/or other breakdown products of APP may contribute to the memory deficits seen in AD. Indeed, a number of transgenic APP mouse models exhibit memory deficits as tested by the Morris water maze and a number of other experimental paradigms (Bryan et al., 2008).

Recently a role has been proposed for APP in the trafficking of NMDAR from the endoplasmic reticulum to the cell membrane (Cousins et al., 2009). However, it is not clear if the interaction between APP and NMDAR is direct, or mediated through a third protein. It remains to be seen if APP is involved in the internalisation and/or recycling of NMDAR, but it could be hypothesised that if APP is cleaved at the membrane into $A\beta_{1-42}$, this may have knock-on effects on the proper insertion,

internalisation and recycling of NMDAR leading to NMDAR-related excitotoxicity and possibly cell death.

1.5.2 The hyperphosphorylated tau theory

Tau was first described in a paper published in 1975 (Weingarten et al., 1975). It was purified from porcine brain and was found to be present in combination with tubulin. Weingarten *et al* (1975) described tau as an extremely heat stable protein required for the polymerization of 6S tubulin (*in vitro*).

1.5.2.1 The expression and structure of tau

Tau proteins are produced by alternative mRNA splicing of a single gene on chromosome 17 (Mi and Johnson, 2006). Tau is mainly found within the brain where there are six isoforms ranging from 352 to 441 amino acids in length. The isoforms differ by the presence of three (3R) or four (4R) 31-35 amino acid C-terminal repeats encoding microtubule binding domains combined with zero, one or two N-terminal inserts caused by alternative splicing of exons 2 and 3 (Figure 1.4) (Mi and Johnson, 2006). Due to the splicing in of exon ten, 4R tau has an extra microtubule binding domain and as such is known to bind to microtubules more effectively than 3R-tau, thereby stabilising them more effectively (Buee et al., 2000). This is an important feature of tau as the differential stabilising abilities of the various isoforms are likely to contribute heavily to the level of plasticity in the brain. Indeed, expression of tau isoforms is developmentally regulated and in foetal brain

only the shortest 3R isoform of tau is present. However by adulthood, all six isoforms are present and the ratio of 3R to 4R tau is largely 1:1 (Buee et al., 2000; Takuma et al., 2003). During early development the requirement for plasticity is naturally very high as the various brain regions and the connections between them form. As such, exclusive expression of the weaker binding 3R tau is an advantage (Takuma et al., 2003). In the adult brain one of two scenarios could exist: either expression of 4R tau reduces the ability of the brain to be plastic or, the reduced requirement for plasticity in a developed adult brain induces the expression of 4R tau isoforms. Due to a high percentage of hydrophilic residues, tau normally exists as an unfolded protein (Jeganathan et al., 2008a). However when it aggregates into filaments and NFT it often adopts higher structures, in particular β-structure (Jeganathan et al., 2008a).

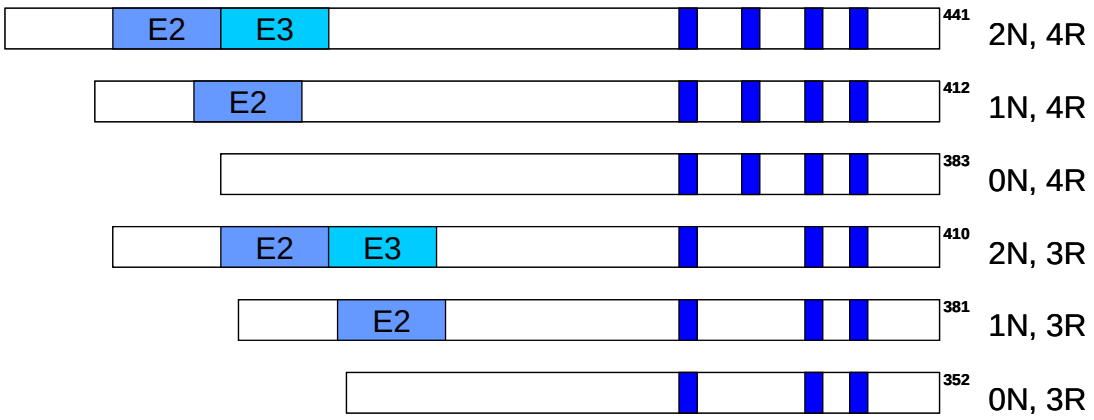

Figure 1.4 Exon organization of the six brain tau isoforms.
Alternative splicing of exons 2, 3 and 10 is responsible for the formation of the six different brain isoforms. Exons 2 and 3 are responsible for the N-terminal inserts termed 0N (exon 2 and 3 absent), 1N (exon 2 present) or 3N (exons 2 and 3 present). Exons 9, 10, 11 and 12 are responsible for the microtubule binding domains. Splicing in of exon 10 in 4R tau causes an extra microtubule binding domain. Exons 4a, 6 and 8 are present in peripheral nervous system (PNS) tau isoforms.

1.5.2.2 The physiological function(s) of tau

Within neurons, tau is mainly localised to the axon where its primary function is to bind to and stabilise microtubules - the crucial tracks used for the intracellular transport of proteins, vesicles and organelles (Mandelkow et al., 2003). This is a physiological process thought to be regulated at least in part by specific phosphorylation of tau. In contrast, *hyper*phosphorylation of tau is thought to contribute to the pathological aggregation of tau into filaments and subsequently NFT, presumably through phosphorylation events distinct to those involved in the physiological function of tau (Burbank and Mitchison, 2006; Hanger et al., 2009). Tau has also been found localised to the ER, Golgi and plasma membranes and a role in src-family tyrosine kinase signalling has been proposed (Brandt et al., 1995; Farah et al., 2005; Farah et al., 2006; Pooler and Hanger, 2010). Indeed, tau can be phosphorylated by members of the src-family of tyrosine kinases such as fyn (Lee et al., 2004). In addition, it has been shown that tau can bind to the SH3 domain of fyn (Lee et al., 1998). The binding of tau to the SH3 domain of fyn is likely to be mediated by tau's phosphorylation status; it has been demonstrated that phosphorylation of tau at threonine 231 decreases this binding (Zamora-Leon et al., 2001; Reynolds et al., 2008).

In addition to its role in microtubule stabilisation, tau is involved in neurite outgrowth and axonal transport. Early studies demonstrated that suppression of tau expression in cerebellar neurons significantly decreased neurite outgrowth (Caceres and Kosik, 1990; Caceres et al., 1991) and it has been demonstrated that over-expression of tau induced outgrowth (Yoshizaki et al., 2004). However, tau

knockout ($tau^{-/-}$) mice are viable and have no major neural phenotypes, suggesting that either tau is not an essential gene or that there is considerable redundancy between tau and the other microtubule-associated proteins, such as MAP1 (Harada et al., 1994; Dawson et al., 2001). The latter situation was confirmed with $tau^{-/-}$ $MAP1B^{-/-}$ double knockout mice in which the neural phenotypes of the double knockouts were exacerbated when compared to $MAP1B^{-/-}$ mice (Takei et al., 2000).

Tau has been shown to inhibit kinesin-dependent fast axonal transport via interference with the ability of the kinesin motors to attach to microtubules (Ebneth et al., 1998; Stamer et al., 2002). In double transgenic mice over-expressing tau and the kinase GSK-3β, there was less impairment of axonal transport (Spittaels et al., 2000). This was related to a decreased affinity of tau for microtubules as a result of increased tau phosphorylation by GSK-3β (Mi and Johnson, 2006). Thus, the involvement of tau in kinesin-dependent fast axonal transport is likely to be mediated by phosphorylation.

1.5.2.3 Pathological aspects of tau

1.5.2.3.1 Mutations in the tau gene and the involvement of tau in tauopathies.

Although tau present in AD brain is generally not mutated, many mutations of the tau gene have been reported and they generally fall into one of two categories: the first category, including missense and deletion mutations in the coding region of tau, produce tau with an altered function. These mutations influence tau's tendency to aggregate into filaments and also its ability to bind to microtubules (Hasegawa et al.,

1998). The second category of mutations mainly affects the splicing of exon ten (Grover et al., 1999). The inclusion of exon ten gives 4R tau its extra microtubule binding domain, and is often associated with an increased ratio of 4R:3R tau. Mutated tau is strongly associated with FTDP-17, a familial form of dementia in which there are tau tangles (comprised of hyperphosphorylated tau) but no amyloid plaques present in the brain. In FTDP-17 brain, tau depositions the same as those seen in AD are observed, however tangles can be detected at younger age and this is associated with the onset of cognitive symptoms.

In progressive supranuclear palsy, tau inclusions consist of 4R isoforms only (Sergeant et al., 1999). However, in AD, inclusions have 3R and 4R tau isoforms, while in Pick's disease only 3R isoforms are found in the aggregates (Sergeant et al., 1997; Buee et al., 2000). This would suggest that neither form of tau is more toxic than the other but that toxicity may arise from altered ratios of 4R:3R tau. Taking into account that tau isoform expression is developmentally regulated, it is probable that isoforms have different functions within the cell. Indeed different tau isoforms have differential effects on microtubule transport (Vershinin et al., 2007). Our understanding of the effect of altering 4R:3R ratios will increase as more information becomes available on the different functions of different isoforms.

Apart from the differences in the composition of tau inclusions described above, to date there is no evidence that tau inclusions found in AD and in the tauopathies are different i.e. they all consist of accumulations (hence tangles) of hyperphosphorylated tau filaments which have a helical structure. Although AD and the tauopathies are clinically and pathologically different diseases, the strong

association between tau tangle load and cognitive symptoms, and the development of a similar dementia to AD in the tauopathies (in the absence of Aβ plaques), forms the basis of the 'tauists' belief that tau tangles in themselves must be pathogenic.

1.5.2.3.2 Phosphorylation.

It was not until 1984 that it was shown that phosphorylation can regulate tau's binding to microtubules (Lindwall and Cole, 1984). It was found that phosphorylated tau promotes significantly less polymerization of microtubules than dephosphorylated tau. In AD and tauopathies, mutant forms of tau become hyperphosphorylated, often within their microtubule binding domains, and subsequently have a reduced ability to bind to microtubules (Iqbal et al., 2005; Marx, 2007).

'Normal' tau has 2-3 mol of phosphate attached per mol of the protein (Iqbal et al., 2005). However, AD tau contains 9-10 mol of phosphate per mol of protein (Ksiezak-Reding et al., 1992; Kopke et al., 1993). It remains unclear if hyperphosphorylation of tau is due to a decrease in the activity of one or more tau phosphatases, an increase in one or more tau kinases, or simply by tau becoming a better substrate (e.g. through a change in conformation of tau or via mis-localisation of tau or a tau kinase/phosphatase). Indeed, it could be a combination of all three. What is clear is that tau found in the aggregated filaments which form the basis of NFTs in the somatodendritic compartment of the cell is phosphorylated on many residues that are not phosphorylated in healthy neurons and at a much higher stochiometry (Hanger et al., 2009). These filaments may be straight or helical in

structure and typically come in pairs (Mandelkow et al., 2007). There are a number of ways in which the presence of NFTs in neurons may cause cell loss. NFTs are a physical barrier in the cell which have been reported to compromise cellular functions including distribution and number of organelles and proteasome activity (Gendron and Petrucelli, 2009). In addition, the sequestration of tau into NFTs causes destruction of the microtubule network and consequently affects axonal transport and synaptic integrity.

Tau is phosphorylated by many kinases (these include GSK-3β, PAR-1/MARK, cdk5 and PKA to name but a few). To date, 40 residues on tau have been reported to be phosphorylated either *in vivo* or *in vitro* (Hanger et al., 2009). Phosphorylation within the microtubule binding domains of tau is reported to have a large effect on the ability of tau to bind to microtubules (Biernat and Mandelkow, 1999). In particular, phosphorylation at serines 262 and 356 has a dramatic effect on binding (numbering based on the longest human tau isoform) (Biernat and Mandelkow, 1999; Biernat et al., 2002; Hanger et al., 2009). However, it has also been shown that phosphorylation in the regions flanking the repeat domains can affect microtubule binding (Cho and Johnson, 2003). It is also postulated that phosphorylation at some residues may cause conformational changes in tau, making the protein either inaccessible to phosphatases or simply a better substrate for additional kinases, or affecting tau's biological function (Jeganathan et al., 2008b; Fischer et al., 2009).

Tau kinases can be broadly divided into two subgroups; the proline-directed kinases (which phosphorylate tau at serine/threonine-proline motifs) and the non proline-directed kinases (which phosphorylate tau within KXGS motifs found in the

microtubule-binding domains; S262, S293, S324 and S356). Two of the most heavily characterised proline-directed kinases are GSK-3β and cyclin-dependent kinase 5 (cdk5). These kinases phosphorylate tau at a large number of common residues. Although increases in the brain expression and/or activation of GSK-3β have not been consistently observed in AD, increased GSK-3β expression (as detected by indirect ELISA) is associated with all stages of neurofibrillary pathology in AD brains (Pei et al., 1997). Additionally, over-expression of GSK-3β in cells causes a dramatic change in tau phosphorylation at a number of residues such as pS202/T205 (Lovestone et al., 1996; Wagner et al., 1996). Treatment of cells with the selective GSK-3β inhibitor lithium decreases tau phosphorylation at the aforementioned sites (Lovestone et al., 1996). These findings implicate tau as an *in vivo* substrate for GSK-3β and suggest that abnormal phosphorylation of tau by GSK-3β may be involved in the pathogenesis of AD. It has been suggested that prior phosphorylation of tau by cdk5 may enhance its subsequent phosphorylation by GSK-3β (Ishiguro et al., 1993). This is suggestive of cdk5 playing a regulatory role in tau phosphorylation. cdk5 is specifically activated in neurons by p35, a protein that can be cleaved by calpain to form the smaller and more stable activator of cdk5, p25 (Lee et al., 2000). This cleavage of p35 into p25 could lead to prolonged activation of cdk5. Indeed, p25 immunoreactivity is high in AD brain, staining neurons and NFTs, whereas p25 immunoreactivity in control brain is very low (Patrick et al., 1999). In addition, Aβ has been demonstrated to increase the cleavage of p35 to p25, which could represent a link between Aβ pathology and tau hyperphosphorylation (Lee et al., 2000; Town et al., 2002). Similar to GSK-3β, cdk5 has been shown to associate with all stages of neurofibrillary pathology in AD brain and over-expression of cdk5 and p25 in cell lines leads to increased tau

phosphorylation (Pei et al., 1998; Cruz et al., 2003). However, inhibition of cdk5 in primary neurons led to increased tau phosphorylation and some studies have found that up regulation of p25 increases cdk5 activity but does not alter tau phosphorylation (Kerokoski et al., 2002; Morfini et al., 2004). This is an issue that remains to be resolved.

Of the non proline-directed kinases, PAR-1 (which is also known as MARK4 in mammals but will be referred to as PAR-1 in this thesis), a member of the AMPK-related family of protein kinases, has been the focus of much research. It has been shown to phosphorylate tau at two serine residues: S262 and S356 (Mandelkow et al., 2004). Phosphorylation at these residues has a large effect on the microtubule-binding properties of tau and it has been suggested that phosphorylation at KXGS motifs may be a pre-requisite for phosphorylation at other residues. Indeed, PAR-1 has been implicated as the initiator of a phosphorylation cascade involving GSK-3β and cdk5 (Nishimura et al., 2004). In addition to PAR-1, other non proline-directed kinases that have been shown to target tau in the KXGS motifs are PKA, CaMKKII and p70S6K (Mandelkow et al., 2007).

Tau can also be phosphorylated on tyrosine (Y) residues, of which there are five in the tau molecule (Y18, Y29, Y197, Y310 and Y394). Kinases that have been implicated in tyrosine phosphorylation of tau include c-Abl, Fyn, Syk, and tau-tubulin kinase 1 (Lee et al., 2004; Derkinderen et al., 2005; Lebouvier et al., 2008). Tau from AD brain has been shown to be tyrosine phosphorylated in some cases and treatment of cultured neurons with Aβ induces tyrosine phosphorylation of tau (Williamson et al., 2002).

Besides protein kinases, protein phosphatases (PPs) also play an important role in the regulation of the phosphorylation status of tau. Phosphatases that have been demonstrated to dephosphorylate tau *in vitro* include PP1, PP2A, PP2B and PP5 (but not PP2C). All of these phosphatases have been shown to dephosphorylate tau at a number of serine and threonine residues. However, the activity of PP2A towards tau has been demonstrated to be ~70% higher than the other phosphatases (Liu et al., 2005a; Rahman et al., 2006). Thus, PP2A is considered to be the 'main' tau phosphatase and it is of interest that its activity is decreased in AD brain (Liu et al., 2005a).

It is becoming clear that no one specific kinase or phosphatase is responsible for the abnormal tau phosphorylation in AD and indeed the literature suggests that there may be a hierarchy among the tau kinases with phosphorylation by one kinase being a pre-requisite for phosphorylation by the next (Nishimura et al., 2004; Mi and Johnson, 2006; Bertrand et al., 2010).

1.5.2.3.3 Tau and axonal transport

Neurons are some of the largest cells in humans and the vast majority of their overall cellular volume consists of the axon. Protein synthesis does not occur in axons and as such a process known as fast axonal transpost (FAT) takes place in order to enable the anterograde transport of essential components (e.g. membrane proteins, mitochondria and synaptic vesicles) from their sites of synthesis in the cell body to synaptic locations along the axon (Morfini et al., 2009). This process is essential for proper synaptic function and is facilitated by a group of molecular motor proteins

known as kinesins (Wagner et al., 1989). In addition, neuronal maintenance requires the reciprocal transport of signalling complexes and degradation products from the synapses to the cell body. Retrogade FAT is carried out by another type of motor protein, dynein (Morfini et al., 2009).

In normal differentiated neurons tau is confined to axons. However it has been demonstrated in a number of neuronal cell types (e.g. hippocampal neurons, N2a neuroblastomas) that expression of tau results in its miss-sorting from axons into the somatodendritic compartments (Thies and Mandelkow, 2007). This observation has also been made in post mortem human AD brain and transgenic mouse models of AD expressing human tau (Terry et al., 1991; Polydoro et al., 2009). Expression of tau in primary cortical neurons leads to the inhibition of anterograde FAT due to interference between tau and kinesins (Stamer et al., 2002). The interference in anterograde FAT seen upon tau expression in hippocampal neurons can be relieved by phosphorylation of tau by kinases such as PAR-1, resulting in the detachment of tau from microtubules (Thies and Mandelkow, 2007). This suggests that the relationship between FAT and tau is closely associated with the phosphorylation status of tau.

1.5.2.3.4 Tau and synaptotoxicity

In addition to inhibiting FAT, expression of tau in cultured hippocampal neurons caused drastic changes in dendritic spine morphology leading to synapse loss, disintegration of processes and cell death (Thies and Mandelkow, 2007). Expression of human tau in lamprey central neurons induces formation of tau filaments similar

to the straight filaments of tau seen in post mortem AD brain tissue. Filament formation in these neurons was associated with a progressive loss of dendritic synapses and microtubules (Hall et al., 2000). In support of a detrimental effect of tau on synapses, it has been demonstrated that aged htau transgenic mice (in which the mouse tau gene is replaced by non-mutated human tau) exhibit an age-dependent perturbation in basal synaptic transmission and LTP in the CA1 region of the hippocampus, an area that develops tau tangles in an age-dependent manner in this model (Polydoro et al., 2009).

1.5.2.3.5 Other post-translational modifications of tau

There are a number of other post-translational modifications of tau found in tangles (Buee et al., 2000; Gong et al., 2005; Gendron and Petrucelli, 2009). A number of proteases and caspases capable of cleaving tau, along with their sites of action, have been identified and the resulting fragments appear to have a higher propensity for aggregation when compared to full length tau (Wang et al., 2009b; Hanger and Wray, 2010). It has been shown that increased phosphorylation of tau inhibits tau cleavage by caspases (Guillozet-Bongaarts et al., 2006). In addition, application of Aβ to cultured hippocampal neurons induced the formation of a 17kDa tau fragment as a result of caspase-3 and calpain activity, and transfection of chinese hamster ovary (CHO) cells with a tau fragment of this molecular weight led to cell death (Canu et al., 1998; Park and Ferreira, 2005). More recently, a different group demonstrated that transfection of CHO cells or primary hippocampal neurons with the 17kDa fragment of tau did not cause cell death and that the calpain-induced fragment was detectable in both human AD and control brains (Garg et al., 2010). Thus it is not

currently clear if the cleavage of tau is part of a normal physiological process or of the cell's attempt to rid itself of pathological tau isoforms. Whatever the contribution of cleavage in tau pathology, it is of interest that tau fragments exhibit strong aggregation properties and are capable of seeding the aggregation of both cleaved and full length tau (Wang et al., 2009b). This could also have implications for current drugs being developed to dissolve NFTs.

Glycosylation (the reaction between the amino group of an amino acid side chain and the carboxyl end of reducing sugars) of AD tau but not control tau has been demonstrated (Wang et al., 1996). It is postulated that glycosylation is a process that precedes tau phosphorylation: tau isolated from AD brain that was not yet hyperphosphorylated was already glycosylated, whereas tau purified form normal control brain was not glycosylated (Liu et al., 2002). In addition, it would seem that aberrant glycosylation induces tau hyperphosphorylation in a site-specific manner both by promoting phosphorylation and inhibiting dephosphorylation (Gong et al., 2005). In contrast, O-GlcNAcylation (a common post-translational modification whereby O-linked-β-N-acetylglucosamine transferase (OGT) catalyses the transfer of GlcNAc from UDP-N-acetylglucosamine to serine or threonine residues of nuclear and cytoplasmic proteins) of tau has been shown to correlate negatively with tau phosphorylation at most sites (Liu et al., 2004; Liu et al., 2009).

It is known that tau in PHFs and NFTs is ubiquitinated, whereas control tau is not. Ubiquitination is considered as a label targeting short-lived, abnormal or damaged proteins for ATP-dependent degradation and removal through the ubiquitin-protease

system (Lace et al., 2007). As such, ubiquitination of tau in PHFs or NFTs may represent a failed attempt by the cell to rid itself of toxic tau species.

The role of these additional post-translational modifications of tau in the pathogenesis of AD and/or the tauopathies is not yet fully understood, but in addition to failed attempts by the cell to rid itself of pathological tau species, it has been proposed that they may be involved in the attempted adaptation of tau function(s) to different cellular locations (Lace et al., 2007).

1.5.3 The mitochondrial cascade (or metabolic) theory

This hypothesis states that genetic inheritance determines mitochondrial function and durability, durability dictates how mitochondria change with age, and AD pathology and symptoms develop when mitochondrial change/impairment rises above a certain level (Swerdlow and Khan, 2004). Reduced brain metabolism is a well documented abnormality in AD which appears before the ability to detect functional impairment by neuropsychological testing (Blass, 2000). Significant changes in the number, size and structure of mitochondria have been reported in AD neurons (Hirai et al., 2001). In addition to damage to the structure of mitochondria, several mitochondrial DNA-encoded enzymes have been shown to be altered in AD, most notably cytochrome c oxidase, which is at the terminal end of the electron transport chain (ETC) and attaches its acquired electrons to oxygen in order to generate water and not reactive oxygen species (ROS) (Zhu et al., 2006; Swerdlow and Khan, 2009). Deficiencies in mitochondrial oxidative phosphorylation lead to an increase in ROS, which is present

in the very early stages of AD, and the degree of impaired mitochondrial oxidative phosphorylation in AD brains correlates with the level of neurodegenerative decline (Rhein and Eckert, 2007). Additionally, mitochondria play a role in buffering cytosolic calcium within cells. When mitochondria are damaged this ability is compromised. However, it would appear that increased cytosolic calcium in neurodegenerative disease is upstream of mitochondrial calcium buffering deficits (Mattson, 2007).

Another prominent change in AD brain is synaptic loss and this is postulated to be important for the pathogenesis of AD (Selkoe, 2002). Under normal physiological conditions, the brain is highly metabolically active and consequently neurons need many mitochondria; especially at synapses, where synaptic transmission demands a constant supply of ATP (Sheehan et al., 1997; Isaacs et al., 2006). It has been proposed that aberrant mitochondrial distribution from an even distribution to a peri-nuclear distribution could be responsible for the synaptic loss seen in AD neurons (Wang et al., 2009a).

Potentially compounding these metabolic defects, *in vitro* Aβ can inhibit enzymes of the mitochondrial respiratory chain such as cytochrome c oxidase, and its toxicity appears to be mediated through effects on mitochondria; mitochondrial DNA depleted NT2 cells are resistant to Aβ-induced toxicity (Cardoso et al., 2001; Crouch et al., 2005). Additionally, it has been demonstrated that the expression of APP (wild-type or mutant) in cultured neurons dramatically increases the percentage of fragmented mitochondria (Wang et al., 2008). Fragmented mitochondria arise as a result of mitochondrial fission, which is a process that allows the sequestration and

elimination of mitochondria that have been damaged irreversibly (Chen et al., 2005; Chen et al., 2007). Mitochondrial fragmentation is also known to be an early event in apoptosis (Frank et al., 2001). Over-expression of APP also results in a profound loss of mitochondrial fusion (Wang et al., 2008), a process that allows the exchange of mitochondrial proteins and DNA. Fusion enables mitochondria that have undergone damage to mitochondrial DNA to replenish their stores of oxidative phosphorylation-related proteins, thus lowering the effect of the mitochondrial DNA defect (Wang et al., 2009a).

Tau has also been shown to affect mitochondrial function. In transgenic mice over-expressing a mutant version of human tau (P301L), respiratory chain components and antioxidant enzymes were dysregulated (David et al., 2005). Additionally, in triple transgenic mice carrying human tau (P301L mutation), APP_{SW} (Swedish mutation) and mutated PS2 (N141I), tau was shown to specifically dysregulate enzymes related to complex I of the oxidative phosphorylation system (Rhein et al., 2009). Furthermore, expression of a cleaved version of tau in cells (mimicking cleavage of tau by caspases) resulted in mitochondrial fragmentation and elevated ROS levels (Quintanilla et al., 2009). Interestingly, it would appear that the detrimental effects of tau on mitochondrial function are reciprocal; inhibition of complex I of the oxidative phosphorylation system in cultured neurons led to miss-sorting of tau from axons to the cell body, retrograde transport of mitochondria and cell death (Escobar-Khondiker et al., 2007).

Although it is clear that Aβ, APP and tau can exert detrimental effects on mitochondria, the cause of the early metabolic and mitochondrial defects observed in

AD remains elusive. That said, the correlation between impaired mitochondrial function and cognitive decline is an interesting subject that warrants further investigation and impaired mitochondrial function may prove to be a useful early indicator of AD.

1.5.4 The calciumopathy model

The calciumopathy model for AD was originally proposed by Khachaturian in 1987 and states that as humans age, their capacity for buffering calcium becomes impaired leading to a dysregulation of calcium homeostasis which if sustained, may provide a trigger for age-associated changes in the brain (Khachaturian, 1987).

A number of studies have shown that elevated cytosolic calcium concentration, through plasma membrane calcium channels or release of calcium from endoplasmic reticulum (ER) stores (mediated by IP_3 and ryanodine receptors), increases the production of intracellular Aβ (Querfurth and Selkoe, 1994; Pierrot et al., 2004; Pierrot et al., 2006). Conversely, increasing cytosolic calcium concentrations by inhibition of the sarco/ER calcium-ATPase (SERCA) pumps with thapsigargin, results in decreased Aβ production (Buxbaum et al., 1994). This suggests that the effects of calcium on APP processing (and the production of Aβ) may be different depending on the source of the calcium ions. Whilst the effect of calcium on the processing of APP and production of Aβ remains unclear, there is strong evidence that the reciprocal situation is true; that Aβ has a detrimental effect on calcium signalling. It has been shown by a number of groups that application of Aβ to

cultured cells increases cytosolic calcium though the formation of cation-selective ion channels by Aβ and via IP_3 and ryanodine receptor-mediated release of calcium from ER stores (Arispe et al., 1993; Mattson et al., 1993; Goodman and Mattson, 1994; Kawahara and Kuroda, 2000; Ferreiro et al., 2004).

Although mutations in presenilins account for less than 10% of all AD cases (Selkoe, 2004), presenilins have also been implicated in the calciumopathy theory; mutations in the PS1 or PS2 genes alter the γ-secretase cleavage pathway leading to increased Aβ production. Additionally, every mutation of PS1 and PS2 that has been studied alters calcium signalling (LaFerla, 2002). It remains unclear as to the exact mechanism by which presenilins affect calcium signalling, but a number of studies have shown that both PS1 and PS2 are involved in the destabilisation of IP_3-mediated calcium release from ER stores (Guo et al., 1996; Begley et al., 1999; Leissring et al., 1999a; Leissring et al., 1999b; Leissring et al., 2000). Indeed, ER calcium stores are diminished in presenilin deficient cells, indicating that presenilins play an important role in the regulation of ER calcium homeostasis (Leissring et al., 2002).

In addition to the calcium-dependent effects mediated by Aβ and the presenilins, tau phosphorylation can be regulated by calcium-dependent mechanisms. Calcium/calmodulin-dependent kinase II (CaMKII) phosphorylates tau at S262 and S356 (Litersky et al., 1996). Additionally, calpain, a calcium-activated protease, can indirectly activate another tau kinase, cdk5 (Kusakawa et al., 2000). Furthermore, the calcium/calmodulin-dependent phosphatase calcineurin (also known as PP2B), has been shown to be able to dephosphorylate tau - albeit to a much lesser extent than the main tau phosphatase, PP2A (Liu et al., 2005a). These data indicate a role

for calcium-activated kinases and phosphatases in the regulation of tau phosphorylation. More recently, it has been shown that treatment of neurons with amyloid proteins led to miss-sorting of tau from axons to dendrites, local elevation of intracellular calcium levels, tau phosphorylation at a number of residues and increased expression and/or activation of tau kinases such as PAR-1 and brain selective kinase 1 (BRSK1) (Zempel et al., 2010).

It remains to be seen if altered calcium signalling is a causative agent in AD, but it cannot be ignored that calcium signalling has been shown to be altered before the development of symptoms in patients who later develop either familial or sporadic AD, and as such may represent an early indicator of AD (Ito et al., 1994; Etcheberrigaray et al., 1998).

1.6 The AMPK-related family of protein kinases

The AMPK-related family of protein kinases were initially identified by their sequence homology to the catalytic domain of the prototypical member of the family, AMP-activated protein kinase (AMPK) (Figure 1.5). AMPK is a kinase that consists of three subunits (α, β and γ) and is involved in the regulation of cellular energy homeostasis and cellular polarity. The α subunit is where the serine/threonine kinase domain resides. This domain also contains a C-terminal regulatory domain. The β subunit is thought to enable the binding of the α and γ subunits to form a complex. The γ subunit is where AMP and ATP bind to the AMPK complex (Carling, 2004). AMPK is activated by a decrease in the cellular ratio of ATP:ADP

which leads to a large increase in the concentration of AMP. Increased intracellular concentrations of AMP activate AMPK which then initiates ATP conserving mechanisms by switching off any ATP depleting processes that are not essential for immediate survival and activating ATP generating pathways (Carling, 2004; Hardie, 2004). These complex actions of AMPK are effected through direct and indirect phosphorylation by AMPK of downstream targets. In addition to its essential role in energy sensing mechanisms, AMPK has recently been implicated in cellular polarity in epithelial cells and *Drosophila* (Hardie, 2007; Lee et al., 2007). The *Drosophila* homologue of AMPK is SNF1A. SNF1A-null mutant *Drosophila* are lethal and exhibit severe polarity and mitotic defects which can be rescued with a phosphomimetic mutant of non-muscle myosin regulatory light chain, a target that is directly phosphorylated by AMPK (Lee et al., 2007).

In a complex with STE20-related adaptor (STRAD) and mouse protein 25 (MO25), the tumour suppressor master kinase LKB1 has been shown to phosphorylate 14 of the 22 AMPK-related family members (including AMPK) on T-loop serine/threonine residues, causing their activation (Hawley et al., 2003). AMPK has also been shown to be regulated by the Ca^{2+}/calmodulin dependent kinase-β (CaMKKβ), and, to a much lesser extent, CaMKKα (Hawley et al., 2005). Although much is known about the regulation and function of AMPK, the regulation and functions of other members of the AMPK-related family of kinases appears to be quite diverse. These functions include the regulation of tumour invasion (NUAK1/2) (Legembre et al., 2004; Suzuki et al., 2004), regulation of gene expression through phosphorylation of CRE-binding protein (SIK1) (Katoh et al., 2004) and the regulation of cell proliferation (QSK) (Bettencourt-Dias et al., 2004). None of the AMPK-related kinases appear to

be activated by the same pharmacological stimuli as AMPK, such as phenformin or AICAR, implying that members of this family are activated and/or regulated by different stimuli to AMPK itself (Lizcano et al., 2004; Sakamoto et al., 2004). This is likely to be because the AMPK-related kinases do not have an AMP binding domain.

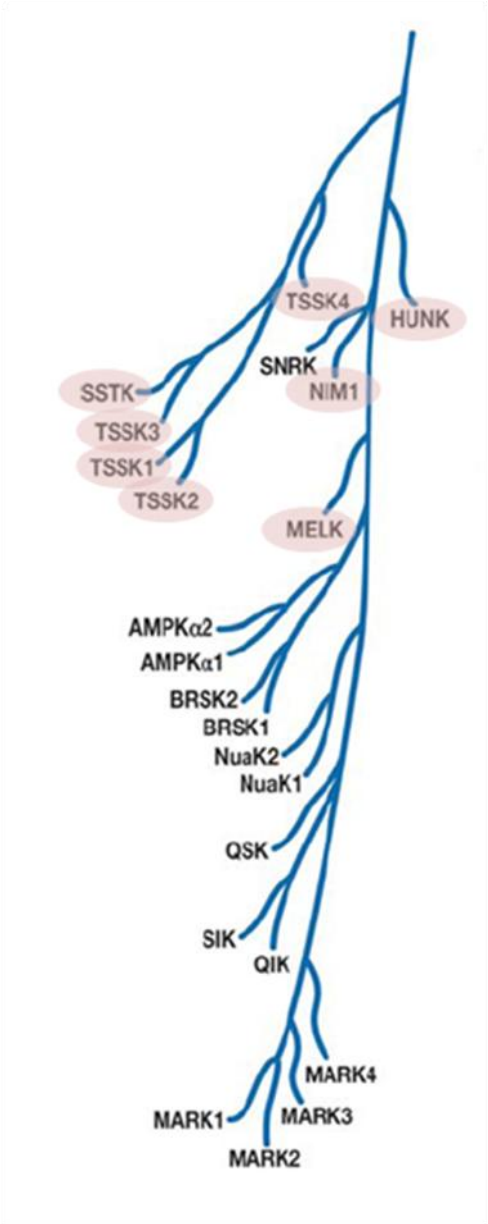

Figure 1.5 The AMPK-related family of protein kinases
Dendrogram revealing the level of relatedness between the human AMPK-related family of protein kinases, a family that is largely regulated by the tumour supressor kinase LKB1(greyed out are non-LKB1 substrates). The diagram shows that there are two isoforms of BRSK (1 and 2) in the human genome and that they are closely related to AMPKα1 and AMPKα2, the prototypical members of this family of protein kinases. Adapted from Alessi et al. (2006).

1.6.1 AMPK-related kinases as tau kinases

It is of interest that at least three members of this family (AMPK, PAR-1 and BRSK) have been reported as tau kinases and that these kinases have (at least partially) overlapping functions.

Probably the more familiar of the three, in terms of being a tau kinase, is the aforementioned PAR-1. PAR-1 was originally identified in a screen to identify determinants of early embryonic polarity in *C.elegans* and was later identified as part of an evolutionarily-conserved group of proteins required for cell polarity in mammals, worms, frogs and flies (Kemphues et al., 1988; Biernat et al., 2002; Hurov and Piwnica-Worms, 2007). PAR-1 has been implicated in the phosphorylation of tau by a number of groups (Drewes et al., 1997; Biernat et al., 2002; Mandelkow et al., 2004; Nishimura et al., 2004; Wang et al., 2007a; Chatterjee et al., 2009). It is known that PAR-1 is able to phosphorylate tau within the KXGS motifs, at S262 and S356, and that this has a dramatic effect on the microtubule binding properties of tau (Mandelkow et al., 2004). In addition, work in *Drosophila melanogaster* has shown that PAR-1 can exacerbate a human tau-induced degenerative eye phenotype, and that PAR-1 may instigate endogenous (fly) and exogenous (human) tau hyperphosphorylation by initiating a phosphorylation cascade which includes GSK-3β and cdk-5 (Shulman and Feany, 2003; Nishimura et al., 2004). Following this, it was shown by Wang *et al* (2007a) that LKB1 lies upstream of PAR-1 and acts as an activator of PAR-1 via phosphorylation at T408.

In addition to PAR-1, AMPK itself has been implicated as a tau kinase *in vitro* (Vingtdeux et al., 2010a; Thornton et al., 2011) and recent data from a post-doctoral

researcher in the laboratories of Prof. Bruno Frenguelli and Dr Kevin Moffat indicates that this is also the case *in vivo* in *Drosophila* (Dr Alessia Galasso, personal communication). AMPK has been shown to phosphorylate tau on a number of sites including S262/S356 and S396. Because patients with diabetes appear to have an increased risk for AD, it was considered a concern that the most widely used pharmacological agent for treating type-2 diabetes, Metformin, is an AMPK activator (Kroner, 2009). However, it has recently been demonstrated that in addition to activating AMPK, metformin, reduces tau phosphorylation via activation of PP2A (Kickstein et al., 2010). Additionally, activation of AMPK has recently been implicated in the mediation of autophagy (Egan et al., 2011) and in the degradation of Aβ peptides, presenting a perplexing situation whereby both activation and inhibition of AMPK could be detrimental (Vingtdeux et al., 2010b; Vingtdeux et al., 2011). Thus it is of vital importance that further research is conducted into the capacity of AMPK as a tau kinase and its potential involvement in the degradation of Aβ species.

1.7 Brain selective kinases (BRSKs)

BRSKs are evolutionarily conserved serine/threonine kinase members of the AMPK-related family of kinases which have orthologues in mouse (SAD-B and SAD-A), *C.elegans* (SAD-1), *Drosophila* (CG6114) and *Ascidians* (HrPOPK-1). For clarity, mammalian orthologues will be referred to as BRSK1 and 2 throughout this thesis. Northern and Western analyses have demonstrated that BRSKs are highly expressed in the brain with lower expression in the testis and the pancreas (Lizcano et al., 2004; Kishi et al., 2005; Hezel et al., 2008).

1.7.1 Physiological function(s) of BRSKs

1.7.1.1 BRSKs and neuronal polarity

Crump *et al* (2001) identified the *C.elegans* orthologue of the BRSKs, SAD-1, and showed that it regulates presynaptic differentiation and axonal polarity (Crump et al., 2001). Work by Crump *et al* (2001) on SAD-1 reported that mutant worms showed axons that failed to terminate properly indicating a deficiency in the signals which control this process. Worms over-expressing SAD-1 had axons which either terminated prematurely or were miss-directed. As a result of these observations Crump *et al* suggest that one of the functions of SAD-1 is to signal to the axons to stop elongating. In support of these findings, Hung *et al* (2007) indicate that SAD-1 directly interacts with the *C.elegans* homologue of Neurabin-1, NAB-1, to confer axonal identity in *C.elegans* dorsal and ventral GABAergic motor neurons (Hung et al., 2007). Additionally, Kim *et al* (2008) show that SAD-1 is required for establishment, but not maintenance, of neuronal polarity in the same *C.elegans* motor neurons (Kim et al., 2008). Consistent with the observations made, SAD-1 has a kinase domain which is related to the kinase domain of the aforementioned embryonic polarity determinant, PAR-1.

Single and double knockout mice have been made for the murine homologue genes of BRSK 1 and 2, SAD-B and SAD-A respectively, to investigate their functions in neuronal polarity (Kishi et al., 2005). Kishi *et al* (2005) found that single knockout mice were healthy and fertile and that lack of one kinase had no compensatory effect on the expression of other. However, the double knockout mice died within two hours of birth and had little response to tactile stimulation, suggesting a neural

phenotype. Examination of the embryonic (E19) nervous system of these mice showed normal formation of the brain, spinal cord and peripheral nervous system, although double knockout animals had visibly thinner cortices when compared to littermate control animals. In addition, the double knock out animals had severely decreased thalamo-cortical projections and the neurons of the forebrain lacked polarity with many of them exhibiting starburst morphology and failing to form distinct axons and dendrites. This confirmed that BRSKs were involved in the establishment of forebrain neuronal polarity, more specifically in the processes that confer distinct axonal and/or dendritic identity.

1.7.1.2 BRSKs and synapses

Presynaptically, *sad-1* mutant worms had a more diffuse distribution of synaptic vesicles than wild type animals at both neuron to neuron and neuromuscular synapses (Crump et al., 2001). In addition, inhibition of SAD-1 activity during the development of DD-type motor neurons disrupted synaptic organisation, an effect which was rescued upon expression of SAD-1 after development (Kim et al., 2008). SAD-1 has been shown to co-localise with SNT-1, a synaptic vesicle protein, and UNC-10, an active zone protein, indicating that SAD-1 is present presynaptically and is associated with active zones and vesicle pools in *C.elegans* (Hung et al., 2007). In support of SAD-1 being involved in presynaptic differentiation, mammalian BRSK1 has also been implicated at the synapse where it was found to localise to, and associate with, synaptic vesicles in mouse hippocampus and cerebellum (Inoue et al., 2006). In addition, it has been suggested that BRSK1 plays a role in neurotransmitter release in cultured rat primary hippocampal neurons by

phosphorylation of the active zone protein RIM1 (Inoue et al., 2006). However, Crump *et al* (2001) suggest that *sad-1* does not regulate all aspects of presynaptic development as other mutants (*rpm-1* and *syd-2*) identified in the same screen exhibit defects in neurons where SAD-1 has little or no effect. *sad-1* and *syd-2* double mutants exhibit an additive phenotype, showing that both genes function in different aspects of synapse development.

1.7.1.3 BRSKs and tau phosphorylation

Because the phosphorylation status of tau regulates its interactions with microtubules (Weingarten et al., 1975; Lindwall and Cole, 1984; Barghorn et al., 2000; Makrides et al., 2004; Wang et al., 2007b) and local variations in the organisation of microtubules affect neuronal polarisation (Mandell and Banker, 1996; Arimura et al., 2004), Kishi *et al* (2005) chose to look at whether BRSKs phosphorylate tau. They found that BRSKs are involved in the basal phosphorylation of tau at S262 - a crucial residue that must be phosphorylated in order for NFTs to form and a residue that is also targeted by PAR-1. In cortical brain slices, immuno-staining for tau phosphorylated at S262 showed a decrease in pS262 in BRSK double knockout mice when compared to wild type animals (Kishi et al., 2005). There was no difference in the amount of total tau detected.

1.7.1.4 BRSKs as checkpoint kinases

In addition to roles in presynaptic differentiation, the establishment of forebrain neuronal polarity and an involvement in the basal phosphorylation of tau, BRSK1

has been identified as a potential checkpoint kinase at the G_2/M transition of the cell cycle (Lu et al., 2004). This was discovered because BRSK1 exhibits homology with the fission yeast kinase Cdr2, which along with Wee1 protein kinase, is involved in the regulation of mitosis (Breeding et al., 1998). *In vivo,* BRSK1 phosphorylates Cdc25-C on Serine 215 (Lu et al., 2004). In HeLa cells, BRSK1 was activated upon DNA damage induced by UV or methyl methane sulphonate and was subsequently translocated to the nucleus. This led to arrest of the cell cycle at the G_2/M transition which could be prevented by treatment with caffeine. It was suggested that these effects on BRSK and the cell cycle arrest were mediated by ataxia-telangiectasia mutated (ATM) or Rad3-related (ATR) protein kinases, both of which are inhibited by caffeine (Lu et al., 2004). In support of this, the BRSK1 sequence contains two consensus phosphorylation sites for ATM or ATR, although there is currently no evidence that BRSKs are targeted by ATM or ATR.

1.7.2 Regulation of BRSKs

Like AMPK and PAR-1, BRSKs can be regulated by the master kinase LKB1 through phosphorylation of a conserved threonine residue in their T-loop (T189 in BRSK1 and T174 in BRSK2) (Lizcano et al., 2004). It has been suggested that LKB1 is constitutively active: under conditions which are known to cause activation of AMPK, no increase in LKB1 activity is seen (Alessi et al., 2006). However, Shelly *et al* (2007) have evidence that phosphorylation of LKB1 at a PKA site (S431) elevates the activity of LKB1. When they mutated the PKA site, so that it was no longer an active site, the increase in LKB1 activity was not seen (axonal

differentiation was prevented) (Shelly et al., 2007). This view is supported by Barnes *et al* (2007) who state that LKB1 is required for axonal polarization, having first been activated by phosphorylation at S431 by PKA (Barnes et al., 2007). In contrast to the work of Shelly *et al* (2007) and Barnes *et al* (2007), a splice variant of LKB1 which lacks S431 has been reported which activates BRSK1/2 and AMPK to the same level as wild type LKB1 (Fogarty and Hardie, 2009). Recently, it was demonstrated that BRSKs act downstream of LKB1 in the establishment of axonal identity; phosphorylation of BRSKs was decreased in the cortices of LKB1 knockout mice and the ability of over-expressed LKB1 to induce the formation of multiple axons was reduced upon BRSK knockdown (Barnes et al., 2007).

In a similar manner to AMPK (Hawley et al., 2005), unpublished data shows that BRSK activity in brain slices is STO-609 sensitive (Prof. Bruno Frenguelli, personal communication). STO-609 is a relatively specific inhibitor of CaMKK and as such, this result suggests that BRSKs are regulated in a calcium dependent manner. Indeed, in mammals, there are two isoforms of CaMKK, α and β, both of which are highly expressed in the brain regions where BRSKs are expressed (Vinet et al., 2003). More recently, it was shown that CaMKKα is an upstream activator of BRSK1 *in vitro* (Fujimoto et al., 2008). This could provide a link between deregulated BRSK activity, tau phosphorylation and aberrant calcium metabolism. In contrast, Bright *et al* showed that CaMKKβ does not activate the BRSKs (Bright et al., 2008), yet it does strongly activate AMPK (Hawley et al., 2005; Woods et al., 2005).

It has also been reported that BRSK2 is directly activated by PKA via phosphorylation at T260 (Guo et al., 2006). This could implicate another signalling

pathway in the control of the BRSKs. However, PKA activation of BRSKs is not via the T-loop threonine residue and it has been reported that PKA has no effect on BRSK activation, so this is an issue that remains unresolved (Bright et al., 2008).

1.8 *Drosophila melanogaster* as a model for neurodegeneration

A process which is pathogenic in humans can be studied in *Drosophila* providing it can be mimicked in a way that shows sufficient correlation of the features of the disease in man (Sang and Jackson, 2005). The fundamental processes of membrane trafficking, the cytoskeleton, gene expression regulation, cell signalling and neuronal connectivity are comparable in flies and man. The lack of redundancy within the fly genome can simplify genetic analysis of processes within the fly: processes which when studied in humans can be difficult due to two or more copies of some genes. A case in point is the presence of only one BRSK homologue in the *Drosophila* genome; CG6114. Arguably the main advantage of using *Drosophila* as a model, is that large numbers of flies can be manipulated, mutagenized and screened in a relatively short time period, allowing insights to be made into disease mechanisms. These experiments would be impractical or even impossible to carry out in a mammalian system over a similar time period (Sang and Jackson, 2005). Perhaps one of the most useful tools for *Drosophila* geneticists is the GAL4/UAS miss-expression system which allows the over-expression of a gene of choice in a wide range of developing and adult tissues in the fly (Brand and Perrimon, 1993).

1.8.1 The eye

The eye is often the focus of *Drosophila* research as the adult animal is highly tolerant of disruption to basic biological processes in this organ, and it is extremely easy to identify eye phenotypes, with many being visible to the naked eye. Additionally, under laboratory conditions, where the flies are kept in vials or bottles, the eye is not required in order to ensure the survival of the fly (Sang and Jackson, 2005). Using the eye-specific driver, GMR-GAL4, the eye has long been utilised for the analysis of developmental patterning and proliferation (Freeman, 1996). It has been shown by a number of groups that expression of 4R human tau isoforms (mainly 0N4R and 2N4R) in the *Drosophila* eye causes a degenerative phenotype which is visible as a rough surface of the eye with disordered and fused lenses, implying disorganization of the ommatidia (photoreceptor clusters) (Shulman and Feany, 2003; Nishimura et al., 2004; Steinhilb et al., 2007a; Steinhilb et al., 2007b; Chatterjee et al., 2009; Iijima-Ando et al., 2010). Shulman and Feany (2003) reported that the observed eye phenotype changes with the level of human tau expression, signifying that the model could be used as a sensitive marker for genetic interactions with tau that influence its toxicity.

Aims of the thesis

Whilst the cause of AD remains elusive, it is apparent that tau pathology in the brain correlates well with the severity of symptoms in life. In addition, the tauopathies are a spectrum of diseases which appear to be caused by aberrant tau protein. Because of the central role of tau phosphorylation in the pathogenesis of tau and the formation of tau tangles, understanding tau phosphorylation is of the utmost importance. As discussed, three members of the AMPK-related family of protein kinases, including AMPK itself, have been implicated as tau kinases. BRSKs have been implicated in the basal phosphorylation of tau and unpublished data suggests that they are regulated in a calcium-dependent manner, via CaMKK. Thus, the aim of my thesis was to investigate the interaction between human BRSKs and 0N4R tau using the *Drosophila* eye as a model, and to further explore the upstream regulation of BRSKs. More specifically, the aims of my thesis were:

1. To transgenically express various mutated forms of human BRSK in the *Drosophila* eye and observe the effect this has on human tau-induced toxic eye phenotypes.
2. To determine if human BRSKs are capable of phosphorylating human tau *in vivo.*
3. To establish the upstream kinases responsible for BRSK activation.
4. To investigate the potential for BRSKs to be regulated in a calcium dependent manner *in vivo*.

5. To investigate the expression levels/activity of BRSK and its upstream activators in human post-mortem brain tissue from AD patients and control subjects.

2| Materials and Methods

All chemicals and reagents were supplied by Sigma Aldrich, UK unless otherwise stated.

2.1 Maintenance of *Drosophila* stocks

2.1.1 Preparation of Sussex fly food

Drosophila stocks were held at 25°C or 18°C in bottles or vials containing Sussex fly food. Sussex fly food was prepared by mixing 518g maize flour, 471g sugar, 93g yeast and 28g agar into 5L water and boiling for 10 minutes in order to kill the live yeast. The food was cooled prior to the addition of 75ml Nipagen M (10% w/v in ethanol) in order to prevent fungal growth, mixed well and poured into bottles and vials. Once set, the food was supplemented with live yeast.

2.1.2 *Drosophila melanogaster* lines used in this work

See Appendix 1.

2.2 Analysis of adult fly phenotypes

2.2.1 Expression of exogenous and endogenous genes in the *Drosophila melanogaster* retina

Over-expression of exogenous (human) and endogenous genes in the retina was achieved using the UAS-GAL4 expression system with the eye specific glass multiple repeat (GMR) driver (Brand and Perrimon, 1993).

2.2.2 Scanning electron microscopy

Female flies were fixed overnight in 4% paraformaldehyde (PFA) made in phosphate buffered saline (PBS, 0.1M sodium phosphate pH 7.3, 0.1M sodium chloride) at 4˚C. Flies were then dehydrated using an acetone series (10%, 30%, 50%, 70%, and 90%), incubated on a rotator in 1ml of solution for 15 minutes at room temperature. Flies were transferred to 100% acetone stored over a molecular sieve (dry acetone), for at least 2 days at 4˚C. Flies were attached to stubs using double-sided tape, sputter coated in gold (or gold and palladium) for 60 seconds and imaged using a Zeiss Supra55 VP SEM at 150X magnification.

2.2.3 Quantitative Edge Detection (QED)

Software for assessing the level of ommatidial disruption in adult fly eyes (QED) was developed in collaboration with Dr John Aston and Mr Quentin Caudron from the Statistics Department at Warwick University. The software was written in Matlab by Mr Quentin Caudron with contributions from Dr John Aston, Prof Bruno Frenguelli, Dr Kevin Moffat and I. A full description of QED (written by Mr Quentin Caudron) is supplied in Appendix 2. Briefly, QED processes SEM images and on the basis of sharp differences in contrast, uses edge detection to identify the edges of ommatidia. The programme then measures the roundness of each ommatidia along with the distance to the six nearest neighbours of the central ommatidia and the angles to the six nearest neighbours of the central ommatidia. For the purpose of this study, only data for the roundness measure (termed ommatidial distortion) has been used as it is a more sensitive measure, sampling hundreds of times per image as opposed to once per image for the distance and angle measures.

Once all the images of a genotype have been analysed, QED plots the distribution of the ommatidial roundness measures for the eye and then proceeds to measure the width of the distribution plot – this is termed the dispersion coefficient. Dispersion coefficients from QED were collected and transferred to GraphPad software (version 4) in order to produce cumulative plots of ommatidial distortion (dispersion coefficients) versus fly count (in percent of total).

2.2.4 Resin embedding

Heads of female flies were dissected on sylgard plates immersed in PBS in order to remove the proboscis and air sacks. Heads were then fixed overnight in 2% gluteraldehyde: 2% paraformaldehyde made in PBS, at 4˚C. Flies were dehydrated using an acetone series (10%, 30%, 50%, 70%, 90% and dry acetone, twice) incubated on a rotator in 1ml of solution for 30 minutes at room temperature. Heads were embedded in Durcupan resin by following the next steps. 1 hour incubation in 3 parts dry acetone: 1 part number 1 Durcupan ACM mixture (11.4g component A, 10g component B, 150µl component D) at room temperature with rotation. 1 hour incubation in 2 parts dry acetone: 2 parts number 1 Durcupan ACM mixture at room temperature with rotation. Overnight incubation in 1 part dry acetone: 3 parts number 1 Durcupan ACM mixture at room temperature with rotation. The following day, two 2 hour incubations in number 1 Durcupan ACM mixture at 50°C followed by a 2 hour incubation in number 2 Durcupan ACM mixture (11.4g component A, 10g component B, 350µl component C, 150µl component D) at 50°C. Heads were transferred individually into moulds containing a thin layer of number 2 Durcupan ACM mixture that had been pre-baked at 70°C for 2-3 hours to prevent the heads

from sinking. The wells were filled with number 2 Durcupan ACM mixture and the heads were orientated. The moulds were baked at 70°C for 2 days to fully set the resin.

2.2.5 Resin sectioning

Resin blocks were trimmed to a trapezoidal shape using a razor blade and 2.5µm sections were cut using a Leica 2065 Supercut Rotary Microtome. The sections were placed on drops of sterile water on superfrost slides (VWR) and allowed to dry on a heated block at 80-82°C.

2.2.6 Toluidine-blue staining

After sectioning, slides were stained with toluidine blue for the visualisation of the structure of photoreceptor cells. For this, a solution of 1% toluidine blue and 1% borax in water was prepared. The solution was re-used and filtered through a 0.2µm filter prior to each use. Slides were stained for 30 seconds on a heated block at 80-82°C, rinsed under tap water and allowed to dry on a heat block. Once dry, slides were mounted in a mixture of dibutyl phthalate and xylene (DPX). Sections were visualised and imaged under brightfield light on an epifluoresence microscope at 100X magnification.

.

2.3 DNA manipulations

2.3.1 DNA isolation

2.3.1.1 Small scale preparation of plasmid DNA

DNA was isolated using the QIAprep Spin Miniprep Kit (Qiagen) according to manufacturer's manual.

2.3.1.2 Large scale isolation of plasmid DNA

DNA was isolated using either the Qiagen Plasmid midi or Hi-Speed maxi kit according to manufacturer's instructions.

2.3.1.3 Preparation of genomic DNA from Drosophila melanogaster

Genomic DNA was prepared according to the method written by E. Jay Rehm (Berkeley Drosophila Genome Project) which was accessed online at:

http://www.fruitfly.org/about/methods/inverse.pcr.html

Briefly, 30 flies were homogenised in 400µl of buffer A (100mM Tris-HCl pH7.5, 100mM EDTA, 100mM NaCl, 0.5% SDS) using a mechanical pestle and incubated at 65°C for 30 minutes. 800µl Lithium Chloride/Potassium Acetate (LiCl/KAc) solution (2.5 parts 6M LiCl: 1 part 5 M KAc) was added and the tube was incubated on ice for 10 minutes before centrifugation for 15 minutes at full speed in a bench-top microcentrifuge (room temperature). 1ml of supernatant was transferred to a new tube avoiding any floating debris and 600µl isopropanol was added. The tube was

re-centifuged as above and the supernatant discarded. The pellet was washed with 70% ethanol and air dried before re-suspending in 100µl sterile water.

2.3.2 Determination of DNA concentration

DNA concentration and purity was measured using a NanoDrop ND-1000 spectrophotometer (Thermo Scientific) and associated NanoDrop 1000 3.6.0 software. Purity was assessed by the 260nm/230nm and the 260nm/280nm ratios, with a ratio below 1.8 indicating a high level of organic contaminants or proteins in the DNA preparation respectively.

2.3.3 Restriction digestion of DNA

This was done in a total reaction volume of between 10 and 100µl using enzymes and buffers supplied by Invitrogen or Fermentas, according to manufacturer's instructions. Enzyme was at 1/10 of the total volume. 100ng-5µg DNA was used. Digests were incubated over night in a 37°C water bath.

2.3.4 Separation of DNA fragments according to size

Method based on Maniatis *et al* (1982) – book 5, chapter 1, pages 150-162

Fragments of DNA were separated according to their size by electrophoresis in agarose gels as previously described (Maniatis et al., 1982). For ease of loading, DNA was mixed with loading buffer containing 30% glycerol, 0.1% bromophenol blue and 0.1% xylene cyanol at a ratio of 1 part loading buffer to 5 parts DNA. Gels

were run at 150V until the dye front had migrated ¾ of the way along the gel. For visualisation of DNA fragments on a UV transilluminator, ethidium bromide or RedSafe DNA stain (Chembio) were incorporated into the gel at 0.5µg/ml.

2.3.5 Purification of DNA from agarose, salts and impurities

This was done using QIAquick Gel Extraction (Qiagen) or Gene Clean II (Q Bio Gene) kits according to manufacturer's instructions.

2.3.6 Subcloning of DNA fragments to plasmid vectors

2.3.6.1 Ligation of DNA fragments to plasmid vectors

Ligations were performed over night at room temperature using a 3:1 or 10:1 molar ratio of insert to vector with T4 DNA ligase (Invitrogen), according to manufacturer's instructions. Vector was pre-treated with Bacterial Alkaline Phosphatase (Invitrogen) according to manufacturer's instructions in order to prevent self-ligation.

2.3.6.2 Transformation of Escherichia coli and selection of colonies

Following 2.3.6.1, chemically competent *E.coli* (high efficiency or subcloning efficiency, both New England Biolabs) was transformed with ligation mixture according to manufacturer's instructions. Transformed cells were identified using antibiotic selection plates.

2.3.7 Bacterial strains

Escherichia coli DH5α derivative (high efficiency, New England Biolabs) genotype: *araD*139 Δ(*ara-leu*)7697 *fhuA lacX74 galK* (Φ80 Δ*(lacZ)M15) mcrA galU recA1 endA1 nupG rpsL* Δ*(mrr-hsdRMS-mcrBC)*

Escherichia coli DH5α derivative (subcloning efficiency, New England Biolabs) genotype: *fhuA2* Δ(*argF-lacZ)U169 phoA glnV44* Φ*80*Δ (*lacZ*)M15 *gyrA96 recA1 relA1 endA1 thi-1 hsdR17*

2.3.8 Media Preparation

2.3.8.1 Luria-Bertani (LB) Broth

LB broth was prepared by mixing 10g NaCl, 10g tryptone and 5g yeast extract into 1L H_2O. This was autoclaved and cooled prior to use. Where antibiotics were used, the antibiotics were added after autoclaving. Ampicillin was used at a final concentration of 100µg/ml and kanomycin at a final concentration of 25µg/ml.

2.3.8.2 LB agar plates

LB broth (see 2.2.7.1.) with 15g/L agar. Autoclaved and cooled before pouring into petri dishes to set. Where antibiotics were used, the antibiotics were added after autoclaving. Ampicillin was used at a final concentration of 100µg/ml and kanomycin at a final concentration of 25µg/ml.

2.3.9 Amplification of DNA using Polymerase Chain Reaction (PCR)

2.3.9.1 Primer design

Sense and antisense primers were designed to gene sequences using Clone Manager Suite software. The software scores potential primer sequences on the basis of a set of criteria including annealing temperature, GC content, primer length, melting temperatures, hairpins, stability, runs of bases and dimers. Primers which satisfied the criteria were ordered from Invitrogen (Custom oligonucleotide service). See Appendix 3 for a list of primers used in this study.

2.3.9.2 PCR conditions

PCR reactions were carried out using the following basic conditions for a 50µl reaction:

5µl 10X PCR buffer (Invitrogen)

1.5µl 50mM $MgCl_2$/$MgSO_4$ (depending on whether standard taq or pfx enzymes were being used)

1.5µl 10mM dNTPs (ATP, CTP, GTP, TTP) (Invitrogen)

5µl of each primer (final concentration of 0.005µg/µl)

x µl DNA (1ng for plasmid and up to 500ng for genomic)

0.4µl polymerase – either taq or pfx (both Invitrogen)

Water to 50µl

An Eppendorf thermocycler was used for all reactions with the following basic conditions:

1. Initial denaturation: 5 minutes, 94°C

2. Denature: 15 seconds, 94°C

3. Anneal primers: 30 seconds, 55°C

4. Extend DNA: 30 seconds per kb of product, 72°C

5. Repeat steps 2-4 for 35 cycles

6. Final Extension: 10 minutes, 72^{o}C

If the PCR was unsuccessful using the basic conditions above, two approaches were taken in order to optimise the conditions. Firstly, the magnesium concentration of the reaction was altered. Magnesium is a cofactor for enzymes and altering its concentration may enhance the stringency of the polymerase. Secondly, the annealing temperature was altered in order to customize the reaction conditions for that particular set of primers.

2.3.10 Sequencing DNA

Using primers designed as described in 2.3.9.1 and plasmid DNA prepared as described in 2.3.1.1 or 2.3.1.2. 50-500ng DNA and 5.5pmol primer were typically used in a total volume of 10ul. Sequencing was carried out by Molecular Biology Services, Biological Sciences, Warwick University on an ABI Prism Genetic Analyser 3130xl, the data from which was collected using ABI Prism 3130xl Genetic Analyser Data Collection Software version 3.0 and edited using ABI Prism Sequencing Analysis Software version 5.2.

2.4 Protein manipulations

2.4.1 Analysis of samples from *Drosophila melanogaster*

2.4.1.1 Protein extraction from Drosophila melanogaster

Lysis buffer contained 50mM tris(hydroxymethyl)aminomethane-hydrochloric acid (Tris-HCl pH 7.5), 0.1mM ethylene glycol tetra-acetic acid (EGTA), 1mM ethylene diamine tetra-acetic acid (EDTA), 1% (v/v) Triton X-100, 1mM Sodium Orthovanadate (Na_3VO_4), 50mM Sodium Fluoride (NaF), 5mM Sodium Pyrophosphate ($Na_4P_2O_7$), 0.27M Sucrose, 0.1% (v/v) β-Mercaptoethanol and 'Complete' protease inhibitor cocktail (Roche, three tablets per 50ml). NaF and $Na_4P_2O_7$ were included in order to inhibit serine/threonine protein phosphatases. Na_3VO_4 was included in order to inhibit protein tyrosine phosphatases. EDTA was used to chelate Mg^{2+} ions which are essential co-factors required for kinase activity. Proteinase inhibitor cocktail tablets were used to inhibit serine, cystein, metallo and aspartyl proteinases. EGTA was included in order to chelate Ca^{2+} ions which are important signalling molecules. This combination of chelators and inhibitors made certain that proteolysis, phosphatase and protein kinase activity was insignificant in the produced lysates.

In order to minimise the effect of tau and BRSK2 expression during eye development, all western blots were conducted on flies which had been reared according to the method described by Iijima-Ando *et al* (2010). Briefly, flies were crossed and reared until eclosion at 18°C in order to minimise GAL4 activity. Once flies had eclosed they were aged at 25°C for 7 days in order to activate GAL4 expression. After aging,

fly heads were dissected and subsequently lysed in 2ul lysis buffer per head with the aid of a mechanical pestle. Lysates were spun in a microcentrifuge at 13000rpm for 20 minutes at 4°C and the supernatant removed. The pellet of cell debris was discarded and the amount of protein in the lysate was determined via the Bradford Assay. Sodium dodecyl sulphate (SDS) loading dye was then added to the lysates which were subsequently heated at 70°C for 10 minutes before snap freezing in liquid nitrogen and storing at -80°C.

2.4.1.2 Sodium dodecyl sulphate polyacrylamide gel electrophoresis (SDS-PAGE)

SDS-PAGE was performed using the BioRad mini system. Protein extracts were thawed and heated at 70˚C for 10 minutes. Following a brief centrifugation to collect the samples at the bottom of the tubes, samples along with Bench Mark Pre-Stained Protein Ladder (Invitrogen) were loaded onto SDS-PAGE gels which constituted of 10% resolving gel and 4% stacking gel (see tables 2.1 and 2.2 for gel compositions). SDS containing loading dye ensured all proteins had an equal mass to charge ratio therefore, the distance travelled through the gel was directly related to a proteins size, with smaller proteins migrating faster than larger ones. Electrophoresis was carried out using running buffer containing (per 1L of distilled water) 1g SDS, 3g Tris and 14.4g Glycine, at a voltage of 100V for 20 minutes for stacking which was then increased to 150V for 30-45 minutes. Proteins were transferred to nitrocellulose using a constant current of 200mAmp for 2 hours. Transfer buffer contained (per 1L of distilled water) 3g Tris, 14.4g Glycine and 20% (v/v) methanol.

	10%
d.water	4.1ml
Lower buffer	3.1ml
30% acrylamide	3.7ml
10% SDS	110ul
TEMED	11ul
20% APS	55.3ul

Table 2.1 Composition of lower (resolving) gel.
Lower buffer consisted of 1.5M Tris at pH 8.8

	4%
d.water	2.8ml
Upper buffer	1.2ml
30% acrylamide	830ul
10% SDS	50ul
TEMED	5.3ul
20% APS	50ul

Table 2.2 Composition of upper (stacking) gel.
Upper buffer consisted of 0.5M Tris at pH 6.8

2.4.1.3 Immunoblotting

Membranes were blocked with either 5% (w/v) skimmed dried milk in PBS or 5% (w/v) bovine serum albumin (BSA) in PBS for 1 hour at room temperature with agitation. Membranes were incubated in various primary antibodies diluted in 1% (w/v) skimmed dried milk in PBS. Primary antibodies were applied at 4°C, with rotation, overnight (see Table 2.3 for primary antibodies used in this study). Following three 10 minute washes in PBS containing 0.05% Tween-20 (PBST) to remove any unbound or non-specific primary antibody, membranes were incubated with horseradish peroxidase (HRP) conjugated secondary antibodies (Thermo Scientific, all used at 1:1000) diluted in 1% (w/v) dried skimmed milk in PBS for 1

hour at room temperature with agitation (see Table 2.4 for secondary antibodies used in this study). Membranes were washed with two 10 minute washes of PBST to remove any unbound or non-specific secondary antibody followed by one 10 minute wash in PBS to remove residual Tween-20 (which can cause a high background signal). Membranes were then incubated with enhanced chemoluminescence (ECL) reagent (GE Healthcare) for one minute before exposing film to the membranes and developing the film. Developed films were scanned using a flat bed scanner and densities of bands were measured using Scion image software.

2.4.2 Analysis of samples from post-mortem human brain tissue

This work was carried out in the lab of Dr Diane Hanger, MRC Centre for Neurodegeneration Research, Institute of Psychiatry, King's College London under the supervision of Dr Wendy Noble and Dr Diane Hanger. Post-mortem frontal cortex tissue from clinically and pathologically confirmed human AD patients and age-matched control subjects was provided by the MRC Neurodegenerative Diseases Brain Bank at the Institute of Psychiatry, King's College London, UK. Written consent was obtained from each subject and/or their families for the purpose of this study. This study was conducted according to the principles expressed by the Declaration of Helsinki.

2.4.2.1 Protein extraction from human post-mortem brain tissue

Human cortex tissue was homogenized on ice at 200 mg/mL (w/v) in modified radioimmunoprecipitation assay buffer (mRIPA) containing 50mM Tris-HCl pH8,

150mM Sodium Chloride (NaCl), 2mM EGTA, 1mM phenyl methane sylfonyl fluoride (PMSF), 10mM NaF, 1mM Na_3VO_4, 1% nonidet P-40, 0.5% sodium deoxycholate ($C_{24}H_{39}O_4Na$), 0.1% SDS and 'Complete' protease inhibitor cocktail lacking EGTA and PMSF (Roche, three tablets per 50ml) using a polytron mechanical homogeniser. PMSF is a serine protease inhibitor, nonidet P-40 is a detergent used for solubilising membranes, sodium deoxycholate is an ionic detergent useful for disrupting and dissociating protein interactions; it is more severe than nonidet P-40 and was included to ensure complete lysis. Homogenates were centrifuged at 13000rpm for 30 minutes and the supernatant was removed. Supernatants were mixed 1:1 with 2x SDS loading dye. 5ul of each sample (approximately 10ug protein) was run on a 10% SDS-PAGE gel and immunoblotted with neuron specific enolase (NSE) primary antibody and a fluorescent conjugated secondary antibody. Membranes were scanned and quantified (see section 2.4.2.2) and subsequent loading was normalised for NSE signal. NSE was chosen for normalisation in order to control for the loss of neurons in AD samples.

2.4.2.2 Sodium dodecyl sulphate polyacrylamide gel electrophoresis (SDS-PAGE) and immunoblotting

SDS-PAGE and immunoblotting was carried out essentially as described in sections 2.4.1.2 and 2.4.1.3 with the following exceptions:

- The apparutus used was the Novex system and all gels consisted of 10% stacking gel and 4% resolving gel.
- SeeBlue Plus2 Pre-Stained Standard (Invitrogen) was used as a molecular weight marker.

- A gel-to-gel loading control was included in order to facilitate normalisation of samples across membranes. This was necessary as the size of the data set necessitated splitting the samples over three gels.
- Membranes were blocked in either 5% (w/v) dried skimmed milk in PBS or Odyssey blocking buffer (made according to manufacturer's instructions) for 1 hour at room temperature with agitation – see Table 2.3 for further details.
- Due to poor signal, some primary antibodies were diluted in Odyssey blocking buffer – see Table 2.3 for further details.
- Fluorescent conjugated secondary antibodies (see Table 2.4. for details) were used followed by scanning of membranes on an Odyssey infrared scanner and quantification of band intensities using Odyssey software (version 3). Membranes were then re-blocked and re-probed for the appropriate loading control and scanned and quantified as before.

2.4.3 Primary antibodies used in this study

Antibody	Source	Species	Application	Blocking	Dilution	Incubation time
pS262 tau	Invitrogen	Rabbit polyclonal	Drosophila	5% milk	1:1000 in 1% milk	Overnight 4°C
			Human	5% milk	1:1000 in 1% milk	
T46 (total tau)	Abcam	Mouse monoclonal	Drosophila	5% milk	1:1000 in 1% milk	Overnight 4°C
BRSK2 N-term	Kind gift of Dr C Sutherland	Sheep polyclonal	Drosophila	5% milk	1:1000 in 1% milk	Overnight 4°C
			Human	Odyssey block	1:500 in odyssey block	
BRSK2 C-term	Kind gift of Dr C Sutherland	Sheep polyclonal	Human	5% milk	1:1000 in 1% milk	Overnight 4°C
Actin	Abcam	Rabbit polyclonal	Drosophila	5% BSA	1:2500 in 1% milk	Overnight 4°C
NSE	Dako	Mouse monoclonal	Human	5% milk	1:10000 in 1% milk	1hr room temperature
LKB1	Kind gift of Dr C Sutherland	Sheep polyclonal	Human	Odyssey block	1:500 in odyssey block	Overnight 4°C
pLKB1	Abcam	Rabbit polyclonal	Human	Odyssey block	1:500 in odyssey block	Overnight 4°C
CaMKK	Kind gift of Dr J Hastie	Sheep polyclonal	Human	5% milk	1:1000 in 1% milk	Overnight 4°C
Total tau	Dako	Mouse monoclonal	Human	5% milk	1:20000 in 1% milk	Overnight 4°C or 1hr room temperature
PHF1	Kind gift of Prof P Davies	Rabbit polyclonal	Human	5% milk	1:200 in 1% milk	Overnight 4°C

Table 2.3 Primary antibodies used in this study.
A table showing the primary antibodies used, their source, species and application, the appropriate block, the dilution and the incubation time and temperature.

2.4.4 Secondary antibodies used in this study

Antibody	Source	Species	Application	Dilution	Incubation
anti-rabbit-HRP	Thermo Scientific	Rabbit	*Drosophila*	1:1000 in 1% milk	1hr room temperature
anti-mouse-HRP	Thermo Scientific	Mouse	*Drosophila*	1:1000 in 1% milk	1hr room temperature
anti-sheep-HRP	Thermo Scientific	Sheep	*Drosophila*	1:1000 in 1% milk	1hr room temperature
anti-rabbit 800	Rockland	Goat	Human	1:5000 in 1% milk	1hr room temperature
anti-sheep 680	Invitrogen	Sheep	Human	1:5000 in 1% milk	1hr room temperature
anti-mouse 800	LICOR	Mouse	Human	1:5000 in 1% milk	1hr room temperature
anti-mouse 680	Invitrogen	Goat	Human	1:5000 in 1% milk	1hr room temperature

Table 2.4 Secondary antibodies used in this study.
A table showing the secondary antibodies used, their source, species and application, the appropriate block, the dilution and the incubation time and temperature.

2.4.5 Recombinant BRSK2 degradation assay

Recombinant BRSK2 protein (10ng/µl) was incubated at 37°C in a water bath. At 0, 1, 2, 4 and 8 hours a 15µl aliquot was removed, placed on ice and SDS sample buffer was added. Equal amounts of protein from each timepoint were analyzed by SDS-PAGE as described in section 2.4.1.2.

2.4.6 Calpain Assay

Method adapted from Patzke and Tsai (2002). Briefly, in calpain reaction buffer (100mM imidazole, 5mM L-cystein and 5mM calcium chloride, pH 7.5) 100ng purified recombinant BRSK2 protein was incubated with increasing concentrations of Calpain-2 (Calbiochem) in the presence or absence of the calpain inhibitor, calpeptin (Calbiochem). Reactions were incubated at 30°C (in a water bath) for 1 hour. Reactions were terminated by the addition of SDS sample buffer and equal amounts of the reactions were analyzed by SDS-PAGE as described in section 2.4.1.2.

3| Cloning of human and *Drosophila* gene sequences into the *Drosophila* expression vector, pUAST.

3.1 Introduction

In order to investigate the effect of co-expression of various human genes (BRSK1, BRSK2, CaMKKα, LKB1) and endogenous *Drosophila* CG6114 (the *Drosophila* homologue of BRSK) with human tau in the *Drosophila* eye, flies which were capable of expressing the genes were constructed. This was achieved by cloning the genes into the *Drosophila* expression vector, pUAST. pUAST is a *Drosophila* vector that confers GAL4 inducibility (Brand and Perrimon, 1993). In the following sections are schematics for the cloning of BRSK1, BRSK2, CaMKKα, LKB1 and CG6114 into the pUAST vector. This chapter serves as a record of the cloning and subsequent transgenic flies used in this thesis.

Two methods were utilised for the cloning of human gene sequences into pUAST. The first method (used for BRSK1, BRSK2 and CG6114 constructs) involved the use of restriction enzymes to release the gene of interest from the construct and ligation of this fragment into pUAST which had been digested with the same enzymes (or enzymes which were isocaudomers). The second method (used for CaMKKα and LKB1 constructs) utilised PCR in order to amplify the sequences. This method was used as cloning of the CaMKKα and LKB1 genes required the insertion of a Kozak sequence, which was absent from the mammalian CaMKKα and LKB1 clones, upstream of the gene in order to ensure that the gene was recognised and able to be expressed and functional in *Drosophila*. Although there is a consensus Kozak sequence for use in *Drosophila*, the BRSK2 Kozak sequence was chosen as the BRSK2 transgenic flies had already been proven to be expressing and functional.

Prospective clones were confirmed with restriction enzyme digests and sequencing, and subsequently the DNA was sent to Best Gene Inc. for transgenesis. Please see Appendix 3 for a list of primers used in this work.

3.2 BRSK1

Four pCMV5.BRSK1 constructs (kind gifts of Prof. Dario Alessi, University of Dundee) were available for cloning; wild type (B-WT), constitutively active (B-CA), kinase dead (B-KD) and non-phosphorylatable (B-NP), see Table 3.1 for a list of the amino acid and DNA codon changes. B1-CA has a conserved threonine (T) residue in the T-loop mutated to glutamic acid (E) in order to mimic phosphorylation. In B1-WT, this threonine residue requires phosphorylation by an upstream kinase in order for BRSK to become active. B1-NP has the same threonine residue mutated to alanine (A), which prevents the residue from becoming phosphorylated and thus causes BRSK to be inactive. Recombinant B1-CA and B1-NP constructs were tested using *in vitro* kinase assays in order to show that the mutations resulted in a functional change (Lizcano et al., 2004). B1-KD has an aspartic acid (D) residue mutated to alanine which prevents BRSK from utilising ATP in order to phosphorylate other proteins, rendering BRSK KD. The B1-KD construct has also been tested using *in vitro* kinase assays and has been confirmed to be inactive (personal communication, Prof Dario Alessi).

Construct	Amino acid change	DNA codon change
B1-CA	T189E	ACC to GAG
B1-KD	D174A	GAC to GCC
B1-NP	T189A	ACC to GCC

Table 3.1 BRSK1 amino acid and DNA codon changes.
Mutations made in wild type BRSK1 to produce B1-CA, B1-KD and B1-NP constructs.

BRSK1 genes were released from the pCMV5 plasmids via restriction enzyme digest with *Eco*RI and *Bam*HI, yielding a fragment (2376bp) containing the BRSK1 gene. The *Drosophila* vector, pUAST, was linearised using *Eco*RI and *Bgl*II and subsequently treated with bacterial alkaline phosphatase (BAP) to prevent re-ligation. *Bgl*II and *Bam*HI are isocaudomers, and as such recognise slightly different sequences (AGATCT and GGATCC respectively) but produce the same sticky ends. The purified BRSK1 fragments were ligated to the linearised pUAST to create pUAST.BRSK1.

Restriction enzyme digest of possible clones were designed so that digestion of a positive clone with *Eco*RI and *Xba*I would release a 2403bp fragment and digestion with *Xho*I would yield a 959bp fragment (see Figure 3.2 for an example digest) – fragments which would differ in size from those produced by digestion of either empty pUAST vector or pCMV5.BRSK1.

Having verified the clones by restriction enzyme digest, the DNA was sequenced using primers 1 a), 1 b) and 1 c) to confirm the ligation and maintenance of the mutation sites.

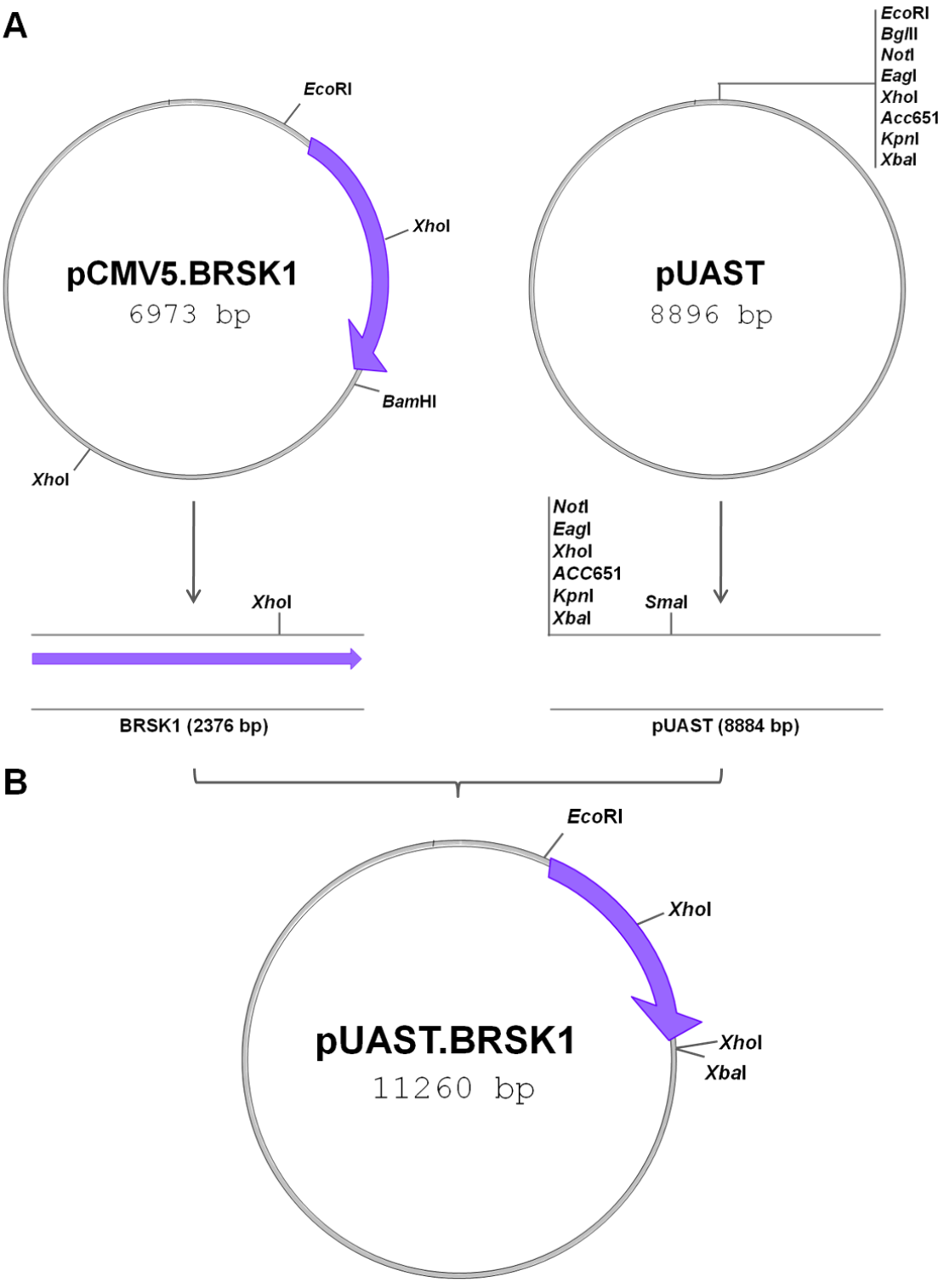

.

Figure 3.1 Schematic for cloning of BRSK1 into pUAST.

A. pCMV5.BRSK1 constructs were digested with EcoRI and BamHI to release a 2376bp fragment containing the BRSK gene. pUAST plasmid was linearised with EcoRI and BglII.

B. The BRSK1 fragment and the linearised pUAST were ligated to create pUAST.BRSK1.

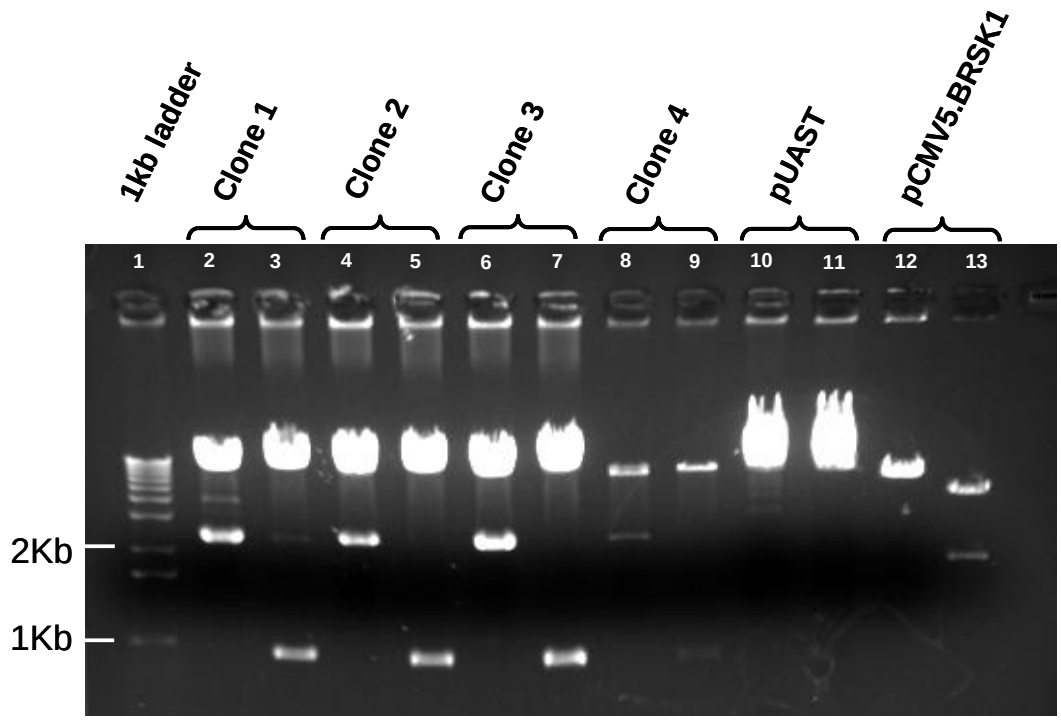

Figure 3.2 Enzyme digest of pUAST.BRSK1 clones.
Agarose gel containing ethidium bromide in order to stain DNA fragments. Lanes 2, 4, 6, 8, 10 and 12 digested with EcoRI and XbaI (to yield a 2403bp fragment from positive clones). Lanes 3, 5, 7, 8, 9, 11 and 13 digested with XhoI (to yield a 959bp fragment from positive clones). pUAST and pCMV5.BRSK1 included as controls.

3.3 BRSK2

As with BRSK1, four pCMV5.BRSK2 constructs (kind gifts of Prof. Dario Alessi, University of Dundee) were available for cloning; B2-WT, B2-CA, B2-KD and B2-NP, see Table 3.2 for a list of the amino acid and DNA codon changes. Recombinant B2-CA and B2-NP constructs have previously been tested using *in vitro* kinase assays in order to confirm that the mutations resulted in functional changes (Lizcano et al., 2004). The B2-KD construct has also been tested using *in vitro* kinase assays and has been confirmed to be inactive (personal communication, Prof Dario Alessi).

Construct	Amino acid change	DNA codon change
B2-CA	T174E	ACC to GAA
B2-KD	D159A	GAC to GCC
B2-NP	T174A	ACC to GCC

Table 3.2 BRSK2 amino acid and DNA codon changes.
Mutations made in wild type BRSK2 to produce B2-CA, B2-KD and B2-NP constructs.

BRSK2 genes were cloned in a similar way to BRSK1. Enzyme digestion of pCMV5.BRSK2 plasmids with *Eco*RI and *Not*I released a fragment (2077bp) containing the BRSK2 sequence. pUAST, was linearised using *Eco*RI and *Not*I and BAP treated. The two DNA fragments were then ligated to create pUAST.BRSK2.

As with BRSK1, restriction enzyme digest of possible clones were designed so that digestion of a positive clone with *Eco*RI and *Not*I would release a 2077bp fragment and digestion with *Sma*I would yield a 3640bp fragment (see Figure 3.4 for an

example digest) - fragments which would be different in size from those resulting from digestion of either empty pUAST vector or pCMV5.BRSK2.

Having verified the clones by restriction enzyme digest, the DNA was sequenced using primers 2 a), 2 b) and 2 c) to confirm the ligation and maintenance of the mutation sites.

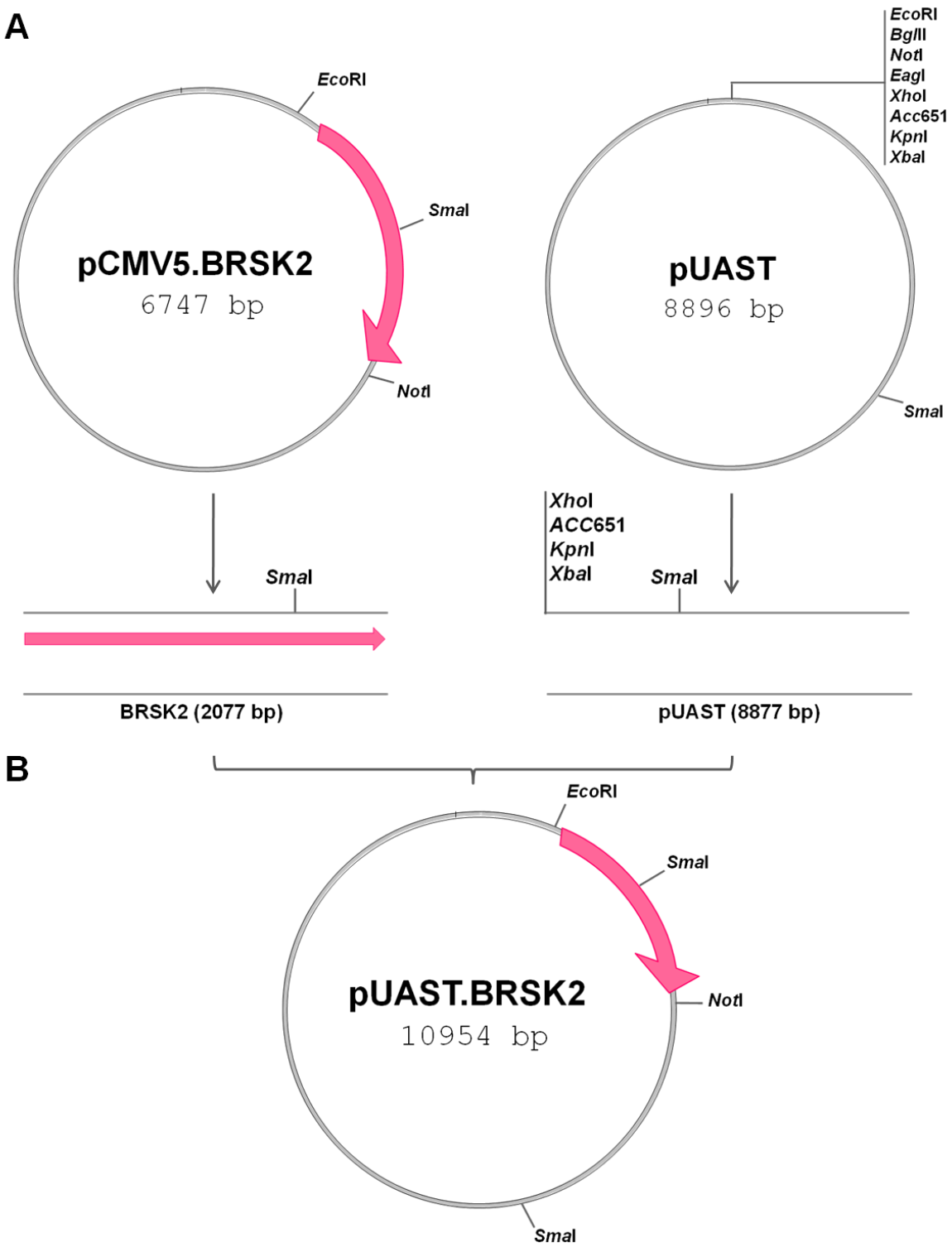

Figure 3.3 Schematic for cloning of BRSK2 into pUAST.
A. BRSK2 constructs were digested with EcoRI and NotI to release a 2077bp fragment containing the BRSK gene. pUAST plasmid was linearised with EcoRI and NotI.
B. The BRSK2 fragment and the linearised pUAST were ligated to create pUAST.BRSK2.

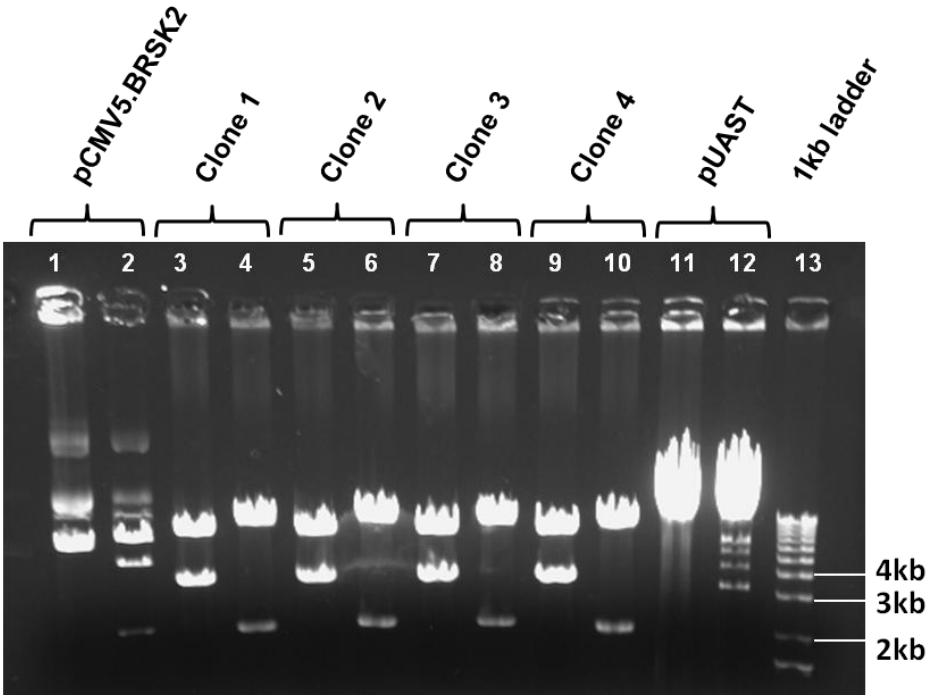

Figure 3.4 Enzyme digest of pUAST.BRSK2 clones.
Agarose gel containing ethidium bromide in order to stain DNA fragments. Lanes 2, 4, 6, 8, 10 and 12 digested with EcoRI and NotI (to yield a 2077bp fragment from positive clones). Lanes 1, 3, 5, 7, 8, 9, and 11 digested with SmaI (to yield a 3640bp fragment from positive clones). pUAST and pCMV5.BRSK2 included as controls.

3.4 Genotyping the BRSK transgenic flies

Upon receipt of the BRSK flies, it was important to confirm that BestGene Inc. had used the correct DNA for transgenesis and that the mutation sites in the BRSK isoforms had been maintained. This was done by genomic PCR using primers 3 a) and 3 b) to amplify a fragment of 492bp from BRSK1 genomic DNA and primers 4 a) and 4 b) to amplify a 990bp fragment from BRSK2 genomic DNA. Subsequently, primer 3 a) was used for direct sequencing of the BRSK1 PCR products and primer 5 a) was used for sequencing the BRSK2 products. Figure 3.5 shows the results for BRSK1 flies and Figure 3.6 the results for BRSK2 flies.

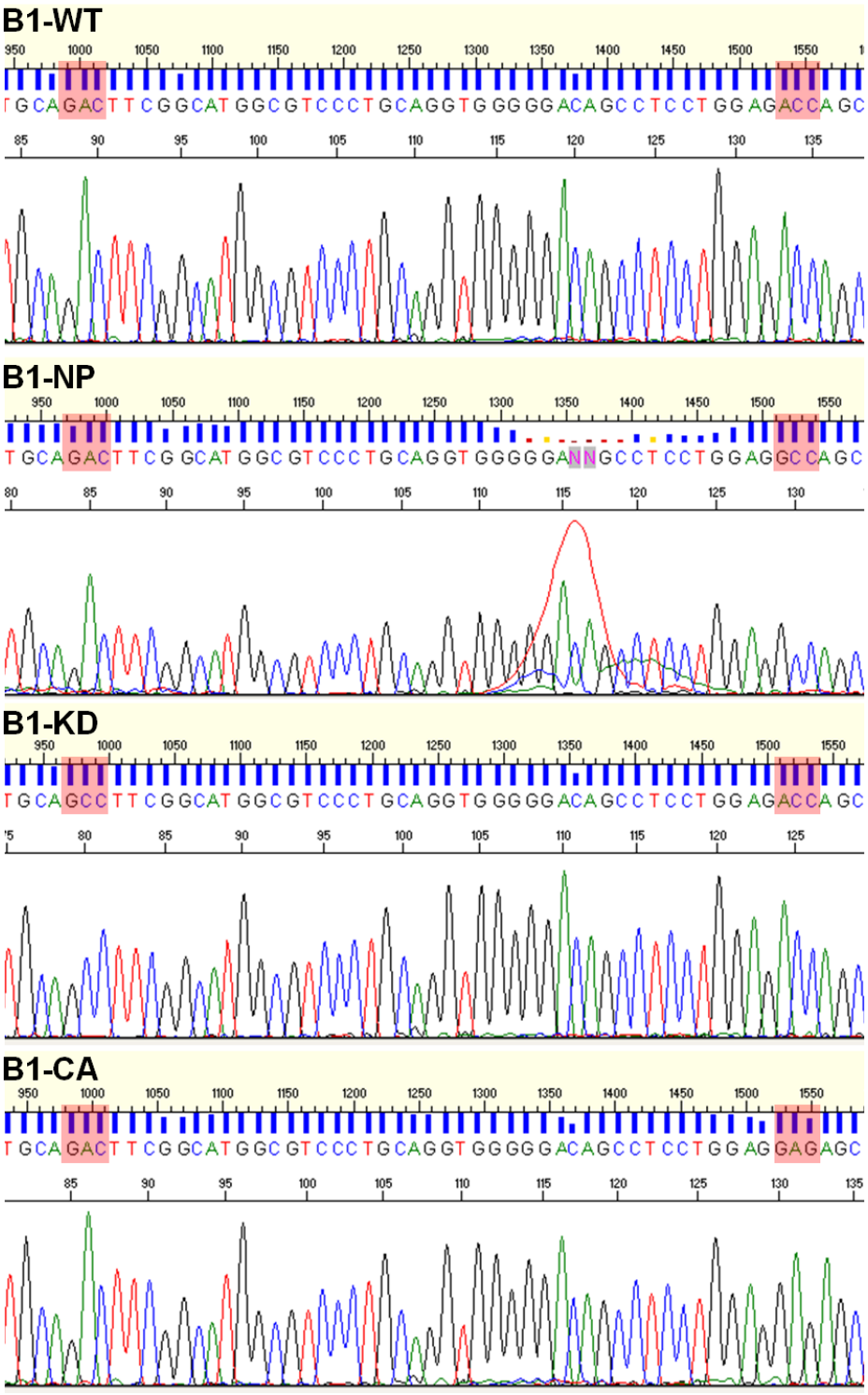

Figure 3.5 BRSK1 genotyping.
Sequences from genotyping of B1-WT, B1-NP, B1-KD and B1-CA transgenic flies. Highlighted in red in the B1-WT sequence, are the two possible mutation sites; GAC (aspartic acid, on the left) and ACC (threonine, on the right). B1-NP is wild type for the GAC site but has an ACC to GCC mutation (threonine to alanine). B1-KD has a GAC to GCC mutation (aspartic acid to alanine) and is wild type for the ACC site. B1-CA is wild type for the GAC site and has an ACC to GAG mutation (threonine to glutamic acid).

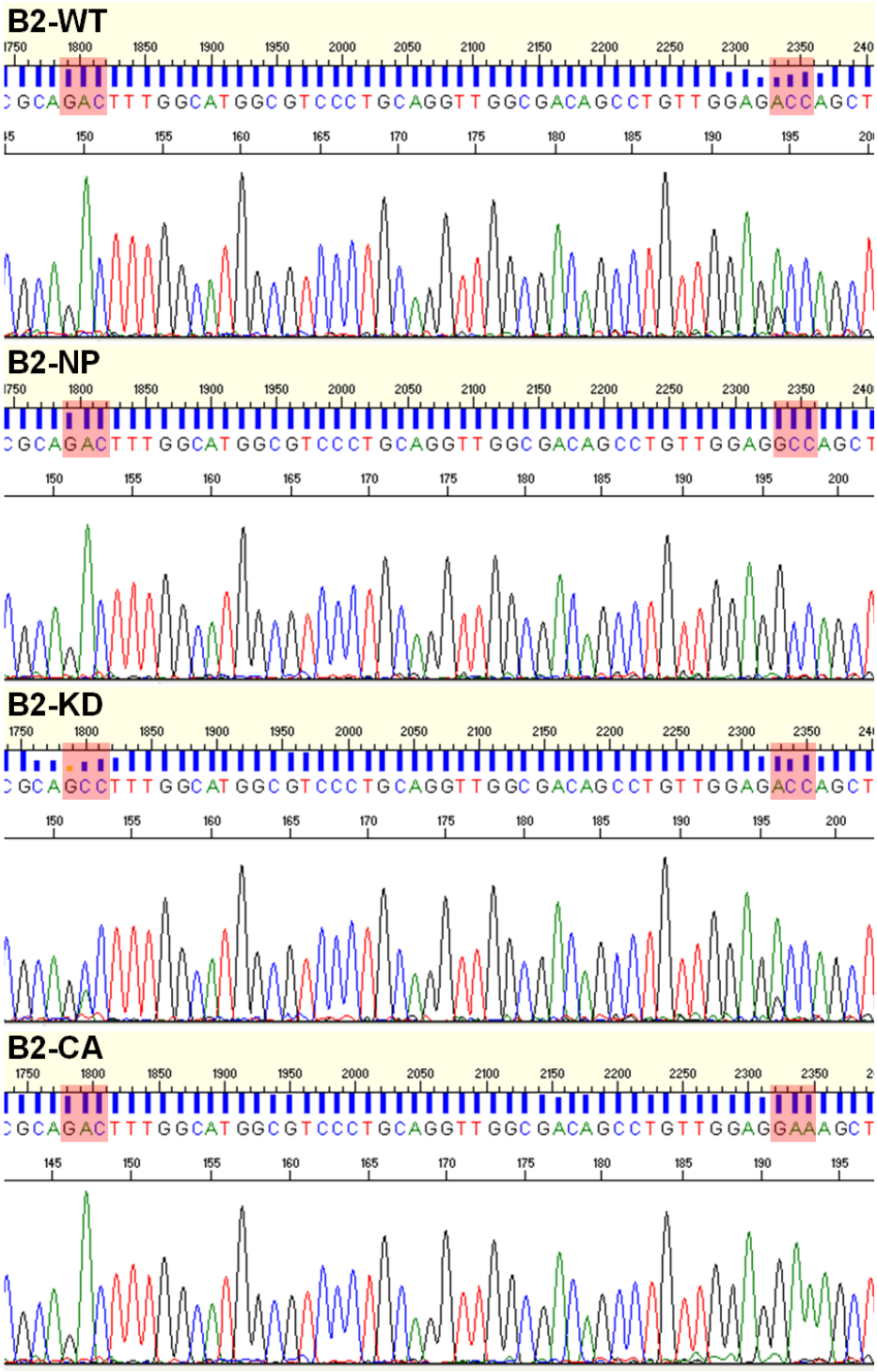

Figure 3.6 BRSK2 genotyping.
Sequences from genotyping of B2-WT, B2-NP, B2-KD and B2-CA transgenic flies. Highlighted in red in the B2-WT sequence, are the two possible mutation sites; GAC (aspartic acid, on the left) and ACC (threonine, on the right). B2-NP is wild type for the GAC site but has an ACC to GCC mutation (threonine to alanine). B2-KD has a GAC to GCC mutation (aspartic acid to alanine) and is wild type for the ACC site. B2-CA is wild type for the GAC site and has an ACC to GAA mutation (threonine to glutamic acid).

3.5 BRSK transgenic line assessment and selection

Due to the redundancy exhibited between BRSK1 and 2 in mammals, most of the experiments in this thesis have been conducted using BRSK2. However, in order to gain some insight into whether BRSK1 and 2 were capable of performing the same function in *Drosophila*, BRSK1 lines were also assessed for their eye phenotype during the selection of BRSK2 lines.

BLASTp showed that BRSK2 has slightly higher sequence identity with CG6114 than BRSK1 (maximum score of 585 with 88% coverage for BRSK2 and maximum score of 572 with 77% coverage for BRSK1).

All BRSK1 and BRSK2 lines were crossed to a line carrying the GMR::GAL4 driver on the second chromosome and the 0N4R isoform of human tau on the third chromosome and the resulting eye phenotypes were scored according to the scale demonstrated in Figure 3.7.

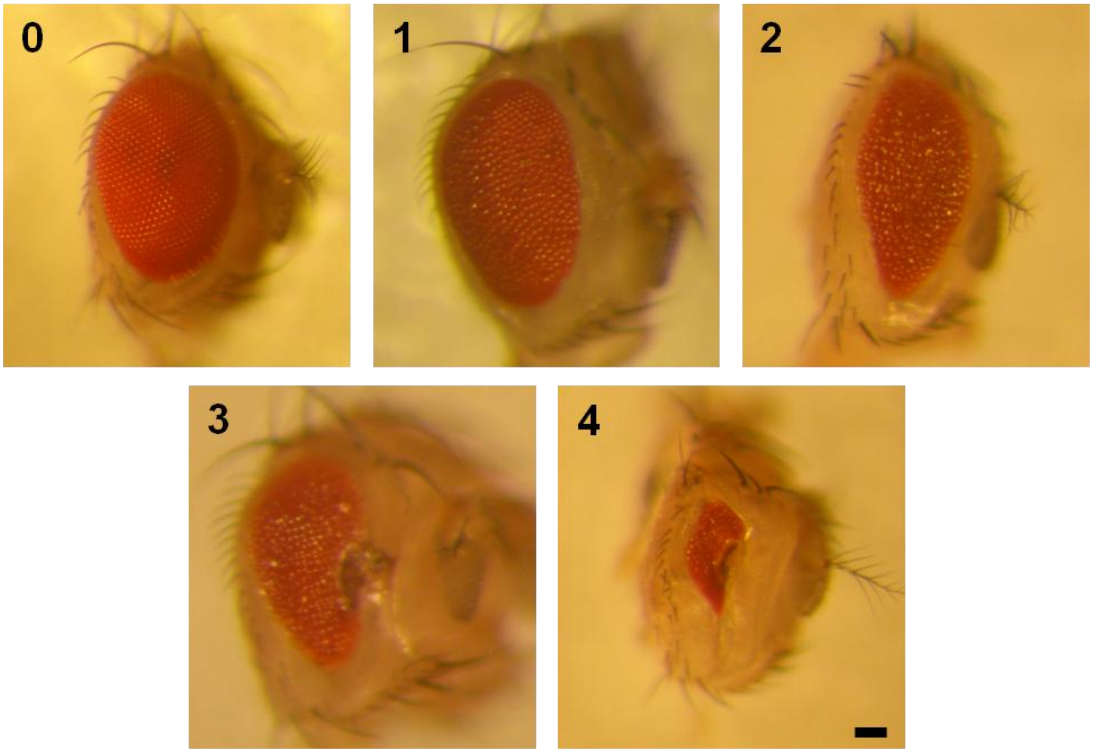

Figure 3.7 Light microscope images of fly eyes to demonstrate the scale used for phenotypic scoring.
The scale used for phenotypic scoring of fly eyes was as follows: 0 – Not rough, 1 – Slightly rough, 2 – Very rough, no signs of necrosis, 3 – Very rough, signs of necrosis, 4 - Very rough, signs of necrosis, eye very small. Scale bar 100µm applies to all panels.

Tables 3.3 and 3.4 show the phenotypic scoring for BRSK1 and BRSK2 flies respectively.

Fly no.	BRSK1 WT Line No.							BRSK1 KD Line No.		BRSK1 NP Line No.			BRSK1 CA Line No.	
	2	3	5	6	7	8	10	6	7	3	4	5	1	2
1	3	3	3	3	3	3	4	2	2	2	2	2	2	2
2	3	3	4	3	2	4		2	2	2	3	2	2	2
3	3	2	4	3	2	3		2	2	2	2	2	2	2
4	3	3	3	2	3	3		2	3	2	2	2	2	2
5	3	2	3	3	3	3		2	2	3	2	3	3	2
6	2	2	4	2	3	4		2	2	3	2	2	2	2
7	2	2	4	3	3	4		2	2	2	2	2	2	3
8	3	3	4	3	2	3		2	2	2	2	2	2	2
9	2	3	3	2	3	3		2	2	2	2	2	2	2
10	3	3	4	3	3	3		2	2	2	2	3	2	3

Table 3.3 Phenotypic scoring of BRSK1.
BRSK1 lines were crossed to GMR;tau and the resulting eye phenotypes scored according to the previously described scale.

Fly No.	BRSK2 WT Line No.					BRSK2 KD Line No.						BRSK2 NP Line No.						BRSK2 CA Line No.				
	1	2	3	4	5	1	3	4	5	7	9	1	2	3	4	6	8	4	5	7	8	10
1	3	3	3	4	3	3	2	2	2	3	2	2	2	3	2	2	3	3	3	3	3	2
2	3	3	3	3	3	2	2	2	2	2	2	2	2	2	2	2	2	3	3	3	3	2
3	2	3	3	2	3	3	2	2	2	2	2	2	3	2	2	2	2	2	2	2	2	2
4	2	2	3	3	4	2	2	2	2	2	2	2	2	2	2	3	2	2	3	2	3	2
5	3	2	2	3	3	2	2	2	2	2	2	2	2	2	2	2	2	2	3	2	2	2
6	2	3	2	3	4	2	2	2	2	2	2	2	3	2	2	2	2	2	2	2	2	3
7	3	4	2	2	3	2	2	2	2	2	2	2	2	2	2	2	2	2	2	2	2	2
8	4	4	3	3	3	2	3	2	3	2	2	2	2	3	2	2	2	2	2	2	2	2
9	4	4	3	3	4	2	2	2	2	2	2	2	2	2	2	2	2	2	2	2	2	2
10	3	3	4	3	3	2	2	2	2	2	2	2	2	2	2	2	2	2	2	2	2	2

Table 3.4 Phenotypic scoring of BRSK2.
BRSK2 lines were crossed to GMR;tau and the resulting eye phenotypes scored according to the previously described scale.

Comparison of the scoring for the BRSK1 and BRSK2 flies, showed that the mutated isoforms of BRSK were capable of producing a similar phenotype, with B-WT isoforms (BRSK1 and BRSK2) having a consistently higher score than either B-NP, B-KD or B-CA. However, this was a surprising result in that B-CA did not appear to have a higher score than B-NP or B-KD. This suggested that the B-CA mutation may not be functional in the transgenic flies.

From the phenotypic scoring in Table 3.4, the BRSK2 lines selected for further use were B2-WT line 5, B2-NP line 4, B2-KD line 4 and B2-CA line 5, henceforth referred to as B-WT, B-NP, B-KD and B-CA respectively. BRSK2 lines were selected on the basis that the flies exhibited a robust and reproducible phenotype. All lines selected had the BRSK2 insertion on the 3rd chromosome in order to minimise any chromosome-specific expression effects.

In addition, with a view to conducting experiments with BRSK and 0N4R human tau in the nervous system, B-WT (line5) and CG6114 RNAi (CG6114 is the *Drosophila* homologue of human BRSKs) were crossed to a number of neuronal GAL4 drivers (elav::GAL4 which expresses in the CNS, tub::GAL4 which expresses everywhere that tubulin is expressed, cha::GAL4 which expresses in cholinergic neurons, d42::GAL4 which expresses in motor neurons and 0k-6::GAL4 which expresses in a subset of motor neurons). However, over-expression of B-WT or knock-down of CG6114 using the aforementioned neuronal drivers was lethal at the embryonic stage and so these experiments were not pursued.

3.6 BRSK2 expression

In order to ascertain that the lack of phenotype in the B-NP and B-KD flies was in fact due to the mutations they carried and not due to a lower level of expression, western blots were carried out on lysates from each of the four selected BRSK2 lines. Figure 3.8 shows that the expression level of total BRSK2 in the four lines was not significantly different (n=3 0.59±0.10 for B-WT, n=3 0.74±0.13 for B-NP, n=3 0.64±0.12 for B-KD and n=3 0.61±0.02 for B-CA, p=0.63 one way anova).

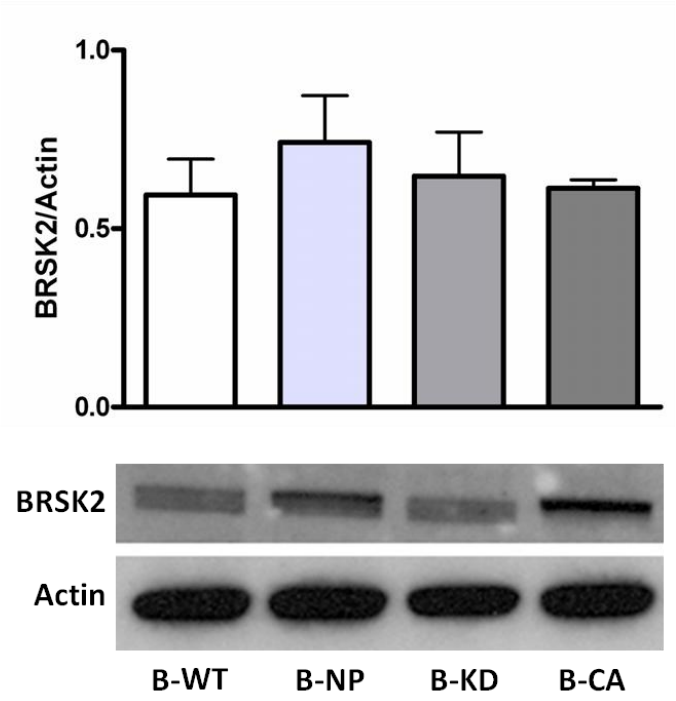

Figure 3.8 Western blots for BRSK2 and actin.
Quantification of western blots to show BRSK2 expression normalised to actin. One way anova analysis showed that expression was not significantly different (n=3 0.59±0.10 for B-WT, n=3 0.74±0.13 for B-NP, n=3 0.64±0.12 for B-KD and n=3 0.61±0.02 for B-CA, p=0.63 one way anova). Representative western blots shown.

3.7 CaMKK alpha

The cloning of CaMKKα into pUAST was done by Mrs Ellie Tucker under my supervision.

One of the upstream regulators of mammalian BRSK identified in the literature is calcium/calmodulin dependent kinase kinase alpha (CaMKKα). CaMKKα acts on BRSKs by phosphorylating the conserved T-loop threonine residue (T189 in BRSK1 and T174 in BRSK2), leading to the activation of BRSKs (Fujimoto et al., 2008).

In order to insert the BRSK2 Kozak sequence at the start of the CaMKK α gene, primers were designed to amplify the gene sequence via PCR. Primer 6 b) was used to engineer an *Eco*RI restriction enzyme site upstream of the BRSK2 Kozak sequence, onto the 5' end of the antisense strand and primer 6 a) was used to insert a *Not*I restriction enzyme site onto the 3' end of the sense strand. This approach allowed the successful PCR of the CaMKKα gene, downstream of the BRSK2 kozak sequence and the insertion of two different restriction enzyme sites allowed the subsequent restriction enzyme digestion and directional cloning of the PCR fragment into pUAST linearised with *Eco*RI and *Not*I. Figure 3.9 shows a schematic of the cloning of CaMKKα.

Restriction enzyme digest of possible clones were designed so that digestion of a positive clone with *Eco*RI and *Not*I would release a 1561bp fragment containing CaMKKα (see Figure 3.10 for an example digest).

Having verified the clones by restriction enzyme digest, the DNA was sequenced using primers 7 a) and 7 b) in order to confirm the ligation before being sent for transgenesis. However, it should be noted that the full CaMKKα insert was not sequenced.

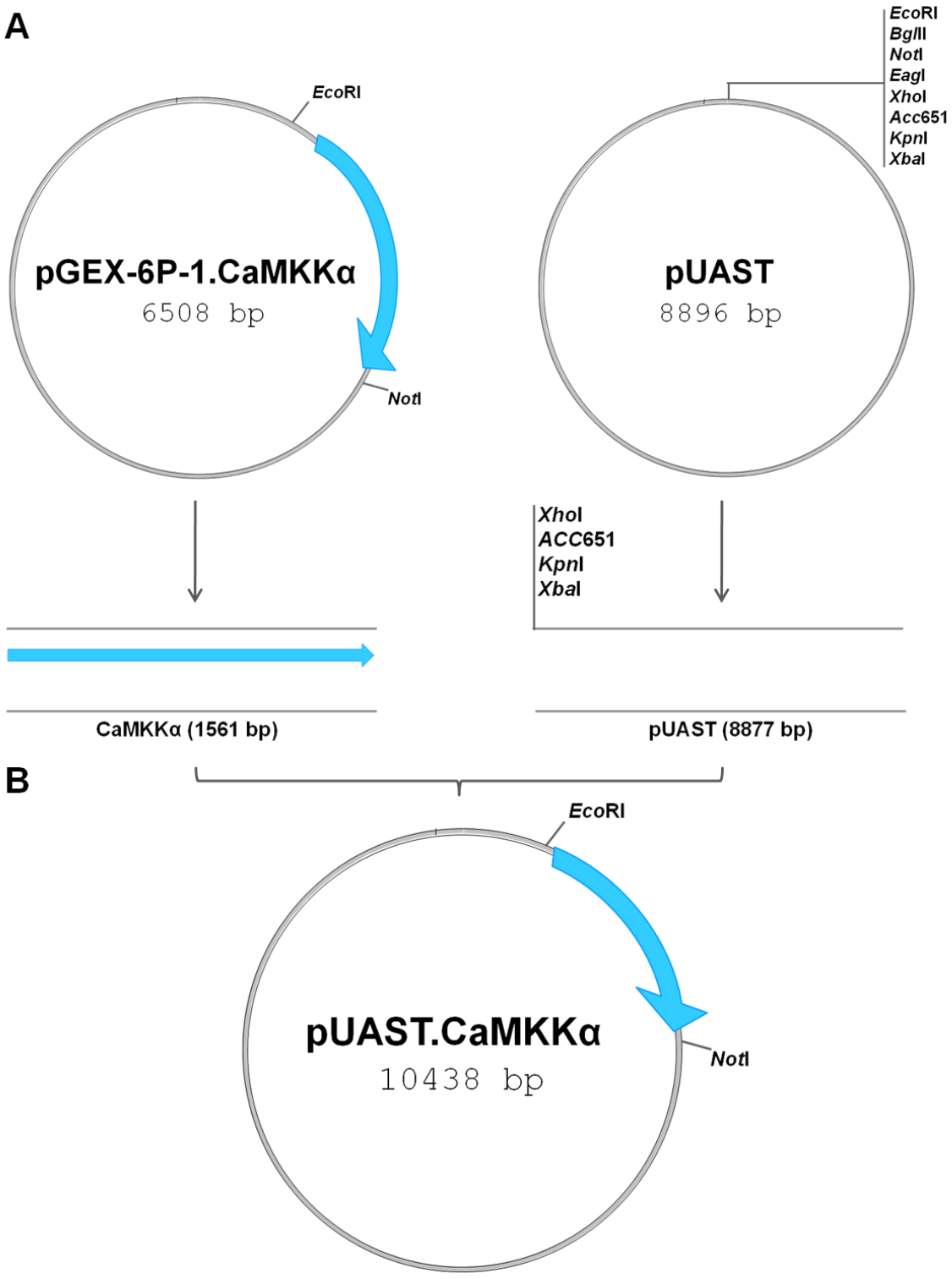

Figure 3.9 Schematic for cloning of CaMKKα into pUAST.
A. CaMKKα was amplified using PCR primers 6 a) and 6 b) and subsequently restriction enzyme digested using EcoRI and NotI. pUAST plasmid was linearised with EcoRI and NotI.
B. The CaMKKα fragment and the linearised pUAST were ligated to create pUAST.CaMKKα.

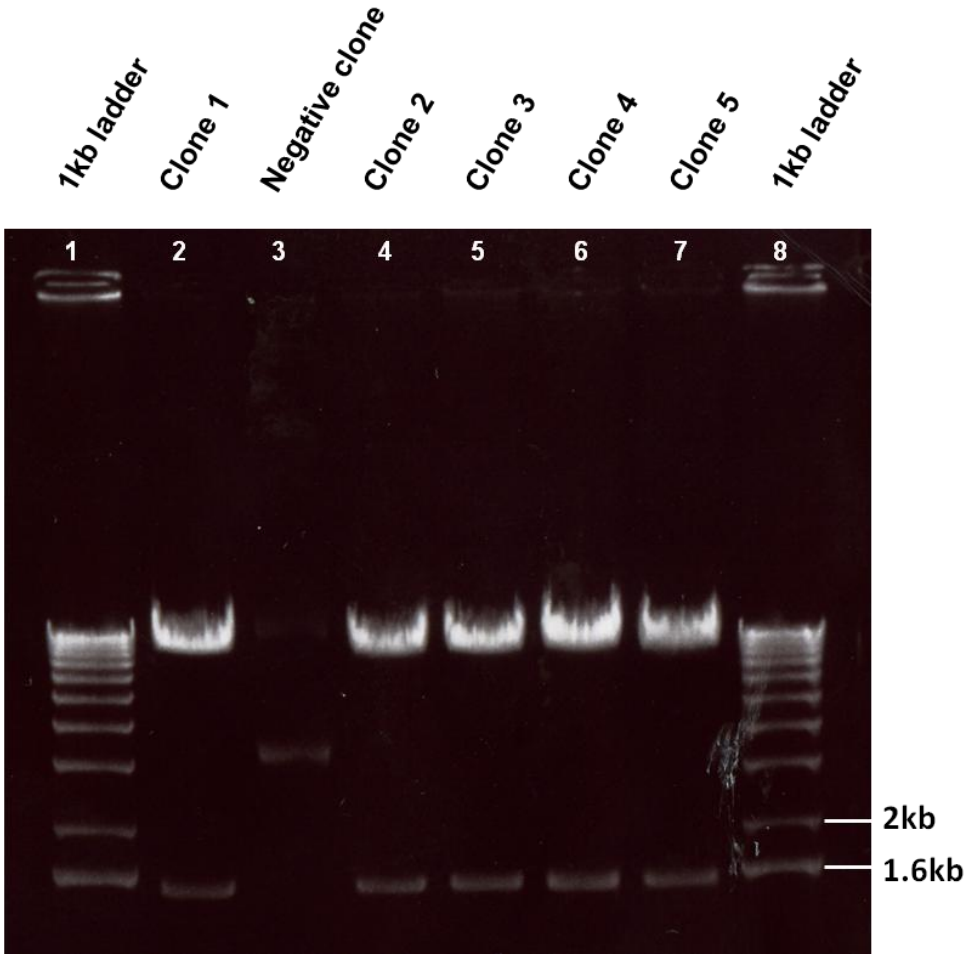

Figure 3.10 Enzyme digest of pUAST.CaMKKα clones.
Agarose gel containing ethidium bromide in order to stain DNA fragments. Lanes 2, 3, 4, 5, 6 and 7 digested with EcoRI and NotI (to yield a 1561bp fragment from positive clones). Lane 3 shows a negative clone, lanes 2, 4, 5, 6 and 7 show positive clones.

3.8 LKB1

Another regulator of mammalian BRSKs identified in the literature is LKB1, which has the same mode of action on BRSK as CaMKKα (Lizcano et al., 2004). LKB1 is a master kinase of the AMPK family of protein kinases.

LKB1 was cloned using the same method as was used for CaMKKα: primer 8 b) was used in order to engineer an *Eco*RI restriction enzyme site upstream of the BRSK2 Kozak sequence onto the 5' end of the antisense strand and primer 8 a) was used to insert a *Not*I restriction enzyme site onto the 3' end of the sense strand. As for CamKKα, this approach allowed the successful PCR of the LKB1 gene, downstream of the BRSK2 Kozak sequence and the insertion of two different restriction enzyme sites allowed the subsequent restriction enzyme digestion and directional cloning of the PCR fragment into pUAST linearised with *Eco*RI and *Not*I. Figure 3.11 shows a schematic of the cloning of LKB1.

Due to the presence of only a few colonies on the transformation plates, pUAST.LKB1 was sequenced using primers 9 a) and 9 b) without being restriction enzyme digested.

LKB1 transgenic flies were not used for any experiments in this thesis, but the cloning is included here as a record of how the LKB1 transgenic flies were constructed.

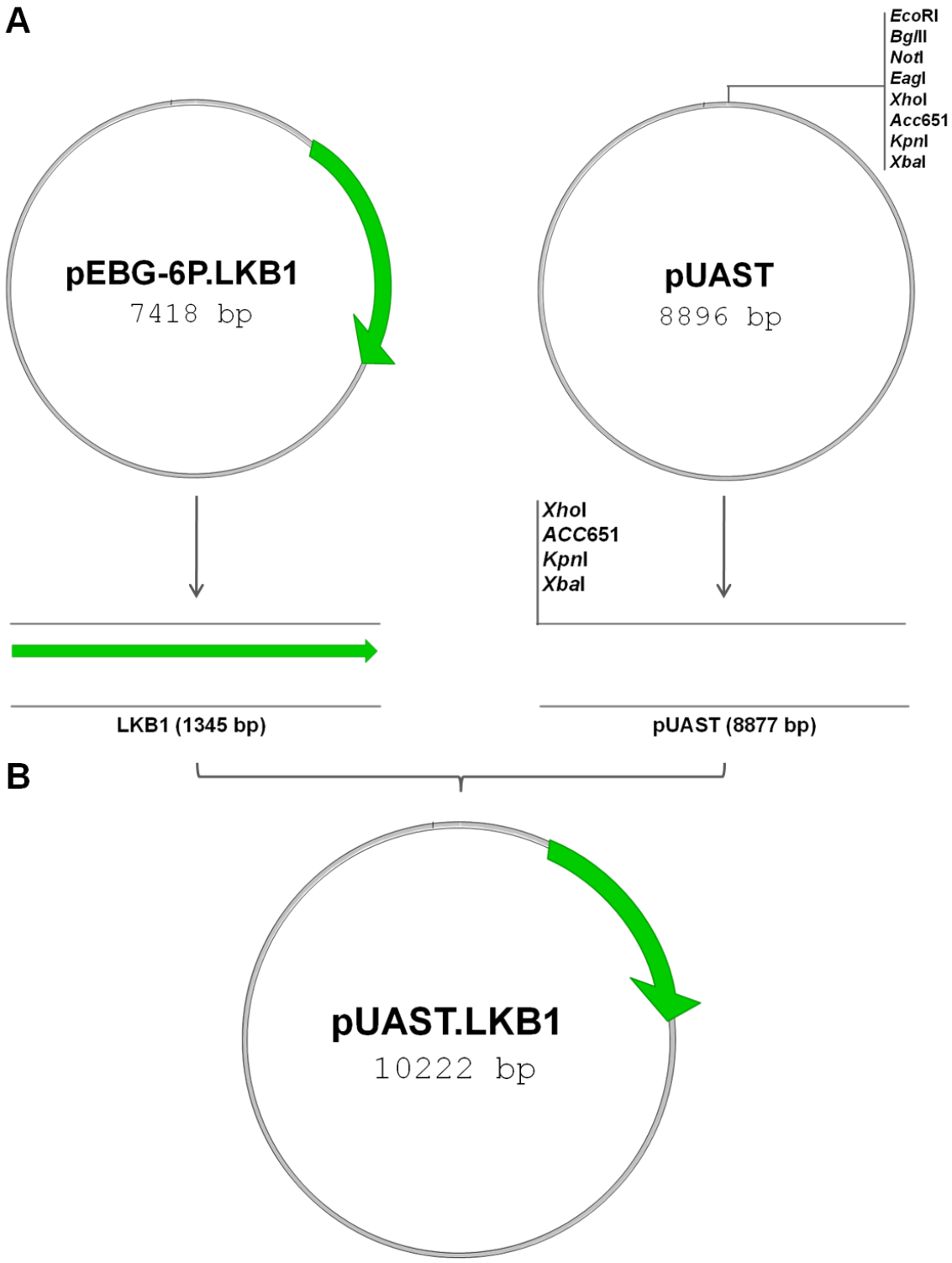

Figure 3.11 Schematic for cloning of LKB1 into pUAST.
A. LKB1 was amplified using PCR primers 8 a) and 8 b) and subsequently restriction enzyme digested using EcoRI and NotI. pUAST plasmid was linearised with EcoRI and NotI.
B. The LKB1 fragment and the linearised pUAST were ligated to create pUAST.LKB1.

3.9 CG6114

CG6114 is the *Drosophila* homologue of BRSKs and was cloned in order to ascertain if CG6114 was capable of interacting with human tau in the same way that is seen for other *Drosophila* kinases such as shaggy (GSK3-β homologue) and PAR-1.

Figure 3.12 shows a schematic for the cloning of CG 6114 into pUAST.

As with previous clones, restriction enzyme digests were designed so that digestion of a positive clone with *Eco*RI and *Xba*I would release a 2548bp fragment and digestion with *Xho*I would release fragments of 578bp and 1162bp in length (see Figure 3.13 for an example digest).

Having verified the clones by restriction enzyme digest, the DNA was sequenced using primers 10 a) and 10 b) in order to confirm the ligation before being sent for transgenesis.

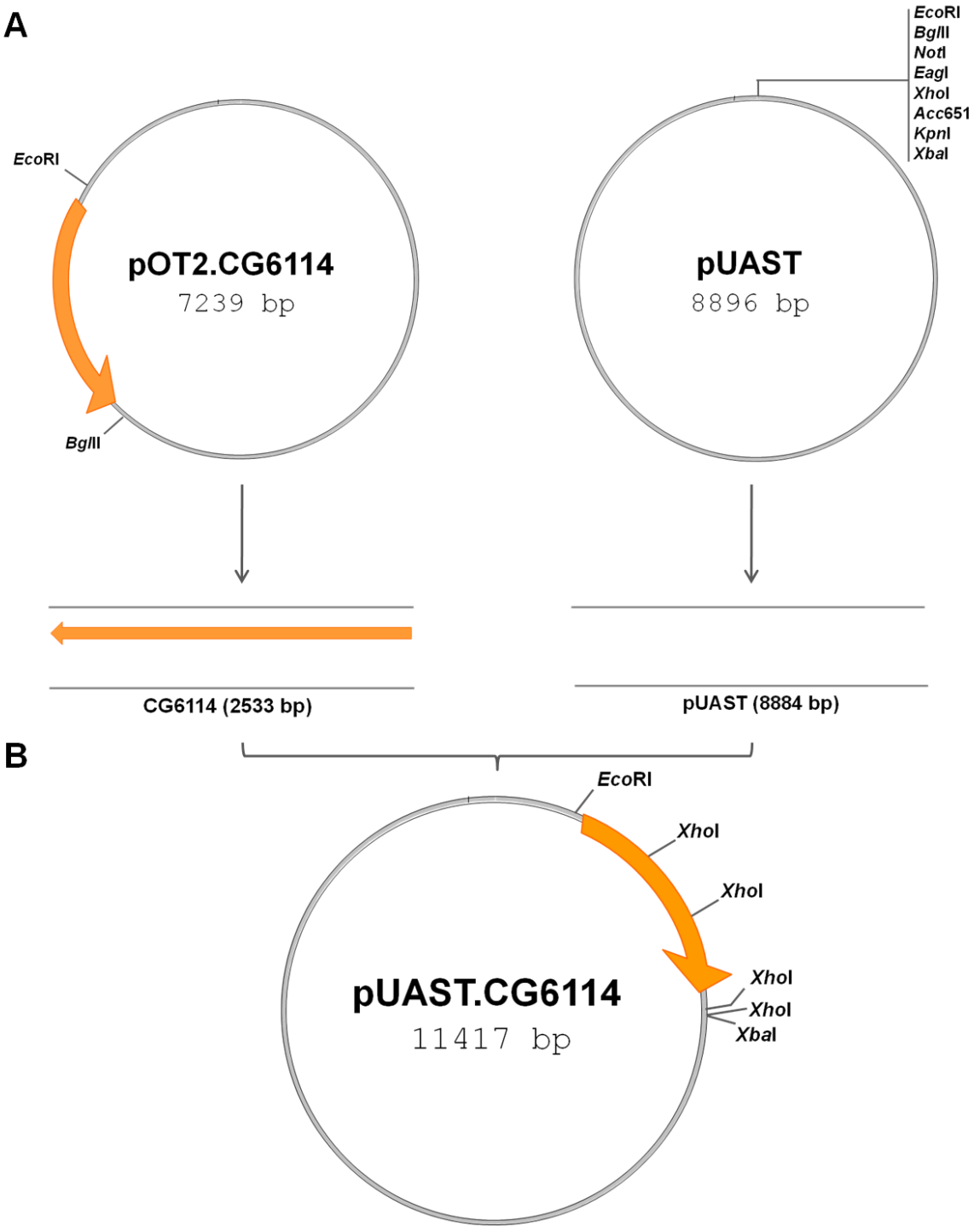

Figure 3.12 Schematic for cloning of CG6114 into pUAST.
A. pOT2.CG6114 was digested with EcoRI and BglII resulting in a 2533bp fragment containing CG6114. pUAST plasmid was linearised with EcoRI and BglII.
B. The CG6114 fragment and the linearised pUAST were ligated to create pUAST.CG6114.

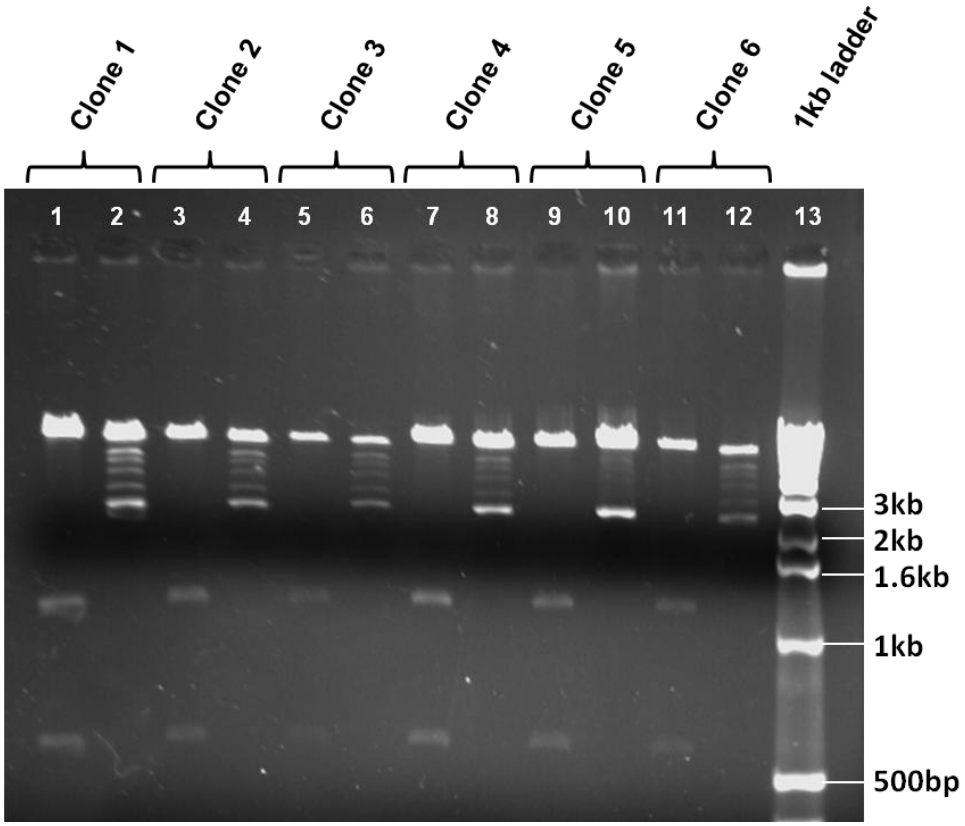

Figure 3.13 Enzyme digest of pUAST.CG6114 clones.
Agarose gel containing ethidium bromide in order to stain DNA fragments. Lanes 2, 4, 6, 8, 10 and 12 digested with EcoRI and XbaI (to yield a 2548bp fragment from positive clones). Lanes 1, 3, 5, 7, 8, 9, and 11 digested with XhoI (to yield 578bp and 1162bp fragments from positive clones).

3.10 Discussion

This chapter serves as a record of the construction of transgenic flies carrying human BRSK1, BRSK2, LKB1 and CaMKKα and endogenous *Dosophila* CG6114.

Phenotypic analysis showed that BRSK1 and BRSK2 isoforms produce similar phenotypes when expressed with GMR::GAL4 and the 0N4R isoform of human tau. B-WT enhanced the tau induced eye phenotype, whilst B-NP, B-KD and B-CA did not (both isoforms). This suggests that B-CA may not be fully constitutively active in the *Drosophila* model. In addition, over-expression of human B-WT or knock-down of the *Drosophila* homologue, CG6114, using a number of neuronal drivers was lethal at the embryonic stage.

Selected BRSK2 transgenic lines (B-WT5, B-NP4, B-KD4 and B-CA5) were confirmed to have similar BRSK expression levels by western blot, indicating that there was no significant position effect of the transgenes in these flies.

Having verified that the BRSK2 flies were expressing and that the protein was functional, the BRSK2 Kozak sequence was used in the construction of CaMKKα and LKB1 transgenic flies in order to ensure that those proteins were also expressed and functional in *Drosophila.*

In Chapter 4, I present data utilising the selected human BRSK2 transgenic flies in combination with human 0N4R, S2A and S262A tau in order to further assess interactions between BRSK2 and tau and to identify the amino acids that are

important for these interactions. I also discuss the data produced with the UAS-CG6114 transgenic flies.

4| Interactions between human BRSK2 isoforms and human tau in the *Drosophila* eye.

4.1 Introduction

At the beginning of this project, little was known about the potential for BRSKs as tau kinases. It had been reported that tau phosphorylation at S262 was reduced in BRSK double knockout mice and that the double knockout mice had a severe neural phenotype which led to death within two hours of birth (Kishi et al., 2005). However, no further exploration had been made into the possibility of BRSK being a direct tau kinase. BRSK was an interesting candidate as a tau kinase due to its mainly neuronal expression and its close relation to PAR-1, another member of the AMPK family of protein kinases, which is a well defined tau kinase and has been studied extensively in both mammalian and *Drosophila* models of AD (Nishimura et al., 2004; Thies and Mandelkow, 2007; Wang et al., 2007a; Zempel et al., 2010).

Four different tau lines were used in this chapter (0N4R tau, R406W tau, S2A tau and S262A tau, for a schematic see Figure 4.1). R406W tau is the 0N4R isoform of tau carrying an R406W mutation (numbering based on the longest human isoform of tau); a mutation that is associated with fronto-temporal dementia with Parkinsonism linked to chromosome 17 (FTDP-17) (Bunker et al., 2006). R406W tau was used as a control in some of the experiments in this chapter as S2A tau was constructed by mutating S262 and S356 in R406W tau to alanine (Nishimura et al., 2004). S262 and S356 are located within KXGS motifs in microtubule binding domains 1 and 4 respectively. S262A tau is the 0N4R isoform of tau carrying a S262A mutation (Iijima-Ando et al., 2010). The tau lines were genotyped in order to confirm isoform identity and mutation status. This work is shown in Appendix 4 along with western blots to show the tau expression level.

Flies expressing human tau (0N4R), BRSK2 (WT, NP, KD, CA) or co-expressing both genes (under the control of the GMR-GAL4 driver) were assessed qualitatively using SEM, and quantitatively using QED software in order to compare the scale of ommatidial distortion. The use of QED allowed me to unambiguously determine the effect various manipulations had on the phenotype of the eye. Semi-thin resin sections of eyes were produced in order to view the effect of human tau and BRSK2 co-expression on the internal cellular structure of the eyes. The S262A tau line (carrying a S262A mutation) was utilised in order to assess the contribution of this site to the BRSK-tau phenotype and this was followed with western blots on lysates from flies expressing 0N4R tau or 0N4R tau with BRSK isoforms in order to elucidate if BRSK was capable of phosphorylating tau. Finally, the S2A tau line (carrying S262A/S356A mutations) was utilised in order to assess the additional contribution of S356 to the BRSK-tau eye phenotype.

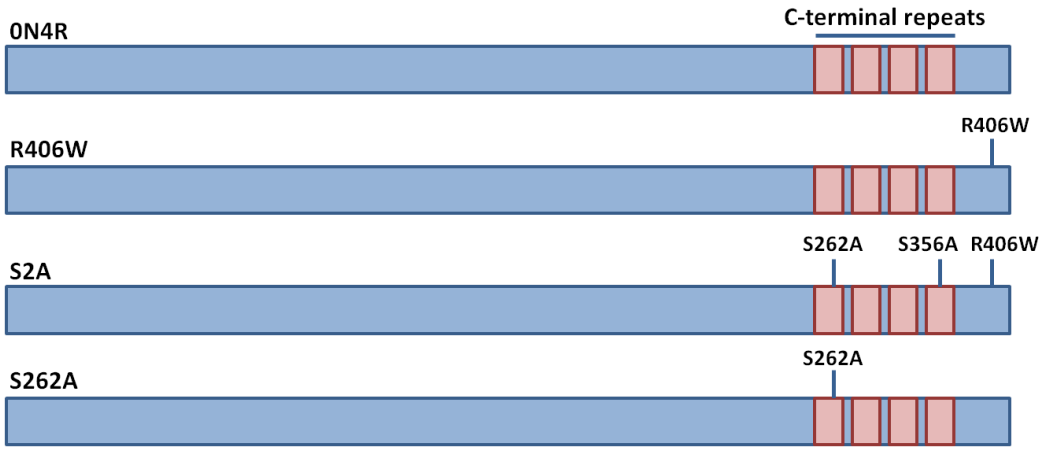

Figure 4.1: Schematic of tau isoforms.
Scheme showing the four tau isoforms used in this chapter: 0N4R, R406W, S2A and S262A along with the relative positions of the R406W, S262A and S356A mutations. In pink are the C-terminal repeats (microtubule binding domains).

4.2 Results

4.2.1 Expression of BRSK2 isoforms in the *Drosophila* eye

In order to ascertain whether expression of human BRSK2 caused an eye phenotype, four different isoforms of BRSK2 were expressed. Visual inspection of SEM images of the eyes showed that expression of wild type (B-WT), non-phosphorylatable (B-NP), kinase dead (B-KD) or constitutively active (B-CA) BRSK was not detrimental to the eye (Figure 4.2) when compared to wild type (CS) eyes or eyes expressing the GAL4 driver alone (GMR).

Figure 4.3 shows a cumulative distribution plot produced by quantification of the SEMs using software designed for this purpose at Warwick University (QED). QED is a software package that was written in Matlab in order to quantify the level of ommatidial distortion in SEMs (described in the Methods section and in Appendix 2). Having processed a number of images per genotype, I have produced a cumulative graph for the distortion coefficients for each genotype, with 0 corresponding to no ommatidial distortion and 1 corresponding to maximal ommatidial distortion on the x-axis and the cumulative fly count on the y-axis (in percent of total). Quantification of the ommatidial distortion using QED confirmed that eyes expressing BRSK2 isoforms were the same as those of the GMR driver.

Looking at the range of distortion coefficients (DCs) produced by QED for each genotype gives an indication as to the variability of the phenotypes; a wide DC range would indicate a genotype with a varied phenotype whilst a narrow DC range would indicate a genotype with little phenotypic variation. Figure 4.4 shows the images

with the lowest and highest DCs for the genotypes analysed in Figure 4.2; it is possible to see that there is little variation in the phenotypes and that the DC ranges are very similar for each of the genotypes (CS: 0.15-0.26, GMR: 0.22-0.29, B-WT: 0.18-0.35, B-NP: 0.19-0.25, B-KD: 0.20-0.31 and B-CA: 0.19-0.28).

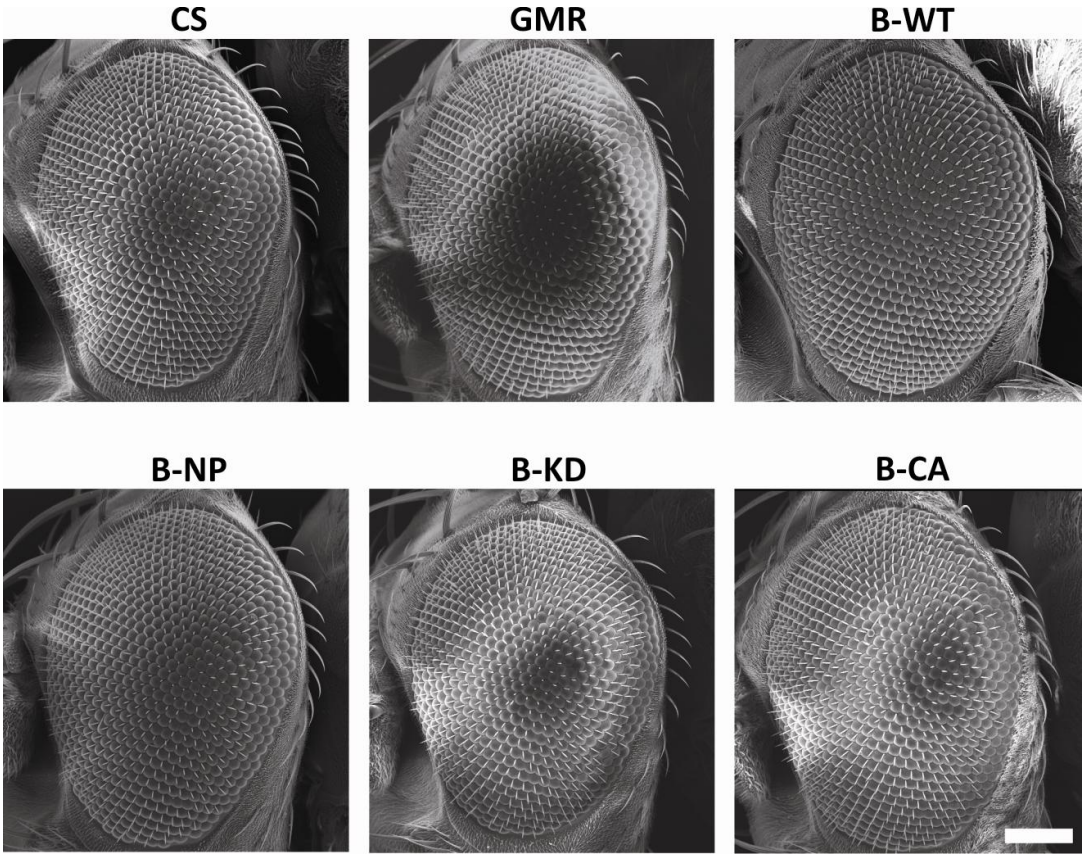

Figure 4.2: SEM images of flies expressing human BRSK2 isoforms.
Scanning electron micrographs showing that expression of human B-WT, B-NP, B-KD or B-CA isoforms under the control of the GMR-GAL4 driver (GMR) did not cause an eye phenotype. Scale bar 100µm applies to all panels.

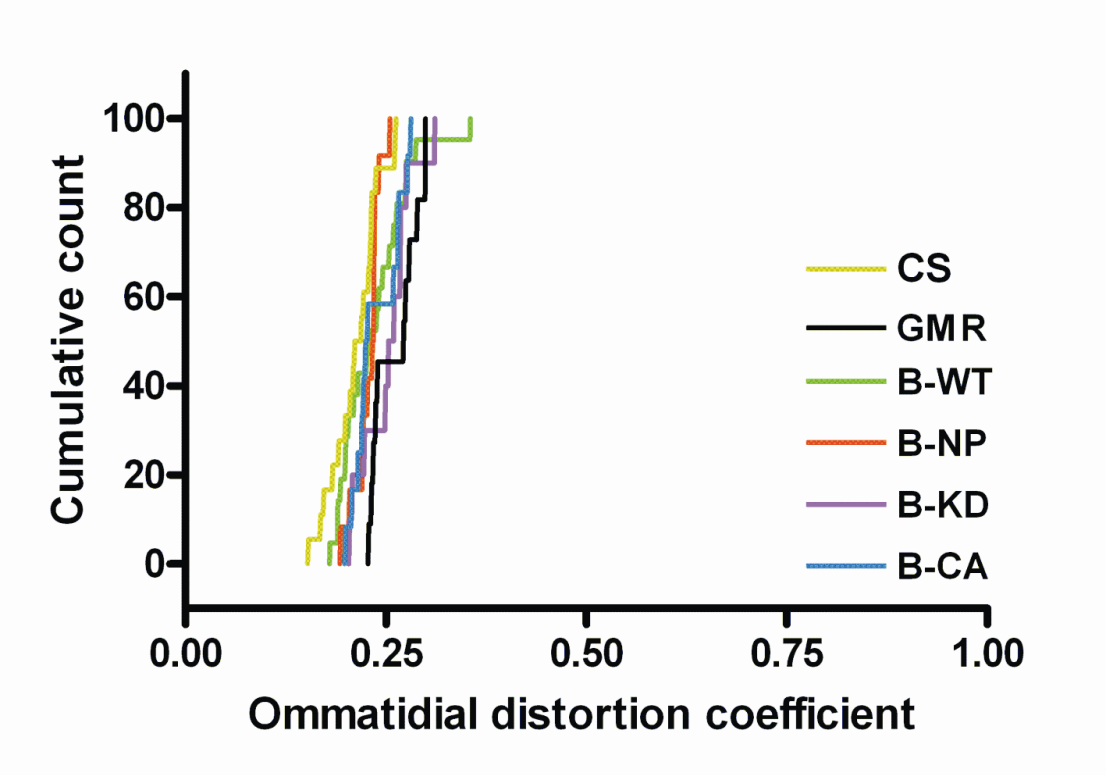

Figure 4.3: Cumulative distribution plot of ommatidial distortion measures (DCs) produced by QED software for flies expressing human BRSK2 isoforms and GMR. *Quantitative analysis of flies expressing BRSK2 isoforms using QED showed that expression of BRSK2 isoforms did not cause an eye phenotype. CS n=18, GMR n=11, B-WT n=21, B-NP n=12, B-KD n=10 and B-CA n=12.*

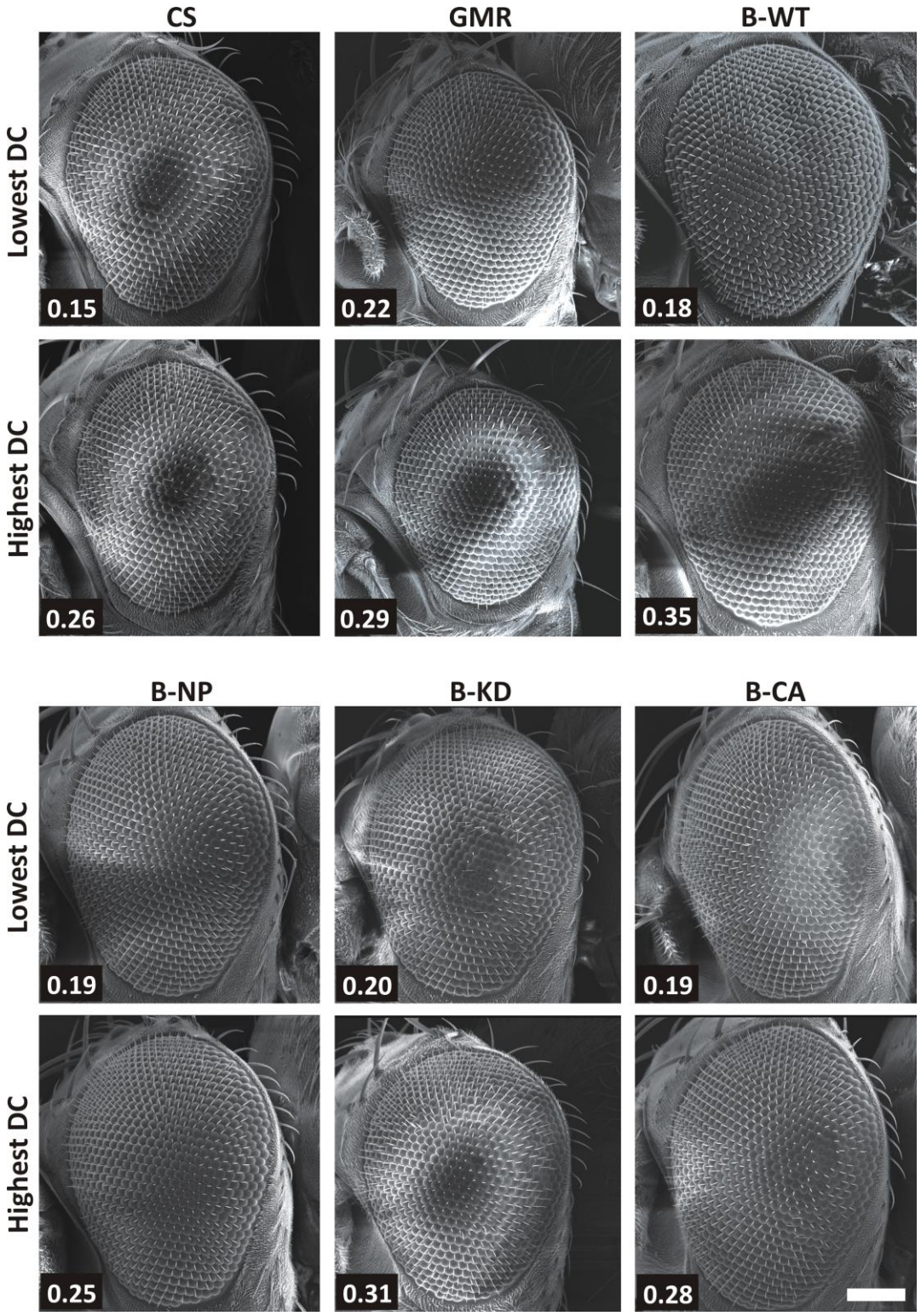

Figure 4.4: SEM images of flies expressing BRSK2 isoforms with the lowest and highest DCs.

Images of flies expressing GMR, B-WT, B-NP, B-KD or B-CA. The range of DCs for the BRSK expressing flies overlapped with that of the GMR flies. DCs are shown on the images. Scale bar 100µm applies to all panels.

4.2.2 Co-expression of human BRSK2 isoforms with human 0N4R tau

It is well known that expression of human tau in the fly eye causes a degenerative 'rough eye' phenotype when visualised externally with SEM (Wittmann et al., 2001; Shulman and Feany, 2003; Steinhilb et al., 2007a). In order to test the hypothesis that human BRSK2 would interact with and phosphorylate human tau in *Drosophila*, UAS-0N4R tau and UAS-BRSK2 (B-WT, B-KD or B-NP) were expressed in the eye (Figure 4.5).

This manipulation caused a drastic exacerbation of the tau phenotype, demonstrating for the first time, that human 0N4R tau and BRSK2 are able to interact *in-vivo* in *Drosophila*. Further to this, it is reasonable to conclude that there is an endogenous *Drosophila* kinase capable of phosphorylating and activating BRSK2. This indicates that intact signalling cascades, composed of both human and *Drosophila* genes and proteins can be observed in the fly.

Expression of B-KD or B-NP with 0N4R tau had no effect on the previously observed degenerative tau phenotype, demonstrating that the exacerbation seen upon B-WT co-expression with 0N4R tau was not simply due to expression of exogenous proteins. Further to this, quantification of western blots for BRSK2 expression (shown in Chapter 3, Figure 3.7) demonstrates that the lack of exacerbation in the flies expressing 0N4R tau with B-NP or B-KD was not due to a lack of BRSK2 expression.

Figure 4.6 shows a cumulative distribution plot produced for the flies of the genotypes in Figure 4.5. As in Figure 4.3, expression of B-WT (green line) had little

or no effect on the ommatidial structure of the eye when compared to GMR (black line). Expression of 0N4R tau caused a degenerative phenotype which can be seen by the shift of the tau curve (red line) further towards 1. However, co-expression of B-WT with 0N4R tau caused a dramatic exacerbation of the 0N4R tau phenotype as can be seen in the large shift to the right of the blue line. This was not the case with B-KD as this line overlies that of the 0N4R tau flies. B-NP appeared to exhibit an intermediate phenotype which was not visually evident from the SEMs.

Figure 4.7 shows the images from the two extremes of the cumulative distribution plot for flies expressing tau, T + B-WT, T + B-NP and T + B-KD; the images with the lowest and highest DCs for each genotype are shown (the images for GMR and B-WT flies were shown in Figure 4.4 and so have not been repeated here). Tau flies had a DC range that was higher than that of the GMR flies (0.31-0.55 and 0.22-0.29 respectively) and correlated with the appearance of a tau-induced degenerative phenotype. Co-expression of B-WT with Tau gave a range of 0.40-0.99. This was visible in the images – the eye with the lowest DC showed signs of B-WT enhancement of Tau, with a smaller eye size and a slightly altered shape. The eye with the highest DC was very degenerated and had almost no ommatidial structure, hence a DC of 0.99. Tau + B-NP and Tau + B-KD flies had ranges of 0.33-0.64 and 0.29-0.72 respectively. These ranges were lower than that of the Tau + B-WT flies and this could be seen in the images; flies of these two genotypes looked more like the Tau flies.

Semi-thin 2.5µm resin sections of eyes from flies of the genotypes shown in Figure 4.5 were produced in order to investigate the underlying cellular morphology of the

eyes. Figure 4.8 shows that expression of the GMR driver caused no phenotype; hexagonally packed ommatidia are visible, each one containing seven rhabdomeres (R8 is not visible). Expression of B-WT did not alter this structured phenotype, whereas expression of 0N4R tau caused marked disruption to the cellular structure. This was manifested as holes where some cells had died at an early stage of development (arrow), merged ommatidia (*) and an incorrect number of rhabdomeres (arrowhead). This phenotype was exacerbated upon co-expression of B-WT, with very few detectable ommatidia and an obvious increase in disorganisation. The effects caused by B-WT were not visible in the sections from eyes co-expressing 0N4R tau and B-NP or B-KD.

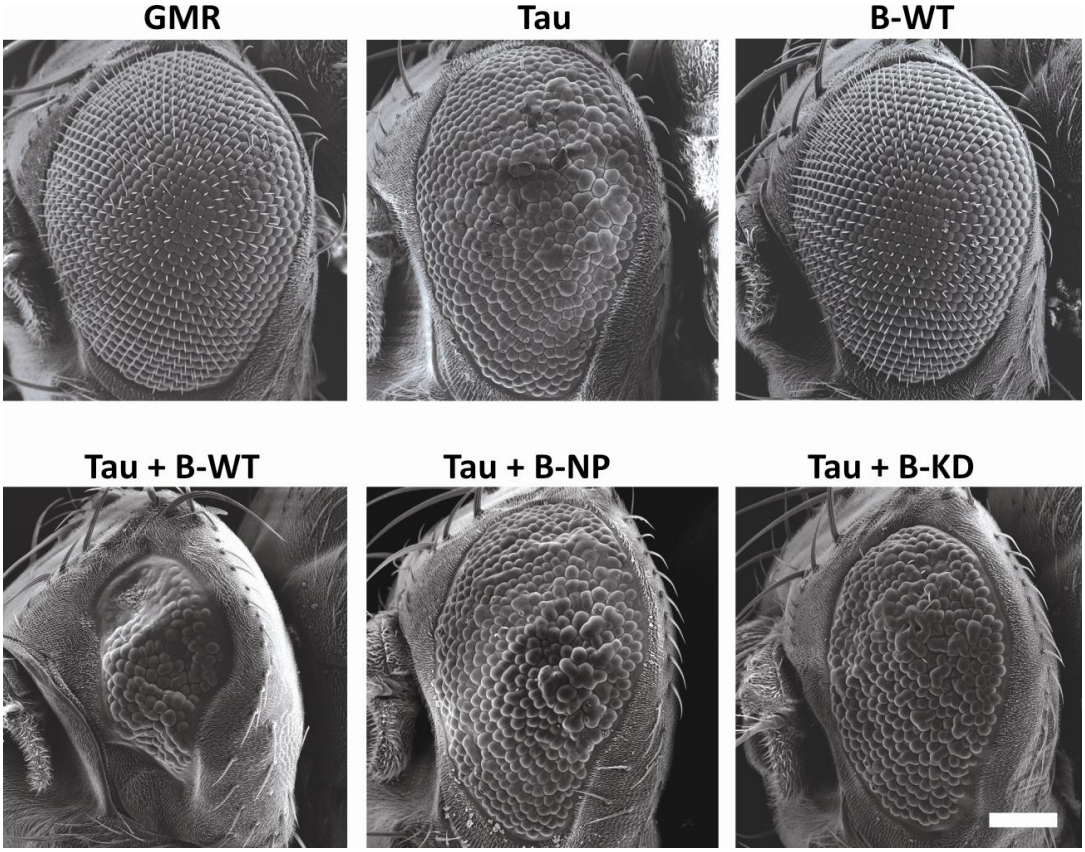

Figure 4.5: SEM images of flies co-expressing human 0N4R tau with human BRSK2 isoforms.

Expression of 0N4R human tau under the GMR::GAL4 driver caused a degenerative eye phenotype (Tau). This was dramatically enhanced upon co-expression of human B-WT (Tau + B-WT). Enhancement was not seen in eyes expressing NP or KD isoforms of human BRSK2 (Tau + B-NP and Tau + B-KD). Scale bar 100µm applies to all panels.

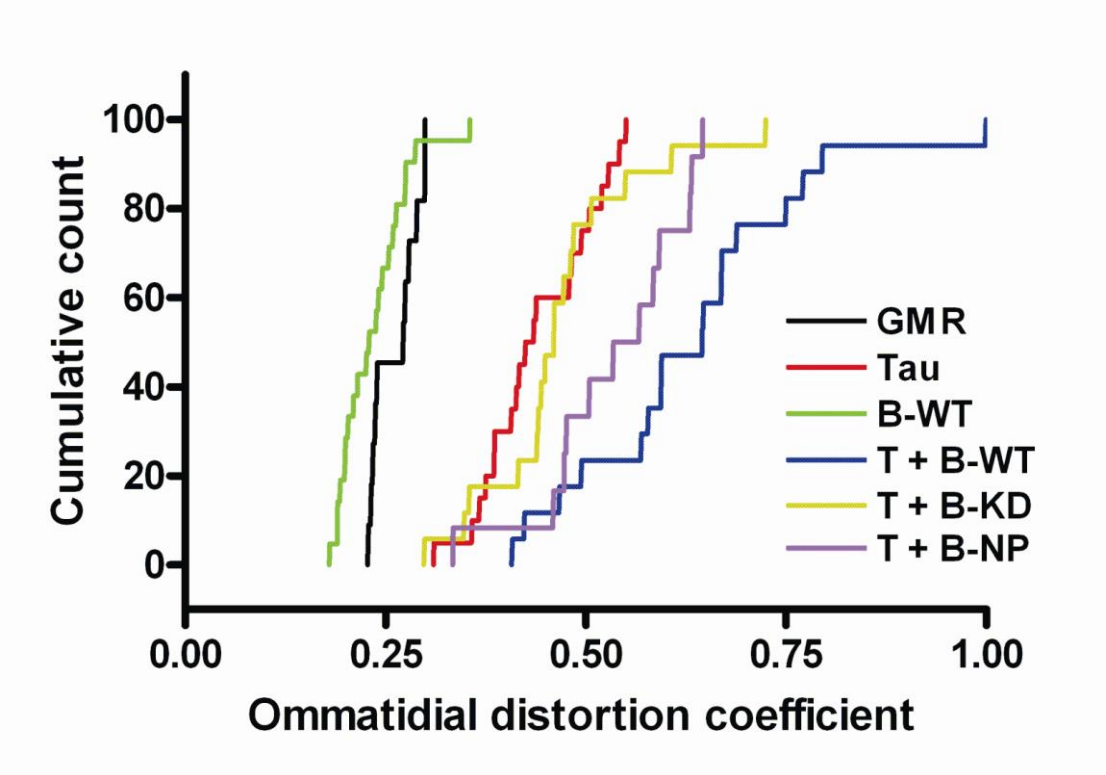

Figure 4.6: Cumulative distribution plot of ommatidial distortion measures (DCs) produced by QED software for flies co-expressing human 0N4R tau and BRSK2 isoforms.

Quantitative analysis of flies co-expressing 0N4R tau and human BRSK2 isoforms under the control of the GMR-GAL4 driver showed that expression of B-WT enhanced the 0N4R tau induced ommatidial distortion (T + B-WT). Enhancement was not seen with B-KD (T + B-KD), whereas B-NP produced an intermediate phenotype (T + B-NP). GMR n=11, Tau n=20, B-WT n=21, T + B-WT n=17, T + B-KD n=17 and T + B-NP n=12.

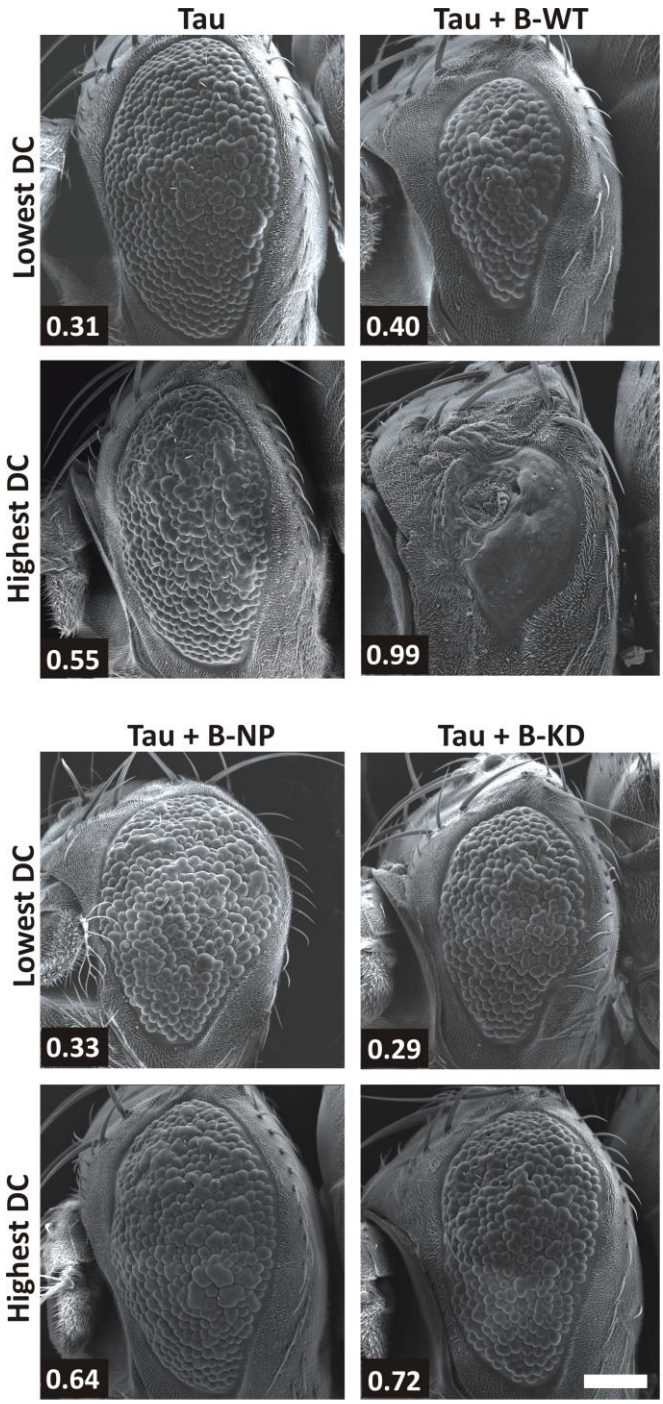

Figure 4.7: Scanning electron micrographs of flies co-expressing 0N4R tau and BRSK2 isoforms with the lowest and highest DCs.

Tau flies had a DC range that was 0.31-0.55, values which were higher than those of the GMR flies (GMR and B-WT flies were shown in Figure 4.3). Co-expression of B-WT with Tau gave a range of 0.40-0.99 indicating a more severe phenotype. Tau + B-NP and Tau + B-KD flies had ranges of 0.33-0.64 and 0.29-0.72 respectively. These ranges were lower than that of the Tau + B-WT flies – this is clear upon visual examination of the images. DCs are shown on each image. Scale bar 100µm applies to all panels.

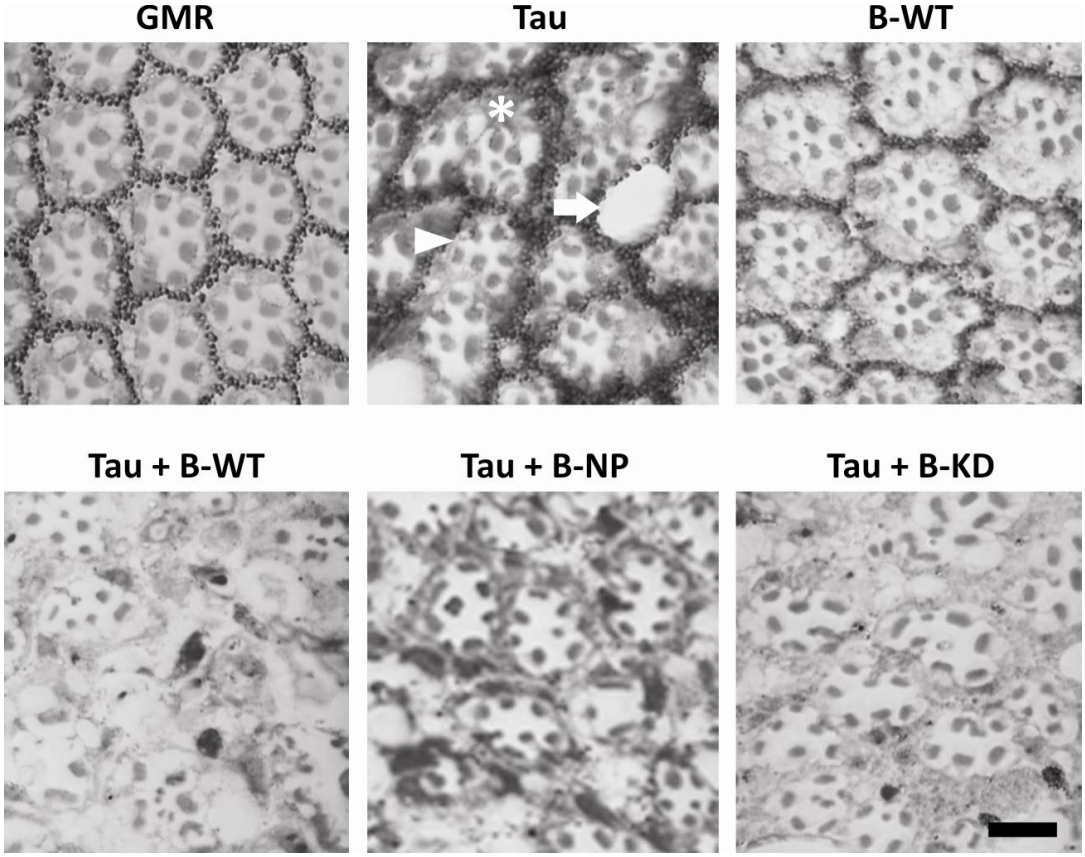

Figure 4.8: Semi-thin 2.5µm resin sections of eyes co-expressing human 0N4R tau with human BRSK2 isoforms.

GMR and B-WT eyes had a very regular sub-cellular structure consisting of hexagonally packed ommatidia, each containing 7 rhabdomeres (R8 was not visible). Expression of 0N4R human tau under the GMR-GAL4 driver caused a degenerative eye phenotype manifested as an incorrect number of rhabdomeres (arrowhead), merged ommatidia (*) and absent cells (arrow). This was enhanced upon co-expression of human B-WT with very little sub-cellular structure visible in the sections. Enhancement was not seen in eyes co-expressing B-NP or B-KD. Scale bar 25µm applies to all panels.

4.2.3 Co-expression of constitutively active human BRSK2 with human 0N4R tau

In addition to B-WT, B-NP and B-KD, I made B-CA flies in which the T-loop threonine had been mutated to glutamic acid in order to mimic phosphorylation at this residue (T174) and produce a constitutively active version of BRSK2 (Lizcano et al., 2004). However, co-expression of B-CA with tau did not cause the enhancement of the tau phenotype seen with B-WT (Figure 4.9). This result was not expected, as B-CA should be able to reproduce the phenotype seen with B-WT. Western blots for BRSK expression (Chapter 3, Figure 3.7) demonstrated that this negative result was not due to a lack of B-CA expression.

QED analysis (Figure 4.10) of flies of the genotypes shown in Figure 4.9 demonstrated that expression of B-CA (blue line) had little effect on the ommatidial structure of the eye when compared to GMR (black line). Additionally, QED confirmed that co-expression of B-CA with 0N4R tau (brown line) did not reproduce the enhancement that was seen with co-expression of B-WT with tau (Figure 4.6), a result that indicates that the T174E mutation in B-CA was not sufficient to render the kinase constitutively active in this model.

The DC range for the tau flies was 0.31-0.55 and the range for the flies co-expressing tau and B-WT was 0.40-0.99 (Figure 4.7), flies co-expressing tau with B-CA had a DC range of 0.39-0.50 (Figure 4.10), indicating that Tau + B-CA flies had a phenotype that was very similar to that of the tau flies.

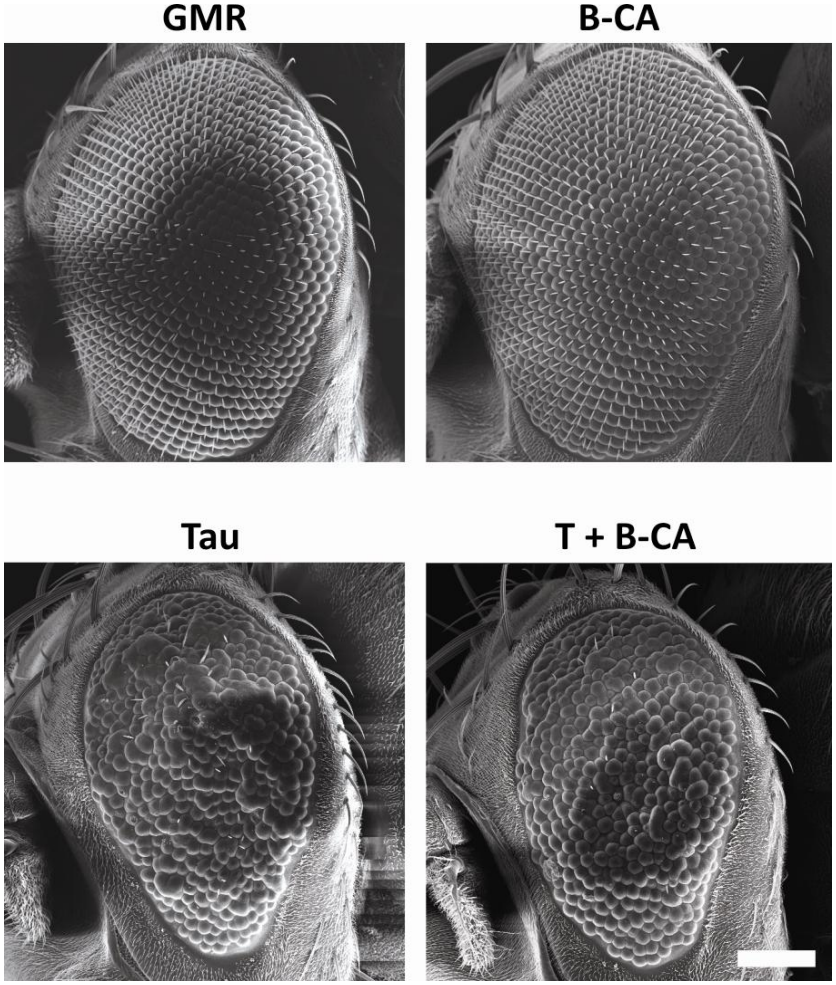

Figure 4.9: SEM images of flies co-expressing human 0N4R tau with constitutively active BRSK2.
Expression of B-CA did not affect the eye phenotype (B-CA). Expression of 0N4R human tau under the GMR-GAL4 driver caused a degenerative eye phenotype which was not enhanced upon co-expression of human B-CA (T + B-CA). Scale bar 100µm applies to all panels.

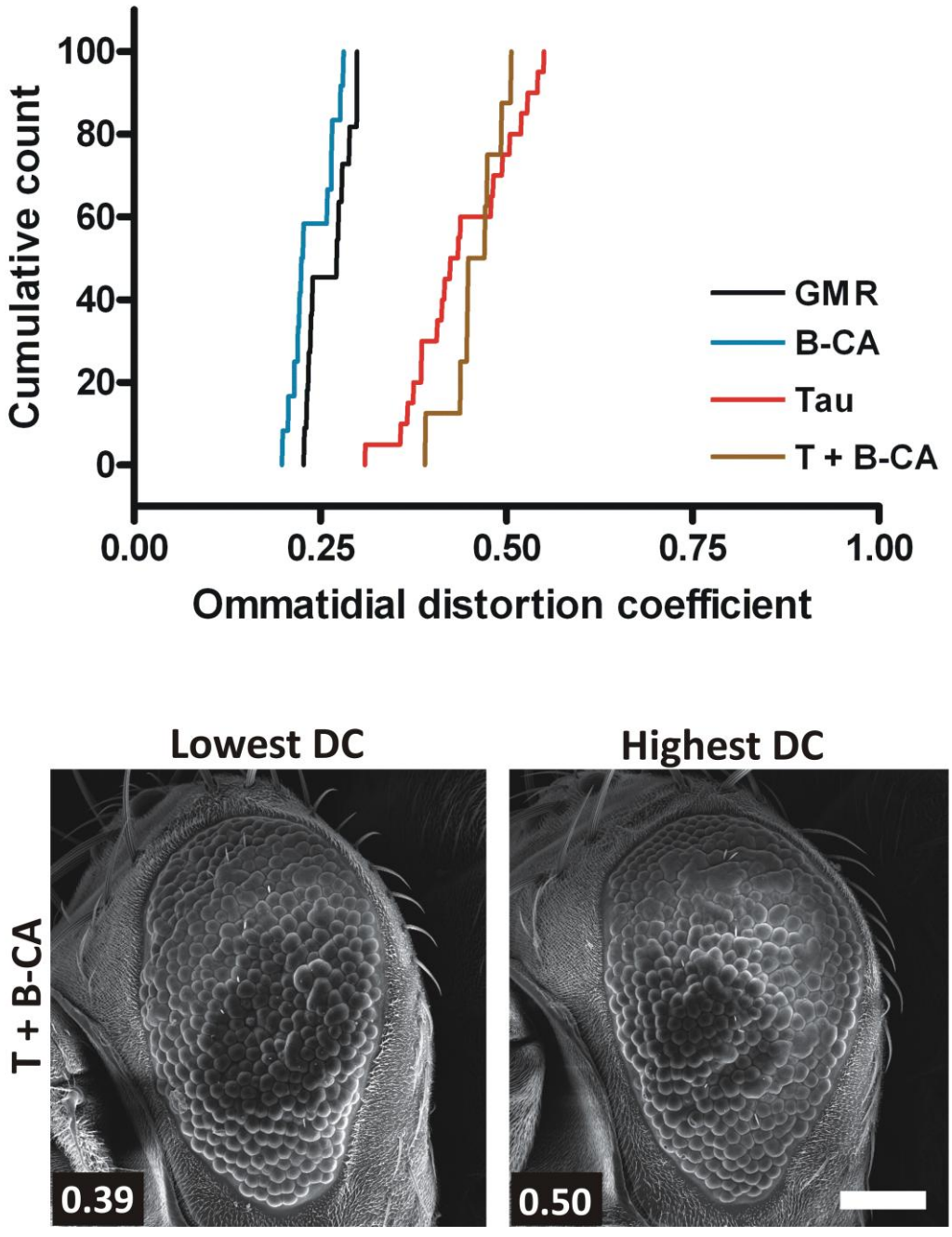

Figure 4.10: Cumulative distribution plot of ommatidial distortion measures (DCs) produced by QED software and images of flies with the lowest and highest DC for flies co-expressing human 0N4R tau and constitutively active BRSK2.
Quantitative analysis of flies co-expressing 0N4R tau and human B-CA under the control of the GMR-GAL4 driver showed that expression of B-CA did not enhance the 0N4R tau induced ommatidial distortion. GMR n=11, B-CA n=12, Tau n=20 and T + B-CA n=8. The range of DC for T + B-CA flies was 0.39-0.50. Scale bar 100µm applies to all panels.

4.3 Co-expression of CG6114 and human tau

Having shown an interaction between B-WT and tau, I wished to explore if CG6114, the *Drosophila* homologue of mammalian BRSKs, was also capable of interacting with human tau.

Over-expression of CG6114 alone resulted in a phenotype similar to that seen upon expression of human B-WT (Figures 4.11, 4.12 and 4.13). Over-expression of CG6114 with tau did not enhance the tau-induced eye phenotype, demonstrating that there is not sufficient conservation between some part of the BRSK-tau pathways between humans and *Drosophila* despite there being 88% sequence identity between CG6114 and human BRSK2. Figure 4.14 shows that the residues that were mutated in the human BRSK proteins (both isoforms), and the residues immediately surrounding the mutation sites, are conserved in CG6114, suggesting that the same kinases which activate the human B-WT would also be capable of activating CG6114.

It should be noted that a potential weakness of QED analysis is that it over-estimates the degree of ommatidial distortion in control flies. For example, Figure 4.14 shows that the GMR CG6114 eye with the highest DC had a value of 0.28 and the T + CG6144 eye with the lowest DC had a value of 0.31. These numbers are fairly close, but the phenotypes are very different as one eye expresses tau and the other doesn't. The reason for this discrepancy is that in the control eyes there are many bristles, and these have an effect on the QED analysis. Depending on the angle that the bristles intersect the ommatidia, some ommatidia may be registered by QED as two smaller

ones because a bristle is lying across the middle. This is generally not a problem in eyes which express tau as they do not have many bristles.

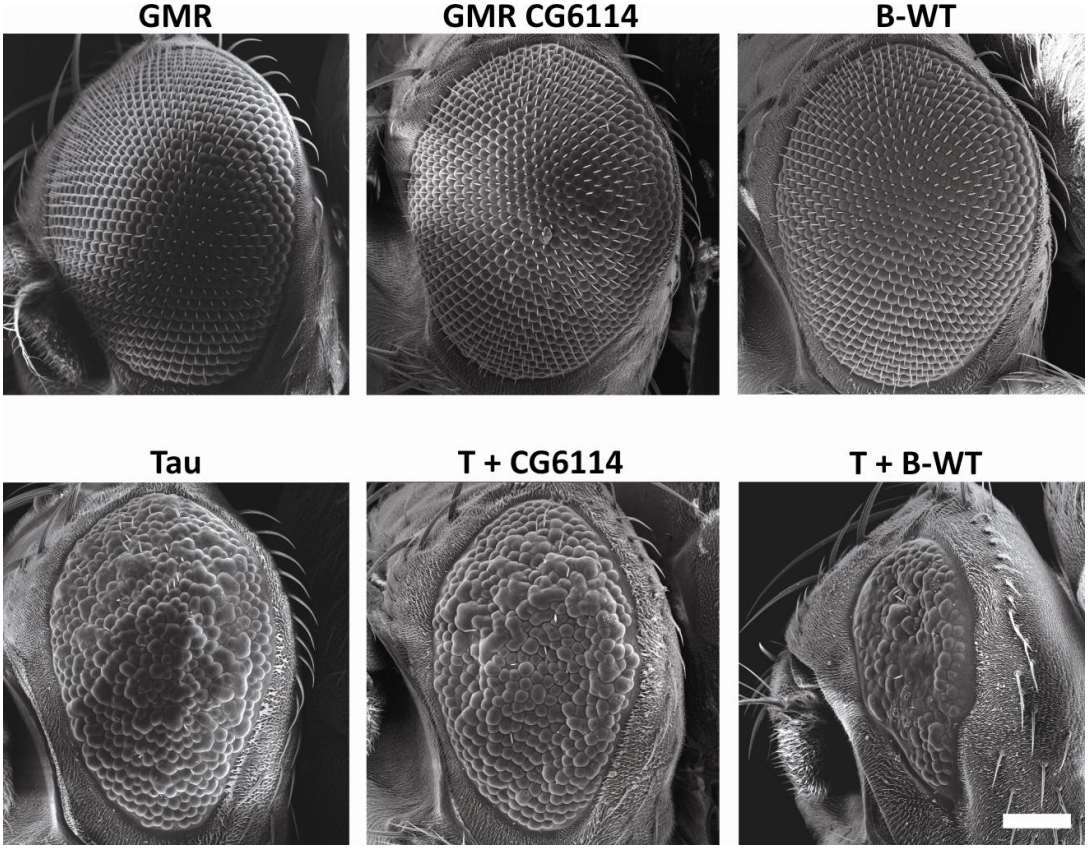

Figure 4.11: SEM images of flies co-expressing human 0N4R tau with CG6114. *Expression of 0N4R human tau under the GMR-GAL4 driver caused a degenerative eye phenotype which was not enhanced upon over-expression of CG6114 (T + CG6114). Over-expression of CG6114 alone (GMR CG6114) resulted in a phenotype similar to that seen with expression of human B-WT. Scale bar 100µm applies to all panels.*

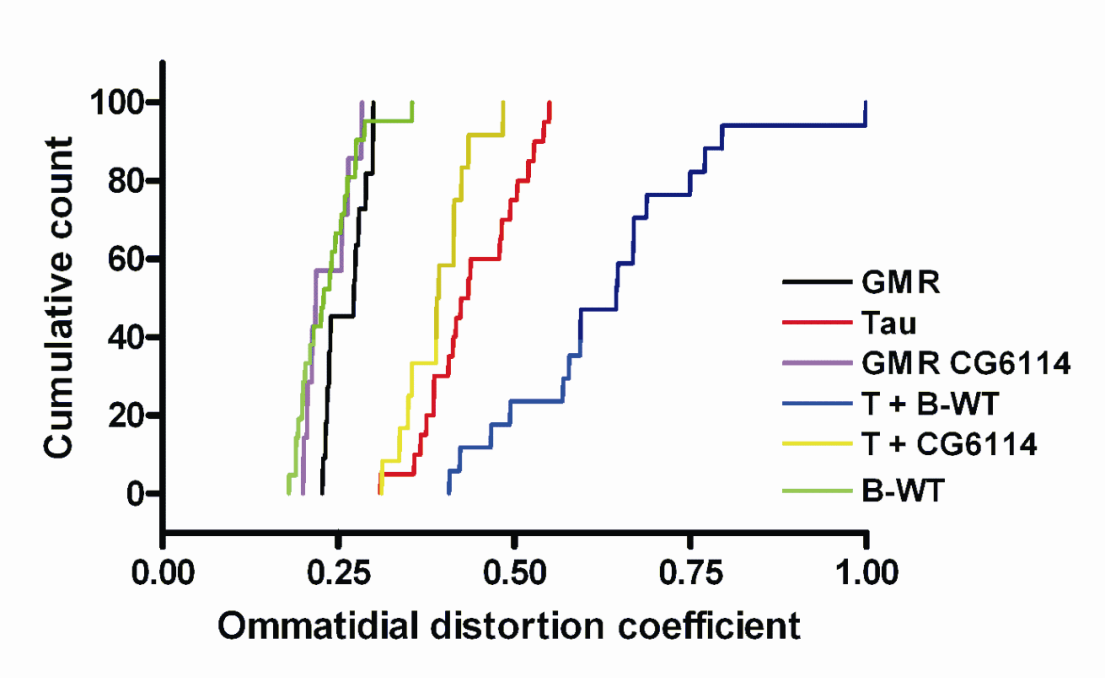

Figure 4.12: Cumulative distribution plot of ommatidial distortion measures (DCs) produced by QED software for flies co-expressing human 0N4R tau and CG6114. *Quantitative analysis of flies co-expressing 0N4R tau and CG6114 under the control of the GMR-GAL4 driver showed that over-expression of CG6114 slightly ameliorated the 0N4R tau induced ommatidial distortion. Expression of CG6114 alone caused a phenotype similar to that seen with expression of human B-WT. GMR n=11, Tau n=20, GMR CG6114 n=7, T + B-WT n=17, T + CG6114 n=12 and B-WT n=21.*

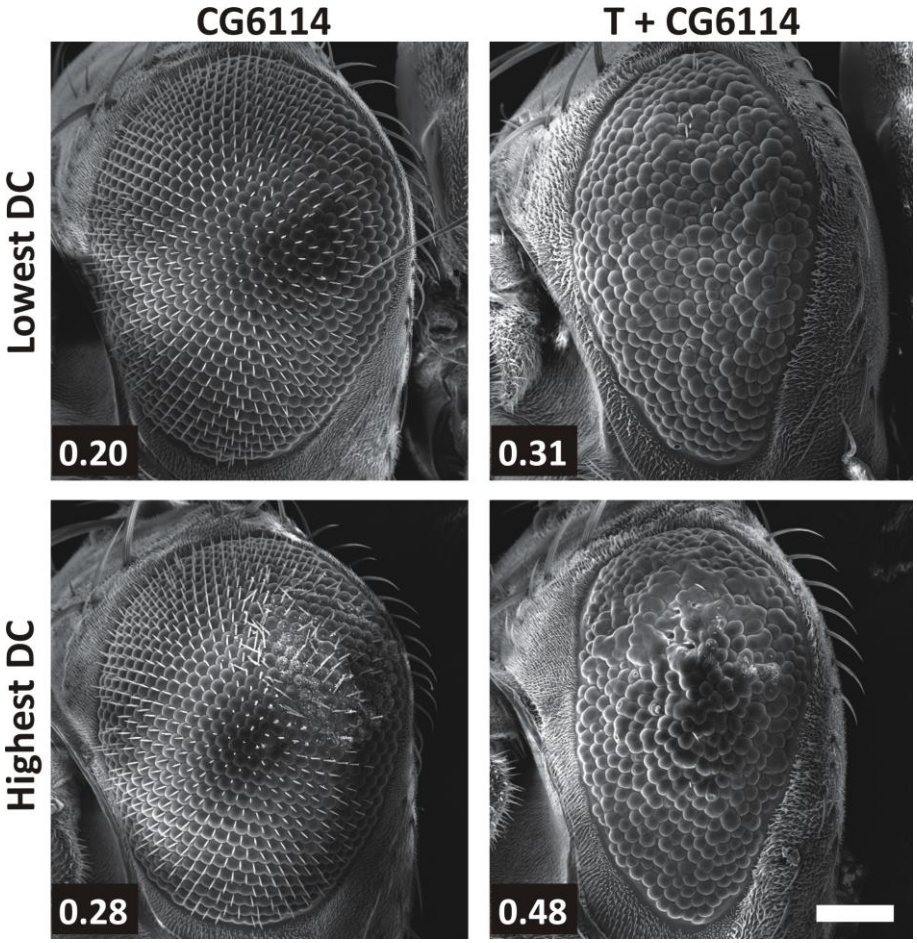

Figure 4.13: Scanning electron micrographs of flies over-expressing CG6114, with or without tau, with the lowest and highest DCs.
Over-expression of CG6114 gave a DC range of 0.20-0.28. Tau + CG6114 flies had a range of 0.31-0.48, which was slightly lower than the DC range of flies expressing tau alone (0.31-0.55). DCs are shown on each image. Scale bar 100µm applies to all panels.

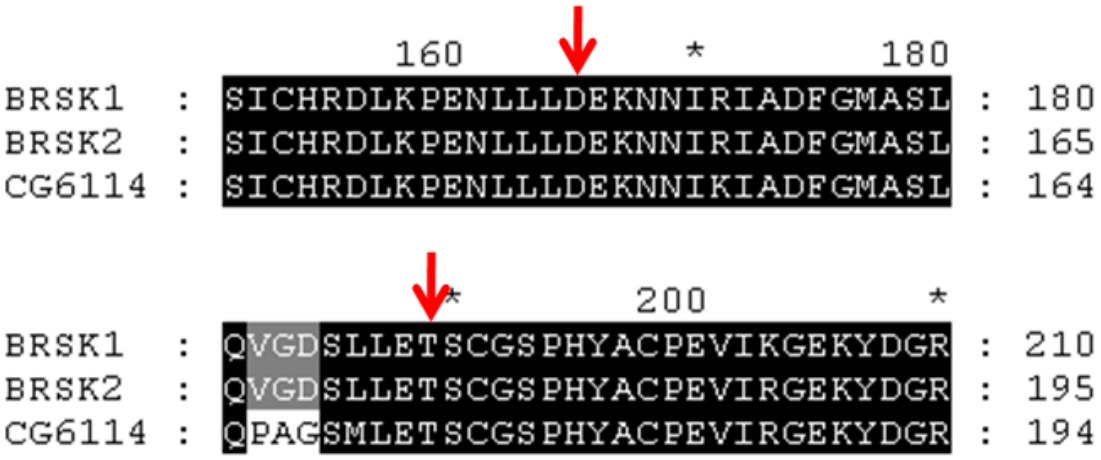

Figure 4.14: Alignment of human BRSK1 and 2 sequences with CG6114 sequence showing conservation of mutated sites.
Alignment of the sequences for human BRSK isoforms with CG6114 shows that the amino acids around the mutation sites are fully conserved between human BRSKs and CG6114. Red arrows indicate the amino acids mutated in kinase dead (D) or non-phosphorylatable (T) human BRSK.

4.4 S262A

Data presented by Kishi *et al* (2005) indicated that BRSKs are involved in the phosphorylation of tau at S262, and so I decided to investigate how important S262 was to the B-WT enhancement of the tau-induced eye phenotype. In order to do this I utilised a version of 0N4R tau which carries a S262A mutation (a kind gift of Dr Koichi Iijima).

Expression of S262A tau caused no eye phenotype (Figure 4.15), and further to this, mutation of S262A almost completely prevented the exacerbation seen upon co-expression of B-WT. This suggests that the phenotype seen upon tau expression, and the enhancement seen with B-WT, is directly linked to the ability of tau to be phosphorylated at S262.

Figure 4.16 shows the cumulative distribution plot for flies expressing S262A tau ± B-WT and flies expressing the relevant controls; GMR, B-WT and 0N4R tau ± B-WT. It clearly shows that expression of S262A tau had no effect on the ommatidial structure of the eyes. The cumulative curve closely overlays that of the GMR flies: demonstrating that the S262A mutation is sufficient to prevent the formation of tau-induced eye phenotypes. Co-expression of S262A tau with B-WT had a small effect on eye phenotype - there was a difference visible between the cumulative curves for S262A and S262A + B-WT flies. This may suggest that there are other sites in tau which are important for the enhancement seen with B-WT.

The DC range of the S262A flies (Figure 4.17) was 0.21-0.30, indicating that this phenotype was very similar to that of the GMR flies. S262A + B-WT flies had DC range of 0.22-0.39, demonstrating that these flies had a slight eye phenotype when compared to the GMR flies. This was due to some disordered and fused ommatidia in the posterior section of the eye in the S262A + B-WT flies.

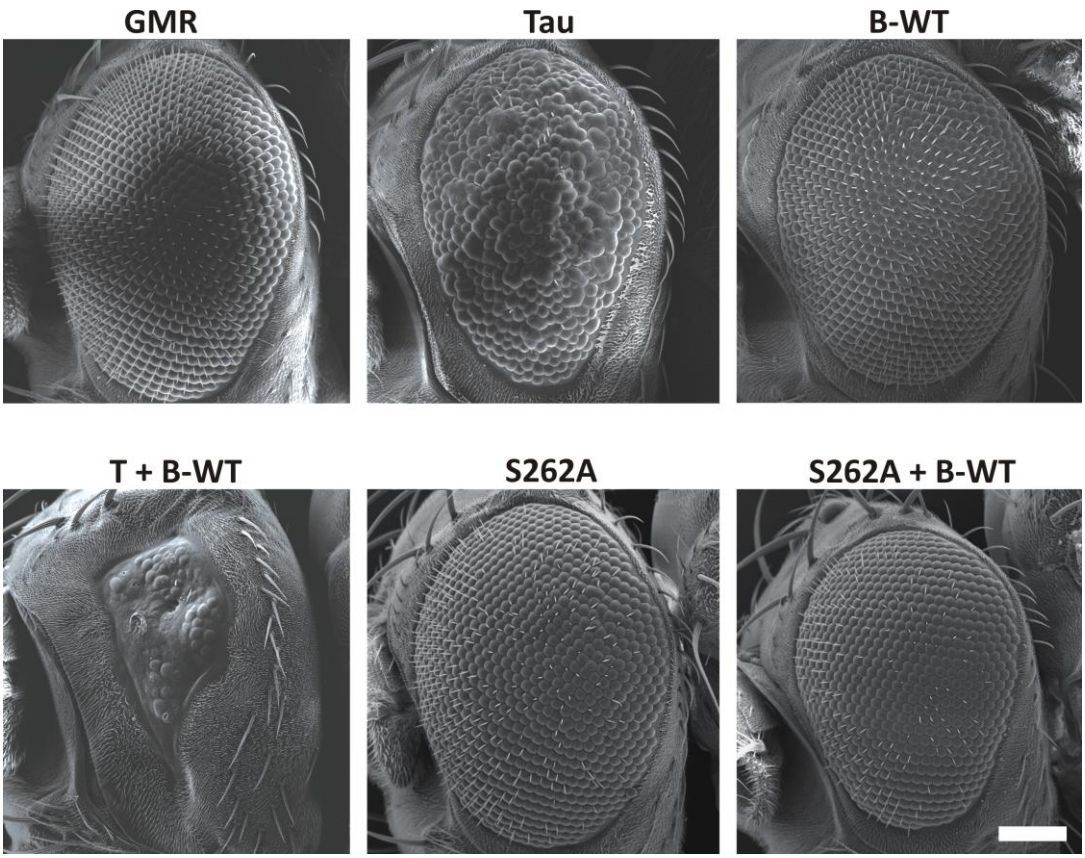

Figure 4.15: Scanning electron micrographs of flies expressing an S262A mutated isoform of tau with or without B-WT.
Expression of S262A tau with or without B-WT caused no visible eye phenotype suggesting that S262 is an important residue for the establishment of both Tau and Tau + B-WT eye phenotypes. Scale bar 100µm applies to all panels.

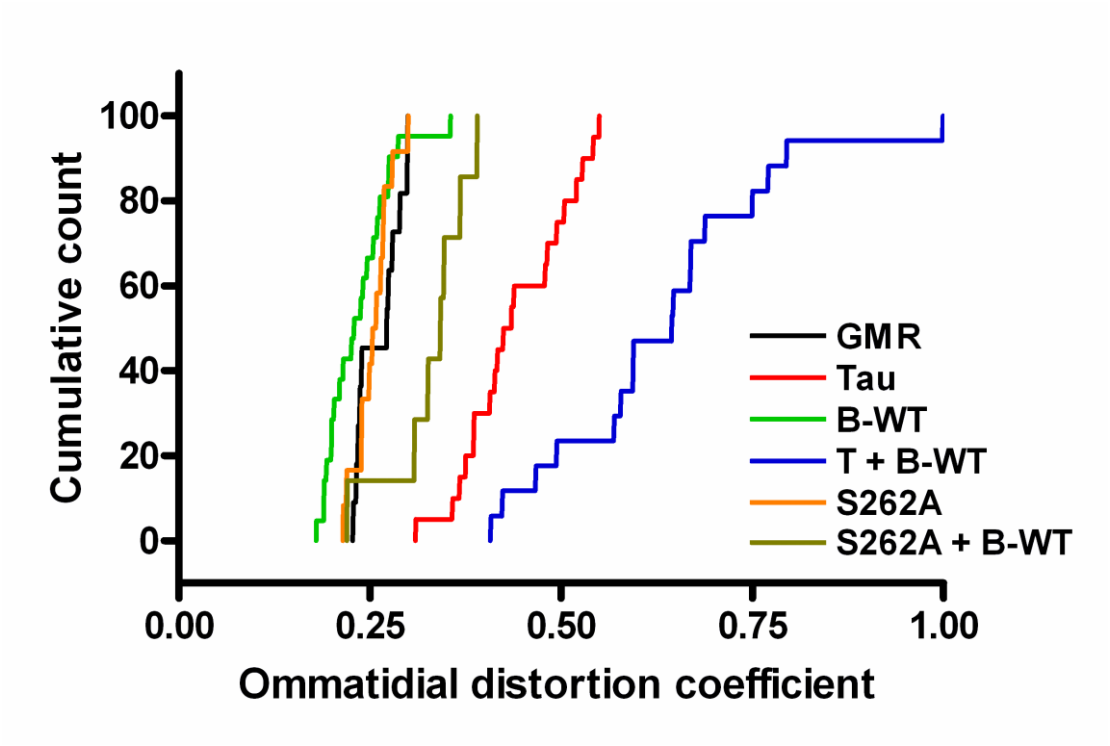

Figure 4.16: Cumulative distribution plot of ommatidial distortion measures (DCs) produced by QED software for flies co-expressing human S262A tau with or without B-WT.

In agreement with the SEM images, expression of S262A tau caused no eye phenotype – the curve for S262A tau overlies that of the GMR flies. Co-expression of B-WT and S262A tau had a small effect on the eye phenotype. GMR n=10, Tau n=20, B-WT n=21, T + B-WT n=17, S262A n=12 and S262A + B-WT n=7.

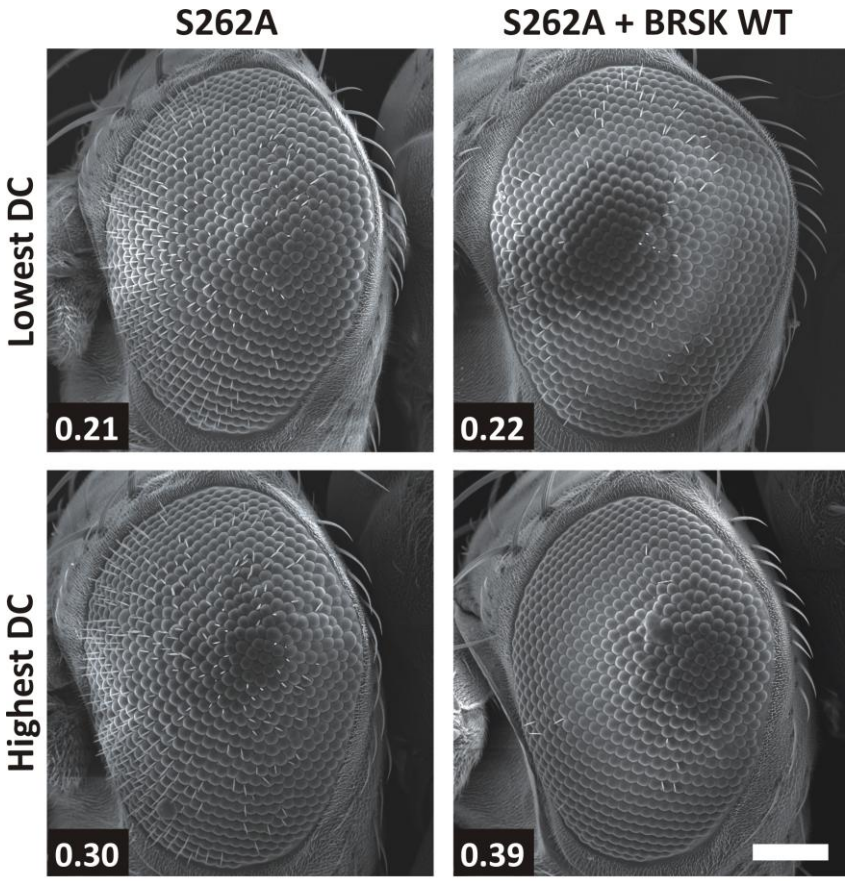

Figure 4.17: Scanning electron micrographs of flies with the lowest and highest DCs expressing S262A tau with or without B-WT.
*DCs are shown on each image**.** The range of DCs for the S262A flies overlapped with the range for the GMR flies (0.22-0.29 for GMR and 0.21-0.30 for S262A). The range of the DCs for the S262A + B-WT flies overlapped with those of the GMR and the S262A flies but ended at a higher value; this was due to a number of disordered and fused ommatidia in the posterior of the eye. Scale bar 100µm applies to all panels.*

4.4.1 Co-expression of sgg S9A and S262A tau

As there was no phenotype with the S262A tau and expression of S262A tau was lower than 0N4R tau (shown in Appendix 4, Figure 12.3), it was important to perform a positive control experiment in order to show that S262A tau could be modulated by kinase activity to produce an eye phenotype. Shaggy (sgg) is the *Drosophila* homologue of human GSK3-β, a serine/threonine kinase which phosphorylates tau at many residues, but is not capable of phosphorylating tau directly at S262 (Kosuga et al., 2005). sgg and PAR-1 appear to be in the same pathway, and phosphorylation of tau by PAR-1 has been shown to induce a cascade of phosphorylation of tau by other kinases including sgg (Nishimura et al., 2004; Kosuga et al., 2005). Previous work showed that expression of sgg with S2A tau caused a rough eye phenotype and so I reasoned that expression of sgg with S262A tau should cause a similar eye phenotype (Chatterjee et al., 2009).

For this experiment, a UAS-sgg S9A line was used which carries an S9A mutation enabling the sgg to be constitutively active (as phosphorylation at S9 deactivates sgg). Figure 4.18 shows that expression of sgg S9A alone caused a rough eye phenotype which was manifested as disordered bristles and some fused ommatidia. Co-expression of sgg S9A with S262A caused an enhancement of the phenotype seen with expression of sgg S9A alone, demonstrating that S262A tau was able to function and cause an eye phenotype.

QED analysis (Figure 4.19) showed that sgg S9A expression caused an eye phenotype when compared to the GMR or S262A tau flies. Co-expression of sgg S9A with S262A tau resulted in an enhanced phenotype that was robust, and had

little variation. This data demonstrated that S262A tau was functional and was able to interact with sgg S9A to produce an eye phenotype. This allowed me to draw the conclusion that the lack of phenotype in the S262A + B-WT flies was due to the S262A mutation, and not due to a lack of expression of S262A tau.

Examination of the flies with the lowest and highest DCs (Figure 4.20) showed that the range of the DCs for the sgg S9A flies was higher than those for the GMR and S262A flies, demonstrating that expression of sgg S9A causes an eye phenotype. The DC range for the S262A + sgg S9A flies was higher than that of the sgg S9A flies, indicating that S262A tau was able to interact with sgg S9A and cause an eye phenotype which was distinct from the phenotype exhibited by the sgg S9A flies (DC ranges: 0.28-0.40 for sgg S9A and 0.44-0.57 for S262A + sgg S9A).

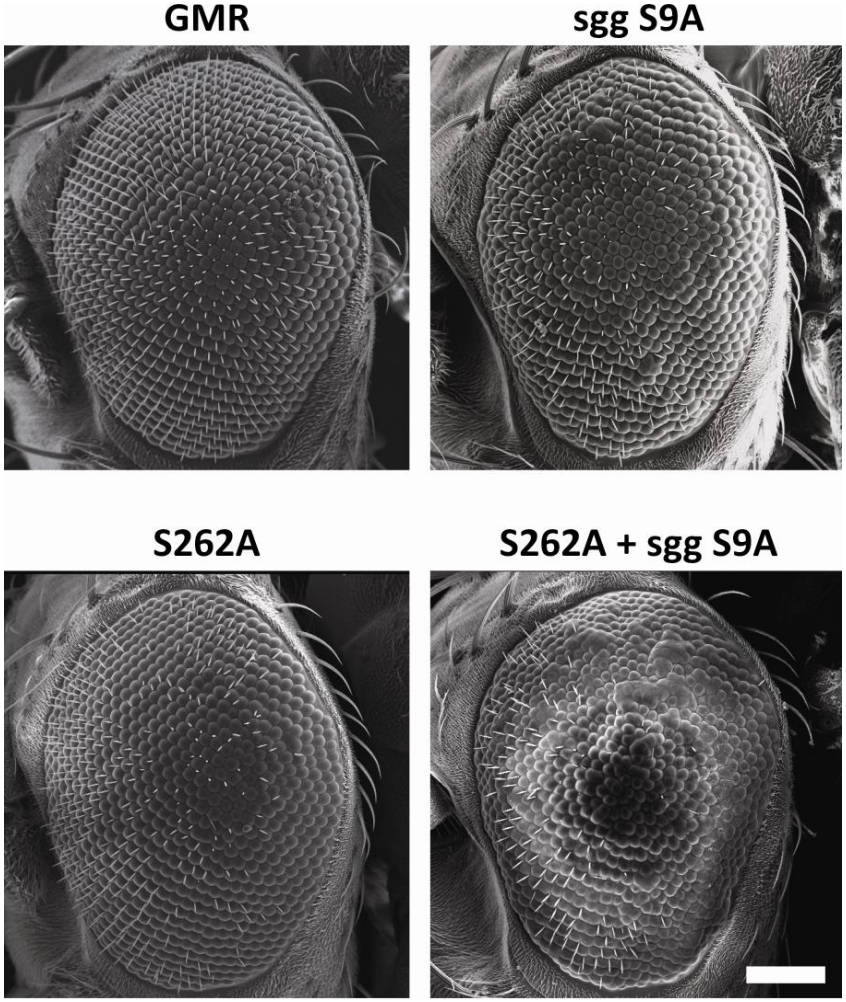

Figure 4.18: Scanning electron microscopy images of flies expressing a S262A mutated isoform of tau with or without sgg S9A.
Expression of sgg S9A alone caused a mild rough eye phenotype whereas co-expression of sgg S9A and S262A resulted in an enhanced eye phenotype, confirming that S262A could be modulated by kinase activity. Scale bar 100µm applies to all panels.

.

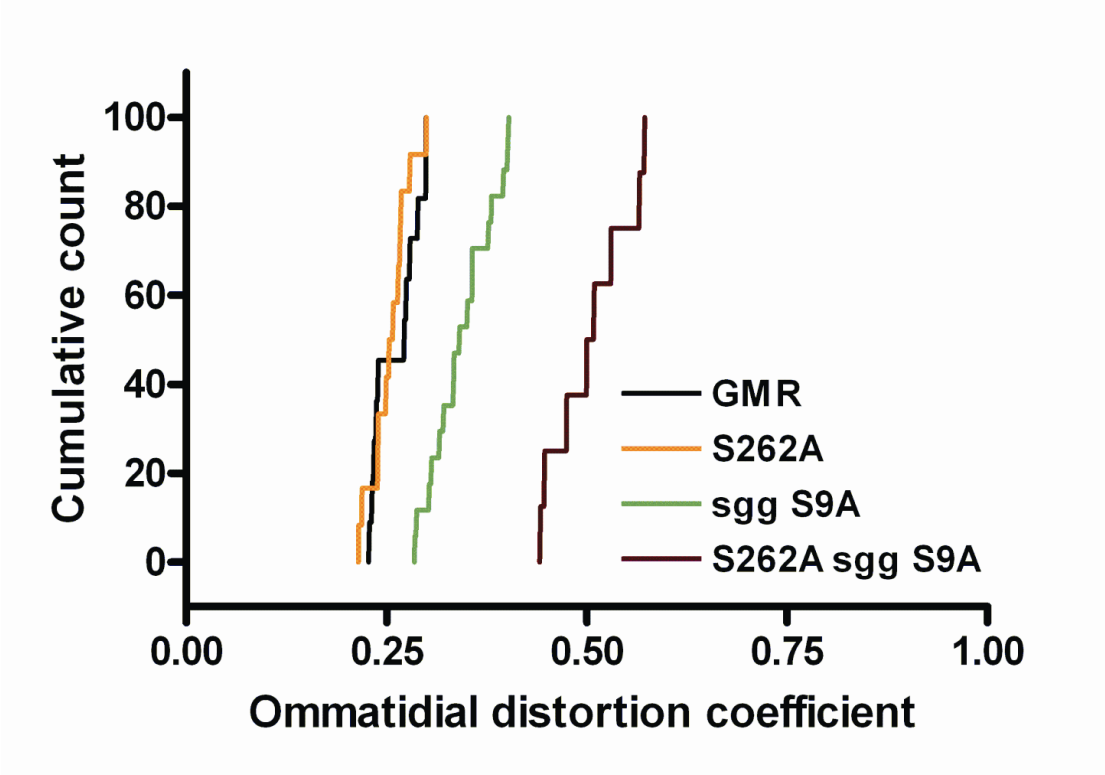

Figure 4.19: Cumulative distribution plot of ommatidial distortion measures (DCs) produced by QED software for flies co-expressing human S262A tau with or without sgg S9A.

Expression of sgg S9A caused an eye phenotype. Co-expression of S262A tau and sgg S9A enhanced this phenotype. This confirmed that S262A was able to be modulated by kinase activity to produce an eye phenotype. GMR n=10, S262A n= 12, sgg S9A n=17 and S262A sgg S9A n=8.

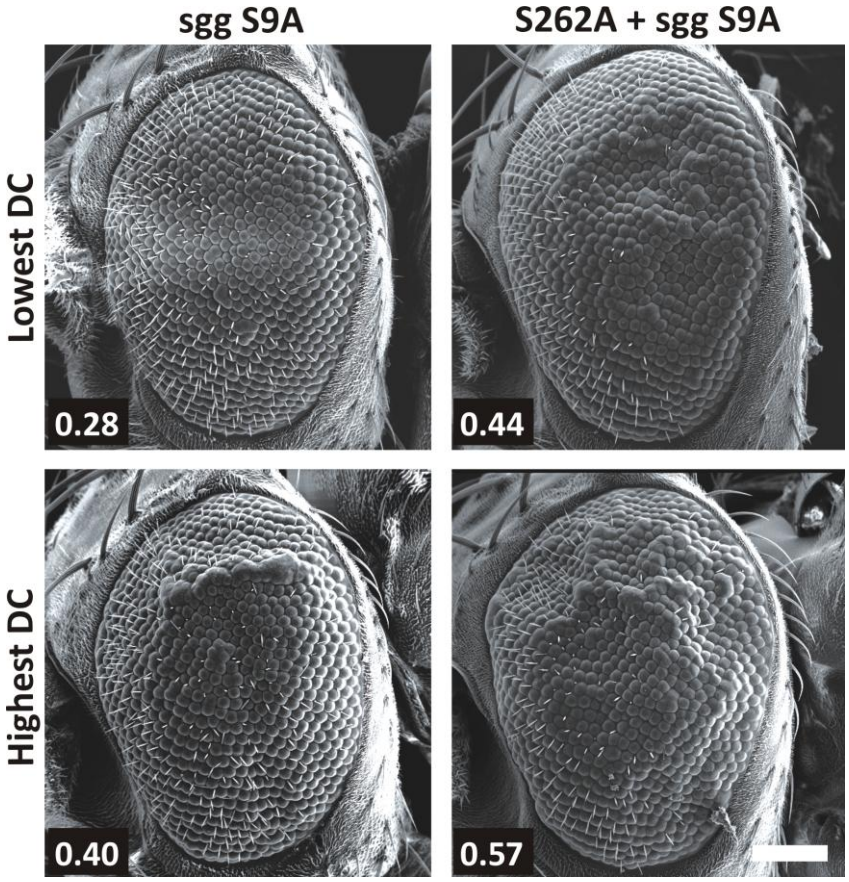

Figure 4.20: Scanning electron micrographs of flies with the lowest and highest DCs expressing sgg S9A with or without S262A tau.
DCs are shown on each image. The range of DCs for the sgg S9A flies was higher than the range for the GMR and S262A tau flies (0.22-0.29 for GMR, 0.21-0.30 for S262A and 0.28-0.40 for sgg S9A) demonstrating that sgg S9A was capable of producing an eye phenotype. The range of the DCs for the S262A + sgg S9A flies was higher than that of the sgg S9A flies, showing that S262A tau was capable of being modulated by sgg S9A and producing an eye phenotype despite the lack of phenotype seen in S262A tau flies. Scale bar 100µm applies to all panels.

4.5 Phosphorylation of tau at S262

Having identified S262 as an important residue for the B-WT enhancement of the tau phenotype I wished to explore whether B-WT was capable of phosphorylating tau at this residue. Figure 4.21 shows that 0N4R tau was phosphorylated at S262 (normalised to total tau, T46) and that co-expression of B-WT caused a significant increase in the intensity of phosphorylated S262 (pS262) signal (n=10, 0.32±0.03 for 0N4R tau and n= 11, 0.62±0.05 for T + B-WT, $p<0.001$, one way anova). No significant increase in pS262 signal was seen upon co-expression of B-NP or B-KD with 0N4R tau (n=8, 0.39±0.05 for T + B-NP and n=9, 0.33±0.05 for T + B-KD). The pS262 signal for T + B-NP and T + B-KD was significantly lower than the signal for T + B-WT ($p<0.05$ and $p<0.01$ respectively, one way anova).

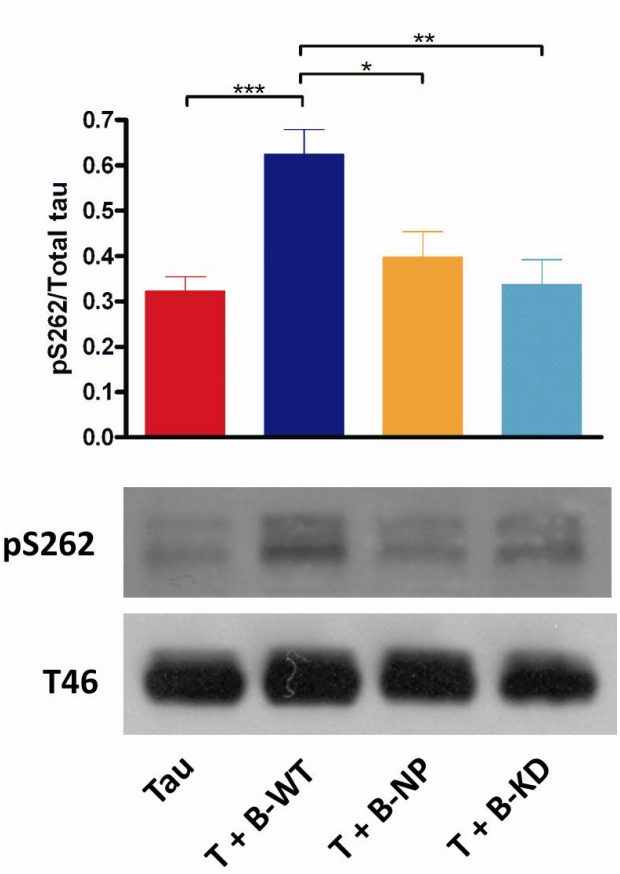

Figure 4.21: Western blots for pS262 and total tau.
*Quantification of western blots from flies expressing tau, T + B-WT, T + B-NP or Tau + B-KD showed that co-expression of B-WT, but not B-NP or B-KD, with 0N4R tau caused a significant increase in tau phosphorylated at S262. T + B-NP and T + B-KD were significantly different from T + B-WT but not from tau alone. Mean ± SEM: 0.32±0.03 for tau (n=10), 0.62±0.05 for T + B-WT (n=11), 0.39±0.05 for T + B-NP (n=8) and 0.33±0.05 for T + B-KD (n=9). *** p<0.001, ** p<0.01, * p<0.05. Representative western blots shown.*

4.6 S2A

PAR-1 is a well characterised tau kinase that has been extensively studied in *Drosophila.* It has been shown to phosphorylate tau at S262 and S356, residues that are within the KXGS repeat motifs in microtubule binding domains 1 and 4 respectively (Nishimura et al., 2004). Mutation of these residues to alanine in tau (hence S2A) prevented PAR-1 associated phosphorylation and PAR-1 enhancement of a tau-induced eye phenotype (Nishimura et al., 2004). Due to the similarity of function between BRSKs and PAR-1, and the data presented in Figure 4.16 which was suggestive of there being another site on tau capable of being phosphorylated by B-WT, I decided to utilise S2A tau in order to assess if S356 could be involved in the enhancement of tau-induced eye phenotypes by B-WT. In order to do this I used S2A and R406W tau flies (kind gifts of Dr Bingwei Lu), with R406W tau replacing 0N4R tau as a control (as the S2A mutations were made in the R406W tau background).

Figure 4.22 shows that expression of R406W tau under the control of the GMR driver caused a similar degenerative eye phenotype to that seen with expression of 0N4R tau and that B-WT was capable of enhancing the R406W phenotype. However, the enhancement of R406W by B-WT was lethal – the fly shown was the only escaper from a number of crosses and as such SEM imaging and phenotypic analysis of R406W + B-WT flies using QED was not possible. Expression of S2A tau, on the other hand, caused no phenotype. Likewise, co-expression of S2A tau with B-WT caused no phenotype either. This data suggests that the sites mutated in

S2A tau (S262/356A) are important for the establishment of both the tau phenotype and the enhancement seen upon co-expression of B-WT.

Figure 4.23 shows SEM images of flies expressing S2A tau with or without B-WT and control eyes expressing GMR, R406W tau, 0N4R tau or 0N4R tau + B-WT. In agreement with the observations made from the light microscope images in Figure 4.22, expression of R406W tau caused a degenerative eye phenotype similar to that of flies expressing 0N4R tau. However, it was evident from the SEM images that the eye phenotype of R406W tau flies was slightly enhanced when compared to the phenotype of 0N4R tau flies, an observation that was confirmed by QED analysis (Figure 4.24).

Expression of S2A tau with or without B-WT did not cause an eye phenotype (Figure 4.23) and this was confirmed by QED analysis (Figure 4.24), demonstrating that the S2A mutations were sufficient to fully rescue the B-WT enhancement of tau-induced eye phenotypes. This suggests that in addition to phosphorylation at S262, phosphorylation at S356 is also involved in the establishment of the tau-BRSK eye phenotype.

Figure 4.25 shows the range of DCs for the R406W, S2A and S2A + B-WT flies. R406W flies had a higher DC range than that of the 0N4R tau flies (0.39-0.63 for R406W and 0.31-0.55 for 0N4R tau) which was likely due to the slightly more toxic nature of R406W tau. The range of the DCs for the S2A and S2A + B-WT flies was similar to that of the GMR flies (0.15-0.25 for S2A, 0.18-0.27 for S2A + B-WT and

0.22-0.29 for GMR), indicating that expression of S2A with or without B-WT did not cause an eye phenotype.

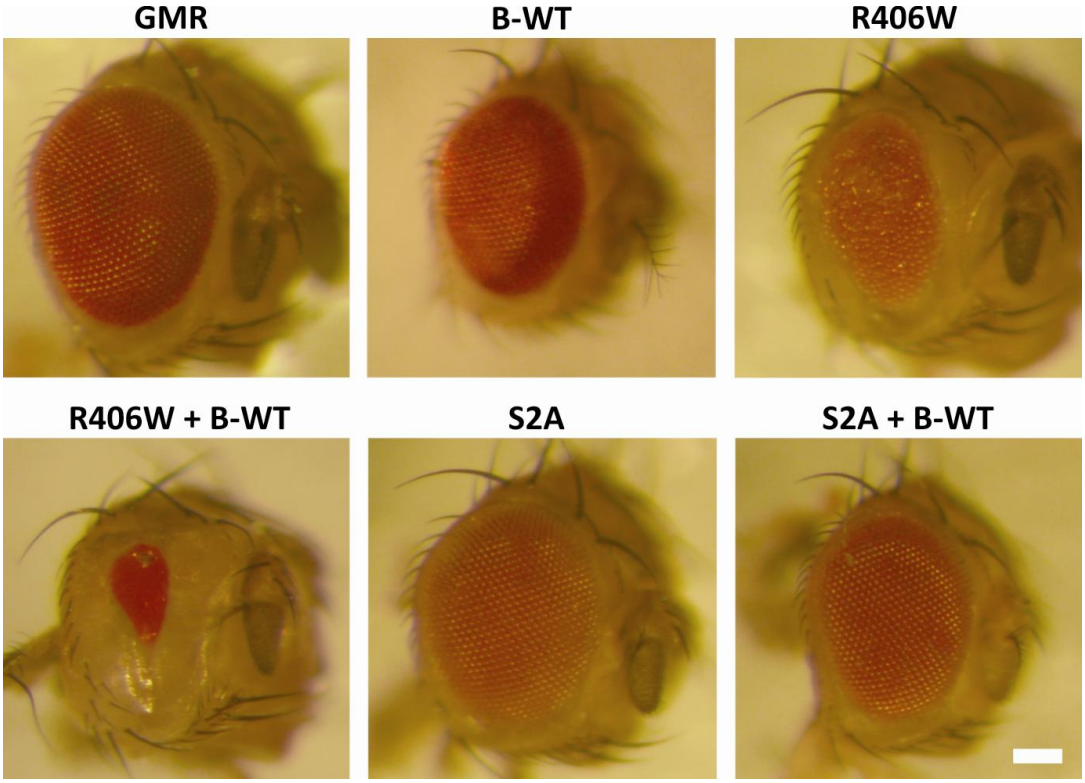

Figure 4.22: Light microscope images of flies expressing R406W or S2A mutated isoforms of tau with or without B-WT.
Expression of R406W tau caused degenerative eye phenotype and B-WT was capable of enhancing the phenotype. Expression of S2A tau, with or without B-WT, caused no eye phenotype suggesting that the S2A residues are important for the establishment of Tau and Tau + B-WT induced eye phenotypes. Scale bar 100µm applies to all panels.

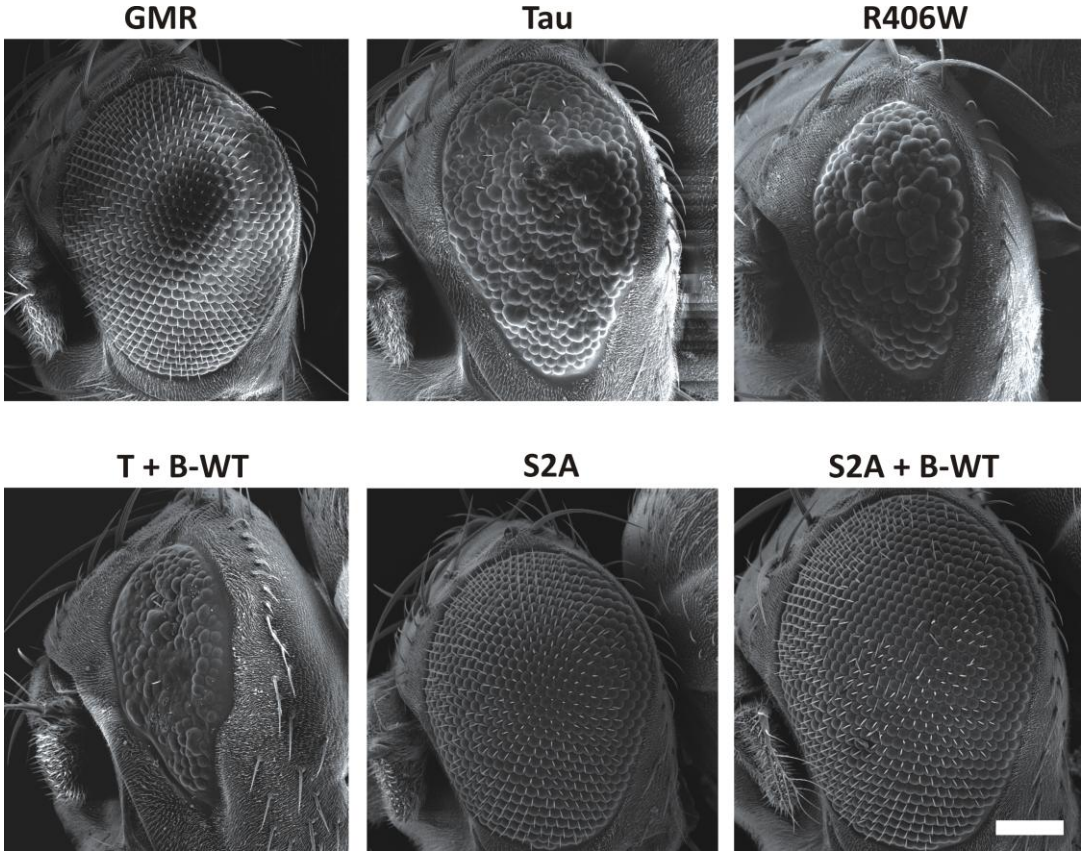

Figure 4.23: Scanning electron micrographs of flies expressing S2A mutated isoforms of tau with or without B-WT.
Expression of R406W tau caused a slightly enhanced eye phenotype when compared to flies expressing 0N4R tau (Tau). Expression of S2A tau, with or without B-WT, caused no eye phenotype suggesting that S356 is also an important residue for the establishment of Tau and Tau + B-WT induced eye phenotypes. Scale bar 100µm applies to all panels.

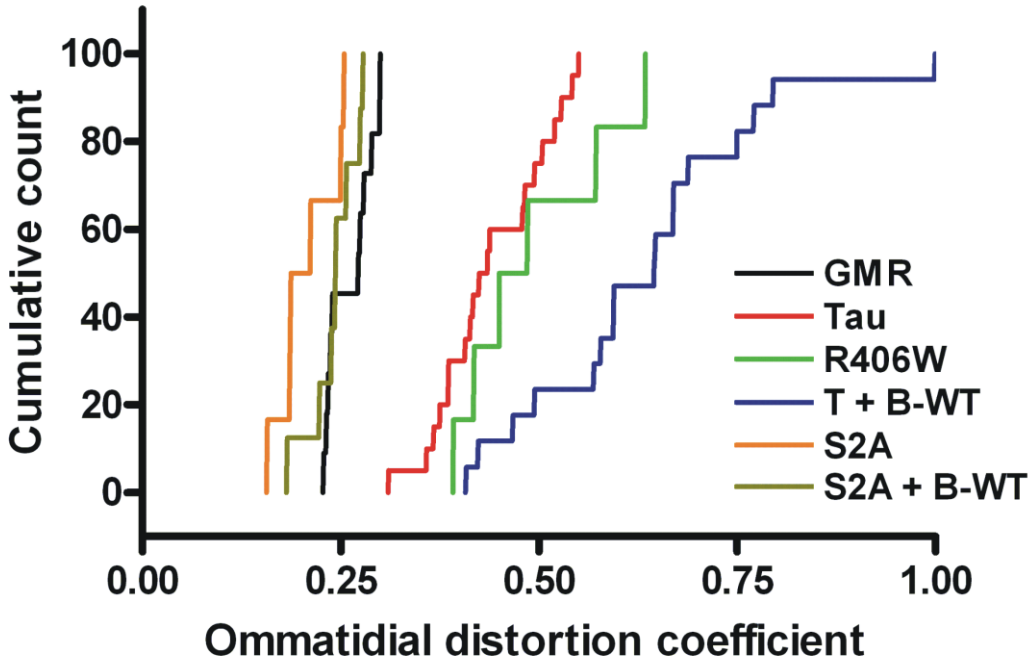

Figure 4.24: Cumulative distribution plot of ommatidial distortion measures (DCs) produced by QED software for flies co-expressing human S2A mutated tau with or without B-WT.

Expression of R406W caused a slightly enhanced phenotype when compared to 0N4R tau (Tau). Expression of S2A tau, with or without B-WT, caused no eye phenotype indicating that the S2A mutations were sufficient to fully rescue the tau-BRSK eye phenotype. GMR n=10, Tau n=20, R406W n=6, T + B-WT n=17, S2A n= 6 and S2A + B-WT n=8.

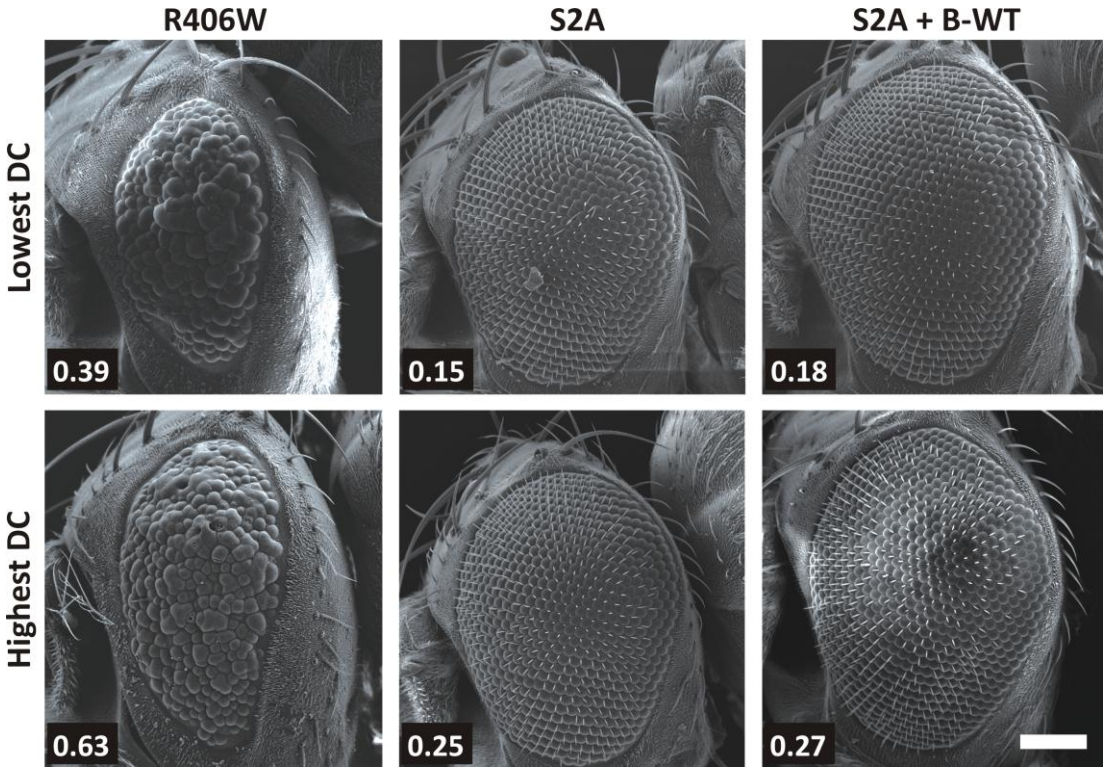

Figure 4.25: Scanning electron micrographs of flies with the lowest and highest DCs expressing R406W, S2A or S2A + B-WT.
DCs are shown on each image. The range of DCs for the R406W flies was higher than the range for the 0N4R tau flies (0.39-0.63 for R406W and 0.31-0.55 for 0N4R tau) demonstrating the slightly more toxic nature of R406W tau. The range of the DCs for the S2A and S2A + B-WT flies was similar to that of the GMR flies (0.15-0.25 for S2A, 0.18-0.27 for S2A + B-WT and 0.22-0.29 for GMR). Scale bar 100µm applies to all panels.

4.7 Discussion

Eyes expressing human BRSK2 isoforms did not have a distinct phenotype to those from GMR flies as assessed by SEM and QED. Previous work in *Drosophila* using endogenous tau kinases over-expressed in the eye has shown that both sgg and PAR-1 are capable of disrupting normal eye phenotypes when expressed in the absence of tau (Nishimura et al., 2004; Chatterjee et al., 2009). On the other hand, not all tau kinases cause a phenotype when over-expressed in the eye; expression of checkpoint kinase 2 (Chk2) does not cause a rough eye phenotype despite it being capable of enhancing a tau-induced deleterious phenotype (Iijima-Ando et al., 2010).

Co-expression of B-WT with 0N4R human tau caused a dramatic exacerbation of the tau-induced degenerative eye phenotype. This was clearly visible in the SEM images, semi-thin resin sections and QED analysis. As the BRSK2 expressed was WT, and as such required activation via phosphorylation at the T-loop T174 residue by an upstream kinase, this demonstrated the presence of upstream kinase(s) in *Drosophila* that could regulate human BRSK. However, over-expression of the *Drosophila* BRSK homologue, CG6114, did not enhance the human tau-induced eye phenotype and in fact seemed to cause a slight amelioration of the human tau-induced phenotype. In contrast to other work on tau kinases in *Drosophila*, this study uses human BRSKs with human tau (rather than endogenous kinases with human tau). It is my belief that this is more relevant to human disease as the functions of *Drosophila* and human genes are not necessarily conserved: endogenous CG6114 does not appear to be able to interact with human tau (as assessed by SEM and QED). This highlights the need to ensure that work with endogenous kinases that are shown

to be able to interact with or phosphorylate human tau is followed up and that the human genes are also validated to be tau kinases. An alignment between the human BRSK isoforms and CG6114 showed that the two sites that were mutated in the human BRSK isoforms were conserved in CG6114. This would suggest that the inability of CG6114 to enhance the human tau-induced eye phenotypes was not due to differential upstream regulation of human BRSKs and CG6144. However, a weakness in the experiments using CG6114 is that the expression of CG6114 was not validated by western blot. Thus it is possible that CG6114 was not being expressed properly or was unstable.

There is a growing body of evidence in AD research showing that oxidative stress causes extensive damage to DNA, RNA and proteins in the brain (Lovell and Markesbery, 2007). This is of interest because BRSK2 has been shown to be activated in response to UV- and methyl methane sulphonate-induced DNA damage in HeLa cells (Lu et al., 2004). With regards to this, the phenotype exhibited upon co-expression of tau and B-WT is strikingly similar to that caused by co-expression of human tau with endogenous checkpoint kinase 2 (Chk2), a kinase which is activated primarily by ataxia telangectasia mutated (ATM) in response to double strand breaks in DNA (Iijima-Ando et al., 2010). When activated by ATM, Chk2 phosphorylates a number of proteins related to DNA damage responses including DNA repair and replication proteins and cell-cycle checkpoint regulators (Stracker et al., 2009). Chk2 has been shown to be able to phosphorylate tau at S262 both *in vitro* and *in vivo* (Iijima-Ando et al., 2010). Further work is required to elucidate the exact role BRSK2 may be playing in response to DNA damage, but at least two DNA damage response kinases (Chk1 and Chk2) have already been shown to

phosphorylate tau and this may infer that tau is implicated in the DNA damage response.

Exacerbation was not seen when B-NP or B-KD was co-expressed with human tau, at similar levels to B-WT (shown in Chapter 3, Figure 3.7), demonstrating that two distinct point mutations that render the recombinant BRSK inactive prevent the genetic interaction with tau in this model. This shows that it is BRSK kinase activity that modulates tau toxicity. However, QED quantification indicated that B-NP was capable of producing an intermediate phenotype not obvious from visual examination of the SEM images. LKB1, the master kinase of the AMPK family, phosphorylates a threonine in the T-loop of BRSKs and another 10 members of the AMPK family causing their activation (Lizcano et al., 2004). The T-loop threonine residue in BRSK1, which is surrounded by the same amino acids as in BRSK2, has been shown to be targeted by CaMKKα *in vitro* (Fujimoto et al., 2008). Mutation of the T-loop residue to alanine in B-NP should prevent B-WT from being activated through phosphorylation by LKB1 or CaMKKα. Conversely, the data shown here for tau + B-NP suggests that either BRSK2 may have other functional interactions of tau independent of phosphorylation, or that mutation of the T-loop threonine to alanine is not sufficient to render the kinase fully inactive in this *Drosophila* model.

Co-expression of B-CA with tau, which should have produced a similar phenotype to that seen in the tau + B-WT flies, did not cause an exacerbation of the tau phenotype. Mutation of the T-loop threonine to glutamic acid in BRSK1 creates a CA isoform of the kinase when expressed in *E.coli* cells (Lizcano et al., 2004). However, it has been shown that the equivalent mutation in BRSK2 is not sufficient to render the

kinase constitutively active in mammalian cells, despite the sequence around the two residues being identical in both isoforms of BRSK (Bright et al., 2008). The reason for differential effects of this mutation on BRSK isoforms is not known but it would seem that my phenotypic data is in agreement with the data of Bright et al (2008); mutation of T174 in BRSK2 is not sufficient to render the kinase constitutively active when expressed in *Drosophila*. In order to test what effect the T174E mutation had on BRSK2 activity, I would co-transfect B-CA or B-WT with tau into HeLa cells in the presence of siRNA against CaMKK and measure the phosphorylation of tau at S262 by western blot. As HeLa cells do not have LKB1, the use of siRNA against CaMKKα should down regulate the other major activator of BRSK2. Thus, if B-CA activity was independent of its activation, then the pS262 signal should be higher in the cells transfected with B-CA compared to B-WT. Although this approach would not enable me to determine the effect of the T174E mutation on BRSK2 activation when expressed in *Drosophila*, it would give an indication as to whether this mutation is sufficient to render BRSK2 constitutively active. To further address whether the mutation can render BRSK2 constitutively active when expressed in *Drosophila*, I could perform a similar experiment in a *Drosophila* cell line such as Schneider 2 cells. However, this would require siRNA targeting both LKB1 and CG17698 (the *Drosophila* homologue of CaMKKα).

Expression of S262A tau prevented both the tau-induced phenotype and the B-WT exacerbation. There was a small effect on ommatidial structure seen with co-expression of S262A and B-WT, which could indicate that there may be other sites in tau that are important for the establishment of the Tau + B-WT phenotype. The most likely candidate for another site would be S356, which is in the fourth microtubule

binding domain of tau and is part of a KXGS motif like the one surrounding S262. PAR-1 is capable of phosphorylating both sites, and due to the similarities in function of PAR-1 and BRSKs, it is likely that BRSKs are also capable of targeting both residues (Chatterjee et al., 2009). That said, a large amelioration in phenotype was obtained by mutating S262, suggesting that S262 is an important residue for the formation of deleterious eye phenotypes caused by the co-expression of tau and B-WT. The production of the tau transgenic flies involves the random insertion of the human tau gene into the *Drosophila* genome. This has led to a number of useful fly lines transgenic for various isoforms of human tau, but due to the nature of the transgenesis, the human genes are likely to have been inserted at different locations in the genome. This is a problem as insertion at different locations leads to differential expression levels; an issue which should not be ignored. When discussing the lack of phenotype produced by flies with mutations in tau (such as the S262A flies used here), the expression level must be taken into consideration as it may not necessarily be the mutations that prevent a phenotype, but a lower expression. There is a way of circumnavigating this issue; it is now possible to perform targeted transgenesis in *Drosophila* where each transgene is inserted into the same genetic location. However, this was not an option for the experiments performed in this thesis and so a positive control experiment using the *Drosophila* homologue of mammalian GSK3-β, sgg (constitutively active from) was conducted. This indicated that the lack of phenotype in the S262A flies was not due to the poor expression of S262A tau (shown in Appendix 4, Figure 12.3) as co-expression of S262A tau with sgg caused an eye phenotype which was worse than the phenotype caused by expression of either sgg or S262A tau alone, indicating that S262A tau

was capable of being modulated by kinase activity and that this modulation resulted in a detectable eye phenotype.

Analysis of lysates from flies expressing 0N4R tau ± B-WT, B-NP or B-KD showed that 0N4R human tau was phosphorylated under basal conditions in the fly, and that co-expression of B-WT significantly elevated the level of phosphorylation. Phosphorylation of S262 has been shown to have a significant effect on the microtubule binding function of tau in both *in vivo* and *in vitro* experiments and is known to be elevated in pre-tangles using a pS262 antibody, and intra-neuronal NFTs using the 12E8 antibody, which also recognises pS356 (Sengupta et al., 1998; Augustinack et al., 2002; Fischer et al., 2009). Pre-tangles and intra-neuronal NFTs are early forms of the extracellular NFTs which characterise AD. Thus, phosphorylation of tau by B-WT may represent an important event in the early stages of AD pathogenesis. Also relevant to this discussion is an experiment performed by a PhD student in the laboratories of Dr Moffat and Prof Frenguelli, demonstrating that co-expression of tau with B-WT causes a decrease in microtubule-bound tau when compared to flies expressing tau alone (personal communication, Mr Charlie Cameron). Thus, it would seem that phosphorylation of tau at S262 by B-WT causes tau to dissociate from microtubules. However, it is yet to be determined if the decrease in microtubule-bound tau is as a direct consequence of B-WT activity (by substituting B-WT for B-KD or B-NP) and whether there is a corresponding increase in tau phosphorylated at S262 in the soluble tau fraction of this assay (the tau which is not bound to microtubules). Elevation of pS262 was not seen upon co-expression with the B-NP or B-KD isoforms of BRSK2 suggesting that the increase in pS262 seen with B-WT expression is as a direct consequence of the kinase activity of B-WT.

The lack of pS262 phosphorylation in the flies co-expressing B-NP with tau does not correlate with the data produced using QED for these flies: QED analysis showed that B-NP slightly exacerbated the tau induced eye phenotype but western blots showed pS262 was not increased. This would suggest that there may be other regulatory sites on BRSK (as shown by the B-NP QED data) and that there may be other residues in tau which are targeted by BRSK. This is supported by the data that shows that co-expression of S262A tau with B-WT causes a slight eye phenotype. However, it should also be taken into consideration that western blotting is a semi-quantitative technique and as such may not be sensitive enough to detect small differences in pS262.

Mutation of two serine residues in S2A tau fully prevented the tau-induced degenerative phenotype and the B-WT enhancement, indicating that both S262 and S356 are important residues for the formation of these phenotypes. With regards to this, an experiment performed recently by Dr Alessia Galasso, a post-doctoral researcher in the laboratories of Dr Moffat and Prof Frenguelli shows that co-transfection of B-WT with human 2N4R tau in human embryonic kidney (HEK) cells increased tau phosphorylation at S356 (personal communication, Dr A. Galasso). This supports the hypothesis that B-WT enhances tau toxicity through phosphorylation of tau at both S262 and S356, but this requires further study. The data on S2A and B-WT is consistent with the observations made by Nishimura *et al*., (2004) who showed that S2A tau had no eye phenotype and that expression of PAR-1 with S2A tau did not cause an enhancement (Nishimura et al., 2004). Expression of B-WT with R406W tau was lethal; the reason for this lethality remains unknown - it could be due to the more toxic nature of R406W tau, or it could be as a result of

GAL4 toxicity (Wittmann et al., 2001; Kramer and Staveley, 2003; Dietzl et al., 2007; Hua et al., 2010). It was not possible to investigate the expression level of S2A tau as the stock became contaminated before the experiment was completed. However, I was able to show that the R406W tau flies expressed significantly less tau than the 0N4R tau flies, and it has been previously published that tau expression in the S2A flies is not significantly different from that of the R406W flies (Nishimura et al., 2004). A positive control experiment for S2A tau (using constitutively active sgg) was not conducted as this has been previously published (Chatterjee et al., 2009).

As an aside, it is interesting that it is very difficult to ameliorate the 'basal' eye phenotype that is formed upon expression of human tau. This raises the question of why does the human tau eye phenotype form? There are a number of possible scenarios: it has been shown that expression of human tau in a *Drosophila* tau null (-/-) background does not affect the human tau-induced eye phenotype, so it is unlikely that the phenotype arises due to sequestration of vital factors away from *Drosophila* tau by human tau, as a result of competition for microtubule binding between human and *Drosophila* tau or due to a simple 'overload' of tau (Feuillette et al., 2010). Further to this, Feuillette *et al.* (2010) indicates that the majority of human tau expressed in the *Drosophila* eye exists as soluble cytosolic hyperphosphorylated species and that the accumulation of soluble cytosolic hyperphosphorylated species correlates with tau toxicity. They draw this conclusion on the basis that expression of human tau^{AP} (in which 14 threonine and serine sites have been mutated to alanine to prevent phosphorylation), in their opinion, does not cause an eye phenotype whereas expression of human tau^{E14} (in which all of the serine sites have been

mutated to glutamic acid to mimic phosphorylation) causes a rough eye phenotype (Feuillette et al., 2010). In contrast, my data shows that mutation of S356 and/or S262 to alanine is sufficient to prevent the human tau-induced eye phenotype, which would suggest that not only is phosphorylation at these residues vital, but that the formation of human tau-induced eye phenotypes may not have a direct relationship to the phosphorylation load of tau; the Feuillette study is based upon the mutation of a large number of residues, whereas I show that mutation of one or two residues (in the S262A and S2A tau respectively) is sufficient to render human tau non-toxic when expressed in the *Drosophila* eye despite all the other residues of tau being available for phosphorylation. In support of this, is the data presented by Chatterjee *et al.*, (2009) whereby S2A tau, which was still highly phosphorylated, was shown to be non-toxic and S11A tau (in which 11 serine residues that are known to be targeted by GSK-3β are mutated to alanine but S262 and S356 are not mutated), which was not highly phosphorylated, was shown to be toxic (Chatterjee et al., 2009). Therefore, it would appear that there is not a direct relationship between the toxicity of human tau and the phosphorylation load. Instead, it may be the case that tau toxicity is more intricately linked to phosphorylation at individual sites and the effect that phosphorylation at each site has on the microtubule binding ability and solubility of tau.

Taken together, the data in this chapter indicate that B-WT is capable of phosphorylating 0N4R human tau at S262. This is the most convincing data to date of an *in vivo* interaction between human tau and BRSK2, although I have no evidence as to whether this interaction is direct or mediated by a third intermediary protein. However, there is no evidence to date of BRSK forming a complex with

other proteins. There is evidence that B-WT is able to interfere with the microtubule binding properties of tau, most likely through its role in phosphorylating tau at S262, a residue which is known to be important for microtubule binding (Sengupta et al., 1998; Fischer et al., 2009) and that B-WT is also capable of phosphorylating tau at S356.

Due to its brain-specific expression, especially in areas affected by AD such as the cortex and the hippocampus, BRSK2 is proving to be a potentially important tau kinase that has been previously overlooked. In the next chapter I will address the regulation of human BRSK2 in the *Drosophila* model, and the possibility that the BRSK2-tau interaction is regulated in a calcium-dependent manner.

5| Upstream regulation of human BRSK2 in *Drosophila*.

5.1 Introduction

Having demonstrated in the previous chapter that BRSK2 was capable of enhancing a tau-induced degenerative eye phenotype and phosphorylating tau at S262, I was interested in identifying endogenous *Drosophila* kinases that were capable of regulating this interaction. According to the literature, there are two upstream regulators of BRSKs; LKB1 and CaMKKα (Lizcano et al., 2004; Fujimoto et al., 2008). As discussed in the Introduction, LKB1 is a master kinase that phosphorylates and regulates 14 members of the AMPK-related family of protein kinases and CaMKKα is a member of the Ca^{2+}/calmodulin-dependent family of protein kinases. Both kinases have been shown to activate BRSKs via phosphorylation at T174 in BRSK2 and T189 in BRSK1. LKB1 and CaMKKα both have homologues in the *Drosophila* genome - LKB1 (referred to as DmLKB1 in order to distinguish between the human and *Drosophila* genes) and CG17698 respectively.

Experiments were conducted in order to elucidate whether DmLKB1 and/or CG17698 were required for the interaction between human tau and human BRSK2 in the *Drosophila* eye. To do this, RNAi lines (obtained from the Vienna *Drosophila* RNAi Collection, VDRC) targeting endogenous DmLKB1 and CG17698 were utilised. To address the specificity of the RNAi, flies transgenic for human CaMKKα (hCaMKKα) were utilised as hCaMKKα is not targeted by the CG17698 RNAi. Due to time constraints it was not possible to do the same rescue experiment using DmLKB1 RNAi and human LKB1. To elucidate whether enhancement of tau-induced eye phenotypes by B-WT occurred in a calcium dependent manner, UAS-

cacophony1 flies (obtained from the Bloomington Stock Center) were used to over-express *cacophony1* (*Drosophila* calcium channel α subunit) in the eye along with tau and B-WT.

Due to the apparent overlap between BRSK and PAR-1 functions, I was interested to ascertain whether endogenous PAR-1 (referred to DmPAR-1 in order to distinguish between the human and *Drosophila* genes) was contributing to B-WT exacerbation of the tau phenotype. To address this, I used a DmPAR-1 RNAi line (obtained from VDRC) to down-regulate the expression of endogenous DmPAR-1 in flies co-expressing tau with B-WT. Finally, western blots on lysates from flies expressing tau and B-WT together with DmLKB1 RNAi, CG17698 RNAi or DmPAR-1 RNAi were performed in order to elucidate the effect of down-regulation of the genes targeted by the RNAi on B-WT induced phosphorylation of tau at S262.

5.2 Results

5.2.1 Co-expression of DmLKB1 RNAi with human tau and human B-WT

In order to ascertain whether endogenous DmLKB1 was required for regulation of human B-WT in *Drosophila*, RNAi targeting DmLKB1 was utilised. Visual examination of flies expressing two copies of DmLKB1 RNAi, with or without tau, showed that DmLKB1 RNAi expression did not have an effect on eye phenotype (Figure 5.1). This was confirmed by QED analysis. GMR flies (shown in Chapter 4, Figure 4.4) had a DC range of 0.22-0.29 whilst flies expressing two copies of DmLKB1 RNAi had a range of 0.19-0.33. Flies expressing Tau (shown in Chapter 4, Figure 4.7) had a DC range of 0.31-0.55 whilst flies expressing two copies of DmLKB1 RNAi with Tau had a range of 0.31-0.65 (data not shown).

Expression of one or two copies of DmLKB1 RNAi in fly eyes expressing human tau with human B-WT resulted in a phenotype which was in-between that of the Tau and Tau with B-WT flies (Figure 5.2). QED analysis confirmed that expression of DmLKB1 RNAi with Tau and B-WT rescued the phenotype, resulting in a phenotype similar to that of flies co-expressing tau and B-NP. This rescue did not appear to be dose-dependent as the curves produced for flies with one copy of the RNAi was very similar to the curve produced for flies with two copies (Figure 5.3).

Figure 5.4 shows that the DC range for flies expressing one copy of DmLKB1 RNAi with Tau and B-WT (0.39-0.62) was intermediate to the ranges of flies expressing Tau alone (0.31-0.55, shown in Chapter 4, Figure 4.7) or Tau with B-WT (0.40-0.99, shown in Chapter 4, Figure 4.7). The DC range of flies expressing two copies of

DmLKB1 RNAi with Tau and B-WT (0.36-0.99) appeared very similar to the range of the Tau + B-WT flies, but this was not the case; it can be seen from figure 5.3 that there is only one fly that had a high DC (0.99) and that the rest of the flies fell in-between the Tau and Tau + B-WT curves.

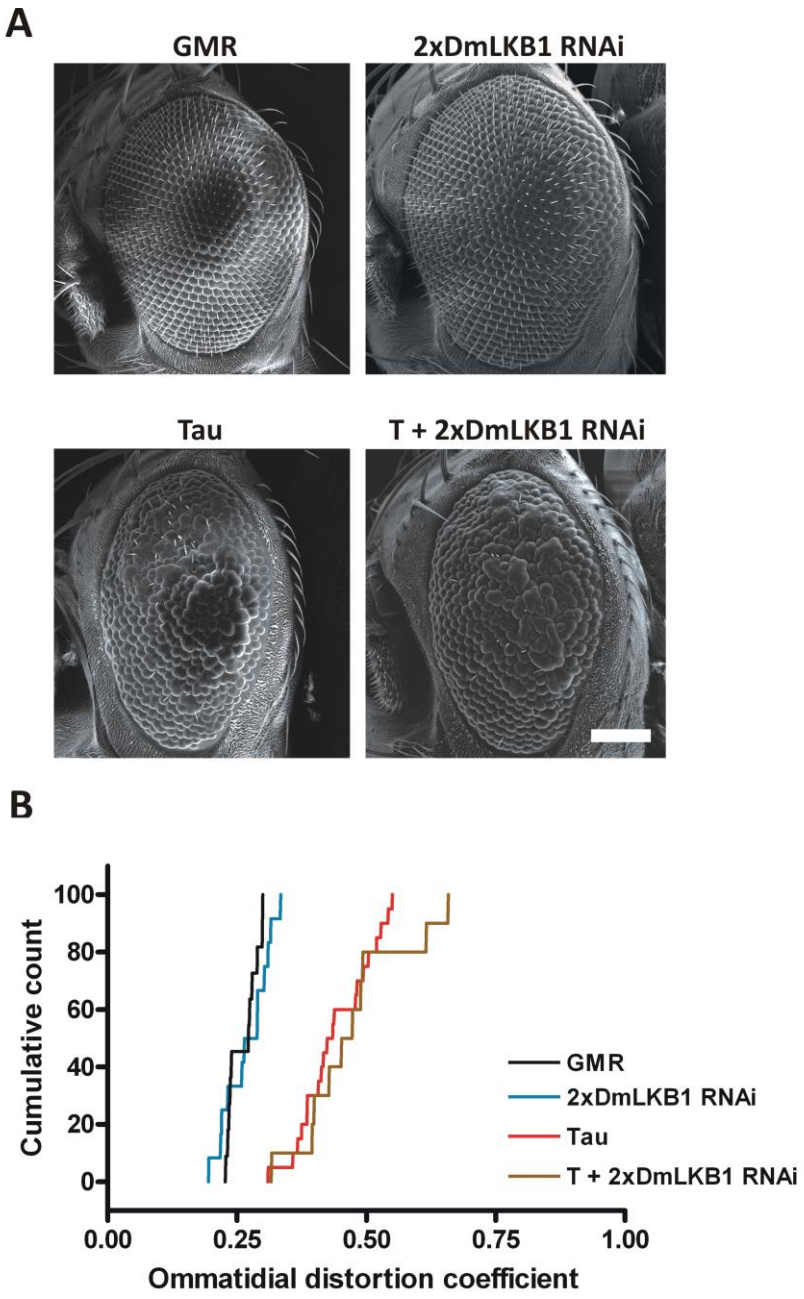

Figure 5.1: SEM images and QED analysis of flies expressing two copies of DmLKB1 RNAi with or without 0N4R tau.

A: Expression of two copies of DmLKB1 RNAi had no visible effect on the eye phenotype when expressed either alone (compared to GMR) or with tau (compared to tau). Scale bar 100µm applies to all panels. B: Quantitative analysis of flies expressing two copies of DmLKB1 RNAi, with or without tau, shows that down-regulation of endogenous DmLKB1 had no effect on eye phenotype in flies either expressing DmLKB1 RNAi alone (compare with GMR) or with Tau (compare with tau). GMR n=11, 2xDmLKB1 RNAi n=12, Tau n=20 and T + 2xDmLKB1 RNAi n=10.

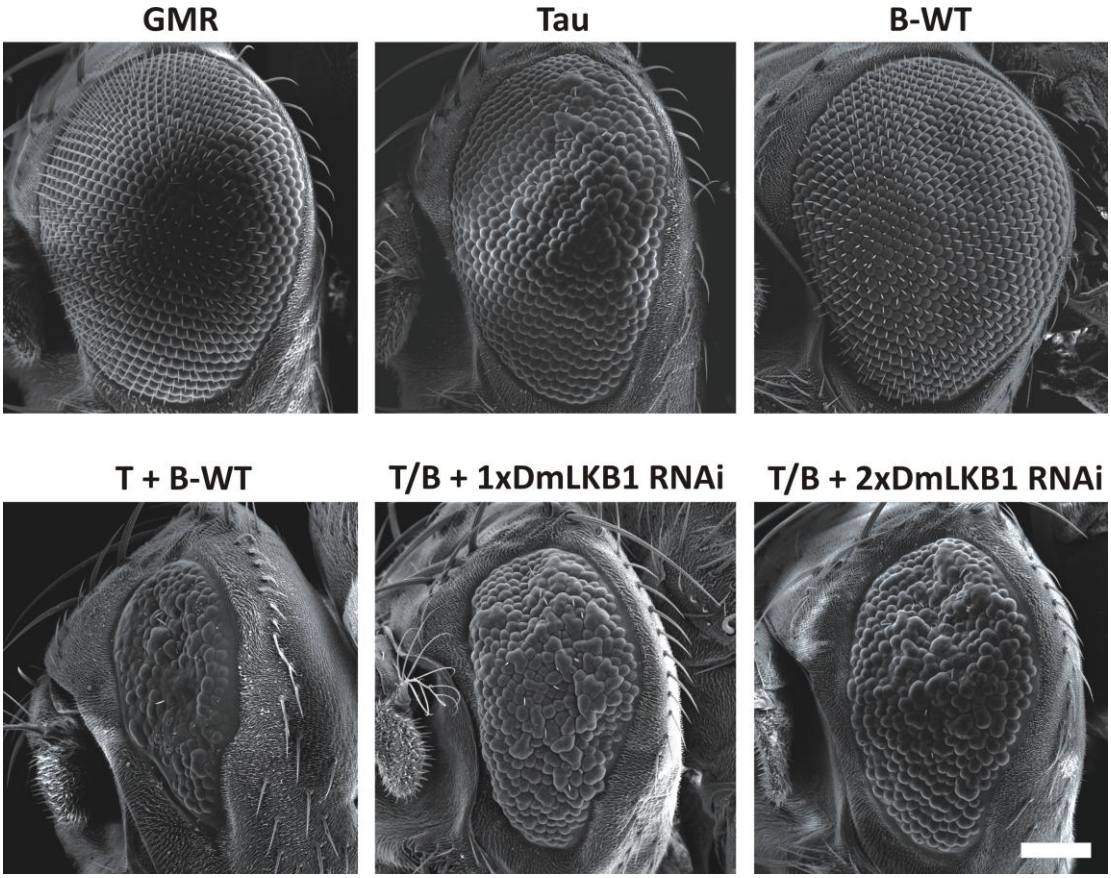

Figure 5.2: SEM images of flies expressing 0N4R tau, B-WT and DmLKB1 RNAi. *Scanning electron micrographs showing that expression of DmLKB1 RNAi (one or two copies) rescues the phenotype caused by co-expression of tau with B-WT (T/B + 1xDmLKB1 RNAi and T/B + 2xDmLKB1 RNAi). Scale bar 100µm applies to all panels.*

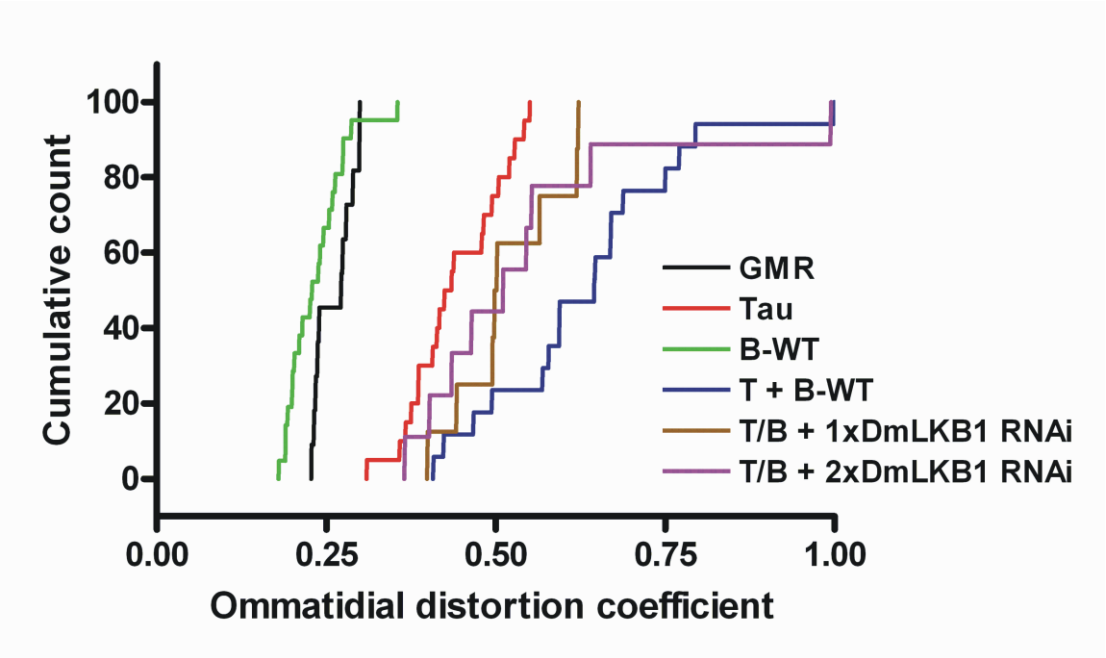

Figure 5.3: Cumulative distribution plot of ommatidial distortion measures (DCs) produced by QED software for flies co-expressing 0N4R tau, B-WT and DmLKB1 RNAi.

Quantitative analysis of flies expressing one or two copies of DmLKB1 RNAi shows that down-regulation of endogenous DmLKB1 rescues the phenotype caused by co-expression of Tau with B-WT (T/B + 1xDmLKB1 RNAi and T/B + 2xDmLKB1 RNAi). The rescue did not appear to be dose-dependent as one copy of DmLKB1 RNAi had the same effect as two copies. GMR n=11, Tau n=20, B-WT n=21, T + B-WT n=17, T/B + 1xDmLKB1 RNAi n=8 and T/B + 2xDmLKB1 RNAi n=9.

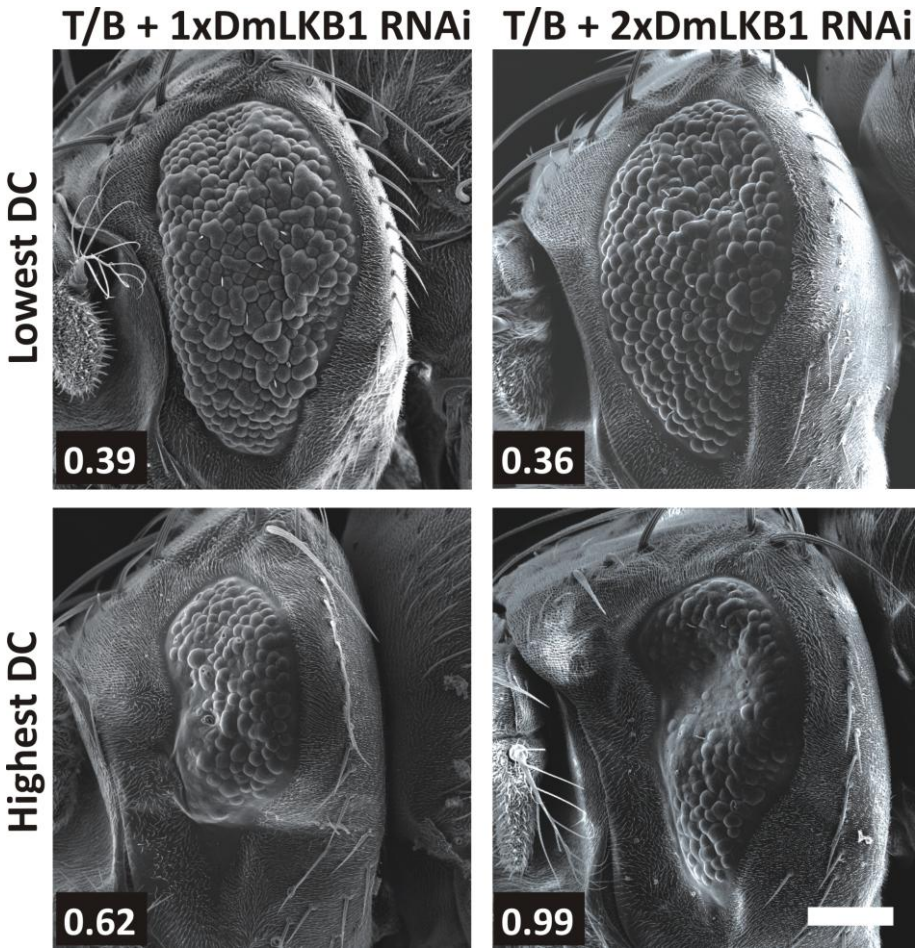

Figure 5.4: SEM images of flies expressing tau, B-WT and one or two copies of DmLKB1 RNAi with the lowest and highest DCs.
Images of flies expressing either one or two copies of DmLKB1 RNAi with 0N4R tau and B-WT. The range of DCs is very similar. DCs are shown on the images. Scale bar 100µm applies to all panels.

5.2.2 Co-expression of CG17698 RNAi with tau and B-WT

In order to ascertain whether endogenous CG17698 was capable of regulating human B-WT in *Drosophila*, RNAi targeting CG17698 was utilised. Visual examination of flies expressing CG17698 RNAi, with or without Tau, showed that CG17698 RNAi expression did not have an effect on eye phenotype when expressed alone, but that it slightly enhanced the phenotype when expressed with Tau (Figure 5.5). This was confirmed by QED analysis: the curve for flies expressing CG17698 RNAi with Tau was shifted to the right of the curve for flies expressing Tau alone (Figure 5.5). The DC range for GMR flies (shown in Chapter 4, Figure 4.4) was 0.22-0.29 whilst flies expressing CG17698 RNAi had a range of 0.22-0.27. Flies expressing Tau (shown in Chapter 4, Figure 4.7) had a DC range of 0.31-0.55 whilst flies expressing CG17698 RNAi with Tau had a higher DC range of 0.46-0.77 (data not shown).

Expression of CG17698 RNAi in fly eyes expressing human tau with human B-WT rescued the Tau-BRSK phenotype (Figure 5.6), resulting in a phenotype that was similar to that of flies co-expressing tau and CG17698 RNAi or tau and B-NP. Further to this, expression of human CaMKKα (hCaMKKα rescue), which was not targeted by the RNAi, reversed the rescue seen upon expression of CG17698 RNAi in the Tau + B-WT background. However, due to the complex genetics involved in producing this fly, the n number is low. Co-expression of hCaMKKα and tau did not alter the tau-induced eye phenotype (assessed using a light microscope, data not shown); this is likely to be due to CG6114 not being able to act on human tau (Chapter 4, Figures 4.11, 4.12 and 4.13).

QED analysis confirmed the results seen upon visual examination of the SEMs; expression of CG17698 RNAi with Tau and B-WT rescued the phenotype and expression of hCaMKKα in this background returned the phenotype to one similar to that of the flies expressing Tau with B-WT (Figure 5.7).

Figure 5.8 shows that the DC range for flies expressing CG17698 RNAi with Tau and B-WT (0.38-0.59) was intermediate to the ranges of flies expressing Tau alone (0.31-0.55, shown in Chapter 4, Figure 4.7) or Tau with B-WT (0.40-0.99, shown in Chapter 4, Figure 4.7). The DC range of flies expressing hCaMKKα in the Tau, B-WT and CG17698 RNAi background (0.48-0.99) was very similar to the DC range of the flies expressing Tau with B-WT.

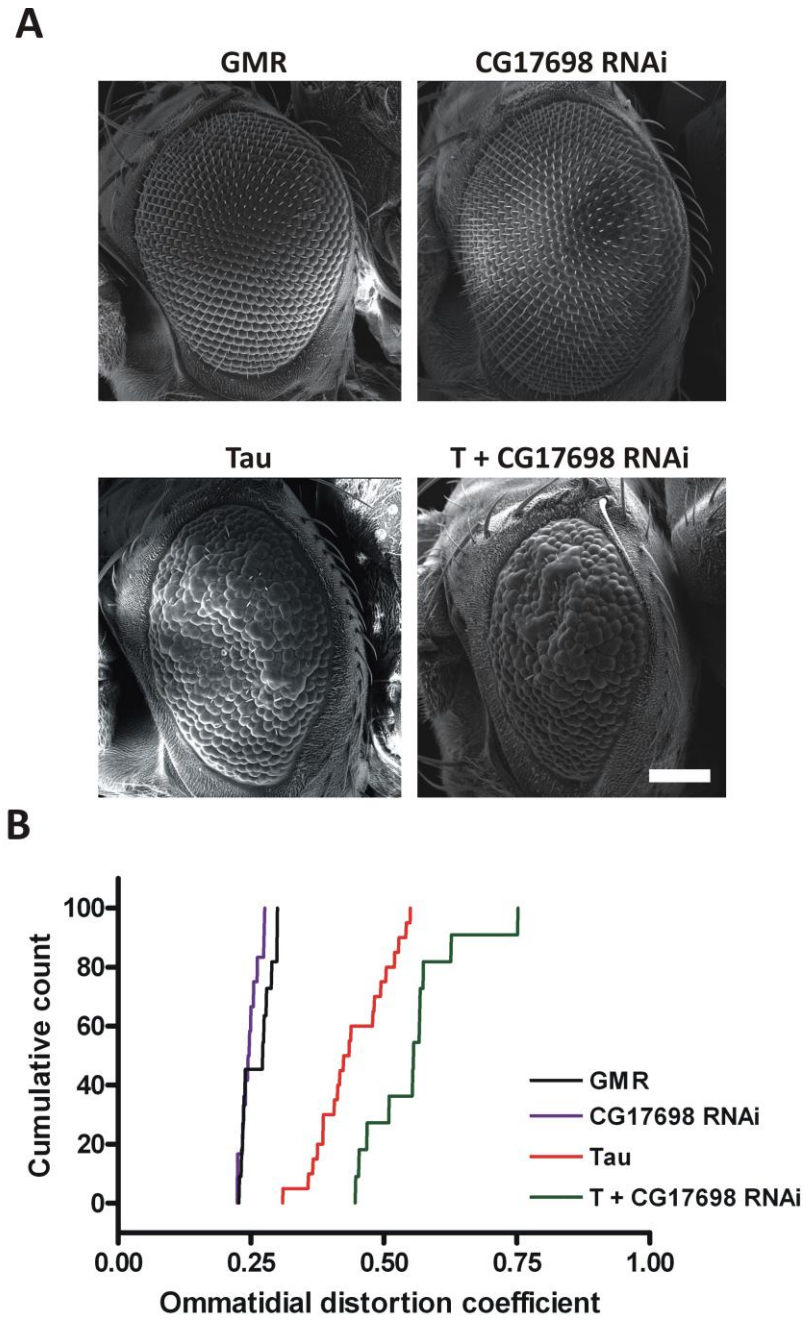

Figure 5.5: SEM images of flies expressing CG17698 RNAi with or without 0N4R tau.

Expression of CG17698 RNAi had no effect on eye phenotype when expressed alone (compare with GMR) but appeared to enhance the eye phenotype when expressed with tau (compare with tau). Scale bar 100µm applies to all panels. Quantitative analysis of flies expressing CG17698 RNAi, with or without tau, shows that down-regulation of CG17698 had no effect on eye phenotype in flies expressing CG17698 RNAi alone (compare with GMR) but that it enhanced the phenotype in flies expressing the RNAi with 0N4R tau (compare with tau). GMR n=11, CG17698 RNAi n=12, Tau n=20 and T + CG17698 RNAi n=11.

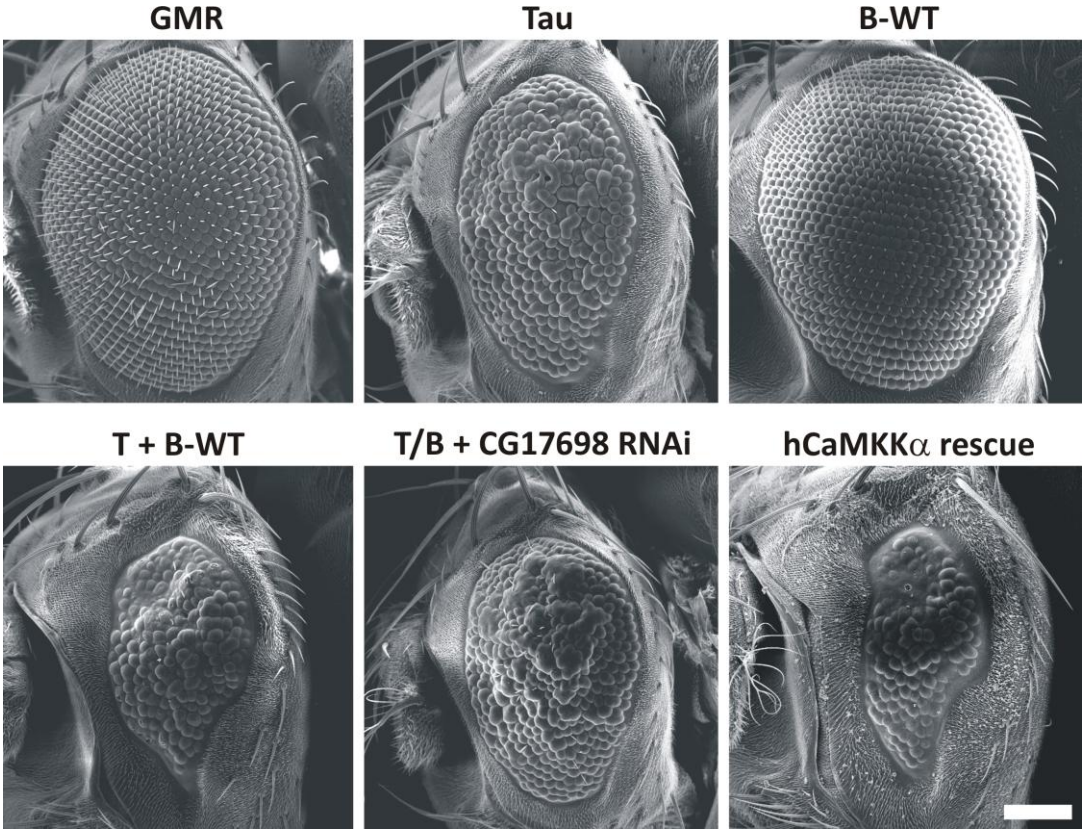

Figure 5.6: SEM images of flies expressing 0N4R tau, B-WT and CG17698 RNAi with or without hCaMKKα.

Scanning electron micrographs showing that expression of CG17698 RNAi can rescue the enhancement seen with co-expression of tau and B-WT. Expression of human CaMKKα in the tau, B-WT, CG17698 RNAi background (hCaMKKα rescue) can over-ride the effect of the RNAi and return the phenotype to something similar to what was seen with expression of tau and B-WT. Scale bar 100µm applies to all panels.

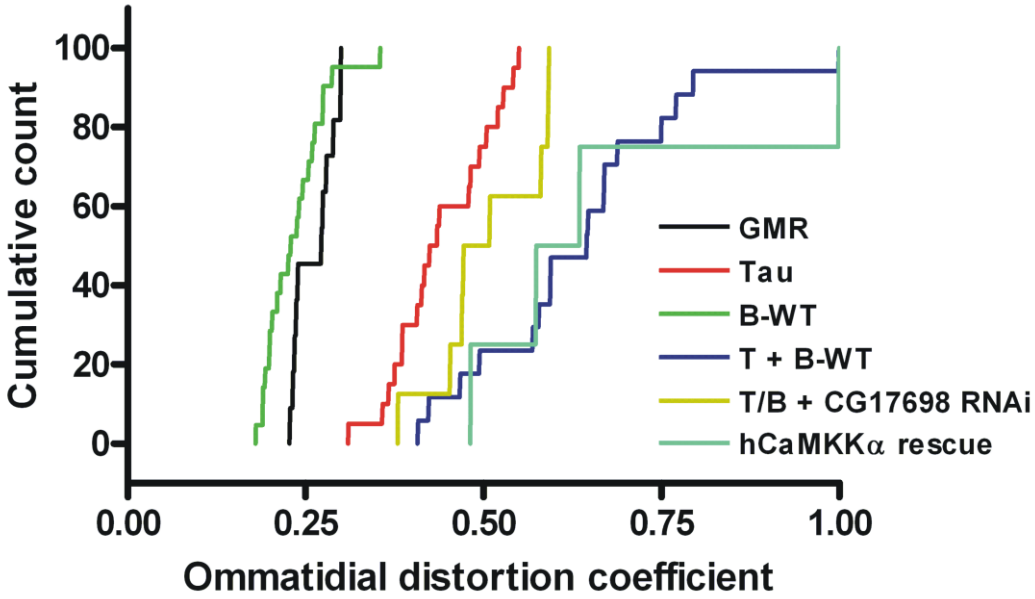

Figure 5.7: Cumulative distribution plot of ommatidial distortion measures (DCs) produced by QED software for flies expressing 0N4R tau, B-WT and CG17698 RNAi with or without hCaMKKα.

Quantitative analysis of flies expressing CG17698 RNAi shows that down-regulation of endogenous CG17698 rescues the phenotype caused by co-expression of 0N4R tau with B-WT. Expression of hCaMKKα in the tau, B-WT, CG17698 RNAi background (hCaMKKα rescue) over-rides the rescue seen with the RNAi. GMR n=11, Tau n=20, B-WT n=21, T + B-WT n=17, T/B + CG17698 RNAi n=8 and hCaMKKα rescue n=4.

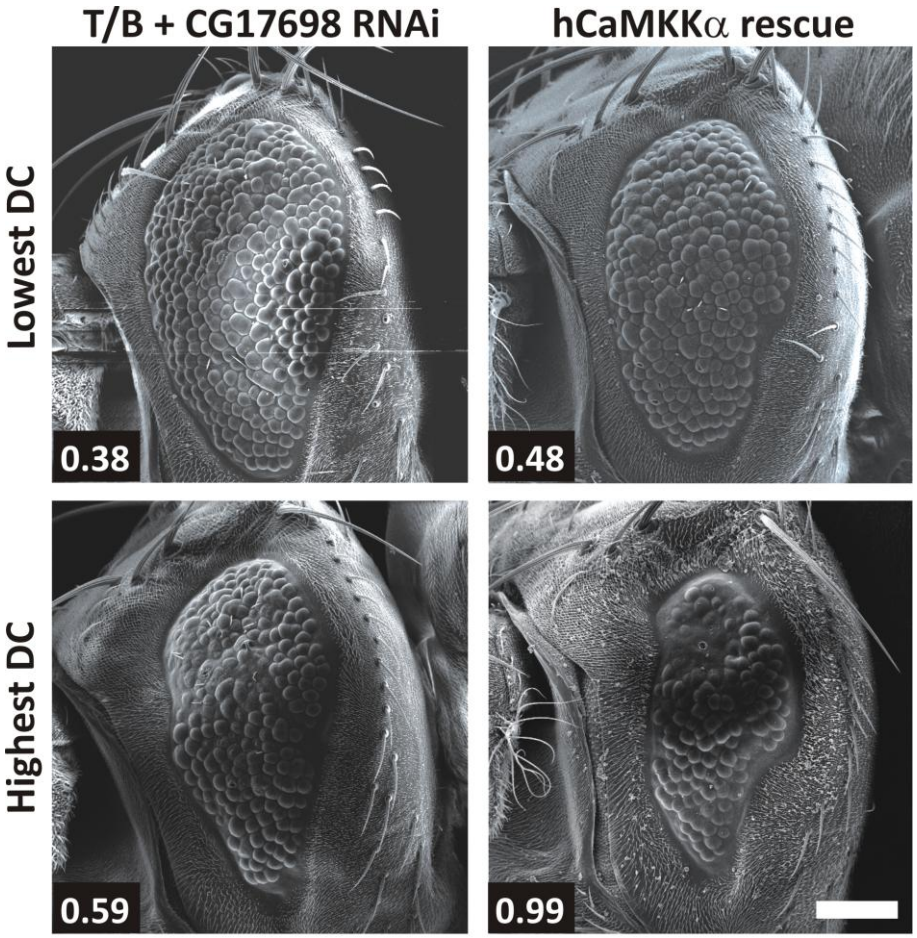

Figure 5.8: SEM images of flies expressing tau, B-WT and CG17698 RNAi with or without hCaMKKα, with the lowest and highest DCs.
The range of DCs for flies expressing tau, B-WT and CG17698 RNAi is in-between the DC ranges of flies expressing tau or tau with B-WT. The range of flies expressing tau, B-WT, CG17698 RNAi and hCaMKKα (hCaMKKα rescue) is similar to the DC range of flies expressing tau with B-WT. DCs are shown on the images. Scale bar 100μm applies to all panels.

5.2.3 Co-expression of both CG17698 and DmLKB1 RNAi with tau and B-WT

Expression of either DmLKB1 RNAi or CG17698 RNAi with tau and B-WT caused a rescue of the eye phenotype. Thus, it could be hypothesised that expression of both RNAi with tau and B-WT could rescue the phenotype to a larger extent (if both RNAi were not 100% effective). However, expression of both RNAi with tau and B-WT did not appear to further rescue the eye phenotype. Instead the phenotype appeared worse than when the RNAi were used individually and the phenotype was returned to something similar to the phenotype seen upon co-expression of tau with B-WT (Figure 5.9).

QED analysis (Figure 5.10) demonstrated that although the n number was quite low (n=5), the eye phenotypes of eyes expressing both RNAi with tau and B-WT were largely similar to the eye phenotypes of flies expressing tau and B-WT but no RNAi. The DC range of the flies expressing both RNAi with tau and B-WT (Figure 5.10) was 0.45-0.72, a range which ended at a lower figure than that of the flies expressing tau and B-WT (0.44-0.99, shown in Chapter 4, Figure 4.7). This could indicate that expression of both RNAi together caused a rescue of the flies with the most severe eye phenotype. However, it is also possible that if more flies were analysed, flies with the more severe eye phenotype would be observed. Unfortunately this was not possible due to difficulties producing flies of this genotype.

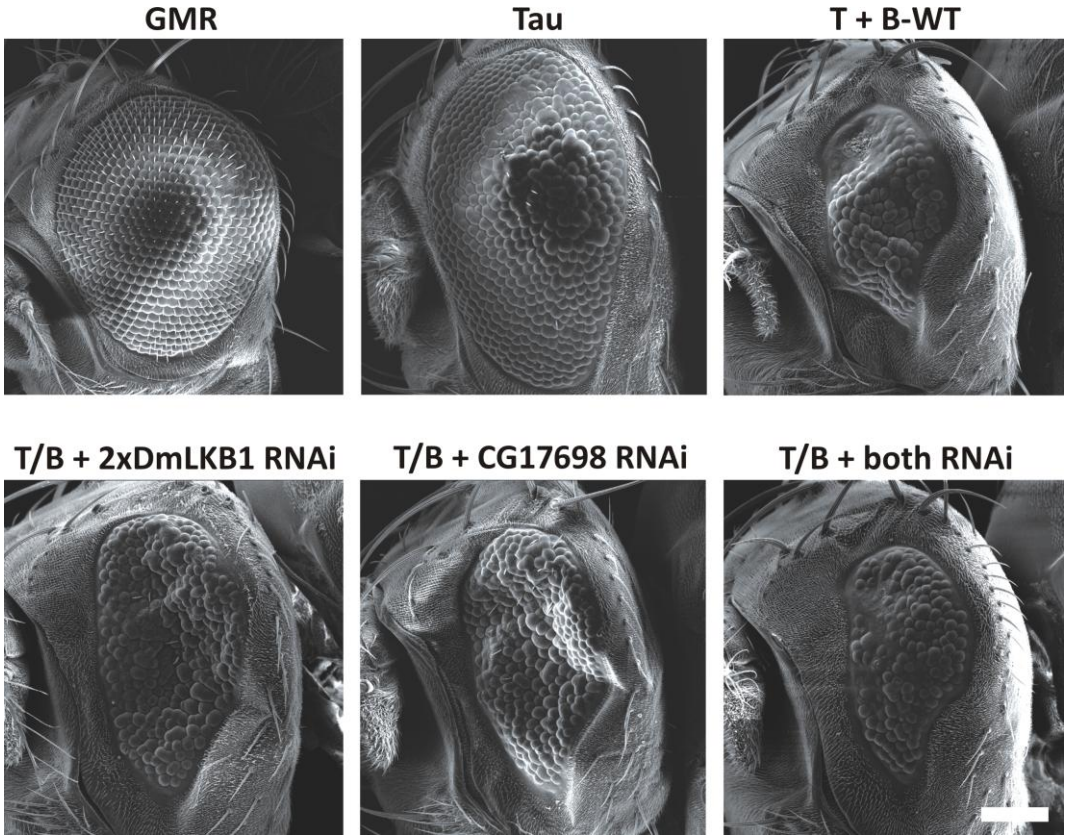

Figure 5.9: SEM images of flies expressing both RNAi with tau and B-WT.
Expression of CG17698 RNAi or two copies of DmLKB1 RNAi with tau and B-WT rescued the eye phenotype. Expression of both RNAi with tau and B-WT did not rescue the phenotype to the same extent as when the single RNAi were utilised. Scale bar 100µm applies to all panels.

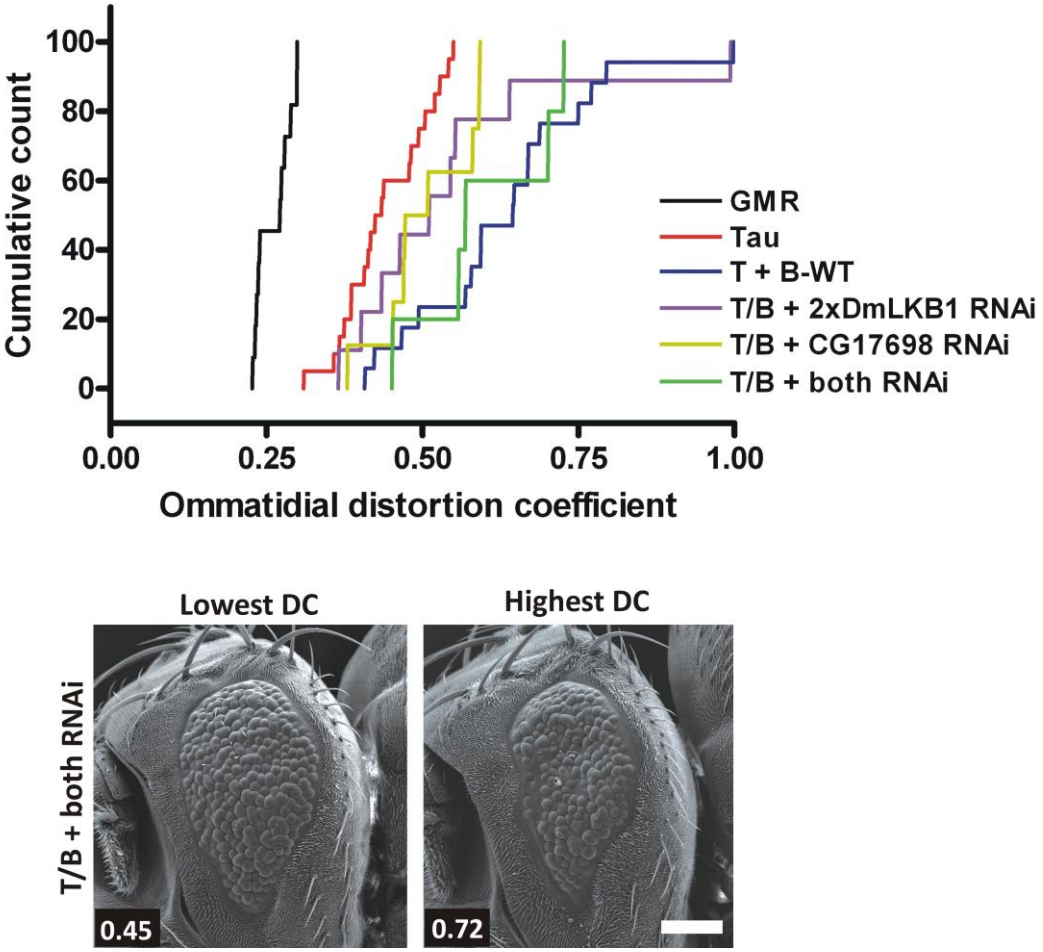

Figure 5.10: Cumulative distribution plot of ommatidial distortion measures (DCs) produced by QED software and images of flies with the lowest and highest DC for flies co-expressing both RNAi with tau and B-WT.
Quantitative analysis of flies co-expressing both RNAi with 0N4R tau and human B-WT under the control of the GMR-GAL4 driver showed that expression of both RNAi did not rescue the eye phenotype. GMR n=11, Tau n=20, T + B-WT n=17, T/B + 2xDmLKB1 RNAi n=9, T/B + CG17698 RNAi n=8 and T/B + both RNAi n=5. The range of DC for T/B + both RNAi flies was 0.45-0.72. Scale bar 100µm applies to all panels.

5.2.4 Co-expression of CG17698 RNAi or DmLKB1 RNAi with tau and B-CA

Co-expression of either CG17698 RNAi or two copies of DmLKB1 RNAi with tau and B-CA showed that B-CA was unable to 'over-ride' the rescue effect of either of the RNAi (data not shown). This is in agreement with the data presented in Chapter 4 (Figures 4.9 and 4.10), which suggested that B-CA was not capable of enhancing the tau-induced eye phenotype, either because it was not constitutively active or because the protein was unstable.

5.2.5 Co-expression of a calcium channel subunit with tau and B-WT

The potential regulation of BRSKs through CaMKK is interesting as it would provide a mechanistic link between the calciumopathy model for AD and tau phosphorylation. The calciumopathy model for AD states that as humans age their capacity for buffering calcium becomes impaired leading to a dysregulation of calcium homeostasis: such changes, if sustained, could trigger age-associated modifications in the brain (Khachaturian, 1987; LaFerla, 2002). In order to investigate whether a rise in intracellular calcium would have an effect on tau and B-WT induced eye phenotypes, I used UAS-cacophony1 flies (obtained from the Bloomington Stock Center). *cacophony1* (*cac1*) is the *Drosophila* homologue of the human voltage-dependent calcium channel alpha-1 subunit. It is predominantly expressed in neuronal tissue and is known to be involved in neurotransmitter release, synaptic transmission and nerve terminal growth (Dason et al., 2009; Gu et al., 2009). Although there is currently no data indicating that expression of *cac1* in the eye leads to an increase in intracellular calcium, it has been shown that cac1 mediates slow-inactivating calcium currents in neurons cultured from late stage pupal brains (Gu et al., 2009).

Over-expression of cac1 under the control of the GMR driver with or without human tau did not cause a visible eye phenotype (Figure 5.11). However, over-expression of cac1 in the presence of both human tau and B-WT caused a dramatic exacerbation of the eye phenotype. This exacerbation was human B-WT dependent, suggesting that B-WT enhancement of tau-induced deleterious eye phenotypes is a process that could be regulated in a calcium-dependent manner.

QED analysis of cac1 flies confirmed that over-expression of cac1 alone, or with tau, caused no eye phenotype and that over-expression with tau and B-WT exacerbated the tau-BRSK phenotype (Figure 5.12). The cumulative curve for flies expressing cac1 with tau and B-WT showed a large shift to the right of the curve for flies expressing tau and B-WT but no cac1.

Figure 5.13 shows the cac1 over-expressing flies with the lowest and highest DCs. GMR cac1 flies had a DC range of 0.21-0.33. T + cac1 flies had a DC range of 0.39-0.52. T/B + cac1 flies had a DC range of 0.70-0.99 and the enhanced phenotype was clearly visible – flies of this genotype had little eye structure, patches of necrosis and smaller eyes than flies expressing tau and B-WT without cac1.

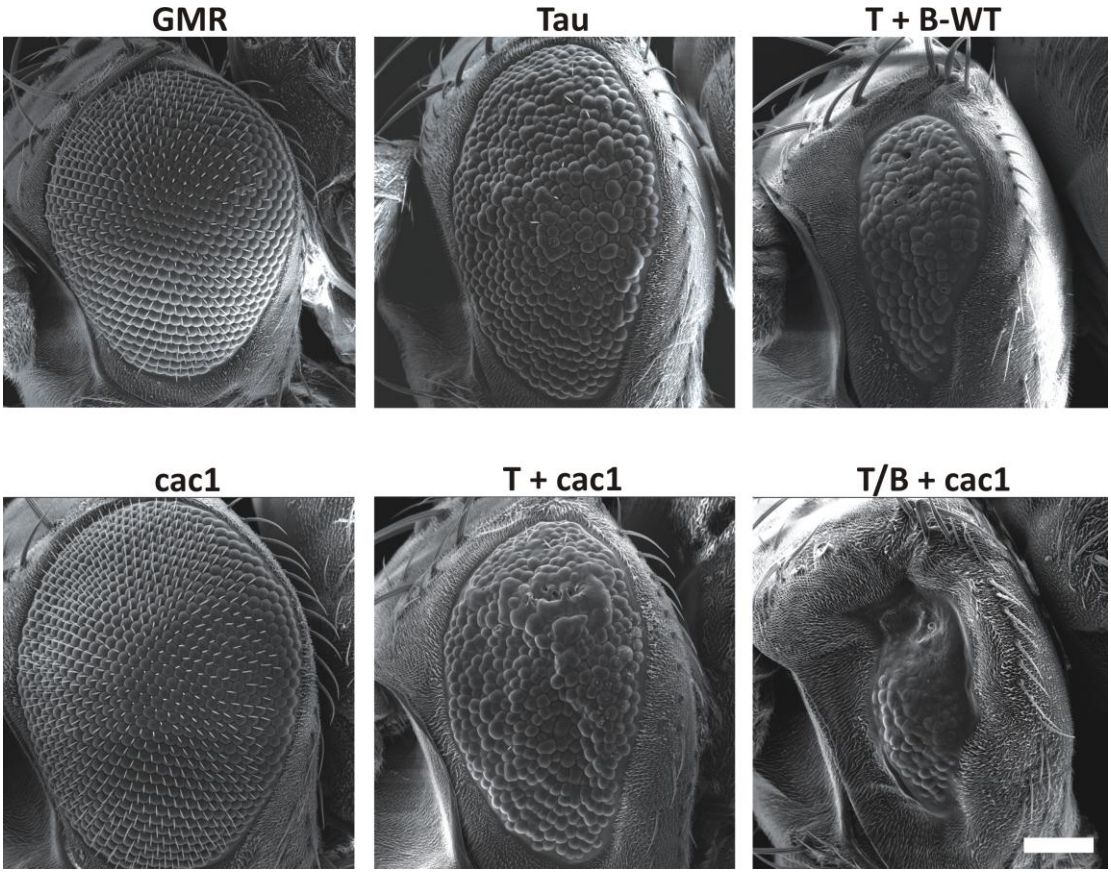

Figure 5.11: SEM images of flies over-expressing cac1 with 0N4R tau and B-WT. *Over-expression of cac1 alone or with tau did not affect the eye phenotype. Over-expression of cac1 with tau and B-WT caused an exacerbation of the eye phenotype. Scale bar 100µm applies to all panels.*

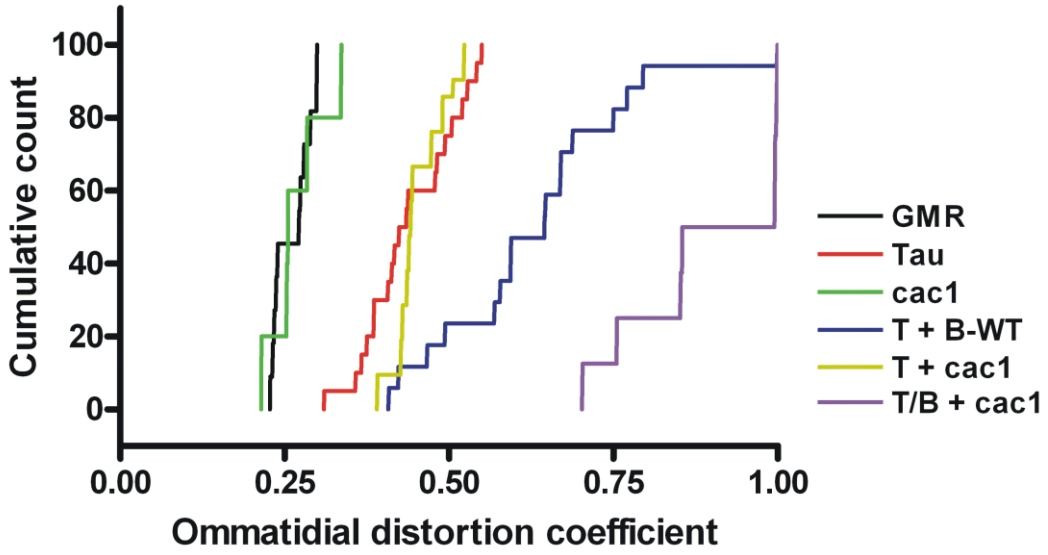

Figure 5.12: Cumulative distribution plot of ommatidial distortion measures (DCs) produced by QED software for flies over-expressing cac1 with tau and B-WT.
Quantitative analysis of flies over-expressing cac1 with or without tau shows that this had no effect on eye phenotype. Over-expression of cac1 with tau and B-WT caused a shift of the cumulative curve to the right of that of the tau + B-WT flies, indicating a more severe phenotype.. GMR n=11, Tau n=20, GMR cac1 n=5, T + B-WT n=17, T + cac1 n=11 and T/B + cac1 n=8.

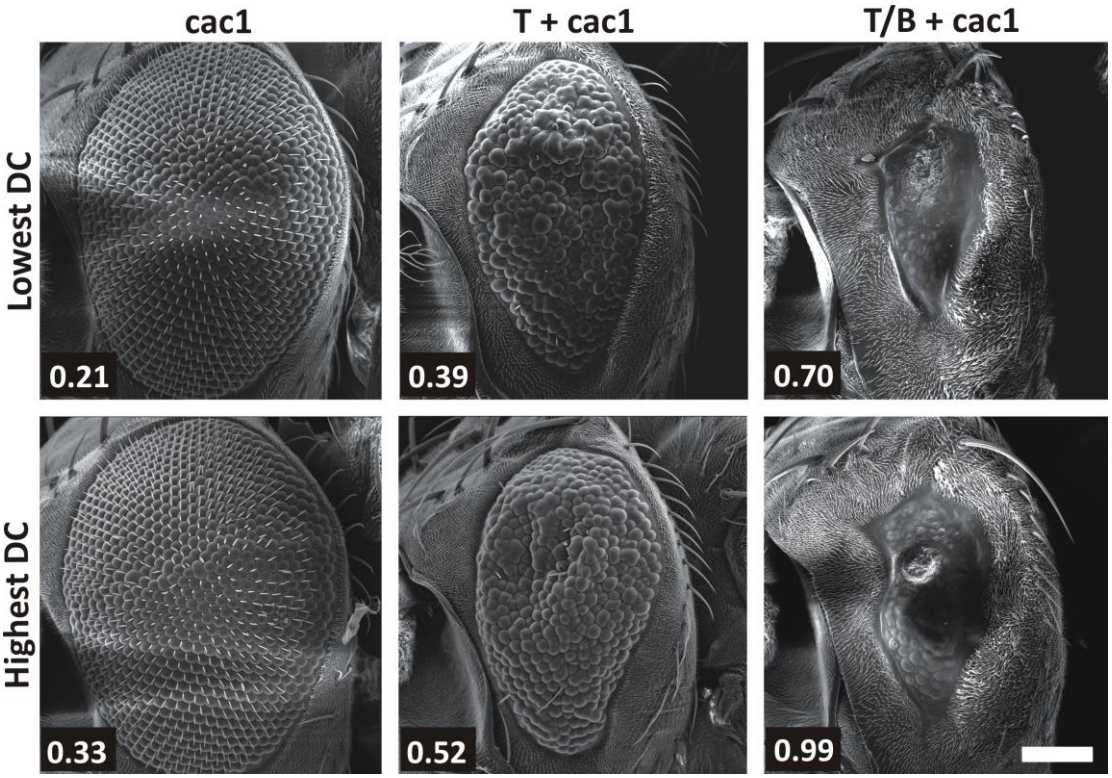

Figure 5.13: SEM images of flies over-expressing cac1 with the lowest and highest DCs.

Images of flies expressing cac1 alone, with 0N4R tau or with 0N4R tau and B-WT. Over-expression of cac1 alone or with tau gives a DC range which is similar to that of the appropriate control (GMR for GMR cac1 and Tau for T + cac1). Co-expression of cac1 with tau and B-WT gives a DC range that is indicative of a more severe eye phenotype that the T + B-WT flies. DCs are shown on the images. Scale bar 100µm applies to all panels.

5.2.6 Co-expression of DmPAR-1 RNAi with tau and B-WT

PAR-1 and BRSKs are members of the AMPK-related family of protein kinases. PAR-1 can phosphorylate tau at two residues in the KXGS motifs; Serine 262 and Serine 356 (Nishimura et al., 2004), and was originally described as a 'major KXGS kinase' (Drewes et al., 1997). Like BRSKs, PAR-1 also has roles in the establishment of neuronal polarity and neurite outgrowth (Biernat et al., 2002; Kishi et al., 2005).

Expression of DmPAR-1 RNAi (obtained from the VDRC) under the control of the GMR driver had no effect on eye phenotype (Figures 5.14 and 5.15). However, expression of DmPAR-1 RNAi with human tau appeared to enhance the tau-induced eye phenotype to some extent (Figure 5.14 and 5.15). This enhancement produced an eye phenotype which was not as severe as that of flies expressing tau with B-WT, but was similar to that of flies expressing tau with CG17698 RNAi (Figures 5.6 and 5.7). Expression of DmPAR-1 RNAi with tau and B-WT resulted in a very variable phenotype (Figure 5.15). QED analysis (Figure 5.15) showed that the phenotype ranged from similar to tau flies at the lower end of the scale, right up to worse than Tau + B-WT flies at the higher end. Figure 5.16 shows that expression of DmPAR-1 RNAi alone gave a DC range of 0.22-0.31, co-expression with tau gave a range of 0.39-0.65 and co-expression with tau and B-WT gave a wide range of 0.32-0.99.

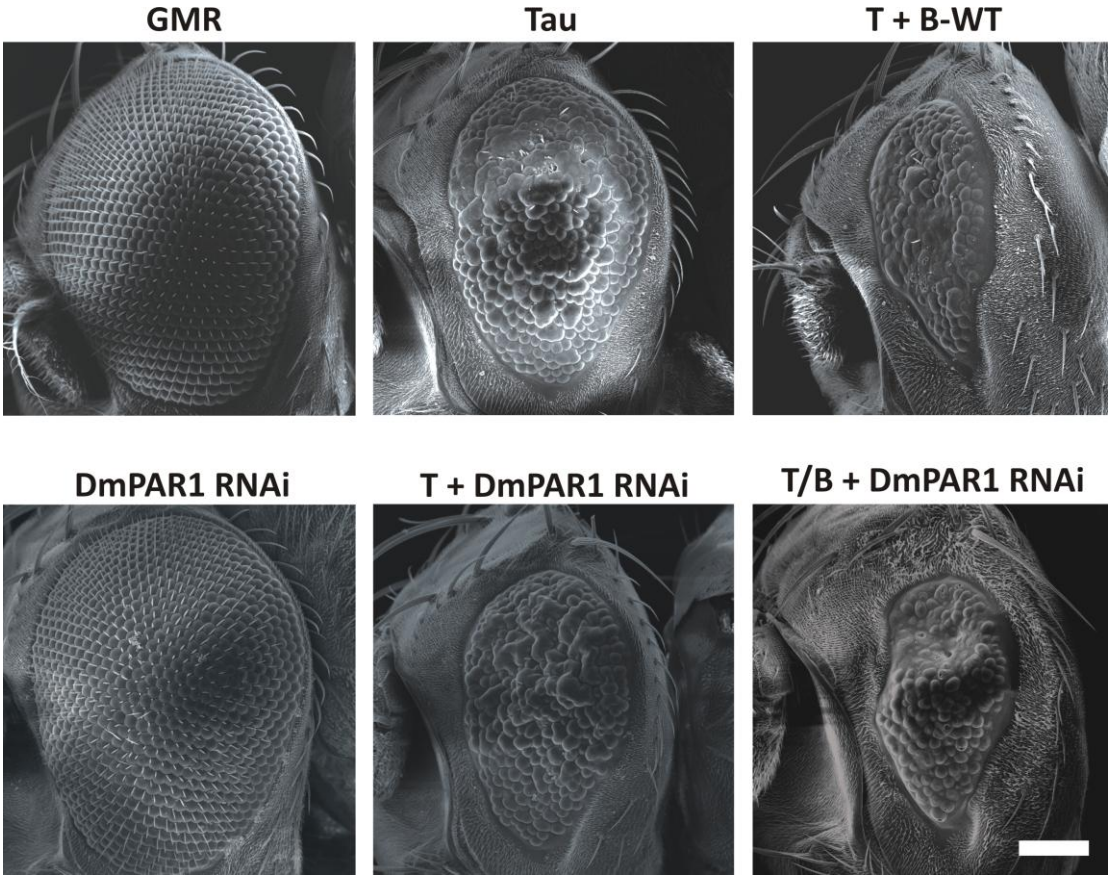

Figure 5.14: SEM images of flies expressing DmPAR-1 RNAi with 0N4R tau and B-WT.

Expression of DmPAR-1 RNAi alone (DmPAR-1 RNAi) did not cause an eye phenotype. Co-expression of DmPAR-1 RNAi with tau (T + DmPAR-1 RNAi) appeared to enhance the tau phenotype. Co-expression of DmPAR-1 RNAi with tau and B-WT caused a variable phenotype; the example shown here is of an eye exhibiting a similar phenotype to a T + B-WT fly. Scale bar 100µm applies to all panels.

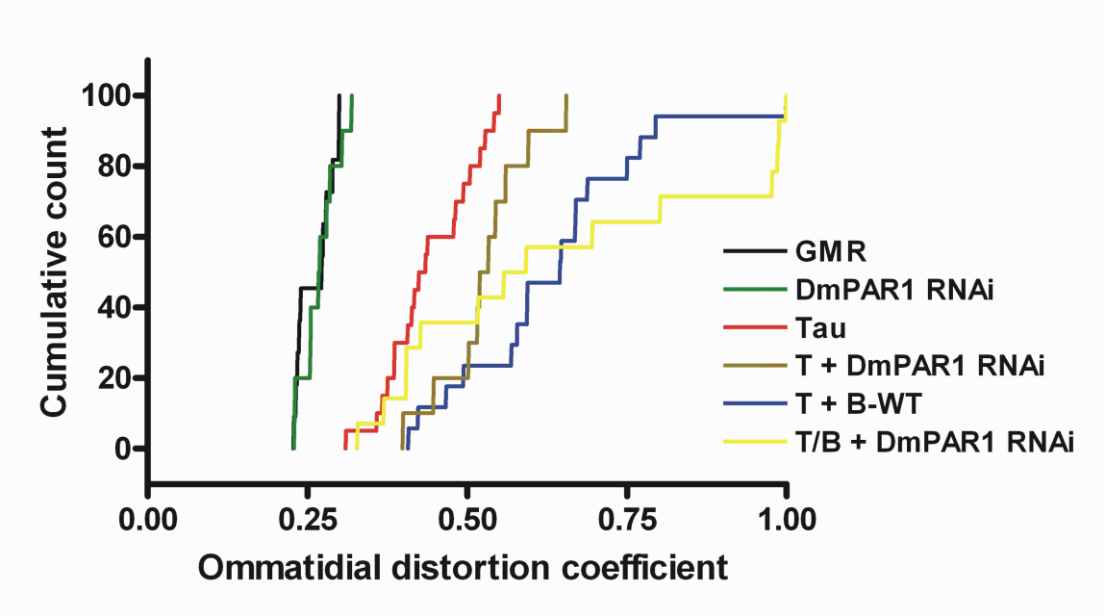

Figure 5.15: Cumulative distribution plot of ommatidial distortion measures (DCs) produced by QED software for flies expressing DmPAR-1 RNAi with 0N4R tau and B-WT.

Quantitative analysis of flies expressing DmPAR-1 RNAi, with or without tau, shows that down-regulation of endogenous DmPAR-1 had no effect on eye phenotype in flies expressing DmPAR-1 RNAi alone (compare with GMR) but that it enhanced the phenotype in flies expressing the RNAi with 0N4R tau (compare with tau). Co-expression of the RNAi with tau and B-WT produced a very variable phenotype. GMR n=11, DmPAR-1 RNAi n=10, Tau n=20 and T + DmPAR-1 RNAi n=10, T + B-WT n=17 and T/B + DmPAR-1 RNAi n=14.

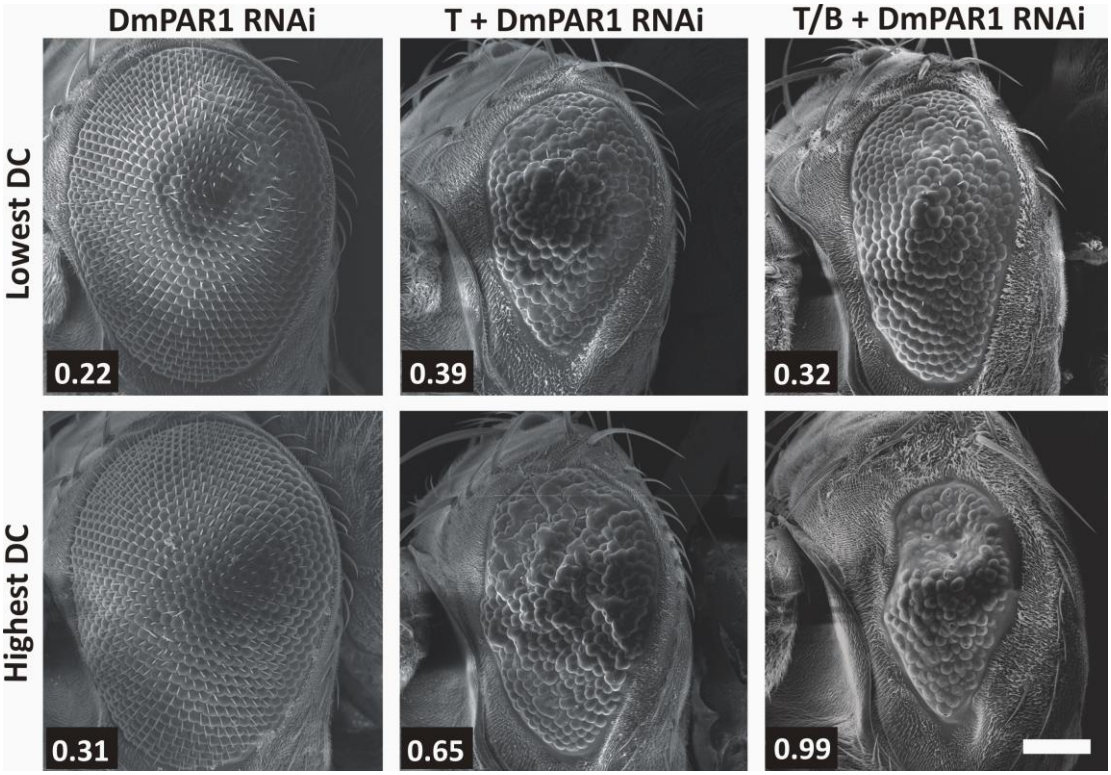

Figure 5.16: SEM images of flies expressing DmPAR-1 RNAi with the lowest and highest DCs.

Images of flies expressing DmPAR-1 RNAi alone, with tau or with tau and B-WT. Expression of DmPAR-1 RNAi alone gives a DC range which is very similar to that of the GMR flies. Co-expression of DmPAR-1 RNAi and tau gives a DC range that is higher than that of the tau flies, demonstrating that expression of DmPAR-1 RNAi enhances the tau-induced phenotype. Expression of DmPAR-1 RNAi with tau and B-WT gives a wide range of DCs; in some flies the phenotype was ameliorated and in some flies the phenotype was enhanced. DCs are shown on the images. Scale bar 100µm applies to all panels.

5.2.7 Phosphorylation of pS262 in RNAi expressing flies

Figure 5.17 shows representative western blots carried out on lysates of flies expressing tau, T + B-WT or T/B with each of the three RNAi lines used in this chapter (CG17698, DmLKB1 and DmPAR-1). The data for tau and T + B-WT flies was originally shown in Chapter 4, Figure 4.21, but has been included here for comparison. Co-expression of B-WT with tau caused a significant increase in the amount of pS262 signal (normalised to total tau, T46) n=10, 0.32±0.03 for 0N4R tau and n= 11, 0.62±0.05 for T + B-WT, $p<0.001$, one way anova. Expression of DmPAR-1 RNAi or CG17698 RNAi with tau and B-WT had no significant effect on the pS262 when compared to flies expressing tau with B-WT, but neither was the pS262 in these flies significantly different from the tau flies (n=7, 0.54±0.08 for T/B + DmPAR-1 RNAi and n=10, 0.50±0.04 for T/B + CG17698 RNAi). Expression of DmLKB1 RNAi with tau and B-WT resulted in pS262 that was not significantly different to pS262 in tau + B-WT flies, but pS262 in the DmLKB1 RNAi flies was significantly elevated when compared to the tau flies (n=9, 0.56±0.05 for T/B + 2xDmLKB1 RNAi, $p<0.05$, one way anova).

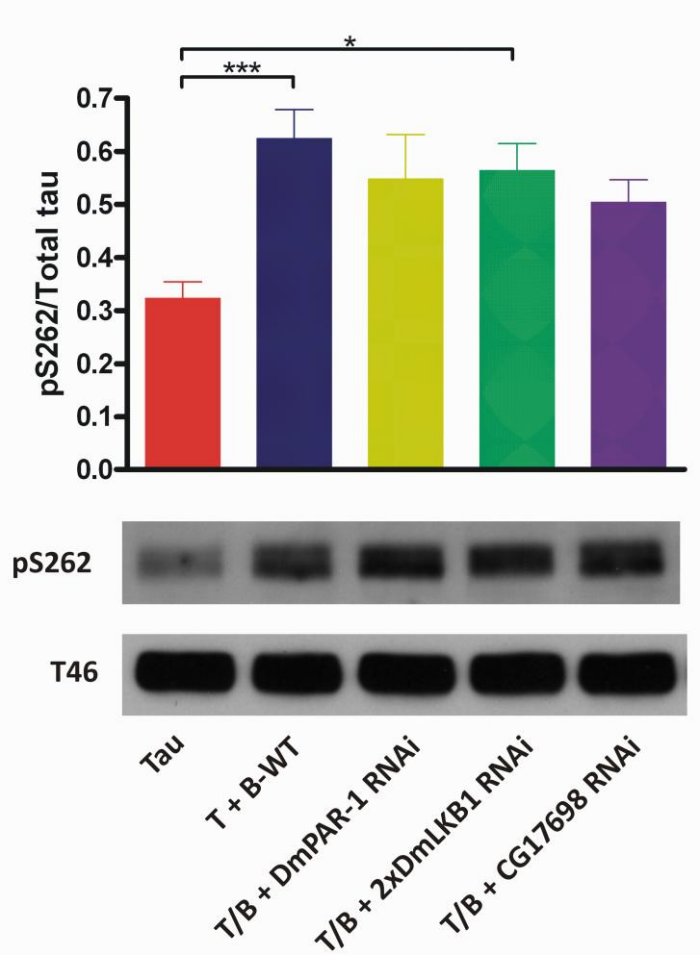

Figure 5.17: Western blots for pS262 and total tau.
*Quantification of western blots from flies expressing tau, T + B-WT, T/B + DmPAR-1 RNAi, T/B + 2xDmLKB1 RNAi or T/B + CG17698 RNAi show that co-expression of B-WT with 0N4R tau caused a significant increase in tau phosphorylated at S262. Expression of DmPAR-1, DmLKB1 or CG17698 RNAi with tau and B-WT had no effect on the increased pS262. Flies expressing DmLKB1 RNAi with tau and B-WT had significantly elevated pS262 when compared to flies expressing tau alone. Mean ± SEM: 0.32±0.03 for tau (n=10), 0.62±0.05 for T + B-WT (n=11), 0.54±0.08 for T/B + DmPAR-1 RNAi (n=7), 0.56±0.05 for T/B + 2xDmLKB1 RNAi (n=9) and 0.50±0.04 for T/B + CG17698 RNAi (n=10). *** $p<0.001$, * $p<0.05$, one way anova. Representative western blots shown.*

5.3 Discussion

Expression of RNAi targeting endogenous DmLKB1 had no effect on control eyes, a finding that is consistent with the literature (Wang et al., 2007a). In addition, there was no effect of DmLKB1 RNAi expression on tau-induced eye phenotypes. The DmLKB1 RNAi has been previously shown to be effective at knocking-down DmLKB1 expression and so the lack of effect on the tau-induced eye phenotypes would suggest that none of the endogenous kinases which are regulated by DmLKB1 (such as PAR-1) contribute significantly to the establishment of 'basal' tau-induced eye phenotypes (Wang et al., 2007a).

Co-expression of DmLKB1 RNAi with tau and B-WT resulted in a rescue of the eye phenotype, as shown by SEM and QED, with flies exhibiting an eye phenotype similar to that of flies co-expressing tau and B-NP. This confirms that DmLKB1 is capable of regulating human B-WT. In mammals, LKB1 is known to regulate 14 members of the AMPK-related family of protein kinases (including BRSKs and PAR-1) and in *Drosophila* DmLKB1 has been shown to regulate endogenous PAR-1 (Lizcano et al., 2004; Wang et al., 2007a). Thus, it would appear that the regulatory pathway from DmLKB1 to members of the AMPK-related kinases has been conserved in *Drosophila.*

Expression of CG17698 RNAi alone had no effect on eye phenotypes. When co-expressed with human tau, there was a slight exacerbation of the tau-induced eye phenotype. The mechanism for this enhancement is unknown; it could be related to the phosphorylation status of tau, indeed it has been suggested that an optimal level of tau phosphorylation is essential to the physiological function of tau (Chatterjee et

al., 2009), but without any evidence for this hypothesis, this interpretation is purely speculative. Equally possible is that the enhancement is due to off target effects of the RNAi.

Co-expression of CG17698 RNAi with tau and B-WT resulted in a rescue of the eye phenotype similar to that seen with DmLKB1 RNAi, confirming that CG17698 is also required for the enhancement of the tau phenotype by human B-WT *in vivo.* Preliminary work in the laboratories of Dr Moffat and Prof Frenguelli has shown that the CG17698 RNAi line knocks-down expression of CG17698 by approximately 70% (personal communication, Mr Sharad Mennon). The similar rescues exhibited upon expression of CG17698 or DmLKB1 RNAi raises the question of whether both genes are acting upon BRSK as part of a linear pathway. It would be relatively straightforward to address this by performing *in vitro* phosphorylation assays, however, in the absence of any evidence for this scenario, it is equally likely that the system is not fully quantitative or that the RNAi are having off target effects that complicate the analysis.

Over-expression of human CaMKKα, which is known to regulate human BRSKs and was not targeted by the RNAi (Fujimoto et al., 2008), prevented the rescue seen with CG17698 RNAi expression, indicating that the RNAi was specific for CG17698. Due to the complex genetics involved in producing this fly, the n number is low (n=4), but QED analysis indicates that the phenotype was not very variable; each of the flies has a phenotype similar to that of tau + B-WT flies. Assessment of flies co-expressing hCaMKKα and tau using a light microscope indicated that hCaMKKα did not alter the tau-induced eye phenotype, providing more evidence that CG6114 is not

able to act on human tau. There is another member of the AMPK family that is regulated by CaMKKs; AMPK, the prototypical member of the AMPK-related family of protein kinases. However, AMPK is mainly regulated by the β-isoform of CaMKKs (Hawley et al., 2005). Thus, the data supports the conclusion that the hCaMKKα 'over-ride' of the CG17968 RNAi was due to a direct activation of human BRSK. Conversely, expression of both RNAi (CG17698 and DmLKB1) simultaneously with tau and B-WT resulted in a phenotype that was more similar to that of flies expressing tau with B-WT than flies expressing tau alone. This could be due to additive off target effects of the RNAi, or because the down regulation of at least 14 kinases in the AMPK family (that are targeted by these two regulators) is in itself toxic. In order to test for toxicity related to the joint use of the CG17698 and DmLKB1 RNAi, I would express the RNAi simultaneously with the GMR driver and with tau (without BRSK). Unfortunately, due to time constraints I was unable to perform these experiments.

In order to elucidate whether BRSKs were activated in a calcium-dependent manner, I over-expressed cac1, a calcium channel α subunit, in an attempt to increase intracellular calcium levels from extracellular sources (rather than via release from the endoplasmic reticulum). Over-expression of cac1 with tau and B-WT dramatically enhanced the eye phenotype, indicating that an increase in intracellular calcium was sufficient to enhance the tau-BRSK eye phenotype. Importantly, the enhancement was human BRSK dependent; no enhancement was seen when cac1 was over-expressed with tau alone, neither did over-expression of cac1 by itself in the eye cause any disruption to the wild type eye phenotype. This experiment provides the first tentative *in vivo* link between increased intracellular calcium, a tau

kinase and increased tau toxicity. Unfortunately I was unable to pursue this further, but it will now be important to demonstrate that tau phosphorylation at S262 and BRSK2 phosphorylation at T174 is increased upon over-expression of cac1 with tau and B-WT, that the calcium induced exacerbation of tau-BRSK eye phenotypes is dependent on CG17698, whether the S262A/S2A mutants are insensitive to cac1 expression with B-WT, that over-expression of cac1 in the eye causes a rise in intracellular calcium and that over-expression of cac1 has no effect when B-NP or B-KD is substituted for B-WT. If this is the case, it would categorically show that BRSKs are activated in response to calcium, leading to tau phosphorylation and an increase in tau toxicity in the *Drosophila* model, as indicated in the summary diagram in Figure 5.18.

This would be highly relevant for AD as perturbed calcium homeostasis has been implicated in the pathogenesis of AD for a number of decades (Khachaturian, 1987; LaFerla, 2002). As discussed in the Introduction, the calciumopathy model for AD proposes that as humans age calcium regulation becomes impaired due to a decrease in buffering capacity and if sustained, dysregulated calcium homeostasis may provide a trigger for age-associated changes in the brain (Khachaturian, 1987). There is a large amount of evidence supporting this theory: calcium signalling has been shown to be impaired before the manifestation of symptoms in familial and sporadic AD patients, increased Aβ and presenilin mutations can increase intracellular calcium and increased cytosolic calcium directly and indirectly activates tau kinases leading to increased tau phosphorylation (Arispe et al., 1993; Ito et al., 1994; Litersky et al., 1996; Etcheberrigaray et al., 1998; Leissring et al., 1999a; Leissring et al., 1999b; Kusakawa et al., 2000; Ferreiro et al., 2004; Zempel et al.,

2010). There is also data suggesting that increasing the cytosolic calcium concentration increases the production of intracellular Aβ (Querfurth and Selkoe, 1994; Pierrot et al., 2004; Pierrot et al., 2006). However, this remains a contentious issue as it has also been demonstrated that increasing cytosolic calcium by a different mechanism leads to decreased Aβ production (Buxbaum et al., 1994). Nevertheless, in AD, the production of Aβ - whether as a result of rising intracellular calcium or not, would serve to greatly exacerbate this process.

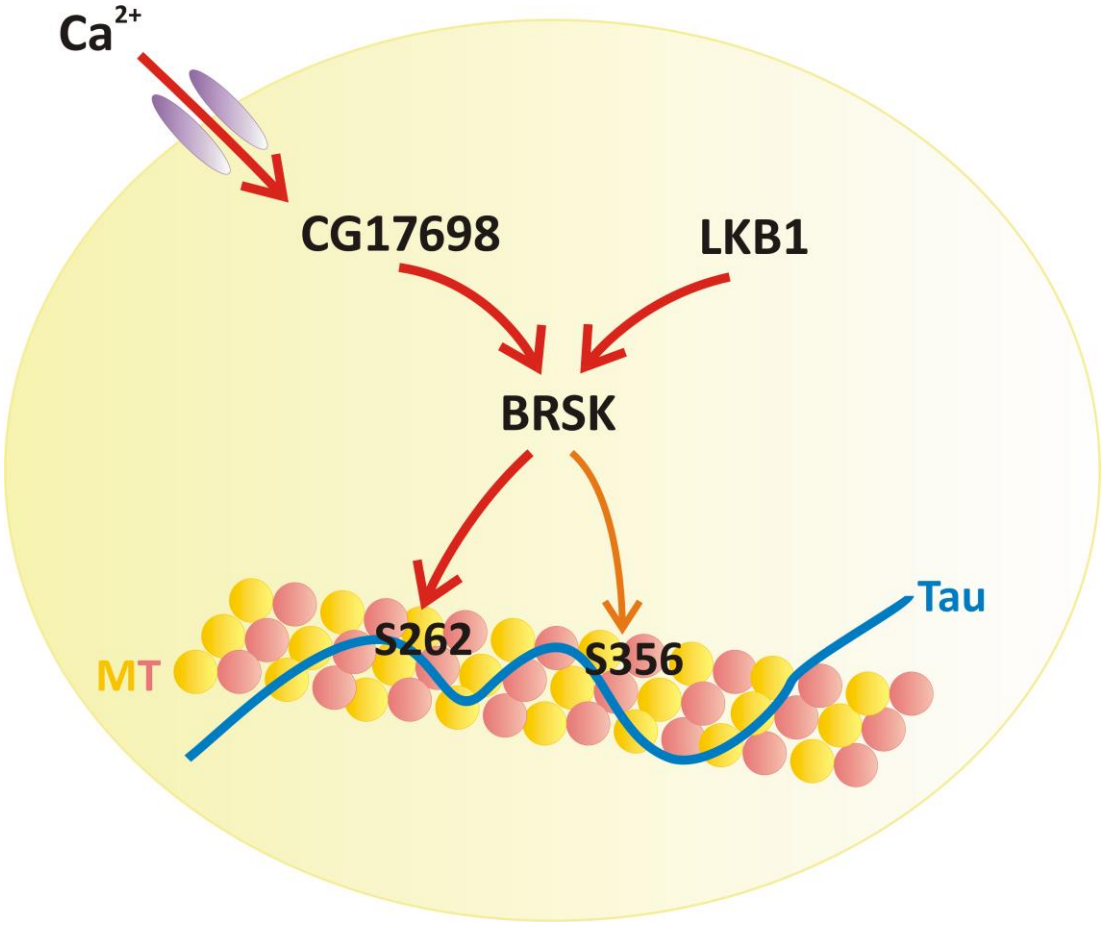

Figure 5.18: Summary schematic of BRSK regulation.
BRSK is regulated by two distinct upstream pathways; LKB1 and CG17698. Calcium influx through plasma membrane calcium channels leads to a rise in intracellular calcium and activation of CG17698 (CaMKKα in humans). CG17698 and LKB1 activate BRSK by phosphorylating at T174 (BRSK2) or T189 (BRSK1). BRSK phosphorylates tau at S262, and possibly at S356.

Due to the similarities in function of PAR-1 and BRSKs, it was important to attempt to establish whether DmPAR-1 and BRSK were in the same pathway to tau that generates the eye phenotype. Experiments were conducted using DmPAR-1 RNAi but the results were mixed and did not allow me to draw any firm conclusions. Expression of DmPAR-1 RNAi under the control of the GMR driver had no effect on eye phenotype. However, co-expression of DmPAR-1 RNAi with human tau led to an exacerbation of the tau-induced eye phenotype. This is an important result as PAR-1 is a potential S262 kinase (Biernat et al., 2002). Thus down regulation of DmPAR-1 may be expected to decrease the toxicity of human tau in the eye if it was the only important S262 kinase and S262 phosphorylation was responsible for the toxicity of human tau in the eye (as is suggested by the S262A data). Co-expression of DmPAR-1 RNAi with tau and B-WT resulted in a very varied phenotype; the RNAi appeared to rescue the phenotype in some flies and to enhance it in others. Due to the degree of variation in the phenotype, no firm conclusions can be drawn as to any interactions between DmPAR-1 and BRSK based on this data; further work is required, beginning with characterisation of the RNAi line. Alternatively, it may be simpler to investigate the potential for interactions between BRSK and PAR-1 using a cellular model.

Analysis of tau phosphorylation in lysates from the various flies showed that none of the RNAi used in this chapter significantly altered pS262 (as detected by western blot). This links back to a point made in the Discussion of Chapter 4; western blotting is a semi-quantitative method and so it is difficult to rank samples with small differences in phosphorylation levels. In addition, it is not known to what extent

phosphorylation and phenotype correlate – it is possible that a small difference in the phosphorylation status of tau (which would be very difficult to detect using a semi-quantitative method) would be sufficient to produce a rescue such as that seen upon expression of DmLKB1 or CG17698 RNAi. This question awaits the development of more sensitive and quantitative approaches, such as an ELISA assay or Mass Spectrometry method to specifically quantify the stoichiometry of tau phosphorylated at S262.

In summary, two upstream regulators of human BRSKs have been identified in the *Drosophila* genome; DmLKB1 and CG17698. Expression of RNAi targeting either gene resulted in rescue of the tau-BRSK phenotype, suggesting a linear regulatory pathway. There is no evidence for this in the literature and as such this warrants further investigation. Whilst the data showing that endogenous DmLKB1 can regulate human BRSKs is interesting, LKB1 is already accepted as a regulator of 14 members of the AMPK family of protein kinases (Lizcano et al., 2004). CaMKKα has previously only been shown to regulate BRSKs *in vitro* and thus my data is the most convincing evidence to date that there is functional regulation of BRSKs by CaMKKα *in vivo* (Fujimoto et al., 2008). In addition, the potentially calcium-dependent nature of the eye phenotype suggests an interesting novel pathway from deregulated intracellular calcium to tau phosphorylation at a disease relevant residue (S262), potentially via CaMKK and BRSKs. In support of this, I have shown that over-expression of a calcium channel results in an enhanced tau-BRSK eye phenotype, providing the first *in vivo* evidence that human BRSKs can be regulated in a calcium-dependent manner and a link between the calciumopathy model for AD and tau phosphorylation. Further work will be required in order to confirm that this

process is mediated by CaMKK and that S262 and B-WT phosphorylation is increased upon co-expression of cac1 with tau and B-WT.

In the following chapter, I extend the present data from flies to humans, in a study conducted using human post-mortem brain tissue to investigate the expression and activation levels of human BRSKs and the two upstream regulators, LKB1 and CaMKK (human homologue of CG17698).

6| Analysis of samples from post-mortem human brain tissue.

6.1 Introduction

The experiments contained in this chapter were conducted in the lab of Dr Diane Hanger, King's College, London, under the supervision of Dr Diane Hanger and Dr Wendy Noble. Post-mortem frontal cortex tissue from clinically and histologically confirmed human AD patients and age-matched control subjects was provided by the MRC Neurodegenerative Diseases Brain Bank at the Institute of Psychiatry, King's College, London. Clinical information on the subjects whose samples were used in this study is shown in Tables 6.1 and 6.2. Written consent was obtained from each subject and/or their family members for the purpose of this study and the study was conducted according to the principles expressed by the Declaration of Helsinki.

The analysis of human samples is a unique opportunity to investigate the expression and/or activity of proteins of interest in disease and control subjects. Although *Drosophila* is an excellent model for basic protein interactions, once proteins of interest have been identified, it is useful to investigate their expression in the tissue and organism affected. The aim of this study was to elucidate if expression of BRSK and/or either of its upstream regulators, LKB1 and CaMKK, was altered in AD samples as this may provide a mechanistic link between the work presented in the previous chapters and the molecular pathology of AD.

Samples were subjected to analysis by Western Blot as described in the Methods section. Membranes were probed with various antibodies and the signals were quantified using Odyssey software (version 3). The strength of signal with each probe was compared between AD and control and analysed for statistical

significance using the student's t-test (for normally distributed data) or the Mann Whitney test (for data with a non-normal distribution). Also tested was the effect of post-mortem delay (PMD) and age using Spearman (for non-normally distributed data) and Pearson tests (for normally distributed data), and sex using t-tests. However, most of the tests for PMD, age and sex were not statistically significant for the antibodies used. Therefore for clarity, statistically significant correlations are shown in the relevant section, and correlations that are not significant are summarised in tabular form at the end of the results section (Table 6.3). In addition, analysis is performed on AD samples grouped according to increasing Braak stage (where that data was available). None of this data was significant (tested by one way anova) and so it was interpreted as 'positive trend', 'negative trend' or 'no trend'. Data which showed a trend is presented in the relevant section and data which didn't show a trend is summarised in Table 6.3 at the end of the results section.

6.2 Results

Tables 6.1 and 6.2 show the clinical information supplied by the MRC Neurodegenerative Diseases Brain Bank on the control and AD subjects whose samples were used in these experiments respectively, sorted according to sex and age. AD cases were histologically confirmed using the original method described by Braak and Braak (1997), and more recently a Brain Net Europe Consortium Scheme method which also takes into account the presence of amyloid plaque pathology (Braak and Braak, 1997; Alafuzoff et al., 2008). All AD cases were Braak stage IV-VI. In the control subjects, cause of death is listed instead of pathological diagnosis. Control subjects had a wide variety of causes of death, however the brain bank attempted to avoid any subjects who had suffered a traumatic brain injury as this can result in the formation of AD pathology in both the acute and chronic phases (Smith et al., 2003; Ikonomovic et al., 2004). In fact, it is well documented that there is a link between a history of traumatic brain injury and subsequent development of AD (Lye and Shores, 2000; Plassman et al., 2000).

Autopsy Number	Sex	Age	Post Mortem Delay (hours)	Cause of Death
A042/01	F	52	44	Carcinoma of the lung
A155/95	F	63	34	Myocardial infarction
A170/00	F	68	9	Systemic lupus erythematosus
A278/96	F	77	29	Pulmonary embolism
A239/95	F	79	38	Chronic obstructive airway disease
A094/95	F	80	31	Left ventricular failure/Bronchopneumonia
A047/02	F	87	22	Carcinoma of the breast
A135/95	M	65	24	Coronary artery occlusion
A077/00	M	68	53	Ischemic heart disease
A223/96	M	80	11	Carcinoma of the prostate
A346/95	M	85	16	Ruptured aortic aneurism
A401/97	M	85	42	Gastrointestinal haemorrhage
A133/95	M	85	48	Left ventricular failure
A134/00	M	86	6	Myocardial infarction
A149/01	M	95	44	Gastrointestinal bleed

Table 6.1: Clinical information on control subjects sorted according to sex and age

Autopsy Number	Sex	Age	Post Mortem Delay (hours)	Pathological Diagnosis
A188/00	F	64	10	Alzheimer's disease: Definite
A010/06	F	67	56	Alzheimer's disease: Braak VI
A074/06	F	69	25	Alzheimer's disease: Braak VI with diffuse neocortical Lewy body disease
A157/00	F	75	9	Alzheimer's disease: Definite
A232/00	F	79	8	Alzheimer's disease: Definite
A221/03	F	81	37	Alzheimer's disease: probable Braak V
A169/05	F	82	43	Alzheimer's disease : Braak V/VI
A309/07	F	83	7	Alzheimer's disease: Braak V with amyloid angiopathy type II and mild neocortical Lewy body disease
A210/05	F	84	<24	Alzheimer's disease: Braak V
A168/05	F	84	36	Alzheimer's disease: Braak V/VI
A203/04	F	84	37	Alzheimer's disease: Braak V with mild amyloid angiopathy
A074/05	F	89	29	Alzheimer's disease: Braak V/VI
A240/06	F	97	12	Alzheimer's disease: Braak V
A186/04	M	71	5	Alzheimer's disease: Braak V/VI
A176/01	M	71	41	Alzheimer's disease: Definite
A249/07	M	74	69	Alzheimer's disease: Braak VI with amyloid angiopathy
A206/07	M	81	47	Alzheimer's pathology: Braak IV
A122/04	M	86	26	Alzheimer's disease: Braak V with moderate amyloid angiopathy

Table 6.2: Clinical information on Alzheimer's disease patients sorted according to sex and age

6.2.1 Tau

Human tau produces a number of bands on western blots due in part to the slight differences in molecular weight of the various isoforms, combined with the range of post-translational modifications of this protein; for the purpose of this study all bands in the molecular weight range of 45-65kDa were quantified (see Figure 6.1 for an example). The boxes for the quantification were of uniform size, and an attempt was made to ensure that they were aligned. However, in the case of the outer lanes of some gels, it was necessary to move the box (e.g. the far right hand lane in Figure 6.1); due to characteristics of the gel, bands in outer lanes may migrate slightly differently, this phenomenon is commonly known as smiling.

Figure 6.2 A(i) shows that there was no difference in the intensity of total tau signal (normalised to neuron specific enolase (NSE) to control for the loss of neurons in AD) between AD and control samples (n=12, 4.67±1.08 for control and n=18, 4.87±1.22 for AD, p=0.45 unpaired t-test).

Consistent with the literature, there was a significant increase in the intensity of the signal for tau phosphorylated at S262 (normalised to total tau), as shown in Figure 6.2 B(i) (n=12, 0.0085±0.0016 for control and n=18, 0.035±0.011 for AD, p=0.031 unpaired t-test), a residue which is known to be important for the microtubule binding properties of tau (Hanger et al., 2007; Fischer et al., 2009). There was no correlation between the pS262 signal and PMD, age or sex (Table 6.3).

Figure 6.3 A(i) shows a significantly higher intensity for the PHF-1 (pS396/pS404) antibody (normalised to total tau) in AD subjects when compared to controls (n=12,

0.29±0.23 for control and n=18, 4.17±0.96 for AD, p=0.0016 unpaired t-test). The PHF-1 antibody recognises two phosphorylated serines which are found in paired helical filament tau (pS396/pS404) and so is generally accepted to be a marker for tau tangles (Otvos et al., 1994). The linear regression in Figure 6.3 B(i) shows a positive correlation between the intensity of PHF1 and pS262 signals in the AD subjects and a Pearson r test for correlation shows that this is significant (n=18, p=0.0012).

Recently a move has been made by the MRC Neurodegenerative Diseases Brain Bank during post-mortem examinations to incorporate assessment of immuno-histochemical staining of brain sections with the AT8 antibody. AT8 is a phospho-specific antibody for tau which recognises pS202/pT205 and it has been suggested that Braak staging of AD brains according to AT8 staining (with more AT8 immuno-reactivity giving a higher Braak stage) is more accurate and reproducible than the traditional Gallyas staining (Alafuzoff et al., 2008).

Figure 6.4 shows graphs grouping the pS262 and PHF1 signals according to the Braak stage of the patients, where that information was available. Despite there being a visible trend for increased pS62 and PHF1 according to Braak stage, this was not significant for either antibody (pS262: n=6, 0.012±0.0074 for stage V, n=4, 0.038±0.031 for stage V/VI and n=3, 0.048±0.027 for stage VI, p=0.43, one way anova PHF1: n=6, 1.65±1.30 for stage V, n=4, 4.48±1.82 for stage V/VI and n=3, 6.49±3.20, for stage VI, p=0.23, one way anova). Data for Braak stage IV was excluded from the statistical analysis due to this group only having one data point.

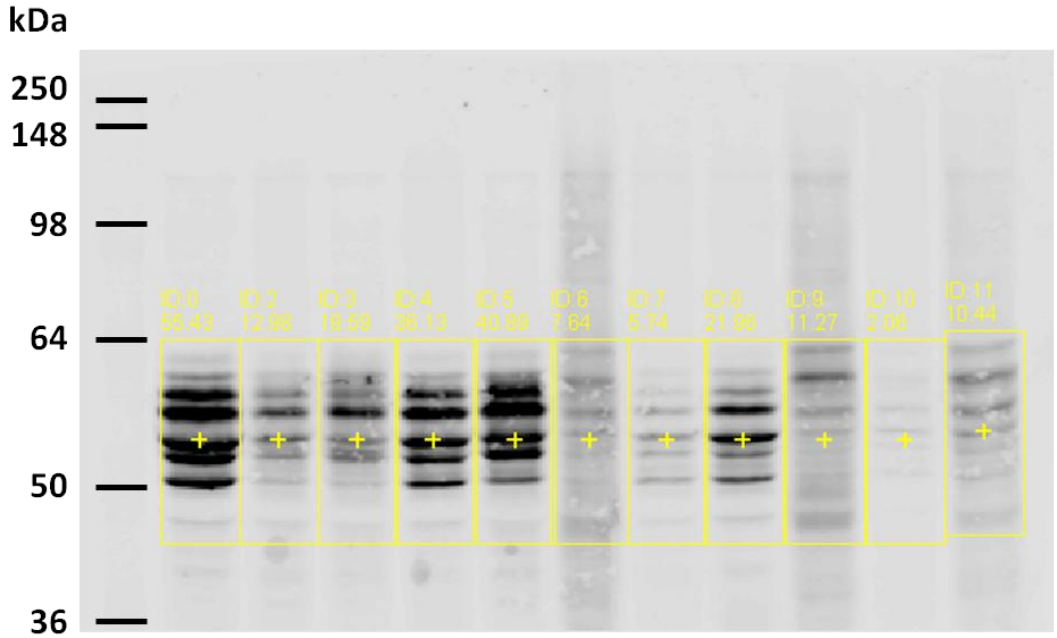

Figure 6.1: An example of quantification for tau western blots.
For tau western blots (total, pS262 and PHF1 antibodies), bands in the molecular weight range of 45-65 kDa were quantified in order to ensure quantification of all tau species. Each box was the same size and an attempt was made to keep the boxes aligned - unless there were lanes on the edges of the gel in which the bands were not straight (e.g. the far right hand lane).

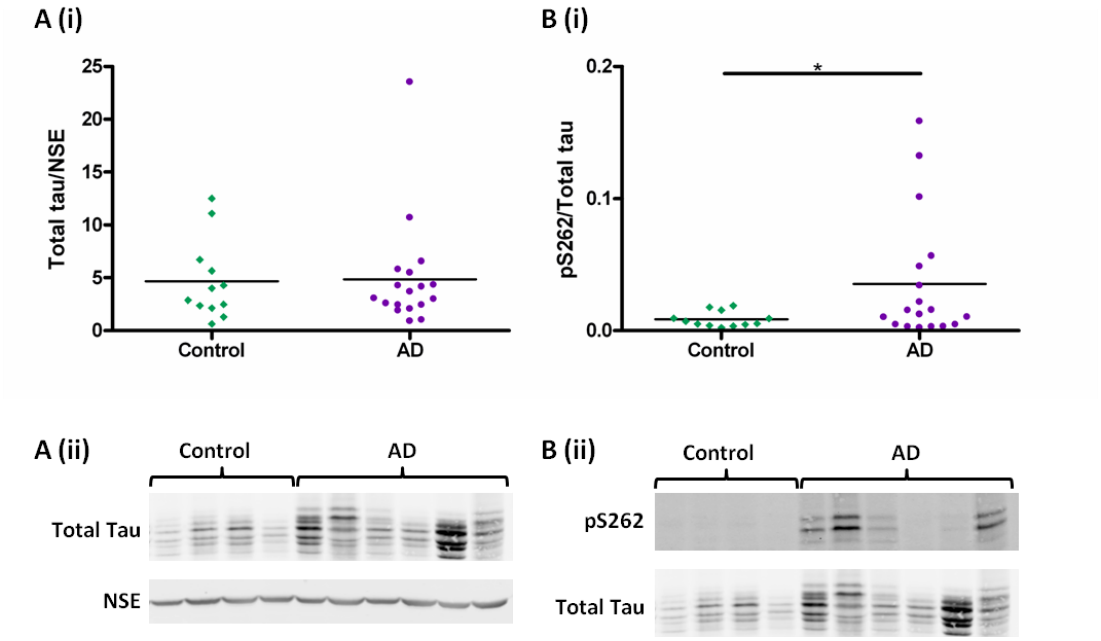

Figure 6.2: Total tau and pS262 tau in Alzheimer brain and aged-matched control brain.

A(i): There is no difference in the level of total tau found in Alzheimer brain (n=18, 4.87±1.22) when compared to age-matched control brain (n=12, 4.67±1.08), p=0.45 unpaired t-test. B (i): Tau phosphorylated at S262 is significantly elevated in Alzheimer brain (n=18, 0.035±0.011) when compared to age-matched control brain (n=12, 0.0085±0.0016), p=0.0315 unpaired t-test. A (ii) and B (ii): Representative western blots for total tau, NSE and pS262 antibodies.

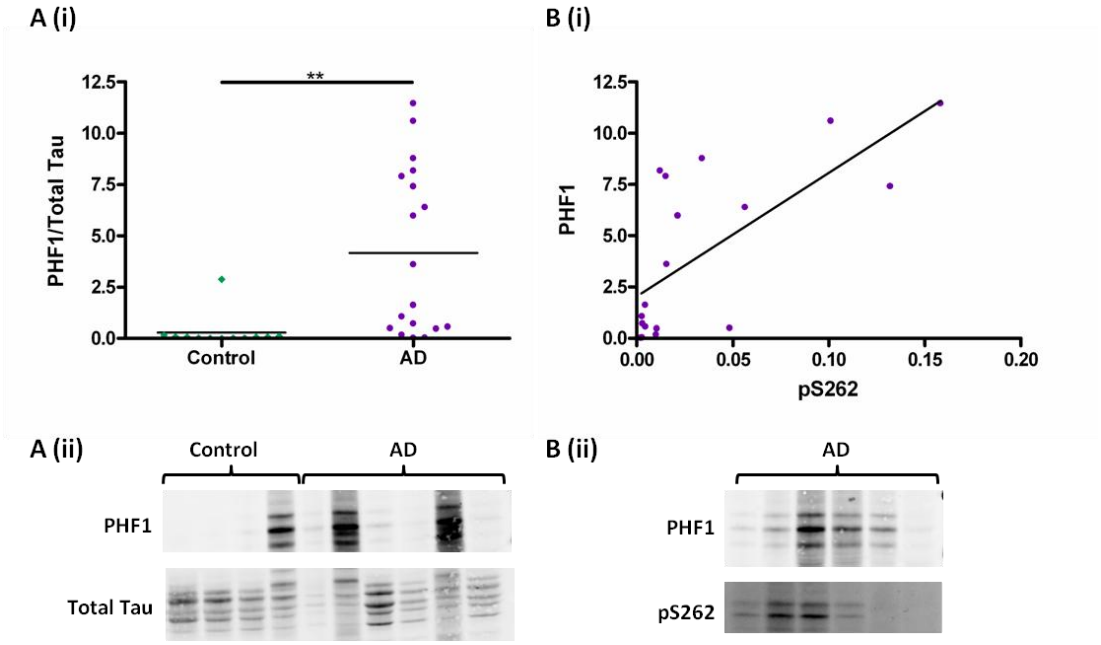

Figure 6.3: PHF1 tau and correlation between PHF1 and pS262 tau in Alzheimer patients and aged-matched controls.

A (i): Tau phosphorylated at residues recognised by the PHF1 antibody (pS396/pS404) is significantly elevated in Alzheimer brain (n=18, 4.17±0.96) when compared to aged-matched control brain (n=12, 0.29±0.23), p=0.0016 unpaired t-test. B (i): There is a significant correlation between the amount of tau phosphorylated at the PHF1 residues and at S262 in Alzheimer brain, p=0.0012 Pearson r test of correlation. A (ii) and B (ii): Representative western blots for PHF1, total tau and pS262 antibodies.

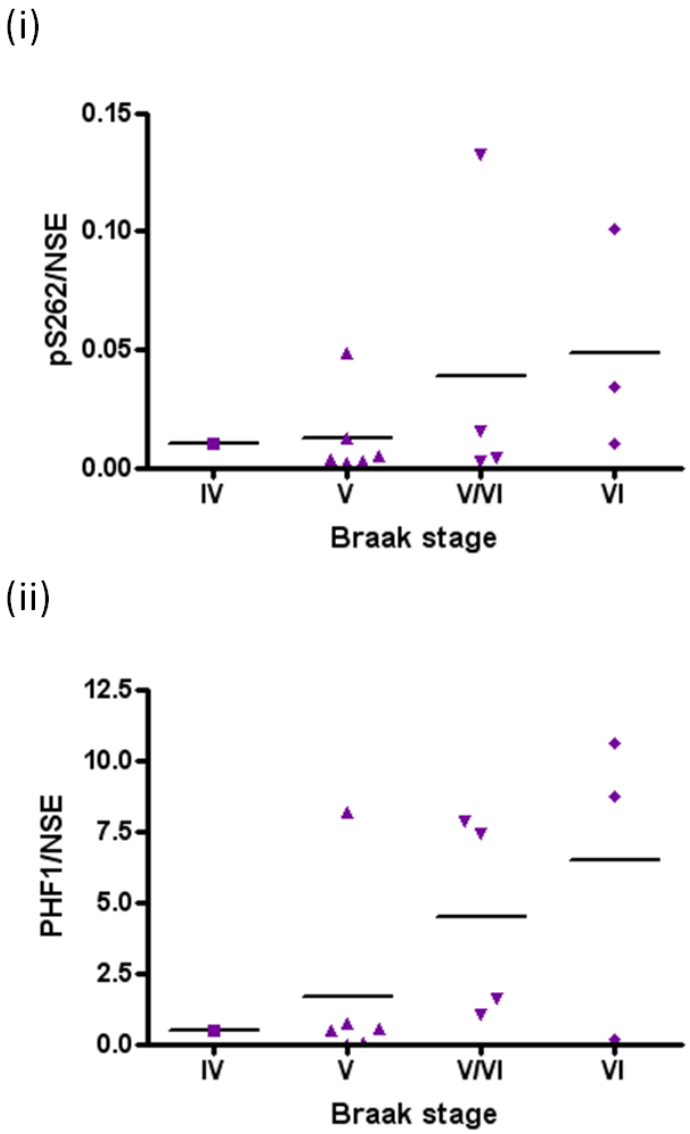

Figure 6.4: PHF1 and pS262 antibody signals grouped according to Braak stage. *Data for stage IV was discounted in the statistical analysis due to only one data point. (i): There is a trend for increased pS262 signal with increasing Braak stage but this was not significant (n=6, 0.012±0.0074 for stage V, n=4, 0.038±0.031 for stage V/VI and n=3, 0.048±0.027 for stage VI, p=0.43, one way anova). (ii): There is a trend for increased PHF1 signal with increasing Braak stage but this was not significant (n=6, 1.65±1.30 for stage V, n=4, 4.48±1.82 for stage V/VI and n=3, 6.49±3.20, for stage VI, p=0.23, one way anova).*

6.2.2 LKB1

LKB1 is the master regulator of 14 members of the AMPK-related family of kinases, including BRSKs (Lizcano et al., 2004). As seen in figure 6.5, there was no significant difference in the intensity of the signal for total LKB1 (normalised to NSE) in the AD samples when compared to the control samples (n=10, 0.08±0.008 for control and n=17, 0.11±0.01 for AD, p=0.12 unpaired t-test).

LKB1 requires phosphorylation at threonine 189 (T189) in order to become active and phosphorylation at this residue is thought to occur through an auto-catalytic property of LKB1 itself. Looking at the phosphorylated (and thus activated) kinase to total kinase ratio gives an indication of the portion of total kinase which is activated at a point in time; the pool of total kinase may not be altered but the amount of that pool which is in the activated state might be. Figure 6.6 shows that there was no significant difference in the ratio of pT189 LKB1 to total LKB1 in AD samples when compared to control samples (n=10, 0.12±0.02 for control and n=17, 0.26±0.11 for AD, p=0.29 Mann Whitney test).

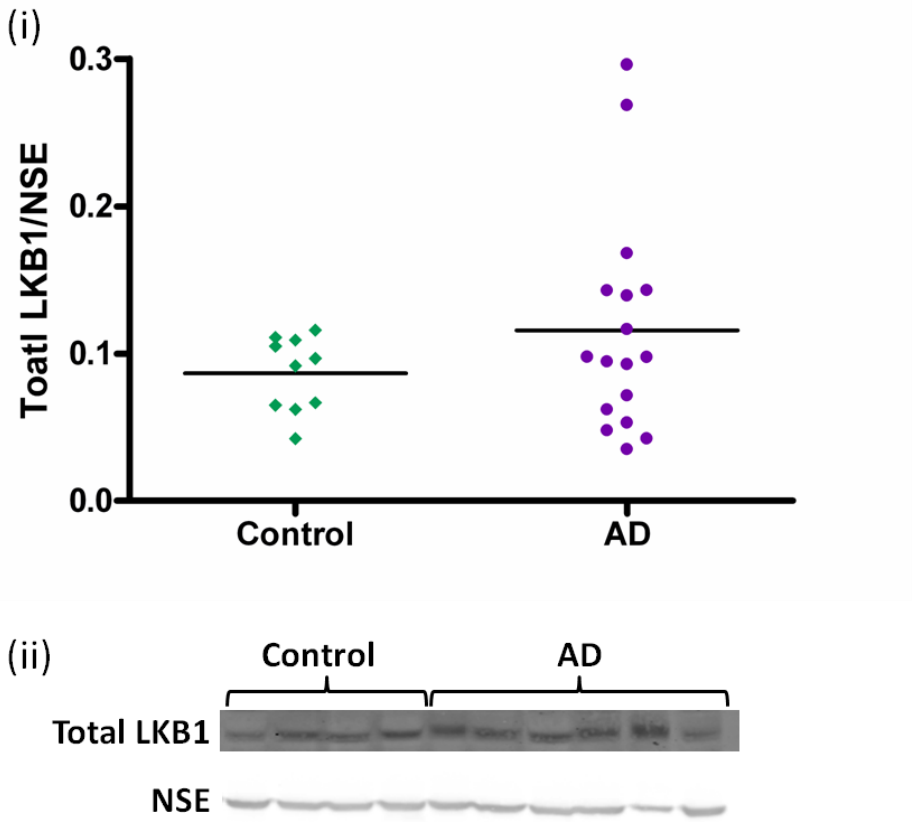

Figure 6.5: Total LKB1 in Alzheimer patients and aged-matched controls.
(i): There is no difference in the intensity of total LKB1 in Alzheimer brain (n=17, 0.11±0.01) when compared to age-matched control brain (n=10, 0.08±0.008) p=0.12 unpaired t-test. (ii): Representative western blots for total LKB1 and NSE antibodies.

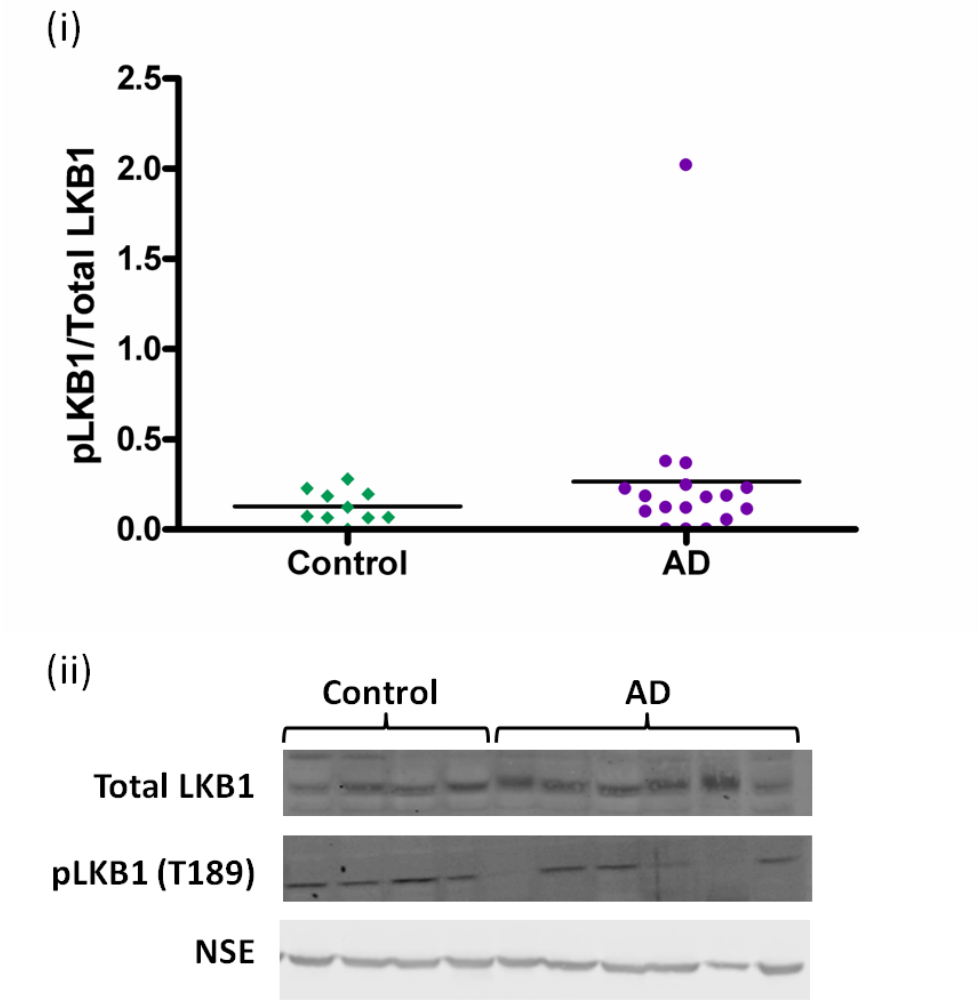

Figure 6.6: Ratio of phosphorylated (T189) LKB1 to total LKB1 in Alzheimer patients and aged-matched controls.
(i): Comparison of the ratio of pLKB1 (T189) to total LKB1 in Alzheimer brain (n=17, 0.26±0.11) and age-matched control brain (n=10, 0.12±0.02) p=0.29 Mann Whitney test. (ii): Representative western blots for pLKB1 (T189), total LKB1 and NSE antibodies.

6.2.3 CaMKK

CaMKKα is a second important regulator of BRSKs (Fujimoto et al., 2008). As shown in figure 6.7, there was no significant difference in the expression of CaMKK in the AD samples when compared to the control samples (using a pan-CaMKK antibody which recognises both the α and β isoforms of CaMKK) (n=11, 1.74±0.22 for control and n=18, 1.58±0.15 for AD, p=0.27 unpaired t-test). Unfortunately, it was not possible to look at the relative activity of CaMKK as there are currently no phospho-specific antibodies available to either isoform of CaMKK.

There was an age-related increase in the expression of the CaMKK in the AD samples (figure 6.8), but this was not present in the control samples (n=11, p=0.8027 for controls and n=18, p=0.02 for AD, Pearson r test).

However, in order to make a fair comparison between the control and AD data sets, the data should be compared over the same age range. This necessitated the removal of one data point from the AD graph; this patient died at the age of 97 and there were no samples from subjects who had an age over 90 in the control data. Removal of this data point from the AD samples rendered the correlation between age of death and CaMKK expression in the AD samples insignificant (n=17, p=0.21 Pearson r test). Removal of this sample from the initial analysis of control and AD groups had no effect on the results; there was no significant difference in the expression of CaMKK between the two groups (n=11, 1.74±0.22 for control and n=17, 1.49±0.12 for AD, p=0.14 unpaired t-test).

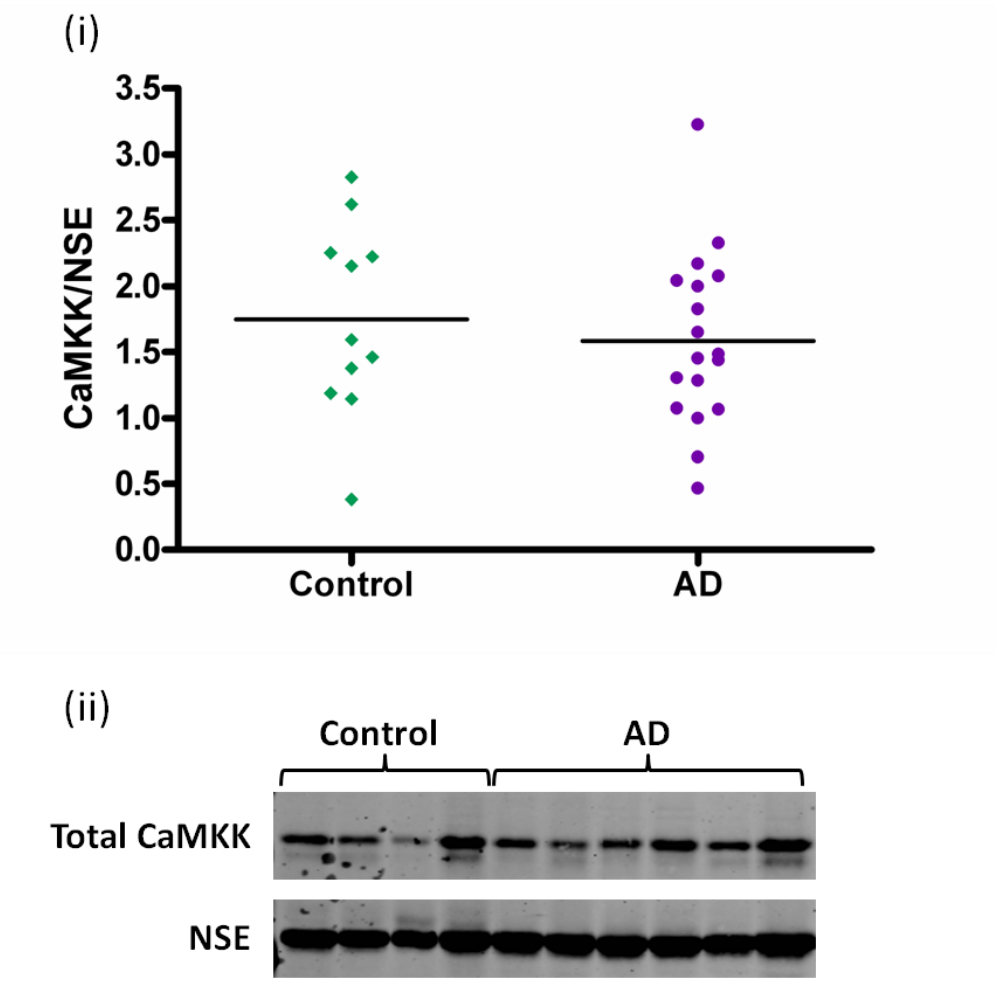

Figure 6.7: Total CaMKK in Alzheimer patients and aged-matched controls.
(i): There is no difference in total CaMKK in Alzheimer brain (n=18, 1.58±0.15) when compared to age-matched control brain (n=11, 1.74±0.22) p=0.27 unpaired t-test. (ii): Representative western blots for total CaMKK and NSE antibodies.

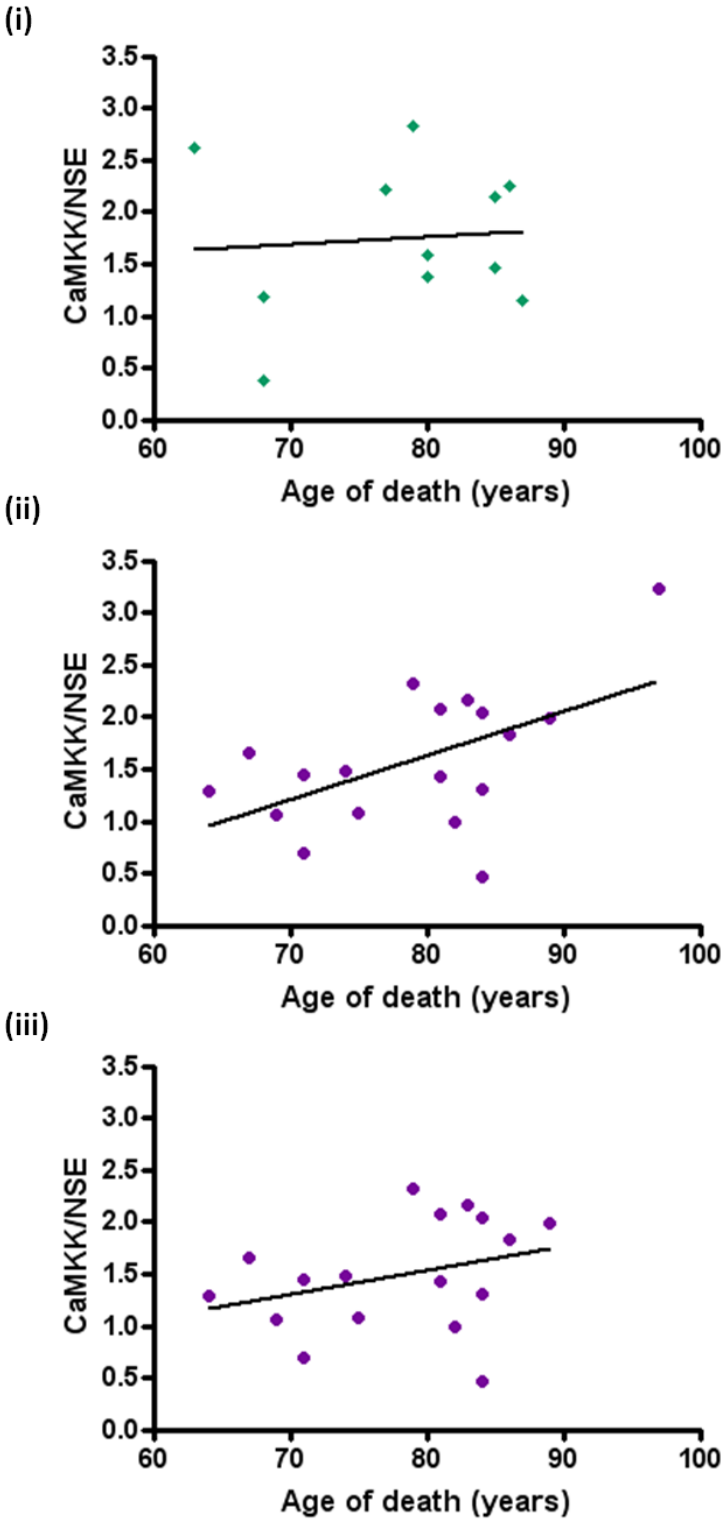

Figure 6.8: Total CaMKK expression and age of Alzheimer patients and aged-matched controls.

(i): There is no correlation between total CaMKK and age in control brain (n=11, p=0.8027 Pearson r test). (ii): There is a significant correlation between total CaMKK and age in AD brain (n=18, p=0.02 Pearson r test). (iii): Removal of the 97 year old patient also removes any significant correlation (n=17, p=0.21 Pearson r test).

6.2.4 BRSK2

Figure 6.9 shows that there was no difference in the expression of BRSK2 as measured by a C-terminal antibody (normalised to NSE) in AD samples when compared to control samples (n=11, 0.37±0.068 for control and n=18, 0.38±0.059 for AD, p=0.42 unpaired t-test). It was not possible to measure phosphorylated (and thus activated) BRSK in each group, since I was unable to detect BRSK phosphorylation in the brain lysates by Western blot.

However, when BRSK was visualised with the antibody raised to the C-terminus of BRSK, a prominent low molecular weight multi-band species running at approximately 44kDa was detected in addition to the full length BRSK (88kDa), (figure 6.10). The novel complex potentially represents fragments of BRSK and is highlighted in the green box (fragment 1) and red box (fragment 2). There has been one previous report of such low molecular weight BRSK species on immunoblots of rat brain probed with affinity purified anti-BRSK2 antibodies isolated from the serum of a patient with limbic encephalitis and small-cell lung cancer (Sabater et al., 2005).

Quantification of individual species (figure 6.11) revealed that fragment 1 is significantly more represented in the AD patient group compared to controls (n=11, 0.02±0.0072 for controls and n=18, 0.16±0.055 for AD, p=0.0278 unpaired t-test). There was no correlation between the expression of fragment 1 and PMD, age or sex (Table 6.3). However, although fragment 1 is significantly elevated in the AD group compared to the control group, it would appear that it is only elevated in a subset of 6

patients (1/3rd) from the 18 AD cases. Further analysis of these six samples showed no correlation between PMD, age or sex.

Figure 6.12 shows that there was no significant difference in the intensity of fragment 2 in AD samples when compared to controls (n=11, 0.57±0.17 for control and n=18, 3.66±2.61 for AD, p=0.33 Mann Whitney test).

There was no correlation between full length BRSK and fragment 1 or fragment 2 in either of the groups, neither was there any correlation between fragment 1 and fragment 2 (Table 6.4).

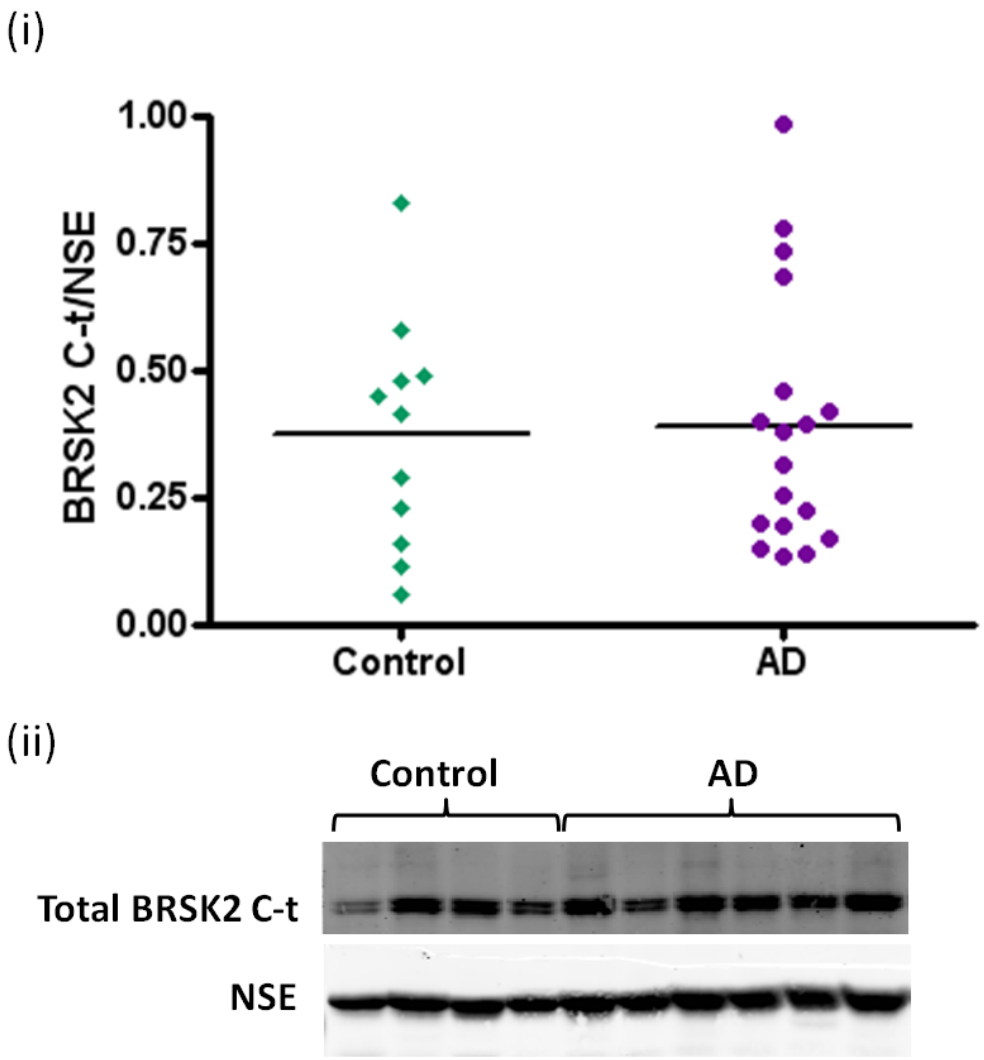

Figure 6.9: Total BRSK2 (C-terminal) in Alzheimer patients and aged-matched controls.
(i): There was no difference in the level of total BRSK2 in Alzheimer brain (n=18, 0.38±0.059) when compared to age-matched control brain (n=11, 0.37±0.068) p=0.42 unpaired t-test. (ii): Representative western blots for total BRSK2 (C-terminal) and NSE antibodies.

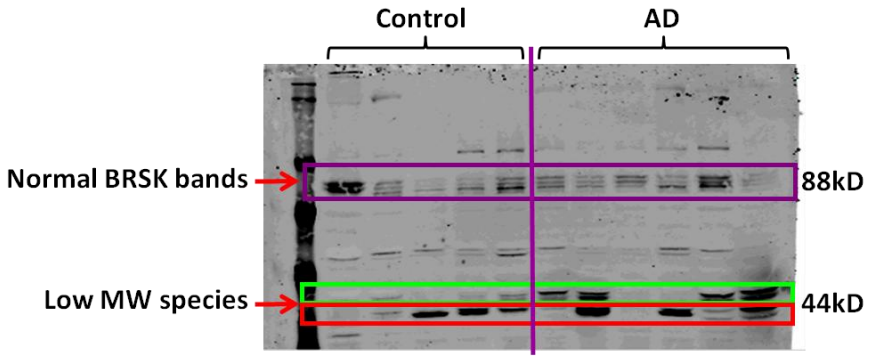

Figure 6.10: Low molecular weight BRSK2 (C-terminal) fragments.
BRSK2 protein usually runs at approximately 88kD (purple box) on a western blot. Using a BRSK2 C-terminal antibody there are also prominent low molecular weight species at approximately 44kDa, termed fragment 1 (green box) and fragment 2 (red box) in future analyses.

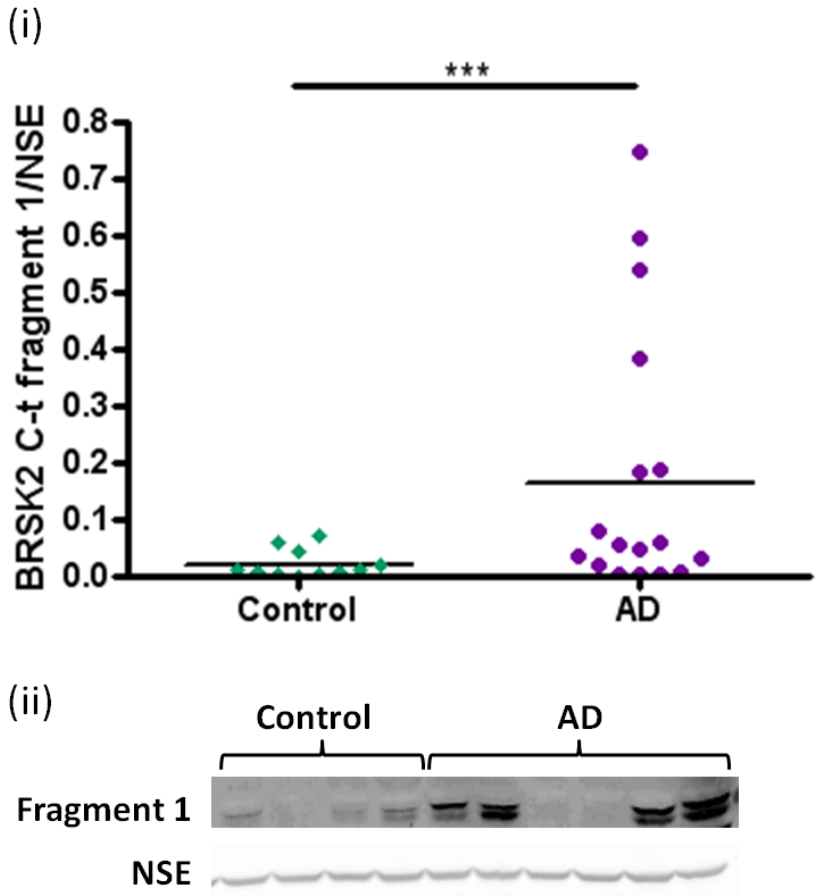

Figure 6.11: BRSK2 (C-terminal) fragment 1 in Alzheimer patients and aged-matched controls.
(i): BRSK2 C-terminal fragment 1 is significantly elevated in Alzheimer brain (n=18, 0.16±0.055) when compared to age-matched control brain (n=11, 0.02±0.0072), p=0.0278 unpaired students t-test. (ii): Representative western blots for BRSK2 C-terminal and NSE antibodies.

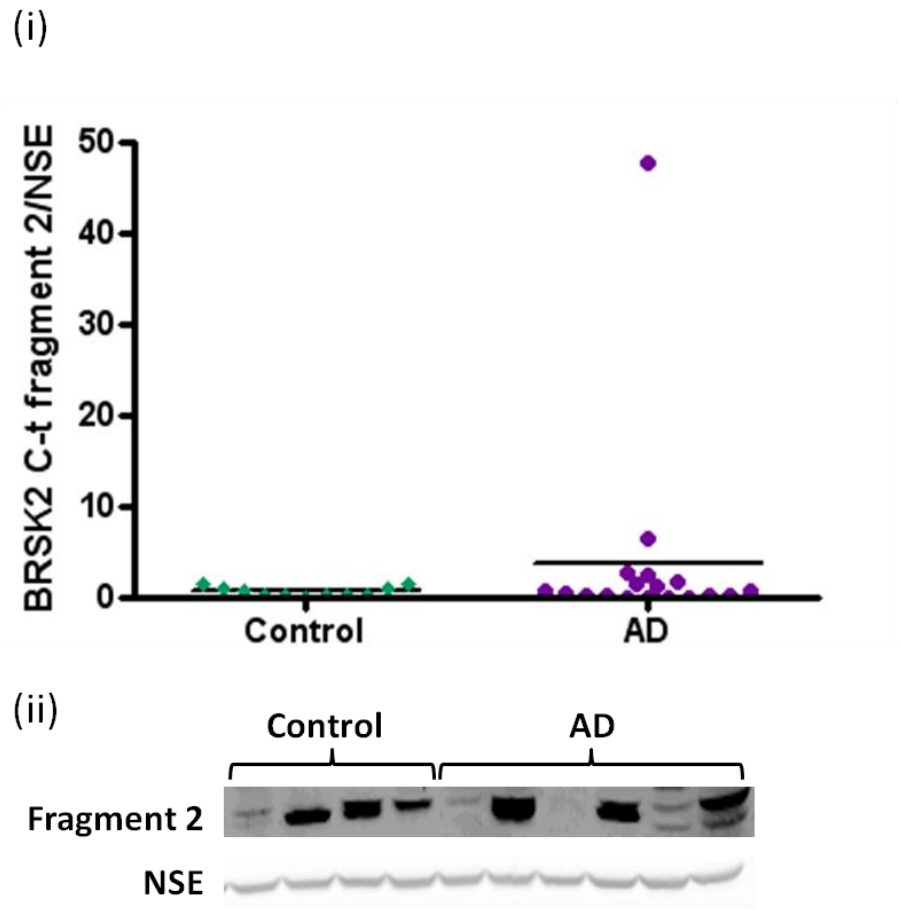

Figure 6.12: BRSK2 (C-terminal) fragment 2 in Alzheimer patients and aged-matched controls.
(i): There is no difference in the level of BRSK2 C-terminal fragment 2 in Alzheimer brain (n=18, 3.66±2.61) when compared to age-matched control brain (n=11, 0.57±0.17) p=0.33 Mann Whitney test. (ii): Representative western blots for BRSK2 C-terminal and NSE.

6.2.4.1 Calpain Assay

Calpain is a calcium dependent cysteine protease which has been shown to be activated upon treatment of neuronal cultures with fibrillary Aβ peptide (Lee et al., 2000). Due to its calcium dependent nature, I was interested in whether calpain may be the protease responsible for the BRSK fragments seen in the AD samples.

In order to address this, I performed a calpain cleavage assay (adapted from Patze and Tsai, 2002). Figure 6.13 shows natural degradation of recombinant His-tagged BRSK2 protein which had been incubated in a 37°C water bath for a number of hours, as detected with the C-terminal BRSK2 antibody. Although BRSK2 was somewhat degraded during the longer incubation times, the most prominent species was still full-length BRSK2 (88kDa) and there were no specific degradation products visible on the gel.

Figure 6.14 shows a representative western blot (using the BRSK2 C-terminal antibody) of the calpain cleavage assay which was conducted in triplicate. Degradation of BRSK2 by calpain produced a band running at approximately 35kDa, which was not present in the lane with no calpain (visible in the lanes where the calpain inhibitor was used). Although this band is of a lower molecular weight than those seen on the western blots from post-mortem brain, it cannot be ruled out that if this assay were to be performed in a cellular system, post-translational modifications of BRSK may cause the fragment to run at a higher molecular weight.

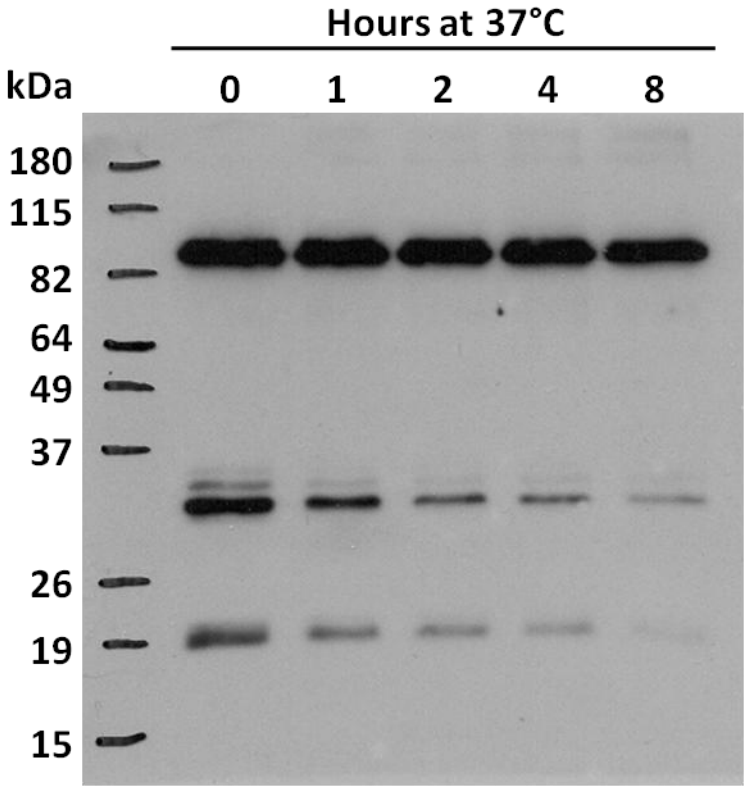

Figure 6.13: Western blot of recombinant His-BRSK2 protein using the C-terminal antibody.
BRSK2 protein is degraded during incubation at 37°C, however the most prominent species is still full-length BRSK (88kDa). There don't appear to be any specific degradation products.

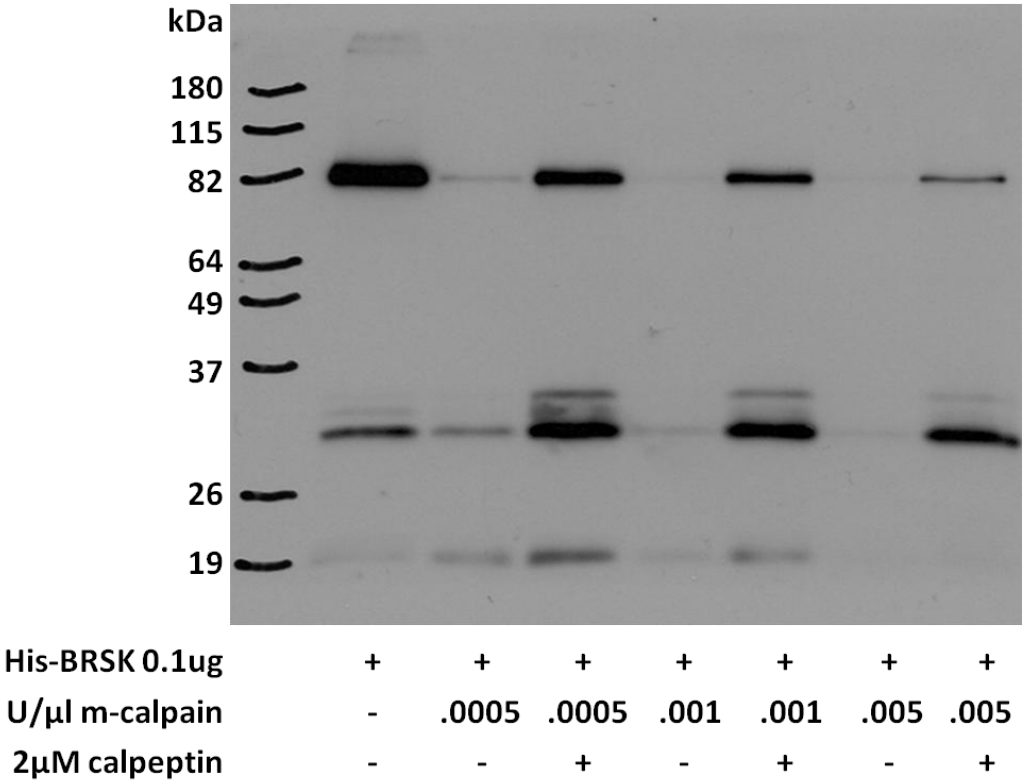

Figure 6.14: m-calpain degradation of BRSK2.
Western blot showing the degradation of his-tagged BRSK2 by m-calpain at three different concentrations, in the presence or absence of 2µM of the m-calpain inhibitor, calpeptin. Degradation of BRSK2 by calpain produced a band of approximately 35kDa which was most prominent in the lanes where the calpain inhibitor was used.

6.2.5 Results of statistical analyses for correlations of antibody signals with PMD, age and sex and trend analysis for AD samples in relation to Braak stage

Antibody	Correlation with						Trend with Braak stage (AD samples)
	PMD		Age		Sex		
	Control	AD	Control	AD	Control	AD	
Total tau	ns	ns	ns	ns	ns	ns	None
pS262	ns	ns	ns	ns	ns	ns	Positive
pS262 subset	-	ns	-	ns	-	n too low	-
PHF-1	ns	ns	ns	ns	ns	ns	Positive
PHF1 subset	-	ns	-	ns	-	ns	-
Total LKB1	ns	ns	ns	ns	ns	ns	None
pLKB1/Total LKB1	ns	ns	ns	ns	ns	ns	None
CaMKK	ns	ns	ns	s (0.02)	ns	ns	None
BRSK2 C	ns	ns	ns	ns	ns	ns	None
BRSK2 C Fragment 1	ns	ns	ns	ns	ns	ns	None
BRSK2 C Fragment 1 subset	-	ns	-	ns	-	ns	-
BRSK2 C Fragment 2	ns	ns	ns	ns	ns	ns	None

Table 6.3: Results for correlation of antibody signals in control and AD tissue with post mortem delay, age and sex and trend analysis for AD samples in relation to Braak stage.
'ns' indicates non-significant data, 's' indicates significant data (p-values are shown in brackets for significant data). Correlations were tested using Pearson r or Spearman r tests of correlation for normally and non-normally distributed data respectively (PMD and age) and parametric or non-parametric t-tests for normally and non-normally distributed data respectively (sex). None of the antibody signals correlated with PMD in either of the groups. CaMKK showed a significant age-dependent increase in signal in the AD samples. Sex had no influence over the antibody signals in either of the groups. It was not possible to analyse the effect of sex on the samples with high pS262 as the n number for the males was too low. For the Braak stage data, none of the antibodies showed a significant correlation (one way anova) and so the data was interpreted as positive trend, negative trend or no trend.

6.2.6 Results of statistical analyses for correlations of full length BRSK, fragment 1 and fragment 2.

Correlation	Result
Full length BRSK to fragment 1 AD	ns
Full length BRSK to fragment 1 Control	ns
Full length BRSK to fragment 2 AD	ns
Full length BRSK to fragment 2 Control	ns
Fragment 1 to fragment 2 AD	ns
Fragment 1 to fragment 2 Control	ns

Table 6.4: Results for correlation of antibody full length BRSK, fragment 1 and fragment 2.
Correlations of full length BRSK to fragment 1 or fragment 2 (AD and Control) were not significant. Correlations of fragment 1 and fragment 2 (AD and Control) were not significant. Correlations were tested using Pearson r or Spearman r tests of correlation for normally and non-normally distributed data respectively.

6.3 Discussion

The work in this chapter examines the expression levels of protein kinases involved in the regulation of BRSKs in human post mortem brain tissue from AD and control subjects. There was no difference in the level of total tau between the two groups, a finding which is consistent with current literature (Causevic et al., 2010). However there was an increase in tau phosphorylation in the AD samples at the epitopes recognised by the pS262 and PHF1 antibodies. The three sites recognised by these phospho-specific antibodies were known to be phosphorylated in AD brain tissue (Hanger et al., 2007), but this is the strongest evidence to date of a significant increase in phosphorylation of S262 of tau associated with AD. In addition, I found a trend toward increased tau phosphorylation at these residues with increasing Braak stage but this was not significant. Braak staging is based upon the tau tangle load in the brain and tangles are largely composed of hyperphosphorylated tau (Augustinack et al., 2002), hence it is plausible that phosphorylation of tau at S262 by BRSK contributes to this association but larger sample sizes will be required to confirm this hypothesis.

I was unable to detect any differences in the expression, or phosphorylation of threonine 189, of LKB1 between the two groups, suggesting that LKB1 activity is not altered in AD. Neither was there any correlation with PMD, age or sex, or any trend associated with Braak stage. Therefore the increase in phosphorylation of tau at S262 in these samples cannot be related to induction of BRSK by abnormally activated LKB1.

Similarly, there was no significant difference in the expression of CaMKK between the AD and control groups and no correlation of CaMKK expression with PMD, sex or Braak stage. However, there was a positive correlation between CaMKK expression and age in the AD samples which was not present in the control samples, suggesting an age-dependent increase in CaMKK expression in AD subjects. Having said this, removal of one data point from the AD data set in order to conduct the control and AD correlations over the same age range rendered the AD data not significant (removal of the same point from the original analysis of CaMKK expression in AD and control subjects had no effect on the results). This suggests that in order to perform such correlations, it would be better to have a larger data set where there is a greater spread of data points. It also highlights the need to perform such comparisons fairly and over the same scale in order to draw conclusions that are not biased by the presence of one data point.

The calciumopathy model for AD states that as humans age their capacity for buffering calcium becomes impaired, leading to a dysregulation of calcium homeostasis which if sustained, may provide a trigger for age-associated changes in the brain (Khachaturian, 1987; LaFerla, 2002). Indeed, in 2001 it was shown that amyloid proteins cause a rise in intracellular calcium in neurons (Kawahara and Kuroda, 2000). More recently, it has been shown that treatment of neurons with amyloid proteins led to missorting of tau from axons to dendrites, local elevation of intracellular calcium levels, tau phosphorylation at a number of residues and increased expression and/or activation of tau kinases such as PAR-1 and BRSK1 (Zempel et al., 2010). The calmodulin kinases (CaMKs) are a family of kinases that are regulated in a calcium and calmodulin dependent manner. Many CaMKs are

capable of phosphorylating and activating calcium-responsive transcription factors such as CREB and ATF-1 and so it could be hypothesised that a rise in intracellular calcium (if sustained) may cause an up-regulation of the expression of many genes via the calcium dependency of such transcription factors, and their activation by CaMKs (Wayman et al., 2008). Thus, increased activation of BRSK in response to increased calcium is likely to be mediated through CaMKKα which is a member of the CaMKs and has been shown to regulate BRSKs *in vitro* (Fujimoto et al., 2008).

Unfortunately, the antibody that I had for CaMKK was pan-CaMKK and as such did not differentiate between the α isoform, which does regulate BRSKs, and the β isoform which does not (Bright et al., 2008; Fujimoto et al., 2008). Possibly more importantly, I was unable to establish the activation status of the CaMKK as currently there are no phospho-CaMKK antibodies (to either isoform). There are two ways of circumnavigating the lack of phospho-CaMKK antibodies; I could have investigated the downstream targets of CaMKKs, however, it would appear that none of the downstream targets of CaMKKs, such as CaMKI and CaMKIV, are targeted specifically by either isoform (Wayman et al., 2008). Alternatively, I could have performed immunoprecipitation kinase assays for CaMKK activity using a synthetic peptide as a substrate for CaMKKs. This was not pursued due to insufficient brain lysate material for such an approach.

There was no significant increase in BRSK expression in the AD samples. Neither was there any effect of PMD or sex on BRSK expression. In addition there was no correlation with age and BRSK2 expression and neither was there any trend toward abnormal BRSK2 expression associated with Braak stage.

Of potential interest were prominent low molecular weight species visible on the Western blots for BRSK2. One of the low molecular weight species (termed fragment 1), was significantly elevated in AD samples compared to control. There was no correlation between fragment 1 and PMD, age or sex. Neither was there any trend associated with Braak stage. This fragment seemed to be highly represented in a subset of the patients ($1/3^{rd}$ of the AD cases), but further analysis of these six samples showed that there was no correlation with PMD, age or sex. It would have been interesting to see if there was a correlation with the age of onset of the disease (age of onset may give an indication as to the type of AD the patients had e.g. familial or sporadic; familial AD, which has a genetically inherited cause, usually has a lower age of onset) but unfortunately this clinical data was not held by the brain bank and so this comparison was not possible.

It was tempting to hypothesise that the low molecular weight fragments were fragmented BRSK proteins, indeed similar low molecular weight fragments have been reported in immunoblots of rat brain probed with affinity purified anti-BRSK2 antibodies isolated from the serum of a patient with limbic encephalitis and small-cell lung cancer (Sabater et al., 2005). However, it is possible that the fragments were due to non-specific binding of the antibodies. Non-specific binding of antibodies to proteins (which are not the targeted antigen) often occurs, especially when using polyclonal antibodies. A relatively simple experiment which would address this would be to perform a peptide blocking experiment. Briefly, the BRSK antibody would be neutralized with the immunizing peptide (the peptide which corresponds to the epitope that the antibody recognises). The blocked antibody

would then no longer be available to bind to the protein immobilised on the membrane and by comparing the results obtained from blocked and non-blocked antibody, the portion of staining which was specific could be determined as this would be absent from the membrane incubated with the blocked antibody.

Before performing any further studies on this fragment it would be important to establish exactly what proteins were present in the 44kDa region and which of these were over-expressed in the 6 AD patients. Proteins present in a BRSK immunoprecipitation from one of the patient samples could be identified by Mass fingerprinting after separation by SDS-PAGE. This would give a clear indication if BRSK was truly the major component of fragment 1 or fragment 2, and indicate the likely region of cleavage. Alternatively a novel potential marker of AD may be identified.

Assuming that the fragments were BRSK proteins, I attempted to generate the fragments from recombinant BRSK. Calpain was an interesting possible protease due to its calcium-dependent nature and the fact that it is activated in neurons treated with fibrillar Aβ peptide (Lee et al., 2000). An *in vitro* calpain cleavage assay (adapted from Lee et al., 2000) showed that calpain degraded BRSK protein with the appearance of a band of approximately 35kDa. However, it was not possible to identify the degradation products under the conditions used in my assay. Further work on this was not possible due to time constraints, but if it were to be re-visited it may be more sensible to take a bioinformatics approach, possibly by scanning the BRSK sequence for known protease motifs and then using *in vitro* cleavage assays to further assess any candidate proteases. It would also be worth examining whether

this fragment is generated in cells exposed to amyloid or calcium, and if it is found in any models of AD or tauopathy where pS262 of tau is increased as post-translational modifications of BRSK in a cellular system may well cause the fragment to run at a higher molecular weight.

As with CaMKK, it was not possible to investigate the phosphorylated BRSK by western blot. Unfortunately there was only one phospho-BRSK antibody available and I was unable to observe a signal using this antibody. It was not clear if this was because there was little or no phospho-BRSK signal in the samples, or because the antibody wasn't good enough. It is likely to be the latter situation as I was also unable to detect a signal when using this antibody on lysates from *Drosophila* expressing human BRSK2. One way to address the lack of sensitive phospho-specific antibodies for many proteins would be to utilise a technology called PhosTag™ (Kinoshita et al., 2006). This is based on the retardation of phosphorylated proteins in SDS-PAGE gels using alkoxide-bridged dinuclear metal complexes as phosphate binding molecules. Incorporation of Mn^{2+} phos-tags into acrylamide gels enables the preferential binding of phosphate molecules bound to Serine, Threonine or Tyrosine residues, causing the phosphorylated proteins to migrate slower than the corresponding non-phosphorylated proteins. This allows the detection of phosphorylated proteins using a total antibody for the protein of interest. However, the weakness of this technology is that it would only show if a particular protein was phosphorylated at a Serine, Threonine or Tyrosine residue; it would not indicate phosphorylation of a specific residue in the protein.

During the analysis, I noticed that on many of the blots there were points which were obviously above the mean (for an example see figure 6.5). Further analysis of such points showed no particular pattern between most antibody signals, for example the 6 samples with the highest pS262 signal were not the same samples that had the highest BRSK2 C-terminal fragment 1 signal and there was no relationship between the expression of full length BRSK and either of the fragments. The only pattern I was able to observe was that 5 of the samples that had high pS262 signal also had high PHF1 signal. It was important to investigate the pattern of the samples with obviously high signals as this could potentially have revealed subsets of patients with a specific pattern of pathological markers. Unfortunately, it would seem that the data sets I used were too small for this kind of analysis; samples which seemed to have unusually high signal in this study may not be so striking in a larger data-set due to a greater spread of data points or alternatively a larger data set may reveal subsets of patients with varying expression levels (as seen with pS262, PHF1 and BRSK2 C-terminal fragment 1).

Currently, there are no other studies investigating the expression of the kinases upstream of tau phosphorylation at S262, as described here. Unfortunately, lack of response to the phospho-specific antibody for BRSK available to me and a lack of phospho-specific antibodies for CaMKK prevented the assessment of activity of BRSK or CaMKK. However, there have been many other studies that have successfully identified altered signalling pathways linked to AD (for example MAP kinases (in particular p38 and SAPK), calpain (a calcium dependent protease), cAMP-dependent protein kinase, CRMP2 and GSK-3β) using the same approach that was utilised in this study (Swatton et al., 2004; Liu et al., 2005b; Cole et al., 2007;

Liang et al., 2007; Causevic et al., 2010). Further challenges to studying the expression and activation level of proteins in post-mortem tissue, beyond those of obtaining reagents, are those posed by the nature of the tissue. The variability seen in post-mortem tissue may arise from several factors; PMD, storage temperature (before post-mortem and the associated sampling) and tissue fixation methods have all been documented to have an effect on the preservation of proteins, DNA and RNA in post-mortem samples (Ferrer et al., 2008). In terms of proteins, PMD and temperature of storage are the most important factors and it has been shown that kinases are particularly sensitive to such variables (Ferrer et al., 2008). Having said this, I found no correlation between PMD and the expression level of any of the kinases in this study, suggesting that for the samples I used, PMD was not a contributing factor to the lack of relationship to AD reported. I did not have any information regarding the storage temperature before post-mortem and so cannot draw any conclusions with regards to this factor.

In conclusion, I have been able to show that there is no difference in the expression of total LKB1, pT189 LKB1, CaMKK and BRSK2 C-terminal between AD and control groups. There was an age-dependent increase in CaMKK expression in the AD samples but I have been unable to elucidate if this was the α isoform or the β isoform. There was no age dependent increase in the signal from the BRSK2 antibody neither was there any trend between the antibody signal and Braak stage. There was a significant increase in a low molecular weight species detected by the BRSK2 antibody in the AD group, suggesting that BRSK2 may be cleaved in AD brain. However, it remains to be elucidated if these fragments are actually BRSK proteins and if so, what effect cleavage may have.

The data I have presented in the previous chapters show that human BRSKs are capable of interacting with and phosphorylating human tau in a *Drosophila* expression model. I show that these interactions are regulated by at least two endogenous upstream kinases, LKB1 and CG17698 and due to the calcium sensitive nature of CaMKKα (the human homologue of CG17698) and the data showing that over-expression of a calcium channel subunit (cac1) enhances the tau-BRSK eye phenotype; I suggest that BRSKs may prove to be important and previously largely unstudied tau kinases. It was important for my thesis to attempt to link the data attained in the *Drosophila* model with the situation in human disease. The data presented in this chapter is as comprehensive as possible - taking into account the limited reagents available and the time constraints. Whilst I was able to show there was no difference in the activation of LKB1 between control and AD samples, I was unable to reach a solid conclusion for BRSK and CaMKK in terms of activation, although their expression was not altered. As such I must conclude that it is still possible that the activity of these kinases is elevated in AD. It should also be taken into consideration that it is feasible that the pathological profile of these kinases may be different according to disease, for example, kinases may play a more important role in the pathogenesis of the tauopathies as these are a spectrum of diseases in which it would appear that tau is the main pathological species (as opposed to AD where amyloid-beta also plays an important role) and so it could be expected that kinases (and/or phosphatases) may play a more pivotal role in the tauopathies.

7| Concluding remarks and perspectives for future work

At the beginning of this project, little was known about BRSKs and their importance to tau phosphorylation in AD. This study provides the first *in vivo* evidence and the most convincing data to date that human BRSKs are able to phosphorylate human tau, exacerbating a human tau-induced degenerative eye phenotype. Importantly, and in contrast to previous studies in *Drosophila*, here I have utilised the human BRSKs in concert with human tau in my experiments. It is my opinion that this approach is more disease relevant, in comparison with studies where human tau and endogenous *Drosophila* kinases were used. However, there is currently no information on the physiological role of BRSK-induced phosphorylation of tau. It would be useful to expand this study in an attempt to determine this, and also to address how the phosphorylation of tau by BRSK fits in with phosphorylation of tau by other kinases.

I have shown, by use of RNAi lines, that human BRSK2 can be regulated by *Drosophila* LKB1 and CG17698. However, data obtained using B-NP, which carries a T174A mutation to prevent activation by phosphorylation at T174 by an upstream kinase, indicates that there may be other regulatory sites on BRSK that act independently of the T-loop T174 residue targeted by LKB1 and CG17698, or that BRSKs possess weak activity in the absence of T-loop T174 phosphorylation. It has been suggested that BRSKs are also regulated by PKA via phosphorylation of threonine 260 (Guo et al., 2006). However this is contradicted by Bright *et al.* (2008) who indicated that PKA was unable to activate BRSKs (Bright et al., 2008). *Drosophila* provides a powerful unbiased model to address this discrepancy, and to identify other regulators of BRSKs. In order to achieve these objectives, a deficiency screen could be performed on B-WT and B-NP, to rapidly isolate enhancers or suppressors of the tau-BRSK eye phenotype. Deficiency stocks have been produced

for all four *Drosophila* chromosomes and are freely available from the stock centres (Thibault et al., 2004; Ryder et al., 2007). Deficiency screens have long been used to successfully identify components of signalling pathways and the eye is by far the most popular tissue in which to conduct such screens because it is not essential for viability or fertility and is easy to score (St Johnston, 2002). Each deficiency is fully mapped to the genome and as such, the genes contained within a deletion can be identified. Using a deficiency screen, in addition to resolving whether PKA is capable of regulating BRSK, new positive and negative regulators of human BRSKs could be identified. Importantly, LKB1 and CG17698 could be used as positive controls in a screen as I have already shown them to be regulators of human BRSK2.

An important observation from my thesis is the apparent calcium-dependent regulation of tau through BRSKs. Here I provide the first direct *in vivo* evidence between an increase in intracellular calcium, a tau kinase and increased tau toxicity; over-expression of cac1, a calcium channel α subunit (in order to increase intracellular calcium levels from extracellular sources), with tau and B-WT dramatically exacerbated the tau-BRSK eye phenotype in a human BRSK2-dependent manner. Although there is much work to be done to characterise this calcium-dependent enhancement of tau toxicity by BRSKs, it is a process that is highly relevant for AD due to the link between AD and perturbed calcium homeostasis. To date, the only other evidence directly linking calcium to tau phosphorylation is the calcium-dependence of another tau kinase, CaMKII, and the cleavage of p35 to p25 (which activates the tau kinase cdk5) by the calcium-activated protease calpain (Litersky et al., 1996; Lee et al., 2000). It will now be important to demonstrate an increase in intracellular calcium levels and in tau phosphorylation at

S262 and BRSK2 phosphorylation at T174 upon over-expression of cac1 with tau and B-WT in the eye. This would provide a biochemical link between the exacerbated eye phenotype and BRSK activation, leading to increased tau phosphorylation at a disease relevant site. In addition, it will be important to elucidate whether the calcium-induced exacerbation of tau-BRSK eye phenotypes is dependent on CG17698, whether the S262A/S2A mutants are insensitive to cac1 expression with B-WT and whether over-expression of cac1 has an effect when B-NP or B-KD are substituted for B-WT. These experiments would give an indication as to whether the exacerbated eye phenotype observed upon over-expression of cac1 in the presence of tau and B-WT is truly mediated by BRSK, through CG17698, and whether S262 and/or S356 are the important residues for this interaction. This seems most likely as the effect of cac1 on the eye phenotypes was only apparent in the presence of B-WT, but the precise details of the interaction require further evidence.

To date, three members of the AMPK-related family of protein kinases have been demonstrated to be tau kinases; PAR-1, AMPK and BRSK2 (Drewes et al., 1997; Nishimura et al., 2004; Vingtdeux et al., 2010a; Thornton et al., 2011). I have shown by phenotypic scoring that BRSK1 is able to enhance a tau-induced degenerative eye phenotype and so it is likely that BRSK1 is also able to phosphorylate tau. Indeed, in the mouse, knockout of each BRSK individually has no effect whereas the double knockout mice have a very severe phenotype, demonstrating redundancy between the two mammalian genes (Kishi et al., 2005). This raises the question of whether any other members of the AMPK-related family of protein kinases are capable of phosphorylating tau. In addition, there are four isoforms of PAR-1/MARK in

humans and two isoforms of AMPK; it would be useful to elucidate whether all of these isoforms also phosphorylate tau or whether it is an isoform-specific activity.

Whilst BRSKs have undoubtedly been demonstrated to be essential during development, there is currently little data on their function in mature organisms. I have shown by western blots on lysates from post-mortem human brain that BRSKs and their upstream regulators are expressed in aged humans (AD and control) and this suggests that their function extends beyond the vital developmental stages. Indeed it has been demonstrated that BRSKs are involved at the synapse in the release of neurotransmitters through the phosphorylation of the active zone protein RIM1 (Inoue et al., 2006). However, it would be interesting to ascertain whether the continued expression of BRSKs beyond developmental stages is also linked to the phosphorylation of tau.

I was able to conclude that the expression of BRSKs was unaltered between post-mortem human brain samples from AD patients and control subjects. However, it was unfortunate that due to insufficient reagents I was unable to investigate the activation of BRSKs in the samples. Thus I was unable to draw any firm conclusions with regards to BRSK activity in AD. With the advent of more sophisticated techniques for measuring phosphorylated proteins such as Mass Spectrometry or ELISAs, it may be possible to readdress this unresolved and clearly vital issue. It may also be worthwhile extending the study to encompass some of the non-AD tauopathies as arguably the pathology in this collection of diseases appears to arise only as a result of tau tangles and as such, phosphorylation of tau may play a more pivotal role in the pathogenesis of the tauopathies as opposed to AD.

The use of *Drosophila* as a model in this study allowed me to take advantage of established genetic techniques, such as the production of recombinant chromosomes, in order to conduct complex experiments where multiple proteins were co-expressed. With the development of more sophisticated genetic tools (such as the recently developed gene-switch system or the temperature-sensitive inhibitor of GAL4, GAL80ts) for temporal control of gene expression, *Drosophila* is rapidly becoming a useful model organism for aging studies (Osterwalder et al., 2001; McGuire et al., 2003; Nicholson et al., 2008; Sofola et al., 2010). This is an attractive benefit as over-expression of human BRSK (and down regulation of CG6114, the *Drosophila* homologue, via RNAi) in the CNS was lethal at the embryonic stage; these new techniques could be utilised for the study of human tau and BRSK expression in neuronal tissue and in aged animals. Although a number of neurodegenerative diseases apart from AD such as ALS, Parkinson's and Huntington's have been modelled in *Drosophila,* new tools such as the gene-switch system enable temporal *and* spatial control of gene expression, greatly enhancing the appeal of *Drosophila* as a model for AD and other neurodegenerative diseases (Marsh et al., 2003; Liu et al., 2008; Ratnaparkhi et al., 2008).

Phosphorylation of tau is highly complex with currently 45 identified phosphorylated residues[3] and little information on the importance of each to tau toxicity, not to mention the signalling pathways that control them. Similar studies to those described in my thesis could be used to map the contribution of every tau phosphorylation site to neurotoxicity, as well as to establish the potential regulatory kinases and phosphatases. This could help clarify the role that specific phosphorylation sites play

[3] http://cnr.iop.kcl.ac.uk/hangerlab/tautable

in tau pathology and identify targets for modulating tau phosphorylation at an early stage *in vivo*.

8| References

Alafuzoff, I. et al. (2008) Staging of neurofibrillary pathology in Alzheimer's disease: a study of the BrainNet Europe Consortium. Brain Pathol 18:484-496.

Alessi, D. R., Sakamoto, K., Bayascas, J. R. (2006) LKB1-Dependent Signaling Pathways. Annu Rev Biochem 75:137-163.

Allinson, T. M., Parkin, E. T., Turner, A. J., Hooper, N. M. (2003) ADAMs family members as amyloid precursor protein alpha-secretases. J Neurosci Res 74:342-352.

Alzheimer, A., Stelzmann, R. A., Schnitzlein, H. N., Murtagh, F. R. (1995) An English translation of Alzheimer's 1907 paper, "Uber eine eigenartige Erkankung der Hirnrinde". Clin Anat 8:429-431.

Apostolova, L. G., Thompson, P. M. (2008) Mapping progressive brain structural changes in early Alzheimer's disease and mild cognitive impairment. Neuropsychologia 46:1597-1612.

Arimura, N., Menager, C., Fukata, Y., Kaibuchi, K. (2004) Role of CRMP-2 in neuronal polarity. J Neurobiol 58:34-47.

Arispe, N., Rojas, E., Pollard, H. B. (1993) Alzheimer disease amyloid beta protein forms calcium channels in bilayer membranes: blockade by tromethamine and aluminum. Proc Natl Acad Sci U S A 90:567-571.

Arnold, S. E., Hyman, B. T., Flory, J., Damasio, A. R., Van Hoesen, G. W. (1991) The topographical and neuroanatomical distribution of neurofibrillary tangles and neuritic plaques in the cerebral cortex of patients with Alzheimer's disease. Cereb Cortex 1:103-116.

Arriagada, P. V., Growdon, J. H., Hedley-Whyte, E. T., Hyman, B. T. (1992) Neurofibrillary tangles but not senile plaques parallel duration and severity of Alzheimer's disease. Neurology 42:631-639.

Augustinack, J. C., Schneider, A., Mandelkow, E. M., Hyman, B. T. (2002) Specific tau phosphorylation sites correlate with severity of neuronal cytopathology in Alzheimer's disease. Acta Neuropathol 103:26-35.

Barghorn, S., Zheng-Fischhofer, Q., Ackmann, M., Biernat, J., von Bergen, M., Mandelkow, E. M., Mandelkow, E. (2000) Structure, microtubule interactions, and paired helical filament aggregation by tau mutants of frontotemporal dementias. Biochemistry 39:11714-11721.

Barnes, A. P., Lilley, B. N., Pan, Y. A., Plummer, L. J., Powell, A. W., Raines, A. N., Sanes, J. R., Polleux, F. (2007) LKB1 and SAD kinases define a pathway required for the polarization of cortical neurons. Cell 129:549-563.

Bartus, R. T., Dean, R. L., 3rd, Beer, B., Lippa, A. S. (1982) The cholinergic hypothesis of geriatric memory dysfunction. Science 217:408-414.

Bayer, A. J., Bullock, R., Jones, R. W., Wilkinson, D., Paterson, K. R., Jenkins, L., Millais, S. B., Donoghue, S. (2005) Evaluation of the safety and immunogenicity of synthetic Abeta42 (AN1792) in patients with AD. Neurology 64:94-101.

Bear, M. F., Connors, B. W., Paradiso, M. A. (2007) Neuroscience: Exploring the brain, Third edition Edition. Baltimore: Lippincott Williams & Wilkins.

Begley, J. G., Duan, W., Chan, S., Duff, K., Mattson, M. P. (1999) Altered calcium homeostasis and mitochondrial dysfunction in cortical synaptic compartments of presenilin-1 mutant mice. J Neurochem 72:1030-1039.

Bertrand, J., Plouffe, V., Senechal, P., Leclerc, N. (2010) The pattern of human tau phosphorylation is the result of priming and feedback events in primary hippocampal neurons. Neuroscience.

Bettencourt-Dias, M., Giet, R., Sinka, R., Mazumdar, A., Lock, W. G., Balloux, F., Zafiropoulos, P. J., Yamaguchi, S., Winter, S., Carthew, R. W., Cooper, M., Jones, D., Frenz, L., Glover, D. M. (2004) Genome-wide survey of protein kinases required for cell cycle progression. Nature 432:980-987.

Biernat, J., Mandelkow, E. M. (1999) The development of cell processes induced by tau protein requires phosphorylation of serine 262 and 356 in the repeat domain and is inhibited by phosphorylation in the proline-rich domains. Mol Biol Cell 10:727-740.

Biernat, J., Wu, Y. Z., Timm, T., Zheng-Fischhofer, Q., Mandelkow, E., Meijer, L., Mandelkow, E. M. (2002) Protein kinase MARK/PAR-1 is required for neurite outgrowth and establishment of neuronal polarity. Mol Biol Cell 13:4013-4028.

Blass, J. P. (2000) The mitochondrial spiral. An adequate cause of dementia in the Alzheimer's syndrome. Ann N Y Acad Sci 924:170-183.

Blennow, K., Nellgard, B. (2004) Amyloid beta 1-42 and tau in cerebrospinal fluid after severe traumatic brain injury. Neurology 62:159; author reply 159-160.

Blessed, G., Tomlinson, B. E., Roth, M. (1968) The association between quantitative measures of dementia and of senile change in the cerebral grey matter of elderly subjects. Br J Psychiatry 114:797-811.

Braak, H., Braak, E. (1991) Neuropathological stageing of Alzheimer-related changes. Acta Neuropathol 82:239-259.

Braak, H., Braak, E. (1997) Diagnostic criteria for neuropathologic assessment of Alzheimer's disease. Neurobiol Aging 18:S85-88.

Brand, A. H., Perrimon, N. (1993) Targeted gene expression as a means of altering cell fates and generating dominant phenotypes. Development 118:401-415.

Brandt, R., Leger, J., Lee, G. (1995) Interaction of tau with the neural plasma membrane mediated by tau's amino-terminal projection domain. J Cell Biol 131:1327-1340.

Breeding, C. S., Hudson, J., Balasubramanian, M. K., Hemmingsen, S. M., Young, P. G., Gould, K. L. (1998) The cdr2(+) gene encodes a regulator of G2/M progression and cytokinesis in Schizosaccharomyces pombe. Mol Biol Cell 9:3399-3415.

Brickman, A. M., Small, S. A., Fleisher, A. (2009) Pinpointing synaptic loss caused by Alzheimer's disease with fMRI. Behav Neurol 21:93-100.

Bright, N. J., Carling, D., Thornton, C. (2008) Investigating the regulation of brain specific kinases 1 & 2 by phosphorylation. J Biol Chem.

Bryan, K. J., Lee, H.-g., Perry, G., Smith, M. A., Casadesus, G. (2008) Chapter 1 - Transgenic Mouse Models of Alzheimer's Disease: Behavioural Testing and Considerations. In: Methods of Behaviour Analysis in Neuroscience, 2nd edition Edition (Buccafusco J, ed). Georgia, America: CRC Press.

Buee, L., Bussiere, T., Buee-Scherrer, V., Delacourte, A., Hof, P. R. (2000) Tau protein isoforms, phosphorylation and role in neurodegenerative disorders. Brain Res Brain Res Rev 33:95-130.

Buerger, K., Ewers, M., Pirttila, T., Zinkowski, R., Alafuzoff, I., Teipel, S. J., DeBernardis, J., Kerkman, D., McCulloch, C., Soininen, H., Hampel, H. (2006) CSF phosphorylated tau protein correlates with neocortical neurofibrillary pathology in Alzheimer's disease. Brain 129:3035-3041.

Buerger, K., Frisoni, G., Uspenskaya, O., Ewers, M., Zetterberg, H., Geroldi, C., Binetti, G., Johannsen, P., Rossini, P. M., Wahlund, L. O., Vellas, B., Blennow, K., Hampel, H. (2009) Validation of Alzheimer's disease CSF and plasma biological markers: the multicentre reliability study of the pilot European Alzheimer's Disease Neuroimaging Initiative (E-ADNI). Exp Gerontol 44:579-585.

Bulic, B., Pickhardt, M., Schmidt, B., Mandelkow, E. M., Waldmann, H., Mandelkow, E. (2009) Development of tau aggregation inhibitors for Alzheimer's disease. Angew Chem Int Ed Engl 48:1740-1752.

Bunker, J. M., Kamath, K., Wilson, L., Jordan, M. A., Feinstein, S. C. (2006) FTDP-17 mutations compromise the ability of tau to regulate microtubule dynamics in cells. J Biol Chem 281:11856-11863.

Burbank, K. S., Mitchison, T. J. (2006) Microtubule dynamic instability. Current Biology 16:R516-R517.

Buxbaum, J. D., Ruefli, A. A., Parker, C. A., Cypess, A. M., Greengard, P. (1994) Calcium regulates processing of the Alzheimer amyloid protein precursor in a protein kinase C-independent manner. Proc Natl Acad Sci U S A 91:4489-4493.

Caceres, A., Kosik, K. S. (1990) Inhibition of neurite polarity by tau antisense oligonucleotides in primary cerebellar neurons. Nature 343:461-463.

Caceres, A., Potrebic, S., Kosik, K. S. (1991) The effect of tau antisense oligonucleotides on neurite formation of cultured cerebellar macroneurons. J Neurosci 11:1515-1523.

Canu, N., Dus, L., Barbato, C., Ciotti, M. T., Brancolini, C., Rinaldi, A. M., Novak, M., Cattaneo, A., Bradbury, A., Calissano, P. (1998) Tau cleavage and dephosphorylation in cerebellar granule neurons undergoing apoptosis. J Neurosci 18:7061-7074.

Cao, X., Sudhof, T. C. (2001) A transcriptionally [correction of transcriptively] active complex of APP with Fe65 and histone acetyltransferase Tip60. Science 293:115-120.

Cardoso, S. M., Santos, S., Swerdlow, R. H., Oliveira, C. R. (2001) Functional mitochondria are required for amyloid beta-mediated neurotoxicity. FASEB J 15:1439-1441.

Carling, D. (2004) Ampk. Curr Biol 14:R220.

Causevic, M., Farooq, U., Lovestone, S., Killick, R. (2010) [beta]-Amyloid precursor protein and tau protein levels are differently regulated in human cerebellum compared to brain regions vulnerable to Alzheimer's type neurodegeneration. Neuroscience Letters In Press, Corrected Proof.

Chapman, P. F., White, G. L., Jones, M. W., Cooper-Blacketer, D., Marshall, V. J., Irizarry, M., Younkin, L., Good, M. A., Bliss, T. V., Hyman, B. T., Younkin, S. G., Hsiao, K. K. (1999) Impaired synaptic plasticity and learning in aged amyloid precursor protein transgenic mice. Nat Neurosci 2:271-276.

Chatterjee, S., Sang, T. K., Lawless, G. M., Jackson, G. R. (2009) Dissociation of tau toxicity and phosphorylation: role of GSK-3beta, MARK and Cdk5 in a Drosophila model. Hum Mol Genet 18:164-177.

Chen, H., Chomyn, A., Chan, D. C. (2005) Disruption of fusion results in mitochondrial heterogeneity and dysfunction. J Biol Chem 280:26185-26192.

Chen, H., McCaffery, J. M., Chan, D. C. (2007) Mitochondrial fusion protects against neurodegeneration in the cerebellum. Cell 130:548-562.

Cho, J. H., Johnson, G. V. (2003) Glycogen synthase kinase 3beta phosphorylates tau at both primed and unprimed sites. Differential impact on microtubule binding. J Biol Chem 278:187-193.

Cole, A. R., Noble, W., van Aalten, L., Plattner, F., Meimaridou, R., Hogan, D., Taylor, M., LaFrancois, J., Gunn-Moore, F., Verkhratsky, A., Oddo, S., LaFerla, F., Giese, K. P., Dineley, K. T., Duff, K., Richardson, J. C., Yan, S. D., Hanger, D. P., Allan, S. M., Sutherland, C. (2007) Collapsin response mediator protein-2 hyperphosphorylation is an early event in Alzheimer's disease progression. J Neurochem 103:1132-1144.

Cooke, S. F., Bliss, T. V. (2006) Plasticity in the human central nervous system. Brain 129:1659-1673.

Cousins, S. L., Hoey, S. E., Anne Stephenson, F., Perkinton, M. S. (2009) Amyloid precursor protein 695 associates with assembled NR2A- and NR2B-containing NMDA receptors to result in the enhancement of their cell surface delivery. J Neurochem 111:1501-1513.

Crouch, P. J., Blake, R., Duce, J. A., Ciccotosto, G. D., Li, Q. X., Barnham, K. J., Curtain, C. C., Cherny, R. A., Cappai, R., Dyrks, T., Masters, C. L., Trounce, I. A.

(2005) Copper-dependent inhibition of human cytochrome c oxidase by a dimeric conformer of amyloid-beta1-42. J Neurosci 25:672-679.

Crump, J. G., Zhen, M., Jin, Y., Bargmann, C. I. (2001) The SAD-1 kinase regulates presynaptic vesicle clustering and axon termination. Neuron 29:115-129.

Cruz, J. C., Tseng, H. C., Goldman, J. A., Shih, H., Tsai, L. H. (2003) Aberrant Cdk5 activation by p25 triggers pathological events leading to neurodegeneration and neurofibrillary tangles. Neuron 40:471-483.

Crystal, H., Dickson, D., Fuld, P., Masur, D., Scott, R., Mehler, M., Masdeu, J., Kawas, C., Aronson, M., Wolfson, L. (1988) Clinico-pathologic studies in dementia: nondemented subjects with pathologically confirmed Alzheimer's disease. Neurology 38:1682-1687.

Dason, J. S., Romero-Pozuelo, J., Marin, L., Iyengar, B. G., Klose, M. K., Ferrus, A., Atwood, H. L. (2009) Frequenin/NCS-1 and the Ca2+-channel {alpha}1-subunit co-regulate synaptic transmission and nerve-terminal growth. J Cell Sci 122:4109-4121.

David, D. C., Hauptmann, S., Scherping, I., Schuessel, K., Keil, U., Rizzu, P., Ravid, R., Drose, S., Brandt, U., Muller, W. E., Eckert, A., Gotz, J. (2005) Proteomic and functional analyses reveal a mitochondrial dysfunction in P301L tau transgenic mice. J Biol Chem 280:23802-23814.

Davis, D. G., Schmitt, F. A., Wekstein, D. R., Markesbery, W. R. (1999) Alzheimer neuropathologic alterations in aged cognitively normal subjects. J Neuropathol Exp Neurol 58:376-388.

Dawson, H. N., Ferreira, A., Eyster, M. V., Ghoshal, N., Binder, L. I., Vitek, M. P. (2001) Inhibition of neuronal maturation in primary hippocampal neurons from tau deficient mice. J Cell Sci 114:1179-1187.

Derkinderen, P., Scales, T. M., Hanger, D. P., Leung, K. Y., Byers, H. L., Ward, M. A., Lenz, C., Price, C., Bird, I. N., Perera, T., Kellie, S., Williamson, R., Noble, W., Van Etten, R. A., Leroy, K., Brion, J. P., Reynolds, C. H., Anderton, B. H. (2005) Tyrosine 394 is phosphorylated in Alzheimer's paired helical filament tau and in fetal tau with c-Abl as the candidate tyrosine kinase. J Neurosci 25:6584-6593.

Deshpande, A., Mina, E., Glabe, C., Busciglio, J. (2006) Different conformations of amyloid beta induce neurotoxicity by distinct mechanisms in human cortical neurons. J Neurosci 26:6011-6018.

Dietzl, G., Chen, D., Schnorrer, F., Su, K. C., Barinova, Y., Fellner, M., Gasser, B., Kinsey, K., Oppel, S., Scheiblauer, S., Couto, A., Marra, V., Keleman, K., Dickson, B. J. (2007) A genome-wide transgenic RNAi library for conditional gene inactivation in Drosophila. Nature 448:151-156.

Drewes, G., Ebneth, A., Preuss, U., Mandelkow, E. M., Mandelkow, E. (1997) MARK, a novel family of protein kinases that phosphorylate microtubule-associated proteins and trigger microtubule disruption. Cell 89:297-308.

Ebneth, A., Godemann, R., Stamer, K., Illenberger, S., Trinczek, B., Mandelkow, E. (1998) Overexpression of tau protein inhibits kinesin-dependent trafficking of vesicles, mitochondria, and endoplasmic reticulum: implications for Alzheimer's disease. J Cell Biol 143:777-794.

Eckert, A., Schulz, K. L., Rhein, V., Gotz, J. (2010) Convergence of amyloid-beta and tau pathologies on mitochondria in vivo. Mol Neurobiol 41:107-114.

Egan, D. F., Shackelford, D. B., Mihaylova, M. M., Gelino, S., Kohnz, R. A., Mair, W., Vasquez, D. S., Joshi, A., Gwinn, D. M., Taylor, R., Asara, J. M., Fitzpatrick, J., Dillin, A., Viollet, B., Kundu, M., Hansen, M., Shaw, R. J. (2011) Phosphorylation of ULK1 (hATG1) by AMP-activated protein kinase connects energy sensing to mitophagy. Science 331:456-461.

Engler, H., Forsberg, A., Almkvist, O., Blomquist, G., Larsson, E., Savitcheva, I., Wall, A., Ringheim, A., Langstrom, B., Nordberg, A. (2006) Two-year follow-up of amyloid deposition in patients with Alzheimer's disease. Brain 129:2856-2866.

Escobar-Khondiker, M., Hollerhage, M., Muriel, M. P., Champy, P., Bach, A., Depienne, C., Respondek, G., Yamada, E. S., Lannuzel, A., Yagi, T., Hirsch, E. C., Oertel, W. H., Jacob, R., Michel, P. P., Ruberg, M., Hoglinger, G. U. (2007) Annonacin, a natural mitochondrial complex I inhibitor, causes tau pathology in cultured neurons. J Neurosci 27:7827-7837.

Etcheberrigaray, R., Hirashima, N., Nee, L., Prince, J., Govoni, S., Racchi, M., Tanzi, R. E., Alkon, D. L. (1998) Calcium responses in fibroblasts from asymptomatic members of Alzheimer's disease families. Neurobiol Dis 5:37-45.

Evin, G., Zhu, A., Holsinger, R. M., Masters, C. L., Li, Q. X. (2003) Proteolytic processing of the Alzheimer's disease amyloid precursor protein in brain and platelets. J Neurosci Res 74:386-392.

Fagan, A. M., Holtzman, D. M. (2010) Cerebrospinal fluid biomarkers of Alzheimer's disease. Biomark Med 4:51-63.

Fagan, A. M., Mintun, M. A., Mach, R. H., Lee, S. Y., Dence, C. S., Shah, A. R., LaRossa, G. N., Spinner, M. L., Klunk, W. E., Mathis, C. A., DeKosky, S. T., Morris, J. C., Holtzman, D. M. (2006) Inverse relation between in vivo amyloid imaging load and cerebrospinal fluid Abeta42 in humans. Ann Neurol 59:512-519.

Farah, C. A., Perreault, S., Liazoghli, D., Desjardins, M., Anton, A., Lauzon, M., Paiement, J., Leclerc, N. (2006) Tau interacts with Golgi membranes and mediates their association with microtubules. Cell Motil Cytoskeleton 63:710-724.

Farah, C. A., Liazoghli, D., Perreault, S., Desjardins, M., Guimont, A., Anton, A., Lauzon, M., Kreibich, G., Paiement, J., Leclerc, N. (2005) Interaction of microtubule-associated protein-2 and p63: a new link between microtubules and rough endoplasmic reticulum membranes in neurons. J Biol Chem 280:9439-9449.

Ferreiro, E., Oliveira, C. R., Pereira, C. (2004) Involvement of endoplasmic reticulum Ca2+ release through ryanodine and inositol 1,4,5-triphosphate receptors

in the neurotoxic effects induced by the amyloid-beta peptide. J Neurosci Res 76:872-880.

Ferrer, I., Martinez, A., Boluda, S., Parchi, P., Barrachina, M. (2008) Brain banks: benefits, limitations and cautions concerning the use of post-mortem brain tissue for molecular studies. Cell and Tissue Banking 9:181-194.

Feuillette, S., Miguel, L., Frebourg, T., Campion, D., Lecourtois, M. (2010) Drosophila models of human tauopathies indicate that Tau protein toxicity in vivo is mediated by soluble cytosolic phosphorylated forms of the protein. J Neurochem.

Fischer, D., Mukrasch, M. D., Biernat, J., Bibow, S., Blackledge, M., Griesinger, C., Mandelkow, E., Zweckstetter, M. (2009) Conformational changes specific for pseudophosphorylation at serine 262 selectively impair binding of tau to microtubules. Biochemistry 48:10047-10055.

Fitzjohn, S. M., Morton, R. A., Kuenzi, F., Rosahl, T. W., Shearman, M., Lewis, H., Smith, D., Reynolds, D. S., Davies, C. H., Collingridge, G. L., Seabrook, G. R. (2001) Age-related impairment of synaptic transmission but normal long-term potentiation in transgenic mice that overexpress the human APP695SWE mutant form of amyloid precursor protein. J Neurosci 21:4691-4698.

Fogarty, S., Hardie, D. G. (2009) C-terminal phosphorylation of LKB1 is not required for regulation of AMP-activated protein kinase, BRSK1, BRSK2, or cell cycle arrest. J Biol Chem 284:77-84.

Frank, S., Gaume, B., Bergmann-Leitner, E. S., Leitner, W. W., Robert, E. G., Catez, F., Smith, C. L., Youle, R. J. (2001) The role of dynamin-related protein 1, a mediator of mitochondrial fission, in apoptosis. Dev Cell 1:515-525.

Freeman, M. (1996) Reiterative use of the EGF receptor triggers differentiation of all cell types in the Drosophila eye. Cell 87:651-660.

Fujimoto, T., Yurimoto, S., Hatano, N., Nozaki, N., Sueyoshi, N., Kameshita, I., Mizutani, A., Mikoshiba, K., Kobayashi, R., Tokumitsu, H. (2008) Activation of SAD Kinase by Ca(2+)/Calmodulin-Dependent Protein Kinase Kinase. Biochemistry.

Garg, S., Timm, T., Mandelkow, E. M., Mandelkow, E., Wang, Y. (2010) Cleavage of Tau by calpain in Alzheimer's disease: the quest for the toxic 17 kD fragment. Neurobiol Aging 32:1-14.

Gendron, T. F., Petrucelli, L. (2009) The role of tau in neurodegeneration. Mol Neurodegener 4:13.

Gilman, S., Koller, M., Black, R. S., Jenkins, L., Griffith, S. G., Fox, N. C., Eisner, L., Kirby, L., Rovira, M. B., Forette, F., Orgogozo, J. M. (2005) Clinical effects of Abeta immunization (AN1792) in patients with AD in an interrupted trial. Neurology 64:1553-1562.

Glenner, G. G., Wong, C. W. (1984) Alzheimer's disease: initial report of the purification and characterization of a novel cerebrovascular amyloid protein. Biochem Biophys Res Commun 120:885-890.

Goedert, M., Spillantini, M. G. (2006) A century of Alzheimer's disease. Science 314:777-781.

Goedert, M., Wischik, C. M., Crowther, R. A., Walker, J. E., Klug, A. (1988) Cloning and sequencing of the cDNA encoding a core protein of the paired helical filament of Alzheimer disease: identification as the microtubule-associated protein tau. Proc Natl Acad Sci U S A 85:4051-4055.

Gong, C. X., Liu, F., Grundke-Iqbal, I., Iqbal, K. (2005) Post-translational modifications of tau protein in Alzheimer's disease. J Neural Transm 112:813-838.

Goodman, Y., Mattson, M. P. (1994) Secreted forms of beta-amyloid precursor protein protect hippocampal neurons against amyloid beta-peptide-induced oxidative injury. Exp Neurol 128:1-12.

Gotz, J., Ittner, L. M. (2008) Animal models of Alzheimer's disease and frontotemporal dementia. Nat Rev Neurosci 9:532-544.

Grimmer, T., Riemenschneider, M., Forstl, H., Henriksen, G., Klunk, W. E., Mathis, C. A., Shiga, T., Wester, H. J., Kurz, A., Drzezga, A. (2009) Beta amyloid in Alzheimer's disease: increased deposition in brain is reflected in reduced concentration in cerebrospinal fluid. Biol Psychiatry 65:927-934.

Grober, E., Dickson, D., Sliwinski, M. J., Buschke, H., Katz, M., Crystal, H., Lipton, R. B. (1999) Memory and mental status correlates of modified Braak staging. Neurobiol Aging 20:573-579.

Grover, A., Houlden, H., Baker, M., Adamson, J., Lewis, J., Prihar, G., Pickering-Brown, S., Duff, K., Hutton, M. (1999) 5' splice site mutations in tau associated with the inherited dementia FTDP-17 affect a stem-loop structure that regulates alternative splicing of exon 10. J Biol Chem 274:15134-15143.

Grundke-Iqbal, I., Iqbal, K., Tung, Y. C., Quinlan, M., Wisniewski, H. M., Binder, L. I. (1986) Abnormal phosphorylation of the microtubule-associated protein tau (tau) in Alzheimer cytoskeletal pathology. Proc Natl Acad Sci U S A 83:4913-4917.

Gu, H., Jiang, S. A., Campusano, J. M., Iniguez, J., Su, H., Hoang, A. A., Lavian, M., Sun, X., O'Dowd, D. K. (2009) Cav2-Type Calcium Channels Encoded by cac Regulate AP-Independent Neurotransmitter Release at Cholinergic Synapses in Adult Drosophila Brain. J Neurophysiol 101:42-53.

Guillozet-Bongaarts, A. L., Cahill, M. E., Cryns, V. L., Reynolds, M. R., Berry, R. W., Binder, L. I. (2006) Pseudophosphorylation of tau at serine 422 inhibits caspase cleavage: in vitro evidence and implications for tangle formation in vivo. J Neurochem 97:1005-1014.

Guo, Q., Furukawa, K., Sopher, B. L., Pham, D. G., Xie, J., Robinson, N., Martin, G. M., Mattson, M. P. (1996) Alzheimer's PS-1 mutation perturbs calcium homeostasis and sensitizes PC12 cells to death induced by amyloid beta-peptide. Neuroreport 8:379-383.

Guo, Z., Tang, W., Yuan, J., Chen, X., Wan, B., Gu, X., Luo, K., Wang, Y., Yu, L. (2006) BRSK2 is activated by cyclic AMP-dependent protein kinase A through phosphorylation at Thr260. Biochem Biophys Res Commun 347:867-871.

Hall, G. F., Chu, B., Lee, G., Yao, J. (2000) Human tau filaments induce microtubule and synapse loss in an in vivo model of neurofibrillary degenerative disease. J Cell Sci 113 (Pt 8):1373-1387.

Hanger, D. P., Wray, S. (2010) Tau cleavage and tau aggregation in neurodegenerative disease. Biochem Soc Trans 38:1016-1020.

Hanger, D. P., Anderton, B. H., Noble, W. (2009) Tau phosphorylation: the therapeutic challenge for neurodegenerative disease. Trends Mol Med 15:112-119.

Hanger, D. P., Byers, H. L., Wray, S., Leung, K. Y., Saxton, M. J., Seereeram, A., Reynolds, C. H., Ward, M. A., Anderton, B. H. (2007) Novel phosphorylation sites in tau from Alzheimer brain support a role for casein kinase 1 in disease pathogenesis. J Biol Chem 282:23645-23654.

Harada, A., Oguchi, K., Okabe, S., Kuno, J., Terada, S., Ohshima, T., Sato-Yoshitake, R., Takei, Y., Noda, T., Hirokawa, N. (1994) Altered microtubule organization in small-calibre axons of mice lacking tau protein. Nature 369:488-491.

Hardie, D. G. (2004) The AMP-activated protein kinase pathway--new players upstream and downstream. J Cell Sci 117:5479-5487.

Hardie, D. G. (2007) AMP-activated/SNF1 protein kinases: conserved guardians of cellular energy. Nat Rev Mol Cell Biol 8:774-785.

Hardy, J. (2006) A hundred years of Alzheimer's disease research. Neuron 52:3-13.

Hardy, J., Allsop, D. (1991) Amyloid deposition as the central event in the aetiology of Alzheimer's disease. Trends Pharmacol Sci 12:383-388.

Hardy, J. A., Higgins, G. A. (1992) Alzheimer's disease: the amyloid cascade hypothesis. Science 256:184-185.

Harvan, J. R., Cotter, V. (2006) An evaluation of dementia screening in the primary care setting. J Am Acad Nurse Pract 18:351-360.

Hasegawa, M., Smith, M. J., Goedert, M. (1998) Tau proteins with FTDP-17 mutations have a reduced ability to promote microtubule assembly. FEBS Lett 437:207-210.

Hashimoto, Y., Niikura, T., Ito, Y., Nishimoto, I. (2000) Multiple Mechanisms Underlie Neurotoxicity by Different Types of Alzheimer's Disease Mutations of Amyloid Precursor Protein. Journal of Biological Chemistry 275:34541-34551.

Hawley, S. A., Boudeau, J., Reid, J. L., Mustard, K. J., Udd, L., Makela, T. P., Alessi, D. R., Hardie, D. G. (2003) Complexes between the LKB1 tumor suppressor, STRAD alpha/beta and MO25 alpha/beta are upstream kinases in the AMP-activated protein kinase cascade. J Biol 2:28.

Hawley, S. A., Pan, D. A., Mustard, K. J., Ross, L., Bain, J., Edelman, A. M., Frenguelli, B. G., Hardie, D. G. (2005) Calmodulin-dependent protein kinase kinase-beta is an alternative upstream kinase for AMP-activated protein kinase. Cell Metab 2:9-19.

Herholz, K., Carter, S. F., Jones, M. (2007) Positron emission tomography imaging in dementia. Br J Radiol 80 Spec No 2:S160-167.

Hezel, A. F., Gurumurthy, S., Granot, Z., Swisa, A., Chu, G. C., Bailey, G., Dor, Y., Bardeesy, N., Depinho, R. A. (2008) Pancreatic lkb1 deletion leads to acinar polarity defects and cystic neoplasms. Mol Cell Biol 28:2414-2425.

Hirai, K., Aliev, G., Nunomura, A., Fujioka, H., Russell, R. L., Atwood, C. S., Johnson, A. B., Kress, Y., Vinters, H. V., Tabaton, M., Shimohama, S., Cash, A. D., Siedlak, S. L., Harris, P. L., Jones, P. K., Petersen, R. B., Perry, G., Smith, M. A. (2001) Mitochondrial abnormalities in Alzheimer's disease. J Neurosci 21:3017-3023.

Hock, C., Konietzko, U., Streffer, J. R., Tracy, J., Signorell, A., Muller-Tillmanns, B., Lemke, U., Henke, K., Moritz, E., Garcia, E., Wollmer, M. A., Umbricht, D., de Quervain, D. J., Hofmann, M., Maddalena, A., Papassotiropoulos, A., Nitsch, R. M. (2003) Antibodies against beta-amyloid slow cognitive decline in Alzheimer's disease. Neuron 38:547-554.

Hua, H., Georgiev, O., Schaffner, W., Steiger, D. (2010) Human copper transporter Ctr1 is functional in Drosophila, revealing a high degree of conservation between mammals and insects. J Biol Inorg Chem 15:107-113.

Hung, W., Hwang, C., Po, M. D., Zhen, M. (2007) Neuronal polarity is regulated by a direct interaction between a scaffolding protein, Neurabin, and a presynaptic SAD-1 kinase in Caenorhabditis elegans. Development 134:237-249.

Hurov, J., Piwnica-Worms, H. (2007) The Par-1/MARK family of protein kinases: from polarity to metabolism. Cell Cycle 6:1966-1969.

Iijima-Ando, K., Zhao, L., Gatt, A., Shenton, C., Iijima, K. (2010) A DNA damage-activated checkpoint kinase phosphorylates tau and enhances tau-induced neurodegeneration. Hum Mol Genet.

Ikonomovic, M. D., Uryu, K., Abrahamson, E. E., Ciallella, J. R., Trojanowski, J. Q., Lee, V. M., Clark, R. S., Marion, D. W., Wisniewski, S. R., DeKosky, S. T. (2004) Alzheimer's pathology in human temporal cortex surgically excised after severe brain injury. Exp Neurol 190:192-203.

Inoue, E., Mochida, S., Takagi, H., Higa, S., Deguchi-Tawarada, M., Takao-Rikitsu, E., Inoue, M., Yao, I., Takeuchi, K., Kitajima, I., Setou, M., Ohtsuka, T., Takai, Y. (2006) SAD: a presynaptic kinase associated with synaptic vesicles and the active zone cytomatrix that regulates neurotransmitter release. Neuron 50:261-275.

Iqbal, K., Alonso Adel, C., Chen, S., Chohan, M. O., El-Akkad, E., Gong, C. X., Khatoon, S., Li, B., Liu, F., Rahman, A., Tanimukai, H., Grundke-Iqbal, I. (2005) Tau pathology in Alzheimer disease and other tauopathies. Biochim Biophys Acta 1739:198-210.

Isaacs, A. M., Senn, D. B., Yuan, M., Shine, J. P., Yankner, B. A. (2006) Acceleration of amyloid beta-peptide aggregation by physiological concentrations of calcium. J Biol Chem 281:27916-27923.

Ishiguro, K., Shiratsuchi, A., Sato, S., Omori, A., Arioka, M., Kobayashi, S., Uchida, T., Imahori, K. (1993) Glycogen synthase kinase 3 beta is identical to tau protein kinase I generating several epitopes of paired helical filaments. FEBS Lett 325:167-172.

Ito, E., Oka, K., Etcheberrigaray, R., Nelson, T. J., McPhie, D. L., Tofel-Grehl, B., Gibson, G. E., Alkon, D. L. (1994) Internal Ca2+ mobilization is altered in fibroblasts from patients with Alzheimer disease. Proc Natl Acad Sci U S A 91:534-538.

Itoh, N., Arai, H., Urakami, K., Ishiguro, K., Ohno, H., Hampel, H., Buerger, K., Wiltfang, J., Otto, M., Kretzschmar, H., Moeller, H. J., Imagawa, M., Kohno, H., Nakashima, K., Kuzuhara, S., Sasaki, H., Imahori, K. (2001) Large-scale, multicenter study of cerebrospinal fluid tau protein phosphorylated at serine 199 for the antemortem diagnosis of Alzheimer's disease. Ann Neurol 50:150-156.

Iwatsubo, T. (2004) The gamma-secretase complex: machinery for intramembrane proteolysis. Curr Opin Neurobiol 14:379-383.

Jacobsen, J. S. (2002) Alzheimer's disease: an overview of current and emerging therapeutic strategies. Curr Top Med Chem 2:343-352.

Jacobsen, J. S., Wu, C. C., Redwine, J. M., Comery, T. A., Arias, R., Bowlby, M., Martone, R., Morrison, J. H., Pangalos, M. N., Reinhart, P. H., Bloom, F. E. (2006) Early-onset behavioral and synaptic deficits in a mouse model of Alzheimer's disease. Proc Natl Acad Sci U S A 103:5161-5166.

Jeganathan, S., von Bergen, M., Mandelkow, E. M., Mandelkow, E. (2008a) The natively unfolded character of tau and its aggregation to Alzheimer-like paired helical filaments. Biochemistry 47:10526-10539.

Jeganathan, S., Hascher, A., Chinnathambi, S., Biernat, J., Mandelkow, E. M., Mandelkow, E. (2008b) Proline-directed pseudo-phosphorylation at AT8 and PHF1 epitopes induces a compaction of the paperclip folding of Tau and generates a pathological (MC-1) conformation. J Biol Chem 283:32066-32076.

Jobst, K. A., Smith, A. D., Szatmari, M., Esiri, M. M., Jaskowski, A., Hindley, N., McDonald, B., Molyneux, A. J. (1994) Rapidly progressing atrophy of medial temporal lobe in Alzheimer's disease. Lancet 343:829-830.

Jobst, K. A., Smith, A. D., Szatmari, M., Molyneux, A., Esiri, M. E., King, E., Smith, A., Jaskowski, A., McDonald, B., Wald, N. (1992) Detection in life of confirmed Alzheimer's disease using a simple measurement of medial temporal lobe atrophy by computed tomography. Lancet 340:1179-1183.

Jolas, T., Zhang, X. S., Zhang, Q., Wong, G., Del Vecchio, R., Gold, L., Priestley, T. (2002) Long-term potentiation is increased in the CA1 area of the hippocampus of APP(swe/ind) CRND8 mice. Neurobiol Dis 11:394-409.

Katoh, Y., Takemori, H., Horike, N., Doi, J., Muraoka, M., Min, L., Okamoto, M. (2004) Salt-inducible kinase (SIK) isoforms: their involvement in steroidogenesis and adipogenesis. Mol Cell Endocrinol 217:109-112.

Kawahara, M., Kuroda, Y. (2000) Molecular mechanism of neurodegeneration induced by Alzheimer's beta-amyloid protein: channel formation and disruption of calcium homeostasis. Brain Res Bull 53:389-397.

Kemphues, K. J., Priess, J. R., Morton, D. G., Cheng, N. S. (1988) Identification of genes required for cytoplasmic localization in early C. elegans embryos. Cell 52:311-320.

Kerokoski, P., Suuronen, T., Salminen, A., Soininen, H., Pirttila, T. (2002) Cleavage of the cyclin-dependent kinase 5 activator p35 to p25 does not induce tau hyperphosphorylation. Biochem Biophys Res Commun 298:693-698.

Khachaturian, Z. S. (1987) Hypothesis on the regulation of cytosol calcium concentration and the aging brain. Neurobiol Aging 8:345-346.

Kickstein, E., Krauss, S., Thornhill, P., Rutschow, D., Zeller, R., Sharkey, J., Williamson, R., Fuchs, M., Kohler, A., Glossmann, H., Schneider, R., Sutherland, C., Schweiger, S. (2010) Biguanide metformin acts on tau phosphorylation via mTOR/protein phosphatase 2A (PP2A) signaling. Proc Natl Acad Sci U S A.

Kim, J. S., Lilley, B. N., Zhang, C., Shokat, K. M., Sanes, J. R., Zhen, M. (2008) A chemical-genetic strategy reveals distinct temporal requirements for SAD-1 kinase in neuronal polarization and synapse formation. Neural Develop 3:23.

Kinoshita, A., Fukumoto, H., Shah, T., Whelan, C. M., Irizarry, M. C., Hyman, B. T. (2003) Demonstration by FRET of BACE interaction with the amyloid precursor protein at the cell surface and in early endosomes. J Cell Sci 116:3339-3346.

Kinoshita, E., Kinoshita-Kikuta, E., Takiyama, K., Koike, T. (2006) Phosphate-binding tag, a new tool to visualize phosphorylated proteins. Mol Cell Proteomics 5:749-757.

Kishi, M., Pan, Y. A., Crump, J. G., Sanes, J. R. (2005) Mammalian SAD kinases are required for neuronal polarization. Science 307:929-932.

Knapp, M., Prince, M., Albanese, E., Banerjee, S., Dhanasiri, S., Fernandez, J. L., Ferri, C., McCrone, P., Stewart, R. (2007) Dementia UK. In. London: Alzheimer's society.

Kopke, E., Tung, Y. C., Shaikh, S., Alonso, A. C., Iqbal, K., Grundke-Iqbal, I. (1993) Microtubule-associated protein tau. Abnormal phosphorylation of a non-paired helical filament pool in Alzheimer disease. J Biol Chem 268:24374-24384.

Kosik, K. S., Joachim, C. L., Selkoe, D. J. (1986) Microtubule-associated protein tau (tau) is a major antigenic component of paired helical filaments in Alzheimer disease. Proc Natl Acad Sci U S A 83:4044-4048.

Kosuga, S., Tashiro, E., Kajioka, T., Ueki, M., Shimizu, Y., Imoto, M. (2005) GSK-3Î² Directly Phosphorylates and Activates MARK2/PAR-1. Journal of Biological Chemistry 280:42715-42722.

Kramer, J. M., Staveley, B. E. (2003) GAL4 causes developmental defects and apoptosis when expressed in the developing eye of Drosophila melanogaster. Genet Mol Res 2:43-47.

Kroner, Z. (2009) The relationship between Alzheimer's disease and diabetes: Type 3 diabetes? Altern Med Rev 14:373-379.

Ksiezak-Reding, H., Liu, W. K., Yen, S. H. (1992) Phosphate analysis and dephosphorylation of modified tau associated with paired helical filaments. Brain Res 597:209-219.

Kumar-Singh, S., Theuns, J., Van Broeck, B., Pirici, D., Vennekens, K., Corsmit, E., Cruts, M., Dermaut, B., Wang, R., Van Broeckhoven, C. (2006) Mean age-of-onset of familial alzheimer disease caused by presenilin mutations correlates with both increased Abeta42 and decreased Abeta40. Hum Mutat 27:686-695.

Kusakawa, G., Saito, T., Onuki, R., Ishiguro, K., Kishimoto, T., Hisanaga, S. (2000) Calpain-dependent proteolytic cleavage of the p35 cyclin-dependent kinase 5 activator to p25. J Biol Chem 275:17166-17172.

Lace, G. L., Wharton, S. B., Ince, P. G. (2007) A brief history of tau: the evolving view of the microtubule-associated protein tau in neurodegenerative diseases. Clin Neuropathol 26:43-58.

LaFerla, F. M. (2002) Calcium dyshomeostasis and intracellular signalling in Alzheimer's disease. Nat Rev Neurosci 3:862-872.

Lebouvier, T., Scales, T. M., Hanger, D. P., Geahlen, R. L., Lardeux, B., Reynolds, C. H., Anderton, B. H., Derkinderen, P. (2008) The microtubule-associated protein tau is phosphorylated by Syk. Biochim Biophys Acta 1783:188-192.

Lee, G., Newman, S. T., Gard, D. L., Band, H., Panchamoorthy, G. (1998) Tau interacts with src-family non-receptor tyrosine kinases. J Cell Sci 111 (Pt 21):3167-3177.

Lee, G., Thangavel, R., Sharma, V. M., Litersky, J. M., Bhaskar, K., Fang, S. M., Do, L. H., Andreadis, A., Van Hoesen, G., Ksiezak-Reding, H. (2004) Phosphorylation of tau by fyn: implications for Alzheimer's disease. J Neurosci 24:2304-2312.

Lee, J. H., Koh, H., Kim, M., Kim, Y., Lee, S. Y., Karess, R. E., Lee, S. H., Shong, M., Kim, J. M., Kim, J., Chung, J. (2007) Energy-dependent regulation of cell structure by AMP-activated protein kinase. Nature 447:1017-1020.

Lee, M., Bard, F., Johnson-Wood, K., Lee, C., Hu, K., Griffith, S. G., Black, R. S., Schenk, D., Seubert, P. (2005) Abeta42 immunization in Alzheimer's disease generates Abeta N-terminal antibodies. Ann Neurol 58:430-435.

Lee, M. S., Kwon, Y. T., Li, M., Peng, J., Friedlander, R. M., Tsai, L. H. (2000) Neurotoxicity induces cleavage of p35 to p25 by calpain. Nature 405:360-364.

Legembre, P., Schickel, R., Barnhart, B. C., Peter, M. E. (2004) Identification of SNF1/AMP kinase-related kinase as an NF-kappaB-regulated anti-apoptotic kinase involved in CD95-induced motility and invasiveness. J Biol Chem 279:46742-46747.

Leissring, M. A., Parker, I., LaFerla, F. M. (1999a) Presenilin-2 mutations modulate amplitude and kinetics of inositol 1, 4,5-trisphosphate-mediated calcium signals. J Biol Chem 274:32535-32538.

Leissring, M. A., Paul, B. A., Parker, I., Cotman, C. W., LaFerla, F. M. (1999b) Alzheimer's presenilin-1 mutation potentiates inositol 1,4,5-trisphosphate-mediated calcium signaling in Xenopus oocytes. J Neurochem 72:1061-1068.

Leissring, M. A., Akbari, Y., Fanger, C. M., Cahalan, M. D., Mattson, M. P., LaFerla, F. M. (2000) Capacitative calcium entry deficits and elevated luminal calcium content in mutant presenilin-1 knockin mice. J Cell Biol 149:793-798.

Leissring, M. A., Murphy, M. P., Mead, T. R., Akbari, Y., Sugarman, M. C., Jannatipour, M., Anliker, B., Muller, U., Saftig, P., De Strooper, B., Wolfe, M. S., Golde, T. E., LaFerla, F. M. (2002) A physiologic signaling role for the gamma -secretase-derived intracellular fragment of APP. Proc Natl Acad Sci U S A 99:4697-4702.

Lemere, C. A., Masliah, E. (2010) Can Alzheimer disease be prevented by amyloid-beta immunotherapy? Nat Rev Neurol 6:108-119.

Liang, Z., Liu, F., Grundke-Iqbal, I., Iqbal, K., Gong, C. X. (2007) Down-regulation of cAMP-dependent protein kinase by over-activated calpain in Alzheimer disease brain. Journal of Neurochemistry 103:2462-2470.

Lindwall, G., Cole, R. D. (1984) Phosphorylation affects the ability of tau protein to promote microtubule assembly. J Biol Chem 259:5301-5305.

Litersky, J. M., Johnson, G. V., Jakes, R., Goedert, M., Lee, M., Seubert, P. (1996) Tau protein is phosphorylated by cyclic AMP-dependent protein kinase and calcium/calmodulin-dependent protein kinase II within its microtubule-binding domains at Ser-262 and Ser-356. Biochem J 316 (Pt 2):655-660.

Liu, F., Grundke-Iqbal, I., Iqbal, K., Gong, C. X. (2005a) Contributions of protein phosphatases PP1, PP2A, PP2B and PP5 to the regulation of tau phosphorylation. Eur J Neurosci 22:1942-1950.

Liu, F., Iqbal, K., Grundke-Iqbal, I., Hart, G. W., Gong, C. X. (2004) O-GlcNAcylation regulates phosphorylation of tau: a mechanism involved in Alzheimer's disease. Proc Natl Acad Sci U S A 101:10804-10809.

Liu, F., Zaidi, T., Iqbal, K., Grundke-Iqbal, I., Merkle, R. K., Gong, C. X. (2002) Role of glycosylation in hyperphosphorylation of tau in Alzheimer's disease. FEBS Lett 512:101-106.

Liu, F., Grundke-Iqbal, I., Iqbal, K., Oda, Y., Tomizawa, K., Gong, C.-X. (2005b) Truncation and Activation of Calcineurin A by Calpain I in Alzheimer Disease Brain. Journal of Biological Chemistry 280:37755-37762.

Liu, F., Shi, J., Tanimukai, H., Gu, J., Grundke-Iqbal, I., Iqbal, K., Gong, C. X. (2009) Reduced O-GlcNAcylation links lower brain glucose metabolism and tau pathology in Alzheimer's disease. Brain 132:1820-1832.

Liu, Z., Wang, X., Yu, Y., Li, X., Wang, T., Jiang, H., Ren, Q., Jiao, Y., Sawa, A., Moran, T., Ross, C. A., Montell, C., Smith, W. W. (2008) A Drosophila model for LRRK2-linked parkinsonism. Proc Natl Acad Sci U S A 105:2693-2698.

Lizcano, J. M., Goransson, O., Toth, R., Deak, M., Morrice, N. A., Boudeau, J., Hawley, S. A., Udd, L., Makela, T. P., Hardie, D. G., Alessi, D. R. (2004) LKB1 is a master kinase that activates 13 kinases of the AMPK subfamily, including MARK/PAR-1. Embo J 23:833-843.

Lovell, M. A., Markesbery, W. R. (2007) Oxidative DNA damage in mild cognitive impairment and late-stage Alzheimer's disease. Nucleic Acids Research 35:7497-7504.

Lovestone, S., Hartley, C. L., Pearce, J., Anderton, B. H. (1996) Phosphorylation of tau by glycogen synthase kinase-3 beta in intact mammalian cells: the effects on the organization and stability of microtubules. Neuroscience 73:1145-1157.

Lu, R., Niida, H., Nakanishi, M. (2004) Human SAD1 kinase is involved in UV-induced DNA damage checkpoint function. J Biol Chem 279:31164-31170.

Luengo-Fernandez, R., Leal, J., Gray, A. (2010) Dementia 2010. In. Oxford: Alzheimer's Research Trust.

Lye, T. C., Shores, E. A. (2000) Traumatic brain injury as a risk factor for Alzheimer's disease: a review. Neuropsychol Rev 10:115-129.

Ma, Q. H., Futagawa, T., Yang, W. L., Jiang, X. D., Zeng, L., Takeda, Y., Xu, R. X., Bagnard, D., Schachner, M., Furley, A. J., Karagogeos, D., Watanabe, K., Dawe, G. S., Xiao, Z. C. (2008) A TAG1-APP signalling pathway through Fe65 negatively modulates neurogenesis. Nat Cell Biol 10:283-294.

Makrides, V., Massie, M. R., Feinstein, S. C., Lew, J. (2004) Evidence for two distinct binding sites for tau on microtubules. Proc Natl Acad Sci U S A 101:6746-6751.

Mandelkow, E., von Bergen, M., Biernat, J., Mandelkow, E. M. (2007) Structural principles of tau and the paired helical filaments of Alzheimer's disease. Brain Pathol 17:83-90.

Mandelkow, E. M., Stamer, K., Vogel, R., Thies, E., Mandelkow, E. (2003) Clogging of axons by tau, inhibition of axonal traffic and starvation of synapses. Neurobiol Aging 24:1079-1085.

Mandelkow, E. M., Thies, E., Trinczek, B., Biernat, J., Mandelkow, E. (2004) MARK/PAR1 kinase is a regulator of microtubule-dependent transport in axons. J Cell Biol 167:99-110.

Mandell, J. W., Banker, G. A. (1996) A spatial gradient of tau protein phosphorylation in nascent axons. J Neurosci 16:5727-5740.

Maniatis, T., Fritsch, E. F., Sambrook, J. (1982) Molecular Cloning, a laboratory approach: Cold Spring Harbor Laboratory Press.

Marsh, J. L., Pallos, J., Thompson, L. M. (2003) Fly models of Huntington's disease. Hum Mol Genet 12 Spec No 2:R187-193.

Marx, J. (2007) Alzheimer's disease. A new take on tau. Science 316:1416-1417.

Masliah, E., Mallory, M., Hansen, L., DeTeresa, R., Alford, M., Terry, R. (1994) Synaptic and neuritic alterations during the progression of Alzheimer's disease. Neurosci Lett 174:67-72.

Masters, C. L., Simms, G., Weinman, N. A., Multhaup, G., McDonald, B. L., Beyreuther, K. (1985) Amyloid plaque core protein in Alzheimer disease and Down syndrome. Proc Natl Acad Sci U S A 82:4245-4249.

Mattson, M. P. (2007) Calcium and neurodegeneration. Aging Cell 6:337-350.

Mattson, M. P., Barger, S. W., Cheng, B., Lieberburg, I., Smith-Swintosky, V. L., Rydel, R. E. (1993) beta-Amyloid precursor protein metabolites and loss of neuronal Ca2+ homeostasis in Alzheimer's disease. Trends Neurosci 16:409-414.

Mattsson, N. et al. (2009) CSF biomarkers and incipient Alzheimer disease in patients with mild cognitive impairment. JAMA 302:385-393.

McGuire, S. E., Le, P. T., Osborn, A. J., Matsumoto, K., Davis, R. L. (2003) Spatiotemporal rescue of memory dysfunction in Drosophila. Science 302:1765-1768.

Mi, K., Johnson, G. V. (2006) The role of tau phosphorylation in the pathogenesis of Alzheimer's disease. Curr Alzheimer Res 3:449-463.

Mizuguchi, M., Ikeda, K., Kim, S. U. (1992) Differential distribution of cellular forms of beta-amyloid precursor protein in murine glial cell cultures. Brain Res 584:219-225.

Morfini, G., Szebenyi, G., Brown, H., Pant, H. C., Pigino, G., DeBoer, S., Beffert, U., Brady, S. T. (2004) A novel CDK5-dependent pathway for regulating GSK3 activity and kinesin-driven motility in neurons. EMBO J 23:2235-2245.

Morfini, G. A., Burns, M., Binder, L. I., Kanaan, N. M., LaPointe, N., Bosco, D. A., Brown, R. H., Jr., Brown, H., Tiwari, A., Hayward, L., Edgar, J., Nave, K. A., Garberrn, J., Atagi, Y., Song, Y., Pigino, G., Brady, S. T. (2009) Axonal transport defects in neurodegenerative diseases. J Neurosci 29:12776-12786.

Mucke, L., Masliah, E., Yu, G. Q., Mallory, M., Rockenstein, E. M., Tatsuno, G., Hu, K., Kholodenko, D., Johnson-Wood, K., McConlogue, L. (2000) High-level neuronal expression of abeta 1-42 in wild-type human amyloid protein precursor transgenic mice: synaptotoxicity without plaque formation. J Neurosci 20:4050-4058.

Nagy, Z., Jobst, K. A., Esiri, M. M., Morris, J. H., King, E. M., MacDonald, B., Litchfield, S., Barnetson, L., Smith, A. D. (1996) Hippocampal pathology reflects memory deficit and brain imaging measurements in Alzheimer's disease: clinicopathologic correlations using three sets of pathologic diagnostic criteria. Dementia 7:76-81.

Naslund, J., Schierhorn, A., Hellman, U., Lannfelt, L., Roses, A. D., Tjernberg, L. O., Silberring, J., Gandy, S. E., Winblad, B., Greengard, P., et al. (1994) Relative abundance of Alzheimer A beta amyloid peptide variants in Alzheimer disease and normal aging. Proc Natl Acad Sci U S A 91:8378-8382.

Nelson, P. T., Braak, H., Markesbery, W. R. (2009) Neuropathology and cognitive impairment in Alzheimer disease: a complex but coherent relationship. J Neuropathol Exp Neurol 68:1-14.

Nicholson, L., Singh, G. K., Osterwalder, T., Roman, G. W., Davis, R. L., Keshishian, H. (2008) Spatial and temporal control of gene expression in Drosophila using the inducible GeneSwitch GAL4 system. I. Screen for larval nervous system drivers. Genetics 178:215-234.

Nishimura, I., Yang, Y., Lu, B. (2004) PAR-1 kinase plays an initiator role in a temporally ordered phosphorylation process that confers tau toxicity in Drosophila. Cell 116:671-682.

Orgogozo, J. M., Gilman, S., Dartigues, J. F., Laurent, B., Puel, M., Kirby, L. C., Jouanny, P., Dubois, B., Eisner, L., Flitman, S., Michel, B. F., Boada, M., Frank, A., Hock, C. (2003) Subacute meningoencephalitis in a subset of patients with AD after Abeta42 immunization. Neurology 61:46-54.

Ost, M., Nylen, K., Csajbok, L., Ohrfelt, A. O., Tullberg, M., Wikkelso, C., Nellgard, P., Rosengren, L., Blennow, K., Nellgard, B. (2006) Initial CSF total tau correlates with 1-year outcome in patients with traumatic brain injury. Neurology 67:1600-1604.

Osterwalder, T., Yoon, K. S., White, B. H., Keshishian, H. (2001) A conditional tissue-specific transgene expression system using inducible GAL4. Proc Natl Acad Sci U S A 98:12596-12601.

Otvos, L., Jr., Feiner, L., Lang, E., Szendrei, G. I., Goedert, M., Lee, V. M. (1994) Monoclonal antibody PHF-1 recognizes tau protein phosphorylated at serine residues 396 and 404. J Neurosci Res 39:669-673.

Park, S. Y., Ferreira, A. (2005) The generation of a 17 kDa neurotoxic fragment: an alternative mechanism by which tau mediates beta-amyloid-induced neurodegeneration. J Neurosci 25:5365-5375.

Patrick, G. N., Zukerberg, L., Nikolic, M., de la Monte, S., Dikkes, P., Tsai, L. H. (1999) Conversion of p35 to p25 deregulates Cdk5 activity and promotes neurodegeneration. Nature 402:615-622.

Pei, J. J., Tanaka, T., Tung, Y. C., Braak, E., Iqbal, K., Grundke-Iqbal, I. (1997) Distribution, levels, and activity of glycogen synthase kinase-3 in the Alzheimer disease brain. J Neuropathol Exp Neurol 56:70-78.

Pei, J. J., Gong, C. X., Iqbal, K., Grundke-Iqbal, I., Wu, Q. L., Winblad, B., Cowburn, R. F. (1998) Subcellular distribution of protein phosphatases and abnormally phosphorylated tau in the temporal cortex from Alzheimer's disease and control brains. J Neural Transm 105:69-83.

Pierrot, N., Ghisdal, P., Caumont, A. S., Octave, J. N. (2004) Intraneuronal amyloid-beta1-42 production triggered by sustained increase of cytosolic calcium concentration induces neuronal death. J Neurochem 88:1140-1150.

Pierrot, N., Santos, S. F., Feyt, C., Morel, M., Brion, J. P., Octave, J. N. (2006) Calcium-mediated transient phosphorylation of tau and amyloid precursor protein followed by intraneuronal amyloid-beta accumulation. J Biol Chem 281:39907-39914.

Plassman, B. L., Havlik, R. J., Steffens, D. C., Helms, M. J., Newman, T. N., Drosdick, D., Phillips, C., Gau, B. A., Welsh-Bohmer, K. A., Burke, J. R., Guralnik, J. M., Breitner, J. C. (2000) Documented head injury in early adulthood and risk of Alzheimer's disease and other dementias. Neurology 55:1158-1166.

Polydoro, M., Acker, C. M., Duff, K., Castillo, P. E., Davies, P. (2009) Age-dependent impairment of cognitive and synaptic function in the htau mouse model of tau pathology. J Neurosci 29:10741-10749.

Pooler, A. M., Hanger, D. P. (2010) Functional implications of the association of tau with the plasma membrane. Biochem Soc Trans 38:1012-1015.

Querfurth, H. W., Selkoe, D. J. (1994) Calcium ionophore increases amyloid beta peptide production by cultured cells. Biochemistry 33:4550-4561.

Quintanilla, R. A., Matthews-Roberson, T. A., Dolan, P. J., Johnson, G. V. (2009) Caspase-cleaved tau expression induces mitochondrial dysfunction in immortalized cortical neurons: implications for the pathogenesis of Alzheimer disease. J Biol Chem 284:18754-18766.

Rahman, A., Grundke-Iqbal, I., Iqbal, K. (2006) PP2B isolated from human brain preferentially dephosphorylates Ser-262 and Ser-396 of the Alzheimer disease abnormally hyperphosphorylated tau. J Neural Transm 113:219-230.

Randall, A. D., Witton, J., Booth, C., Hynes-Allen, A., Brown, J. T. (2010) The functional neurophysiology of the amyloid precursor protein (APP) processing pathway. Neuropharmacology 59:243-267.

Raskind, M. A., Peskind, E. R., Wessel, T., Yuan, W. (2000) Galantamine in AD: A 6-month randomized, placebo-controlled trial with a 6-month extension. The Galantamine USA-1 Study Group. Neurology 54:2261-2268.

Ratnaparkhi, A., Lawless, G. M., Schweizer, F. E., Golshani, P., Jackson, G. R. (2008) A Drosophila model of ALS: human ALS-associated mutation in VAP33A suggests a dominant negative mechanism. PLoS One 3:e2334.

Reisberg, B., Doody, R., StÃ¶ffler, A., Schmitt, F., Ferris, S., MÃ¶bius, H. J. r. (2003) Memantine in Moderate-to-Severe Alzheimer's Disease. New England Journal of Medicine 348:1333-1341.

Reynolds, C. H., Garwood, C. J., Wray, S., Price, C., Kellie, S., Perera, T., Zvelebil, M., Yang, A., Sheppard, P. W., Varndell, I. M., Hanger, D. P., Anderton, B. H. (2008) Phosphorylation regulates tau interactions with Src homology 3 domains of phosphatidylinositol 3-kinase, phospholipase Cgamma1, Grb2, and Src family kinases. J Biol Chem 283:18177-18186.

Rhein, V., Eckert, A. (2007) Effects of Alzheimer's amyloid-beta and tau protein on mitochondrial function -- role of glucose metabolism and insulin signalling. Arch Physiol Biochem 113:131-141.

Rhein, V., Song, X., Wiesner, A., Ittner, L. M., Baysang, G., Meier, F., Ozmen, L., Bluethmann, H., Drose, S., Brandt, U., Savaskan, E., Czech, C., Gotz, J., Eckert, A. (2009) Amyloid-beta and tau synergistically impair the oxidative phosphorylation system in triple transgenic Alzheimer's disease mice. Proc Natl Acad Sci U S A 106:20057-20062.

Robakis, N. K. (2010a) Mechanisms of AD neurodegeneration may be independent of Abeta and its derivatives. Neurobiol Aging 32:372-379.

Robakis, N. K. (2010b) Are Abeta and its derivatives causative agents or innocent bystanders in AD? Neurodegener Dis 7:32-37.

Rogers, S. L., Doody, R. S., Pratt, R. D., Ieni, J. R. (2000) Long-term efficacy and safety of donepezil in the treatment of Alzheimer's disease: final analysis of a US multicentre open-label study. Eur Neuropsychopharmacol 10:195-203.

Rosler, M., Anand, R., Cicin-Sain, A., Gauthier, S., Agid, Y., Dal-Bianco, P., Stahelin, H. B., Hartman, R., Gharabawi, M. (1999) Efficacy and safety of rivastigmine in patients with Alzheimer's disease: international randomised controlled trial. BMJ 318:633-638.

Ryder, E. et al. (2007) The DrosDel Deletion Collection: A Drosophila Genomewide Chromosomal Deficiency Resource. Genetics 177:615-629.

Sabater, L., Gomez-Choco, M., Saiz, A., Graus, F. (2005) BR serine/threonine kinase 2: a new autoantigen in paraneoplastic limbic encephalitis. J Neuroimmunol 170:186-190.

Sabbagh, M. N. (2009) Drug development for Alzheimer's disease: where are we now and where are we headed? Am J Geriatr Pharmacother 7:167-185.

Sakamoto, K., Goransson, O., Hardie, D. G., Alessi, D. R. (2004) Activity of LKB1 and AMPK-related kinases in skeletal muscle: effects of contraction, phenformin, and AICAR. Am J Physiol Endocrinol Metab 287:E310-317.

Sang, T. K., Jackson, G. R. (2005) Drosophila models of neurodegenerative disease. NeuroRx 2:438-446.

Selkoe, D. J. (1991) The molecular pathology of Alzheimer's disease. Neuron 6:487-498.

Selkoe, D. J. (1999) Translating cell biology into therapeutic advances in Alzheimer's disease. Nature 399:A23-31.

Selkoe, D. J. (2002) Alzheimer's disease is a synaptic failure. Science 298:789-791.

Selkoe, D. J. (2004) Alzheimer disease: mechanistic understanding predicts novel therapies. Ann Intern Med 140:627-638.

Sengupta, A., Kabat, J., Novak, M., Wu, Q., Grundke-Iqbal, I., Iqbal, K. (1998) Phosphorylation of tau at both Thr 231 and Ser 262 is required for maximal inhibition of its binding to microtubules. Arch Biochem Biophys 357:299-309.

Sergeant, N., Wattez, A., Delacourte, A. (1999) Neurofibrillary degeneration in progressive supranuclear palsy and corticobasal degeneration: tau pathologies with exclusively "exon 10" isoforms. J Neurochem 72:1243-1249.

Sergeant, N., David, J. P., Lefranc, D., Vermersch, P., Wattez, A., Delacourte, A. (1997) Different distribution of phosphorylated tau protein isoforms in Alzheimer's and Pick's diseases. FEBS Lett 412:578-582.

Sheehan, J. P., Swerdlow, R. H., Miller, S. W., Davis, R. E., Parks, J. K., Parker, W. D., Tuttle, J. B. (1997) Calcium homeostasis and reactive oxygen species production in cells transformed by mitochondria from individuals with sporadic Alzheimer's disease. J Neurosci 17:4612-4622.

Shelly, M., Cancedda, L., Heilshorn, S., Sumbre, G., Poo, M. M. (2007) LKB1/STRAD promotes axon initiation during neuronal polarization. Cell 129:565-577.

Shulman, J. M., Feany, M. B. (2003) Genetic modifiers of tauopathy in Drosophila. Genetics 165:1233-1242.

Small, G. W., Kepe, V., Ercoli, L. M., Siddarth, P., Bookheimer, S. Y., Miller, K. J., Lavretsky, H., Burggren, A. C., Cole, G. M., Vinters, H. V., Thompson, P. M., Huang, S. C., Satyamurthy, N., Phelps, M. E., Barrio, J. R. (2006) PET of brain amyloid and tau in mild cognitive impairment. N Engl J Med 355:2652-2663.

Small, S. A. (2003) Measuring correlates of brain metabolism with high-resolution MRI: a promising approach for diagnosing Alzheimer disease and mapping its course. Alzheimer Dis Assoc Disord 17:154-161.

Smith, A. D., Jobst, K. A. (1996) Use of structural imaging to study the progression of Alzheimer's disease. Br Med Bull 52:575-586.

Smith, C., Graham, D. I., Murray, L. S., Nicoll, J. A. (2003) Tau immunohistochemistry in acute brain injury. Neuropathol Appl Neurobiol 29:496-502.

Sofola, O., Kerr, F., Rogers, I., Killick, R., Augustin, H., Gandy, C., Allen, M. J., Hardy, J., Lovestone, S., Partridge, L. (2010) Inhibition of GSK-3 ameliorates Abeta pathology in an adult-onset Drosophila model of Alzheimer's disease. PLoS Genet 6.

Sokoloff, L. (1977) Relation between physiological function and energy metabolism in the central nervous system. J Neurochem 29:13-26.

Spittaels, K., Van den Haute, C., Van Dorpe, J., Geerts, H., Mercken, M., Bruynseels, K., Lasrado, R., Vandezande, K., Laenen, I., Boon, T., Van Lint, J., Vandenheede, J., Moechars, D., Loos, R., Van Leuven, F. (2000) Glycogen synthase kinase-3beta phosphorylates protein tau and rescues the axonopathy in the central nervous system of human four-repeat tau transgenic mice. J Biol Chem 275:41340-41349.

St Johnston, D. (2002) The art and design of genetic screens: *Drosophila melanogaster*. Nat Rev Genet 3:176-188.

Stamer, K., Vogel, R., Thies, E., Mandelkow, E., Mandelkow, E. M. (2002) Tau blocks traffic of organelles, neurofilaments, and APP vesicles in neurons and enhances oxidative stress. J Cell Biol 156:1051-1063.

Steinhilb, M. L., Dias-Santagata, D., Fulga, T. A., Felch, D. L., Feany, M. B. (2007a) Tau phosphorylation sites work in concert to promote neurotoxicity in vivo. Mol Biol Cell 18:5060-5068.

Steinhilb, M. L., Dias-Santagata, D., Mulkearns, E. E., Shulman, J. M., Biernat, J., Mandelkow, E. M., Feany, M. B. (2007b) S/P and T/P phosphorylation is critical for tau neurotoxicity in Drosophila. J Neurosci Res 85:1271-1278.

Stracker, T. H., Usui, T., Petrini, J. H. J. (2009) Taking the time to make important decisions: The checkpoint effector kinases Chk1 and Chk2 and the DNA damage response. DNA Repair 8:1047-1054.

Sunderland, T., Linker, G., Mirza, N., Putnam, K. T., Friedman, D. L., Kimmel, L. H., Bergeson, J., Manetti, G. J., Zimmermann, M., Tang, B., Bartko, J. J., Cohen, R. M. (2003) Decreased beta-amyloid1-42 and increased tau levels in cerebrospinal fluid of patients with Alzheimer disease. JAMA 289:2094-2103.

Suzuki, A., Lu, J., Kusakai, G., Kishimoto, A., Ogura, T., Esumi, H. (2004) ARK5 is a tumor invasion-associated factor downstream of Akt signaling. Mol Cell Biol 24:3526-3535.

Swatton, J. E., Sellers, L. A., Faull, R. L., Holland, A., Iritani, S., Bahn, S. (2004) Increased MAP kinase activity in Alzheimer's and Down syndrome but not in schizophrenia human brain. European Journal of Neuroscience 19:2711-2719.

Swerdlow, R. H., Khan, S. M. (2004) A "mitochondrial cascade hypothesis" for sporadic Alzheimer's disease. Med Hypotheses 63:8-20.

Swerdlow, R. H., Khan, S. M. (2009) The Alzheimer's disease mitochondrial cascade hypothesis: an update. Exp Neurol 218:308-315.

Takei, Y., Teng, J., Harada, A., Hirokawa, N. (2000) Defects in axonal elongation and neuronal migration in mice with disrupted tau and map1b genes. J Cell Biol 150:989-1000.

Takuma, H., Arawaka, S., Mori, H. (2003) Isoforms changes of tau protein during development in various species. Brain Res Dev Brain Res 142:121-127.

Tariot, P. N., Farlow, M. R., Grossberg, G. T., Graham, S. M., McDonald, S., Gergel, I. (2004) Memantine Treatment in Patients With Moderate to Severe Alzheimer Disease Already Receiving Donepezil: A Randomized Controlled Trial. JAMA 291:317-324.

Taylor, K. I., Probst, A. (2008) Anatomic localization of the transentorhinal region of the perirhinal cortex. Neurobiol Aging 29:1591-1596.

Terry, R. D., Masliah, E., Salmon, D. P., Butters, N., DeTeresa, R., Hill, R., Hansen, L. A., Katzman, R. (1991) Physical basis of cognitive alterations in Alzheimer's disease: synapse loss is the major correlate of cognitive impairment. Ann Neurol 30:572-580.

Thibault, S. T. et al. (2004) A complementary transposon tool kit for Drosophila melanogaster using P and piggyBac. Nat Genet 36:283-287.

Thies, E., Mandelkow, E.-M. (2007) Missorting of Tau in Neurons Causes Degeneration of Synapses That Can Be Rescued by the Kinase MARK2/Par-1. J Neurosci 27:2896-2907.

Thinakaran, G., Koo, E. H. (2008) Amyloid precursor protein trafficking, processing, and function. J Biol Chem 283:29615-29619.

Thompson, R. F. (1985) The Brain: An introduction to Neuroscience. New York: W H Freeman and Company.

Thornton, C., Bright, N. J., Sastre, M., Muckett, P. J., Carling, D. (2011) AMP-activated protein kinase (AMPK) is a tau kinase, activated in response to beta-amyloid exposure. Biochem J.

Tolboom, N., Yaqub, M., van der Flier, W. M., Boellaard, R., Luurtsema, G., Windhorst, A. D., Barkhof, F., Scheltens, P., Lammertsma, A. A., van Berckel, B. N. (2009) Detection of Alzheimer pathology in vivo using both 11C-PIB and 18F-FDDNP PET. J Nucl Med 50:191-197.

Tomlinson, B. E., Blessed, G., Roth, M. (1968) Observations on the brains of non-demented old people. J Neurol Sci 7:331-356.

Tomlinson, B. E., Blessed, G., Roth, M. (1970) Observations on the brains of demented old people. J Neurol Sci 11:205-242.

Town, T., Zolton, J., Shaffner, R., Schnell, B., Crescentini, R., Wu, Y., Zeng, J., DelleDonne, A., Obregon, D., Tan, J., Mullan, M. (2002) p35/Cdk5 pathway mediates soluble amyloid-beta peptide-induced tau phosphorylation in vitro. J Neurosci Res 69:362-372.

Townsend, M., Qu, Y., Gray, A., Wu, Z., Seto, T., Hutton, M., Shearman, M. S., Middleton, R. E. (2010) Oral treatment with a gamma-secretase inhibitor improves long-term potentiation in a mouse model of Alzheimer's disease. J Pharmacol Exp Ther 333:110-119.

Vershinin, M., Carter, B. C., Razafsky, D. S., King, S. J., Gross, S. P. (2007) Multiple-motor based transport and its regulation by Tau. Proc Natl Acad Sci U S A 104:87-92.

Vinet, J., Carra, S., Blom, J. M., Harvey, M., Brunello, N., Barden, N., Tascedda, F. (2003) Cloning of mouse Ca2+/calmodulin-dependent protein kinase kinase beta (CaMKKbeta) and characterization of CaMKKbeta and CaMKKalpha distribution in the adult mouse brain. Brain Res Mol Brain Res 111:216-221.

Vingtdeux, V., Davies, P., Dickson, D. W., Marambaud, P. (2010a) AMPK is abnormally activated in tangle- and pre-tangle-bearing neurons in Alzheimer's disease and other tauopathies. Acta Neuropathol 121:337-349.

Vingtdeux, V., Chandakkar, P., Zhao, H., d'Abramo, C., Davies, P., Marambaud, P. (2011) Novel synthetic small-molecule activators of AMPK as enhancers of autophagy and amyloid-{beta} peptide degradation. FASEB J 25:219-231.

Vingtdeux, V., Giliberto, L., Zhao, H., Chandakkar, P., Wu, Q., Simon, J. E., Janle, E. M., Lobo, J., Ferruzzi, M. G., Davies, P., Marambaud, P. (2010b) AMP-activated protein kinase signaling activation by resveratrol modulates amyloid-beta peptide metabolism. J Biol Chem 285:9100-9113.

Wagner, M. C., Pfister, K. K., Bloom, G. S., Brady, S. T. (1989) Copurification of kinesin polypeptides with microtubule-stimulated Mg-ATPase activity and kinetic analysis of enzymatic properties. Cell Motil Cytoskeleton 12:195-215.

Wagner, U., Utton, M., Gallo, J. M., Miller, C. C. (1996) Cellular phosphorylation of tau by GSK-3 beta influences tau binding to microtubules and microtubule organisation. J Cell Sci 109 (Pt 6):1537-1543.

Walsh, D. M., Selkoe, D. J. (2004) Deciphering the molecular basis of memory failure in Alzheimer's disease. Neuron 44:181-193.

Wang, J. W., Imai, Y., Lu, B. (2007a) Activation of PAR-1 kinase and stimulation of tau phosphorylation by diverse signals require the tumor suppressor protein LKB1. J Neurosci 27:574-581.

Wang, J. Z., Grundke-Iqbal, I., Iqbal, K. (1996) Glycosylation of microtubule-associated protein tau: an abnormal posttranslational modification in Alzheimer's disease. Nat Med 2:871-875.

Wang, J. Z., Grundke-Iqbal, I., Iqbal, K. (2007b) Kinases and phosphatases and tau sites involved in Alzheimer neurofibrillary degeneration. Eur J Neurosci 25:59-68.

Wang, X., Su, B., Zheng, L., Perry, G., Smith, M. A., Zhu, X. (2009a) The role of abnormal mitochondrial dynamics in the pathogenesis of Alzheimer's disease. J Neurochem 109 Suppl 1:153-159.

Wang, X., Su, B., Siedlak, S. L., Moreira, P. I., Fujioka, H., Wang, Y., Casadesus, G., Zhu, X. (2008) Amyloid-beta overproduction causes abnormal mitochondrial dynamics via differential modulation of mitochondrial fission/fusion proteins. Proc Natl Acad Sci U S A 105:19318-19323.

Wang, Y., Martinez-Vicente, M., Kruger, U., Kaushik, S., Wong, E., Mandelkow, E. M., Cuervo, A. M., Mandelkow, E. (2009b) Tau fragmentation, aggregation and clearance: the dual role of lysosomal processing. Hum Mol Genet 18:4153-4170.

Wayman, G. A., Lee, Y. S., Tokumitsu, H., Silva, A. J., Soderling, T. R. (2008) Calmodulin-kinases: modulators of neuronal development and plasticity. Neuron 59:914-931.

Weingarten, M. D., Lockwood, A. H., Hwo, S. Y., Kirschner, M. W. (1975) A protein factor essential for microtubule assembly. Proc Natl Acad Sci U S A 72:1858-1862.

Williamson, R., Scales, T., Clark, B. R., Gibb, G., Reynolds, C. H., Kellie, S., Bird, I. N., Varndell, I. M., Sheppard, P. W., Everall, I., Anderton, B. H. (2002) Rapid tyrosine phosphorylation of neuronal proteins including tau and focal adhesion kinase in response to amyloid-beta peptide exposure: involvement of Src family protein kinases. J Neurosci 22:10-20.

Wilson, C. A., Doms, R. W., Lee, V. M. (2003) Distinct presenilin-dependent and presenilin-independent gamma-secretases are responsible for total cellular Abeta production. J Neurosci Res 74:361-369.

Wittmann, C. W., Wszolek, M. F., Shulman, J. M., Salvaterra, P. M., Lewis, J., Hutton, M., Feany, M. B. (2001) Tauopathy in Drosophila: neurodegeneration without neurofibrillary tangles. Science 293:711-714.

Woods, A., Dickerson, K., Heath, R., Hong, S. P., Momcilovic, M., Johnstone, S. R., Carlson, M., Carling, D. (2005) Ca2+/calmodulin-dependent protein kinase kinase-beta acts upstream of AMP-activated protein kinase in mammalian cells. Cell Metab 2:21-33.

Xu, H., Greengard, P., Gandy, S. (1995) Regulated formation of Golgi secretory vesicles containing Alzheimer beta-amyloid precursor protein. J Biol Chem 270:23243-23245.

Yao, C., Williams, A. J., Ottens, A. K., May Lu, X. C., Chen, R., Wang, K. K., Hayes, R. L., Tortella, F. C., Dave, J. R. (2008) Detection of protein biomarkers using high-throughput immunoblotting following focal ischemic or penetrating ballistic-like brain injuries in rats. Brain Inj 22:723-732.

Yoshizaki, C., Tsukane, M., Yamauchi, T. (2004) Overexpression of tau leads to the stimulation of neurite outgrowth, the activation of caspase 3 activity, and accumulation and phosphorylation of tau in neuroblastoma cells on cAMP treatment. Neurosci Res 49:363-371.

Zamora-Leon, S. P., Lee, G., Davies, P., Shafit-Zagardo, B. (2001) Binding of Fyn to MAP-2c through an SH3 binding domain. Regulation of the interaction by ERK2. J Biol Chem 276:39950-39958.

Zekanowski, C., Golan, M. P., Krzysko, K. A., Lipczynska-Lojkowska, W., Filipek, S., Kowalska, A., Rossa, G., Peplonska, B., Styczynska, M., Maruszak, A., Religa, D., Wender, M., Kulczycki, J., Barcikowska, M., Kuznicki, J. (2006) Two novel presenilin 1 gene mutations connected with frontotemporal dementia-like clinical phenotype: genetic and bioinformatic assessment. Exp Neurol 200:82-88.

Zempel, H., Thies, E., Mandelkow, E., Mandelkow, E.-M. (2010) A{beta} Oligomers Cause Localized Ca2+ Elevation, Missorting of Endogenous Tau into Dendrites, Tau Phosphorylation, and Destruction of Microtubules and Spines. J Neurosci 30:11938-11950.

Zhu, X., Perry, G., Moreira, P. I., Aliev, G., Cash, A. D., Hirai, K., Smith, M. A. (2006) Mitochondrial abnormalities and oxidative imbalance in Alzheimer disease. J Alzheimers Dis 9:147-153.

9| Appendix 1 – *Drosophila melanogaster* strains used in this study

Label	Description	Full Genotype	Source
Canton S	Wild type	+ ; + ; +	Lab stock
GMR::GAL4	Driver of GAL4 in eye photoreceptors	$w^{[1118]}$; {w[$^{+}$mc],UAS-GMR::GAL4} ; +	Lab stock
0N4R tau	0N4R human tau	$w^{[1118]}$; + ; {w[$^{+}$mc],UAS-4R tau}	Kind gift of Mel Feany
0N3R tau	0N3R human tau	$w^{[1118]}$; w[$^{+}$mc],UAS-3R tau}; +	Kind gift of Mel Feany
R406W tau	0N4R R406W human tau	$w^{[1118]}$; + ; {w[$^{+}$mc],UAS-0N4R R406W}	Kind gift of Bingwei Lu
S2A tau	0N4R R406W S2A human tau	$w^{[1118]}$; {w[$^{+}$mc],UAS-0N4R R406W S2A}; +	Kind gift of Bingwei Lu
S262A tau	0N4R S262A human tau	$w^{[1118]}$; +; {w[$^{+}$mc],UAS-0N4R S262A}	Kind gift of Koichi Iijima
B2WT1	Wild type (WT) human BRSK2	$w^{[1118]}$; {w[$^{+}$mc],UAS-B2WT1}/Cyo ; +	This work
B2WT2	WT human BRSK2	$w^{[1118]}$; {w[$^{+}$mc],UAS-B2WT2}/CyO ; +	This work
B2WT3	WT human BRSK2	$w^{[1118]}$; + ; {w[$^{+}$mc],UAS-B2WT3}/TM3	This work
B2WT4	WT human BRSK2	$w^{[1118]}$; + ; {w[$^{+}$mc],UAS-B2WT4}/TM3	This work
B2WT5	WT human BRSK2	$w^{[1118]}$; + ; {w[$^{+}$mc],UAS-B2WT5}/TM3	This work
B2NP1	Non-phosphorylatable (NP) human BRSK2	$w^{[1118]}$; {w[$^{+}$mc],UAS-B2NP1}/CyO ; +	This work

Label	Description	Full Genotype	Source
B2NP2	NP human BRSK2	$w^{[1118]}$; {w[$^{+}$mc],UAS-B2NP2}/CyO ; +	This work
B2NP3	NP human BRSK2	$w^{[1118]}$; + ; {w[$^{+}$mc],UAS-B2NP3}/TM3	This work
B2NP4	NP human BRSK2	$w^{[1118]}$; + ; {w[$^{+}$mc],UAS-B2NP4}/TM3	This work
B2NP5	NP human BRSK2	$w^{[1118]}$; + ; {w[$^{+}$mc],UAS-B2NP4}/TM3	This work Stock died
B2NP6	NP human BRSK2	$w^{[1118]}$; + ; {w[$^{+}$mc],UAS-B2NP6}/TM3	This work
B2NP7	NP human BRSK2	$w^{[1118]}$; {w[$^{+}$mc],UAS-B2NP7}/CyO ; +	This work Stock died
B2NP8	NP human BRSK2	$w^{[1118]}$; {w[$^{+}$mc],UAS-B2NP8}/CyO ; +	This work
B2KD1	Kinase dead (KD) human BRSK2	$w^{[1118]}$; {w[$^{+}$mc],UAS-B2KD1}/CyO ; +	This work
B2KD2	KD human BRSK2	$w^{[1118]}$; {w[$^{+}$mc],UAS-B2KD2}/CyO ; +	This work Stock died
B2KD3	KD human BRSK2	$w^{[1118]}$; {w[$^{+}$mc],UAS-B2KD3}/CyO ; +	This work
B2KD4	KD human BRSK2	$w^{[1118]}$; + ; {w[$^{+}$mc],UAS-B2KD4}/TM3	This work
B2KD5	KD human BRSK2	$w^{[1118]}$; {w[$^{+}$mc],UAS-B2KD5}/CyO ; +	This work
B2KD6	KD human BRSK2	$w^{[1118]}$; {w[$^{+}$mc],UAS-B2KD6}/CyO ; +	This work Stock died
B2KD7	KD human BRSK2	$w^{[1118]}$; + ; {w[$^{+}$mc],UAS-B2KD7}/TM3	This work
B2KD8	KD human BRSK2	$w^{[1118]}$; + ; {w[$^{+}$mc],UAS-B2KD8}/TM3	This work Stock died
B2KD9	KD human BRSK2	$w^{[1118]}$; + ; {w[$^{+}$mc],UAS-B2KD9}/TM3	This work
B2KD10	KD human BRSK2	$w^{[1118]}$; {w[$^{+}$mc],UAS-B2KD10}/CyO ; +	This work Stock died
B2CA1	Constitutively active (CA) human BRSK2	$w^{[1118]}$; {w[$^{+}$mc],UAS-B2CA1}/ CyO; +	This work Stock died
B2CA2	CA human BRSK2	$w^{[1118]}$; + ; {w[$^{+}$mc],UAS-B2CA2}/TM3	This work Stock died

Label	Description	Full Genotype	Source
B2CA3	CA human BRSK2	$w^{[1118]}$; {w[$^{+}$mc],UAS-B2CA3}/ CyO; +	This work Stock died
B2CA4	CA human BRSK2	$w^{[1118]}$; {w[$^{+}$mc],UAS-B2CA4}/ CyO; +	This work
B2CA6	CA human BRSK2	$w^{[1118]}$; {w[$^{+}$mc],UAS-B2CA6}/ CyO; +	This work Stock died
B2CA7	CA human BRSK2	$w^{[1118]}$; {w[$^{+}$mc],UAS-B2CA7}/ CyO; +	This work
B2CA8	CA human BRSK2	$w^{[1118]}$; {w[$^{+}$mc],UAS-B2CA8}/ CyO; +	This work
B2CA9	CA human BRSK2	$w^{[1118]}$; {w[$^{+}$mc],UAS-B2CA9}/ CyO; +	This work Stock died
B2CA10	CA human BRSK2	$w^{[1118]}$; {w[$^{+}$mc],UAS-B2CA10}/ CyO; +	This work
B1WT1	WT human BRSK1	$w^{[1118]}$; {w[$^{+}$mc],UAS-B1WT1}/CyO ; +	This work Stock died
B1WT2	WT human BRSK1	$w^{[1118]}$; {w[$^{+}$mc],UAS-B1WT2}/CyO ; +	This work
B1WT3	WT human BRSK1	$w^{[1118]}$; {w[$^{+}$mc],UAS-B1WT3}/CyO ; +	This work
B1WT4	WT human BRSK1	$w^{[1118]}$; {w[$^{+}$mc],UAS-B1WT4}/CyO ; +	This work Stock died
B1WT5	WT human BRSK1	$w^{[1118]}$; {w[$^{+}$mc],UAS-B1WT5}/CyO ; +	This work
B1WT6	WT human BRSK1	$w^{[1118]}$; + ; {w[$^{+}$mc],UAS-B1WT6}/TM3	This work
B1WT7	WT human BRSK1	$w^{[1118]}$; {w[$^{+}$mc],UAS-B1WT7}/CyO ; +	This work
B1WT8	WT human BRSK1	$w^{[1118]}$; + ; {w[$^{+}$mc],UAS-B1WT8}/TM3	This work
B1WT9	WT human BRSK1	$w^{[1118]}$; + ; {w[$^{+}$mc],UAS-B1WT9}/TM3	This work Stock died
B1WT10	WT human BRSK1	$w^{[1118]}$; {w[$^{+}$mc],UAS-B1WT10}/CyO ; +	This work
B1KD1	KD human BRSK1	$w^{[1118]}$; + ; {w[$^{+}$mc],UAS-B1KD1}/TM3	This work Stock died
B1KD2	KD human BRSK1	$w^{[1118]}$; + ; {w[$^{+}$mc],UAS-B1KD2}/TM3	This work Stock died
B1KD3	KD human BRSK1	$w^{[1118]}$; {w[$^{+}$mc],UAS-B1KD3}/CyO ; +	This work Stock died
B1KD4	KD human BRSK1	$w^{[1118]}$; {w[$^{+}$mc],UAS-B1KD4}/CyO ; +	This work Stock died

Label	Description	Full Genotype	Source
B1KD5	KD human BRSK1	$w^{[1118]}$; + ; {w[$^{+}$mc],UAS-B1KD5}/TM3	This work Stock died
B1KD6	KD human BRSK1	$w^{[1118]}$; {w[$^{+}$mc],UAS-B1KD6}/CyO ; +	This work
B1NP1	NP human BRSK1	$w^{[1118]}$; + ; {w[$^{+}$mc],UAS-B1NP1}/TM3	This work Stock died
B1NP2	NP human BRSK1	$w^{[1118]}$; {w[$^{+}$mc],UAS-B1NP2}/CyO ; +	This work Stock died
B1NP3	NP human BRSK1	$w^{[1118]}$; + ; {w[$^{+}$mc],UAS-B1NP3}/TM3	This work
B1NP4	NP human BRSK1	$w^{[1118]}$; + ; {w[$^{+}$mc],UAS-B1NP5}/TM3	This work
B1NP5	NP human BRSK1	$w^{[1118]}$; {w[$^{+}$mc],UAS-B1NP6}/CyO ; +	This work
B1CA1	CA human BRSK1	$w^{[1118]}$; + ; {w[$^{+}$mc],UAS-B1CA1}/TM3	This work
B1CA2	CA human BRSK1	$w^{[1118]}$; + ; {w[$^{+}$mc],UAS-B1CA2}/TM3	This work
hCaMKKα1	human hCaMKKα isoform	$w^{[1118]}$; {w[$^{+}$mc],UAS-hCaMKKα1}/CyO ; +	This work
hCaMKKα2	human hCaMKKα isoform	$w^{[1118]}$; + ; {w[$^{+}$mc],UAS-hCaMKKα2}/TM3	This work
hCaMKKα3	human hCaMKKα isoform	$w^{[1118]}$; {w[$^{+}$mc],UAS-hCaMKKα3}/CyO ; +	This work
hCaMKKα4	human hCaMKKα isoform	$w^{[1118]}$; + ; {w[$^{+}$mc],UAS-hCaMKKα4}/TM3	This work
hCaMKKα5	human hCaMKKα isoform	$w^{[1118]}$; {w[$^{+}$mc],UAS-hCaMKKα5}/CyO ; +	This work
hCaMKKα6	human hCaMKKα isoform	$w^{[1118]}$; + ; {w[$^{+}$mc],UAS-hCaMKKα6}/TM3	This work
hCaMKKα7	human hCaMKKα isoform	$w^{[1118]}$; + ; {w[$^{+}$mc],UAS-hCaMKKα7}/TM3	This work
hCaMKKα8	human hCaMKKα isoform	$w^{[1118]}$; {w[$^{+}$mc],UAS-hCaMKKα8}/CyO ; +	This work

Label	Description	Full Genotype	Source
hCaMKKα9	human hCaMKKα isoform	$w^{[1118]}$; + ; {w[$^{+}$mc],UAS-hCaMKKα9}/TM3	This work
GMR ; tau	0N4R human tau driven by GMR::GAL4	$w^{[1118]}$; {w[$^{+}$mc],UAS-GMR::GAL4}/CyO ; {w[$^{+}$mc],UAS-4R tau}/TM6B	This work
GMR ; tau, B2WT5	Recombinant 0N4R human tau and B2WT5 driven by GMR::GAL4	$w^{[1118]}$; {w[$^{+}$mc],UAS-GMR::GAL4}/CyO ; {w[$^{+}$mc],UAS-B2WT5},{w[$^{+}$mc],UAS-4R tau}/TM6B	This work
CG17698 RNAi	RNAi to CG17698 (*Drosophila* homologue of CaMKK)	$w^{[1118]}$; {w[$^{+}$mc],UAS-CG17698 RNAi} ; +	VDRC
LKB1 RNAi	RNAi to *Drosophila* LKB1	$w^{[1118]}$; {w[$^{+}$mc],UAS-LKB1 RNAi} ; {w[$^{+}$mc],UAS-LKB1 RNAi}	Kind gift of Bingwei Lu
PAR-1 RNAi	RNAi to *Drosophila* PAR-1	$w^{[1118]}$; +; {w[$^{+}$mc],UAS-PAR-1 RNAi}	VDRC
CG6114 RNAi	RNAi to CG6114 (*Drosophila* homologue of BRSK)	$w^{[1118]}$; {w[$^{+}$mc],UAS-CG6114 RNAi} ; +	VDRC
LKB1;LKB1,tau	0N4R and LKB1 RNAi recombinant	$w^{[1118]}$; {w[$^{+}$mc],UAS-LKB1 RNAi}/CyO ; {w[$^{+}$mc],UAS-LKB1 RNAi}, {w[$^{+}$mc],UAS-4R tau}/TM6B	This work
UAS-CG6114-2	CG6114 (*Drosophila* homologue of BRSK)	$w^{[1118]}$; + ; {w[$^{+}$mc],UAS-CG6114-2}/TM3	This work
UAS-LKB1-2	human LKB1	$w^{[1118]}$; + ; {w[$^{+}$mc],UAS-LKB1-2}/TM3	This work
CG17698; B2WT5	CG17698 RNAi and B2WT5	$w^{[1118]}$; {w[$^{+}$mc],UAS-CG6114 RNAi}/+ ; {w[$^{+}$mc],UAS-B2WT5}/TM6B	This work
GMR, CG17698; hCaMKKα6	CG17698 RNAi and hCaMKKα6 driven by GMR::GAL4	$w^{[1118]}$; {w[$^{+}$mc],UAS-GMR::GAL4}/{w[$^{+}$mc],UAS-CG6114 RNAi} ; {w[$^{+}$mc],UAS-hCaMKKα6}/TM6B	This work

Label	Description	Full Genotype	Source
CyO/If; Tau, B2WT5	Recombinant 0N4R human tau and B2WT5	$w^{[1118]}$; If /CyO ; {w[$^{+}$mc],UAS-B2WT5},{w[$^{+}$mc],UAS-4R tau}/TM6B	This work
sgg S9A	Shaggy S9A	w[1118] ; P{w[+mC]=UAS-sgg.S9A}MB14	Bloomington
sgg; B2WT5	Shaggy S9A and B2WT5	$w^{[1118]}$; {w[$^{+}$mc],UAS-sgg S9A}/CyO ; {w[$^{+}$mc],UAS-B2WT5}/TM6B	This work
sgg; S262A	Shaggy S9A and 0N4R S262A tau	$w^{[1118]}$; {w[$^{+}$mc],UAS-sgg S9A}/CyO ; {w[$^{+}$mc],UAS-0N4R S262A}/TM6B	This work
GMR, CG17698; B2WT5	CG17698 RNAi and B2WT5 driven by GMR::GAL4	$w^{[1118]}$; {w[$^{+}$mc],UAS-GMR::GAL4}/{w[$^{+}$mc],UAS-CG6114 RNAi} ; {w[$^{+}$mc],UAS-B2WT5}/TM6B	This work
GMR, CG17698; TM6B/MKRS	CG17698 RNAi driven by GMR::GAL4	$w^{[1118]}$; {w[$^{+}$mc],UAS-GMR::GAL4}/{w[$^{+}$mc],UAS-CG6114 RNAi} ; MKRS/TM6B	This work
CG17698; B2CA5	CG17698 RNAi and B2CA5	$w^{[1118]}$; {w[$^{+}$mc],UAS-CG6114 RNAi}/+ ; {w[$^{+}$mc],UAS-B2CA5}/TM6B	This work
GMR; B2CA5	B2CA5 driven by GMR::GAL4	$w^{[1118]}$; {w[$^{+}$mc],UAS-GMR::GAL4}/CyO; {w[$^{+}$mc],UAS-B2CA5}/TM6B	This work
DB	Double Balancer	$w^{[1118]}$; CyO/If; TM6B/MKRS	Lab stock
CyO/If; B2WT5, hCaMKKα	Recombinant hCaMKKα and B2WT5	$w^{[1118]}$; If /CyO ; {w[$^{+}$mc],UAS-B2WT5},{w[$^{+}$mc],UAS-hCaMKKα}/TM6B	This work
cac1	cacophony 1 (calcium channel α subunit)	$w^{[1118]}$; + ; P{w[+mC]=UAS-cac1-EGFP}786C	Bloomington

10| Appendix 2 – QED Documentation

Quantitative Edge Detection

Q E D

http://go.warwick.ac.uk/qcaudron/qed

Quentin CAUDRON
q.caudron@warwick.ac.uk
http://go.warwick.ac.uk/qcaudron

Centre for Complexity Science
The University of Warwick

January 21, 2010

Contents

1 Introduction

Quantitative Edge Detection (QED) is a software package, written in Matlab, that assesses the extent of structural diferences in biomedical images. QED's website is located at `http://go.warwick.ac.uk/qcaudron/qed`.

1.1 About QED

This package is geared towards analysing phenotypic differences in *Drosophila melanogaster* eyes, caused by genetic manipulations such as the expression of *Tau* protein, or in the general use of fruit flies as neurodegenerative disease models. QED uses implementations of the edge detection algorithms to extract information from images, namely the Marr-Hildreth and Sobel edge detectors. It accounts, to some extent, for the curvature of the eye by a perspective transformation and uses morphological operations on the resulting images to obtain connected edgesets - a pixel-thin net that defines the location of all edges (of a specific width) on the original image. From these edgesets, information is extracted and metrics are defined. Comparing these between genotypes with statistical tests leads to a quantitative evaluation of the difference between physical features of the two genotypes.

1.2 Acknowledgements

QED was written by Quentin Caudron, with contributions from John Aston of the Department of Statistics, and from Bruno Frenguelli, Kevin Moffat and Ceri Lyn-Adams of the Department of Biological Sciences, all at the University of Warwick.

2 Installation

QED can be downloaded, both in the form of a standalone Windows executable and of the source code. The Windows installer contains both the QED executable and the Matlab Component Runtime libraries (MCR). The MCR libraries are essential for the running of QED on your system, as they contain all of the functions required for QED to work if Matlab is not installed on your computer.

2.1 First Installation

The Windows installer is available for download on QED's website. Whilst the installer itself is less than 50 KB, please note that in order to maintain QED up-to-date, all installation components are downloaded upon installation. You will therefore need an internet connection to install QED. Please note that this is a relatively large download (approximately 150 MB) and that installation of the MCR component may take some time. Once the MCR libraries have been installed, QED will be downloaded and installed into your *Program Files* directory.

3 Running QED

3.1 Image Preparation

QED will analyse the contents of a folder on your computer. This folder should contain only the images you wish to process, in greyscale `.tif` or `.tiff` format, and no other files or folders. You should copy images from both the control genotype and the genotype of interest into this folder. The more images present, the more accurate the results.

3.2 Launching QED

QED can be run from the Start Menu or Desktop shortcut. Because QED is written in Matlab and uses a large number of external runtime components, it may appear to run relatively slowly. Please be patient and only run the program once ! Whilst graphical elements are demanding on system resources, the information processing and analysis, once underway, is fast.

3.3 Runtime Output

A black terminal window will appear. This window is purely used for verbose output, and in fact, the vast majority can be ignored. Only in the case of a program crash should the contents of this window be studied.

3.4 Selecting the Directory to Analyse

When QED has loaded all of its functions, you will be prompted to select a folder to analyse. Browse through your system, select the relevant folder, and click OK.

3.5 Entering Genotypes

The first time a folder is processed, you will be asked to enter the names of the two genotypes. You should ideally enter plain text, though spaces, dashes and underscores are acceptable. Examples are, `GMR`, `GMR-Tau` or `Control Eyes`. Press *OK* when done.

3.6 Defining the Eye Region

QED will begin processing images alphabetically. You are first told what the filename of the current image is, and asked to cut around the eye. This is done by clicking around the eye. Each time you click, a point is placed on the image. Points automatically connect to the last point, so you should click around the eye to draw a polygon, following the contour as closely as possible. Once you are finished, either click on the first point you placed to close the shape, or double-click while placing your final point.

At this stage, all points can be moved by clicking and dragging them, and the entire shape can be moved by clicking in the middle of the polygon and dragging. You can delete a point by right-clicking on it and selecting *Delete*. If you wish to add a point, hover the mouse over the edge of the polygon and press the *A* key on your keyboard, and then click to insert a new point. Once you are satisfied with the cutout, double-click inside the shape to confirm your selection.

3.7 Optimising the Edgeset

Once you have defined the eye region, you will be shown the original image, alongside an edgeset. You can then modify two parameters and one setting in order to obtain a better edgeset.

The first is the width of the Gaussian kernel, which defines the width of edges that are extracted from the image. As an example, a 650 x 650-pixel image, close-cropped onto the eye of a wild-type fly, may have edge widths between four and six pixels. The default value, in this case, is five pixels. The selected value must be in the correct edge width range, or the algorithm will begin to pick up features that are not true edges.

The second parameter is the Sobel threshold. This defines how sharp changes in luminosity should be in order to be considered edges. The default, for the above image dimensions, is four. Lowering this tends to bring out more edges, but also more noise, whereas increasing it will break up edges. Because it is very important to have connected edgesets, this parameter should be set to remove as much noise as possible, but not be set so high as to begin breaking up edges. The lower bound for this threshold is zero, but

it does not necessarily have to take integer values. If extreme sensitivity is required, the Sobel threshold can be dropped to 0.001, for example. On the other end of the scale, if the edges are very well-defined, a higher threshold may be better, and can be increased to values in the tens or above.

You can apply Contrast-Limited Adaptive Histogram Equalisation to the image, by using the checkbox below the parameter modification area. You will see the original image on the left change, such that contrast is enhanced. This is good if the original image contains a shadow, for example, but is not appropriate for all images. If you select this contrast enhancement, the luminosity values of the image will change, and the above parameters will thus need to be altered. The important parameter to modify, in the case of a contrast-adapted image, is the Sobel threshold, which should generally be increased to account for the increased contrast in the image.

Modifying these parameters is possibly equal parts science and art, and will require a large amount of trial and error. For the example image dimensions listed above, it could be found that decreasing the Gaussian kernel width to four, and increasing the Sobel threshold to approximately fifteen, can provide an improvement on the default values, though these can often remain superior for a majority of images.

If an adequate edgeset cannot be found, the option to reject the image exists. The image will simply be moved to another folder, an edgeset will not be generated, and QED will ignore its existence during the analysis.

3.8 Selecting the Image Genotype

After accepting the edgeset for an image, you will be asked to specify the genotype of that image, and will be presented with a list of the two genotypes you entered earlier. Make your selection, and click *OK*.

3.9 Collating Edgesets

Once all images in the directory have been processed, QED will gather all edgeset data into memory and begin extracting structural information from them. This information is used in the metrics that are used to compare between genotypes : roundness of ommatidia, distances between ommatidia

and angles between ommatidia around the centre of the eye. You are then presented with a results graph window, which is automatically saved in both `.eps` and `.tif` formats in the *Results* directory, created in the folder being analysed.

4 Results

4.1 Generated Files

The graphs that appear on your screen show the dispersion coefficients for each metric. A dispersion coefficient is a measure of how wide a distribution is, and thus, the lower it is, the more regular and ordered a measure is. Dispersion coefficients are calculated for ommatidial roundness and for interommatidial distances and angles. For a control genotype, dispersion coefficients are expected to be small, as we expect hexagonal packing (60° and equal distances between ommatidia) of ommatidia, which should all be round. When ommatidia begin to fuse, they lose their roundness (they are now oval or more "blob"-shaped) and the regularity of the hexagonal lattice is reduced, leading to higher dispersion coefficients.

Each graph shows two sets of points. Blue points are the first genotype, which should be your control. Points in red are from the second genotype. Each point represents the dispersion coefficient for a particular image, and the three graphs show these for the three different measures.

Numerical results are also saved in the *Results* folder, as `.csv` files. Dispersion coefficients are saved in three files - one per metric - with the left column containing the first (control) genotype. Full results for metrics are also saved in the *Results* directory, under *Raw Data*.

Images showing the progress of edge detection are also generated, in folders created for each image.

4.2 Repeat Analyses

If you wish to add or remove images, or simply attempt to improve an edgeset, you should be aware of the files created by QED. The folder you have just

analysed will now contain the following :

- The `.tif` or `.tiff` images you placed there for analysis
- A `.qed` file for each image, containing genotype and edgeset information
- `genotypes.qed`, a file containing information regarding the genotypes being analysed
- A `Rejected` folder, containing any images which had their edgesets rejected
- A `Results` folder, containing numerical and graphical results from the analysis

The second item in this list determines whether or not an image will be analysed. Any image in the directory without an associated `.qed` file will be analysed, and you will be prompted to create an edgeset for it. Any image with an associated `.qed` file will be analysed, but its edgeset will have been already created, allowing repeat analyses of a directory to be done much more rapidly. If you wish to recreate the edgeset for an image, simply delete its `.qed` file and rerun the program. Likewise, to add images to be analysed, simply copy the image into the directory along with the other images, and an edgeset will be created for it when you run QED. If you believe an image should not be being analysed, delete its `.qed` and move the `.tif` or `.tiff` into the *Rejected* folder.

5 Code

The code for QED is available for download on its website.

5.1 File Breakdown

- `qed.m` is the central file. It prompts for a directory and genotype information, collates edgeset results, and calculates the metrics from the extracted information. It also computes the p-values from the Mann-Whitney test and generates the results plot as well as saving all results to file.

- `qextract.m` opens an image, prompts the user to cut out the eye region and opens the GUI for generating the edgeset. It applies the perspective transform to the edgeset and searches for boundaries.
- `QGUI.m` is the functionality behind the edgeset creation. It defines the behaviour of buttons on the GUI.
- `qedgeset.m` returns the edgesets from an image, given the Gaussian kernel width and Sobel threshold values.
- `qdispersion.m` calculates a dispersion coefcient given a distribution.
- `qgauss2D.m` computes the 2D derivates of a Gaussian.
- `qsurface.m` generates a semiellipsoidal surface based on x and y dimensions, with an empirically-defined curvature.
- `qresult.m` generates CSV files containing results.
- `QGUI.fig` contains information on what the GUI looks like.
- `itriu.m` extracts half of a diagonal matrix.

6 Help

Please contact the author with any questions or queries.

6.1 Contact Details

Email: `q.caudron@warwick.ac.uk`
Address: Quentin CAUDRON
Centre for Complexity Science D2.05,
Mathematics Institute
University of Warwick
Coventry, CV4 7AL

11| Appendix 3 – Primer sequences

1. Sequencing pUAST.BRSK1 clones:

a) Sense primer: 5' TAGACGTCGTGGAGCTTGAG 3'

b) M (sequences over the mutation sites): 5' CGCCATCCTGAAGCTCATAG 3'

c) Anti-sense primer: 5' TGGTTCGGGAACTTCATCTC 3'

2. Sequencing pUAST.BRSK2 clones:

a) Sense primer: 5' GGTAGGGCCCAACATACTGC 3'

b) M (sequences over the mutation sites): 5' TTCTTCCGGCAGATCATCTC 3'

c) Anti-sense primer: 5' GTCACCTTCACCCTGCTCTC 3'

3. BRSK1 genotyping PCR primers (also used for sequencing the PCR products):

a) Sense primer: 5' TGCTCCAGACTGAGCCTTTT 3'

b) Anti-sense primer: 5' GTTCTTCCGCCAGATTGTGT 3'

4. BRSK2 genotyping PCR primers:

a) Sense primer: 5' CAGCAGCTTGTTGCGGTCTC 3'

b) Anti-sense primer: 5' CGCCACCATGTACCCATACG 3'

5. BRSK2 genotyping sequencing primer

a) Antisense primer: 5’ TGTCAGGTGGTGAGCTCTTC 3’

6. CaMKKα cloning primers (PCR primer pair)

a) Sense primer: 5’ TTCACCGTCATCACCGAAAC 3’

b) Anti-sense primer: 5’ GAATTC GCC CTT GGA TTC GCC ACC ATG GAG GGG GGT CCA GCT GT 3’

7. pUAST.CaMKKα sequencing primers

a) Sense primer: 5’ CGCAGCTGAACAAGCTAAAC 3’

b) Antisense primer: 5’ CTGCTCCCATTCATCAGTTC 3’

8. LKB1 cloning primers (PCR primer pair)

a) Sense primer:
5’ ATAAGAATGCGGCCGCTAAACTATCGCCCTTTCACTGCTGCTGT 3’

b) Anti-sense primer:
5’ CCGGAATTCCGGGCCCTTGGATCCGCCACCATGGAGGTGGACCCGCA 3’

9. pUAST.LKB1 sequencing primers

a) Sense primer: 5’ GCCGGTTCGTACTCAAGCATCC 3’

b) Anti-sense primer: 5’ GTTCATCCACCGCATCGACTCC 3’

10. pUAST.CG 6114 sequencing primers

a) Sense primer: 5'GTCACACCACAGAAGTAAGG 3'

b) Anti-sense primer: 5' GCGATGTGTACGAGAACAAG 3'

11. Tau genotyping PCR primers (also used for sequencing the PCR products)

N terminal:

a) Sense primer: 5' CAGAGCTGGGTGGTGTCTTTGG 3'

b) Anti-sense primer: 5' AAGATCACGCTGGGACGTACGG 3'

C terminal:

c) Sense primer: 5' CCCGTGGTCTGTCTTGGCTTTG 3'

d) Anti-sense primer: 5' AAGGTGGCAGTGGTCCGTACTC 3'

12| Appendix 4 – Genotyping tau flies

12.1 Genotyping tau flies by PCR and sequencing

In this work, a number of *Drosophila* stocks transgenic for human tau isoforms which were generously donated form other laboratories were utilised. There are six different isoforms of human tau, ranging from 352 to 441 amino acids in length, differing by the presence of three (3R tau) or four (4R tau) 31-35 amino acid C-terminal repeats encoding microtubule binding domains combined with zero, one or two N-terminal inserts caused by alternative splicing of exons 2 and 3. We had transgenic flies carrying the 0N3R, 0N4R, R406W, S2A and S262A isoforms and so I decided to genotype the tau stocks in order to confirm that the flies carried the stated isoform and/or mutations.

This was done via PCR from genomic DNA using PCR primers 11 a) and 11 b) for the N-terminal and 11 c) and 11 d) for the C-terminal. N-terminal primers were designed so that 0N isoforms would yield a 348bp fragment, 2N isoforms a 435bp fragment and 3N isoforms a 521bp fragment. The C-terminal primers were positioned such that 3R tau would yield a 402bp fragment and 4R tau a 494bp fragment.

It was possible to clearly genotype each tau stock from the PCR fragments (Figure 12.1). The S356A and/or S262A mutations in the S2A and S262A stocks were checked by direct sequencing of the PCR products (Figure 12.2) using primers 11 b) and 11 c).

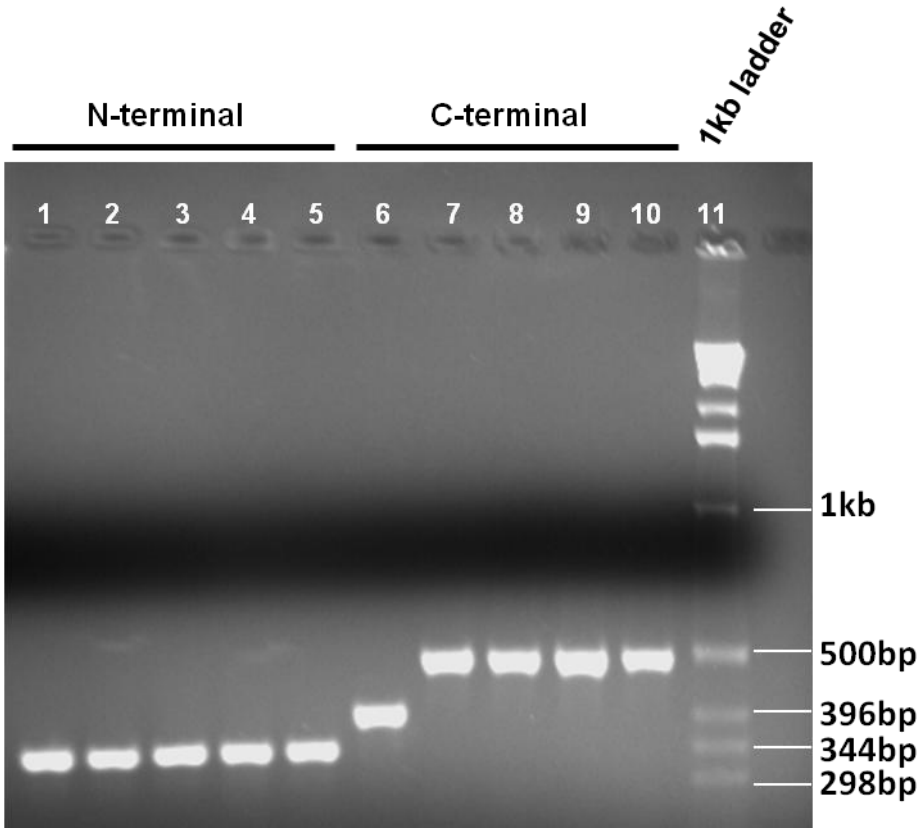

Figure 12.1 Tau Fly genotyping PCRs
Loading of genomic DNA: Lanes 1+6 – 0N3R. Lanes 2+7 – 0N4R. Lanes 3+8 – 0N4R (R406W). Lanes 4+9 – 0N4R (R406W S2A). Lanes 5+10 – 0N4R (S262A). N-terminal primers were designed so that 0N isoforms would yield a 348bp fragment, 2N isoforms a 435bp fragment and 3N isoforms a 521bp fragment. The C-terminal primers were positioned such that 3R tau would yield a 402bp fragment and 4R tau a 494bp fragment. All of the N-terminal primers yielded a band of ~344bp and so all of the isoforms are 0N (lanes 1-5). Lane 6 yielded a band of ~396bp with the C-terminal primers and so this lane contains 3R tau. Lanes 7-10 yielded bands of ~500bp with the C-terminal primers and so these lanes contain 4R tau.

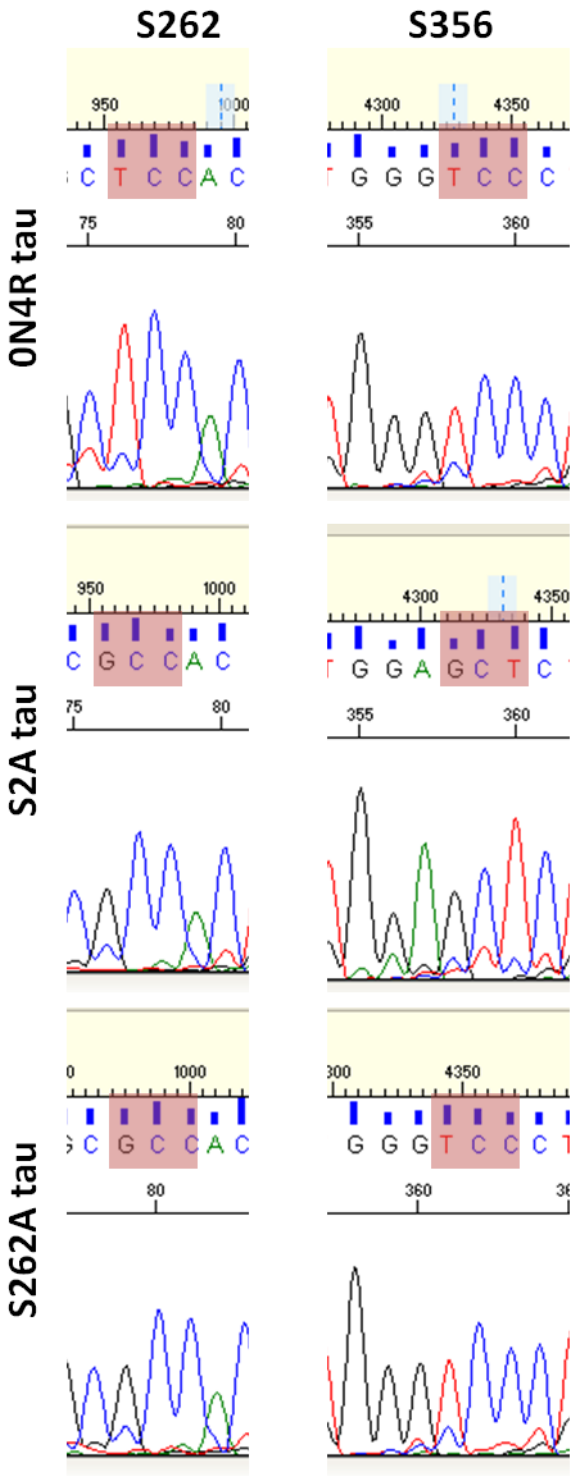

Figure 12.2 Genotyping tau flies
Highlighted in red are the relevant nucleotides which form the codons for S262 and S356. Both S2A and S262A tau carry a TCC to GCC (serine to alanine) mutation of the codon for S262. S2A tau carries a TCC to GCT (serine to alanine) mutation of the codon for S356 whilst S262A tau is wild type for this codon.

12.2 Tau expression

Having confirmed the genotypes of the flies, western blots were performed on lysates from flies expressing the 4R tau isoforms (3R was not included as it has not been used in this study) as described in the Methods section. Densitometric quantification of the bands was performed using Scion image software. Figure 12.3 shows that expression of S262A tau and R406W tau was significantly lower when compared to the control of 0N4R tau (normalised to actin) (n=3 2.91±0.14 for 0N4R tau, n=3 1.94±0.06 for S262A tau and n=3 1.54±0.05 for R406W tau, $p<0.01$, Dunnett's multiple comparison test). Unfortunately it was not possible to investigate the expression of the S2A flies as the stock became contaminated before the experiment could be completed. However, it has been shown previously that the expression of tau in the S2A tau flies was not significantly different from that of the R406W tau flies (Nishimura et al., 2004).

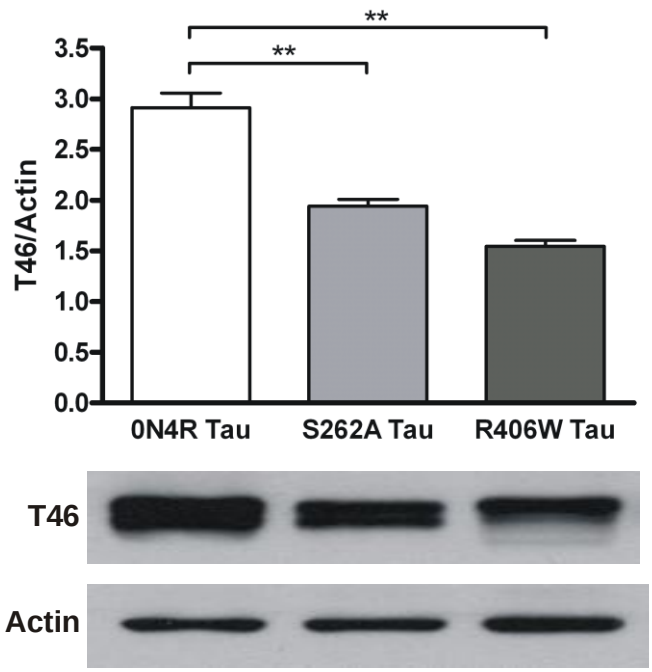

Figure 12.3: Western blots for total tau (T46) and actin.
*Quantification of western blots from flies expressing 0N4R tau, S262A tau and R406W tau show that expression of tau was significantly lower in S262A tau and R406W tau flies than in the control 0N4R tau flies. Mean ± SEM: 2.91±0.14 for 0N4R tau (n=3), 1.94±0.06 for S262A tau (n=3) and 1.54±0.05 for R406W tau (n=3). ** p<0.01, Dunnett's multiple comparison test. Representative western blots shown.*